



TRAKYA UNIVERSITY



# JOURNAL OF NATURAL SCIENCES

**26** Volume

**1** Number

April

**2025**

TRAKYA  
UNIVERSITY  
JOURNAL OF  
NATURAL  
SCIENCES

TUJNS

Trakya Univ J Nat Sci  
ISSN 2528-9691



# **Trakya University Journal of Natural Sciences**

**Volume: 26**

**Number: 1**

**April**

**2025**

## **Trakya Univ J Nat Sci**

<http://dergipark.org.tr/trkjnat>

e-mail: [tujns@trakya.edu.tr](mailto:tujns@trakya.edu.tr)

ISSN 2528-9691





**Owner**

On behalf of Trakya University Rectorship, Graduate  
School of Natural and Applied Sciences  
Doç. Dr. Filiz UMAROĞULLARI

**Editor-in-Chief**

Prof. Dr. Kadri KIRAN

**Editorial Board**

Abdel Hameed A. AWAD	Egypt	Ionnias BAZOS	Greece
Albena LAPEVA-GJONOVA	Bulgaria	İskender KARALTI	Türkiye
Arzu ALTIN YAVUZ	Türkiye (Biostatistics Editor)	İpek SÜNTAR	Türkiye
Ayşegül ÇERKEZKAYABEKİR	Türkiye (Copyeditor)	Kürşad TÜRKŞEN	Canada
Bálint MARKÓ	Romania	Mehmet Bora KAYDAN	Türkiye
Beata ZIMOWSKA	Poland	Mehmet MENDEŞ	Türkiye (Biostatistics Editor)
Belgin SÜSLEYİCİ	Türkiye	Melike SAPMAZ METİN	Türkiye
Boris ASSYOV	Bulgaria	Mustafa YAMAÇ	Türkiye
Burak ÖTERLER	Türkiye (Design Editor)	Mykyta PEREGRYM	Hungary
Bülent YORULMAZ	Türkiye	Naime ARSLAN	Türkiye
Celal KARAMAN	Türkiye (Copyeditor)	Özgür EMİROĞLU	Türkiye
Cem VURAL	Türkiye	Özkan DANIŞ	Türkiye
Coşkun TEZ	Türkiye	Panagiotis MADESIS	Greece
Davide BARRECA	Italy	Regina KAROUSOU	Greece
Dimitrios MOSSIALOS	Greece	Reşat ÜNAL	Türkiye
Enes TAYLAN	United States	Saliha ÇORUH	Türkiye
Emre EVLİCE	Türkiye	Seray TÖZ	Türkiye
Etil GÜZELMERİÇ	Türkiye	Tuğba ONGUN SEVİNDİK	Türkiye
Gamze ALTINTAŞ KAZAR	Türkiye (Design Editor)	Vedat BEŞKARDEŞ	Türkiye
Graham SAUNDERS	England	Volkan AKSOY	Türkiye (Eng Language Editor)
Güray DOĞAN	Türkiye	Yerlan TURUSPEKOV	Kazakhstan
Hatice KORKMAZ GÜVENMEZ	Türkiye	Yeşim SAĞ	Türkiye
Herdem ASLAN	Türkiye	Yıldız AYDIN	Türkiye

**Correspondence Address**

Trakya Üniversitesi Fen Bilimleri Enstitüsü Binası, Balkan Yerleşkesi – 22030 Edirne / TÜRKİYE

e-mail: [tujns@trakya.edu.tr](mailto:tujns@trakya.edu.tr)

Tel: +90 284 2358230

Fax: +90 284 2358237

*This Journal is a peer reviewed journal and is indexed by Biological Sciences, BIOSIS Previews, CAB Abstract, DOAJ (Directory of Open Access Journal), ESCI (Emerging Sources Citation Index), SCOPUS, TUBITAK-ULAKBIM Life Sciences Database (Turkish Journal Index) and Zoological Record.*

**Publisher**

Trakya University Press (<https://yayinevi.trakya.edu.tr/>)

## REVIEWER LIST

Aysegul Yildiz (Muğla, TÜRKİYE)  
Cüneyt Kırkıl (Elazığ, TÜRKİYE)  
Derya Birikten (Kütahya, TÜRKİYE)  
Duygu Yaşar Şirin (Tekirdağ, TÜRKİYE)  
Ece Şimşek (Antalya, TÜRKİYE)  
Ecesu Sezen (İstanbul, TÜRKİYE)  
Elif Begüm Yıldırım (İstanbul, TÜRKİYE)  
Emre Deniz (Washington, USA)  
Figen Esin Kayhan (İstanbul, TÜRKİYE)  
Funda Demirtaş Korkmaz (Giresun, TÜRKİYE)  
Ilker Kiliccioglu (Muğla, TÜRKİYE)  
Jie Chen (Illinois, USA)  
Jülide Tozkır (Edirne, TÜRKİYE)  
Kevser Taban (Sivas, TÜRKİYE)  
Kübra Yıldırım (Antalya, TÜRKİYE)  
Luis Alberto Parra Sanchez (Burgos, SPAIN)  
Mehmet Varol (Muğla, TÜRKİYE)  
Mustafa Çakır (Van, TÜRKİYE)  
Nazlı Öztürk (İstanbul, TÜRKİYE)  
Nuray Varol (Ankara, TÜRKİYE)  
Özlem Gök (Elazığ, TÜRKİYE)  
Seniye Zengin (İstanbul, TÜRKİYE)  
Serkan Örtücü (Erzurum, TÜRKİYE)  
Yasemin Yenilmez (İstanbul, TÜRKİYE)

## CONTENTS

### Research Article

1. *Dilek Bahar, Senem Akkoç, Buket Banu Özkan* **1-8**  
**Antiproliferative effect of silver compounds containing benzimidazole ring**
2. *Zeynep Tokcaer Keskin* **9-17**  
***In silico* analysis of IL7RA missense mutations in lung, breast and skin cancers**
3. *Elif Kale Bakir, Asuman Deveci Ozkan, Ozlem Aksoy, Yonca Yuzugullu Karakus* **19-27**  
***Eisenia foetida* (Sav.) coelomic fluid protect human umbilical vein endothelial cells against metformin-induced cell toxicity**
4. *Aysegül Cerkezkayabekir, Elvan Bakar, Deniz Yüksel Yence* **29-37**  
**Brominated flame retardant BDE-99 promotes apoptosis by intrinsic mitochondrial pathway in rat liver**
5. *Kaniga Pandi, Binoy Varghese Cheriyan, Srinithi Manikandan, Jayavarthini Jayaraman, Lokesh Kumar Harikrishnan, Vijaykumar Sayeli, Elumalai Perumal* **39-47**  
**6,3'-dimethoxy flavonol: Evidence-based insights into anti-proliferative and apoptotic effect on osteosarcoma cells**
6. *Fatma Akçakale Kaba, Ersin Akıncı, Mehmet Fatih Cengiz, Adem Kaba* **49-59**  
**Comparison of DCAS9-activator complexes for the activation of *PDX1* and *NGN3* pancreatic genes using the CRISPR system**
7. *Esra Merve Dizge, Duygu Göksay Kadaifçiler* **61-72**  
**Fungal contamination in residential water systems: A comparative study between hot and cold water samples**

### Review

8. *Moh Aijaz, Arun Kumar* **73-91**  
**Astaxanthin: Unveiling biochemical mysteries, expanding horizons, and therapeutic opportunities in health science and biomedical research**
9. *Bülent Gündüz, Emine İnci Balkan* **93-102**  
**Melatonin - leptin interaction and obesity-related genes**



## Antiproliferative effect of silver compounds containing benzimidazole ring

Dilek Bahar<sup>1\*</sup>, Senem Akkoç<sup>2,3</sup>, Buket Banu Özkan<sup>1</sup>

<sup>1</sup> Erciyes University, Genkok Genome and Stem Cell Center, Kayseri, 38030, TÜRKİYE

<sup>2</sup> Suleyman Demirel University, Faculty of Pharmacy, Department of Basic Pharmaceutical Sciences, Isparta, 32260, TÜRKİYE

<sup>3</sup> Bahçeşehir University, Faculty of Engineering and Natural Sciences, Istanbul, 34353, TÜRKİYE

### Cite this article as:

Bahar D., Akkoç S. & Özkan B.B. 2025. Antiproliferative effect of silver compounds containing benzimidazole ring. *Trakya Univ J Nat Sci*, 26(1): 1-8, DOI: 10.23902/trkjinat.1549105

Received: 13 September 2024, Accepted: 02 November 2024, Online First: 20 December 2024, Published: 15 April 2025

### Edited by:

Yeşim Sağ Açıkel

### \*Corresponding Author:

Dilek Bahar

[dilekbahar@erciyes.edu.tr](mailto:dilekbahar@erciyes.edu.tr)

### ORCID iDs of the authors:

DB. 0000-0002-4916-5071

SA. 0000-0002-1260-9425

BBÖ. 0000-0002-1589-9464

### Key words:

Apoptosis

Cytotoxic activity

Ag-NHC

Oxidative stress

Cancer

**Abstract:** The benzimidazole nucleus is a crucial pharmacophore in medicine, due to its significant biological activities. Recent studies have focused on the synthesis and biological activity of benzimidazole compounds. Therefore, in the present study, a series of *N*-heterocyclic silver compounds containing benzimidazole nuclei were prepared, and *in vitro* cell culture experiments were performed to evaluate their effects. The compounds were cultured with lung (A549), colon (CaCo2), breast (MCF7), prostate (PC3) cancer cell lines, and healthy lung (WI38) cell line, and their anticancer effects were investigated through the MTT cell proliferation test, apoptosis determination, and oxidative stress tests on these cell lines. The results revealed that the presence of drug candidates was more practical than that of commercially used cisplatin.

**Özet:** Benzimidazol çekirdeği önemli biyolojik aktiviteleri ile tıpta önemli bir farmakofordur. Son çalışmalar benzimidazol bileşiklerinin sentezi ve biyolojik aktivitesine odaklanmıştır. Bu nedenle, bu çalışmada benzimidazol çekirdekleri içeren bir dizi *N*-heterosiklik gümüş bileşiği hazırlanmıştır. Bileşiklerin etkilerini incelemek için *in vitro* hücre kültür deneyleri yapılmıştır. Bileşikler akciğer (A549), kolon (CaCo2), meme (MCF7), prostat (PC3) kanser hücre hatları ve sağlıklı akciğer (WI38) hücre hattı ile kültüre edilmiş ve bileşiklerin antikanser etkileri bu hücreler üzerinde MTT hücre çoğalma testi, apoptoz tayini ve oksidatif stres testleri yapılarak araştırılmıştır. Sonuçlar ilaç adaylarının varlığının ticari olarak kullanılan sisplatinden daha pratik olduğunu ortaya koymuştur.

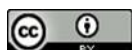
### Introduction

Cancer is a growing global threat to human life, with increasing mortality rates due to numerous factors such as disease diversity and drug resistance (Block *et al.* 2015). Over 14 million cancer cases are reported worldwide annually, and this number is estimated to reach 19.3 million by 2025. Although cancer is a treatable disease, late diagnosis, risky surgical procedures, prolonged and severe side effects of chemotherapy, and resistance to chemotherapeutic drugs make treatment challenging (Chaicharoenaudomrung *et al.* 2019). The incidence and mortality rates of breast cancer are expected to show an increase pattern in recent future. Indeed, breast cancer accounted for 11.6% of all cancer cases worldwide in 2018. Colon cancer is the most common cancer affecting both sexes, with one in ten cancer patients diagnosed with metastatic colon cancer. Approximately 600,000 people die from metastatic colon cancer annually (Siegel *et al.* 2024).

While the effectiveness of cancer drugs is debatable, toxic risks have been observed in drugs developed against

cancer, and resistance to cancer drugs is increasing. This underscores the urgent need for the development of new methods for disease treatment. Despite significant advancements in treatment methods and improvements, cancer remains unbeaten, fueling the ongoing demand for more effective drugs in this sector. The present research, focusing on the synthesis and determination of antiproliferative effects of silver compounds containing benzimidazole ring, has the potential to contribute significantly to this fight.

Benzimidazoles, with their 'Hem' structure, a key component of hemoglobin, and the presence of the 'heme ion' system, which is crucial for oxygen transport in the body, play a vital role in functions of some biological molecules, such as metalloproteins and B12 vitamins (Akkoç *et al.* 2019). Naturally occurring nucleotides containing adenine and guanine are isoesters of the benzimidazole ring, allowing interaction with biopolymers in organisms. Benzimidazole and its



OPEN ACCESS

derivatives are among the most synthesized and investigated heterocyclic compounds in reactivity (Gök *et al.* 2014, Akkoç *et al.* 2016a, Akkoç *et al.* 2017, Akkoç 2019). The anticancer effects of benzimidazole derivatives may arise from their cytotoxic effects on cancer cells (Bansal & Silakari 2012, Tonelli *et al.* 2014, Akkoç *et al.* 2016b, Gök *et al.* 2019).

Therefore, our study investigated the cytotoxic effects of a series of *N*-heterocyclic silver compounds containing benzimidazole nuclei on lung (A549), colon (CaCo2), breast (MCF7), and prostate (PC3) cancer cell lines and WI38 healthy epithelial cell line.

## Materials and Methods

### Synthesis of silver metal compounds

The process of synthesizing the silver metal compounds involved stirring the synthesized benzimidazolium salt (2 mmol), silver oxide (1 mmol), and molecular sieve (5-10 beads) in dried dichloromethane (15 mL) at room temperature for 18 hours (Gök *et al.* 2014, Gök *et al.* 2019). The solution was then filtered through celite, and the resulting silver complexes were crystallized in a dichloromethane-diethyl ether mixture. The cis-platin that used as positive control drug were purchased from Sigma (SigmaAldrich, USA).

### Evaluation of compounds' anticancer effect

For this purpose, breast (MCF-7) lung (A-549), prostate (PC-3), and colon (CaCo2) cancer cell lines, and WI38 healthy lung epithelial cell line were cultured. The culture media included 10% Fetal bovine serum (FBS), 1% L-glutamine, 1% penicillin-streptomycin, and EMEM (Eagle's Minimum Essential Medium) for MCF-7 cell line, F-12K for A-549 and PC-3 cell lines, and RPMI 1640 for CaCo2 cell line.

Cells were thawed from liquid nitrogen, seeded into 75 cm<sup>2</sup> flasks, and placed in a 37°C, 5% CO<sub>2</sub> incubator. The culture medium was changed every 3-4 days. When the cell density in the culture dishes reached 90-95%, trypsinization was performed, and cells were subcultured to obtain a higher number. Excess cells were cryopreserved in a freezing medium containing 10% FBS, 80% culture medium, and 10% Dimethyl sulfoxide (DMSO), stored at -80°C, and then transferred to liquid nitrogen for further studies. Once an adequate number of cells were obtained, they were subjected to trypsinization again and seeded into 96-well culture plates at a density of 3x10<sup>3</sup> cells per well for the 3-(4,5-dimethylthiazol-2-yl)-2,5-diphenyltetrazolium bromide (MTT) assay. After 24 hours of cell seeding, cells were cultured in triplicates with different concentrations of each silver metal compounds (200, 100, 50, 25, 12.5, and 6.25 µM) and following a 48-hour incubation, MTT solution prepared in Phosphate-buffered saline (PBS) was added to each well at a final concentration of 0.5 mg/mL, and the plates were further incubated for three hours. The medium containing formazan crystals formed

within the cells was aspirated, and DMSO was added to dissolve the formazan crystals. The color developed after dissolving the formazan crystals in DMSO was measured at 560 nm using a Promega Glomax Elisa reader. Each test was performed at least in triplicate. The obtained absorbance values were analyzed using the GraphPad Prism statistical software, and the half-maximal inhibitory concentrations (IC<sub>50</sub>) of the drugs on cells were determined (Aslan *et al.* 2020).

The impact of effective doses on apoptosis and reactive oxygen species (ROS) activity in cells was determined using the Muse™ Annexin V & Dead Cell Kit (Catalog No: MCH100105) and Muse® Oxidative Stress Kit (Catalog No: MCH100111), respectively. For this purpose, cells were seeded into 6-well culture plates, and silver metal compounds doses that induced IC<sub>50</sub> values in the cells, as determined by MTT assay, were used. After a 48-hour incubation with drugs, apoptosis and oxidative stress tests were performed. The kits were used according to the manufacturer's instructions, and data were analyzed using TURCOSA statistical software. A dependent two-sample t-test was used to evaluate the effects of different drugs on the same cells.

Cells were stained with propidium iodide (PI) and Hoechst double staining to visualize apoptosis and cell membrane integrity. Like the MTT assay, cells were seeded into 96-well culture plates, and drug doses resulting in IC<sub>50</sub> values were added. After 48 hours, cells were washed three times with DPBS, incubated with DPBS containing PI and Hoechst for 15 minutes in the dark and imaged using a fluorescence microscope at x20 objective (Nikon, Ti Eclipse).

### Statistics

The half-maximal inhibitory concentrations (IC<sub>50</sub>) values were analyzed using the GraphPad Prism statistical software and other statistical evaluations were made using a t-test.

## Results

### Preparation of Silver Metal Compounds

The open structures of benzimidazol ring contained silver metal complexes were given in Fig. 1. The known complex, [1-phenyl-3-(2,4,6-trimethylbenzyl) benzimidazole-2-ylidene]chlorosilver(I), SE-231, was synthesized according to the literature (Gök *et al.* 2014). The known complexes, 1-(2-diethylaminoethyl)-3-(2,3,5,6-tetramethylbenzyl)benzimidazole-2-ylidene]chlorosilver(I), SE-208, and 1-(2-diethylaminoethyl)-3-(2,3,4,5,6-pentamethylbenzyl) benzimidazole-2-ylidene]chlorosilver(I), SE-209, were prepared according to the literature (Akkoç *et al.* 2014, Gök *et al.* 2014).

NMR data of the synthesized known compounds are given below. Both proton and carbon NMR data prove the accuracy of the structures.

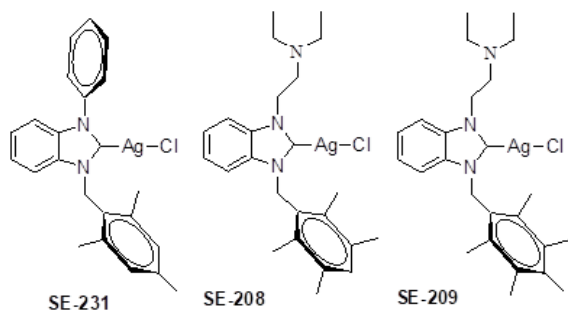


Fig. 1. Synthesized Ag-NHC complexes.

[1-Phenyl-3-(2,4,6-trimethylbenzyl)benzimidazol-2-ylidene]chlorosilver(I), SE-231

$^1\text{H}$  NMR (300.13 MHz,  $\text{DMSO-d}_6$ );  $\delta$ : 1.65 and 2.52 [s, 9 H,  $\text{NCH}_2\text{C}_6\text{H}_2(\text{CH}_3)_3$ -2,4,6]; 5.55 [s, 2 H,  $\text{NCH}_2\text{C}_6\text{H}_2(\text{CH}_3)_3$ -2,4,6]; 6.71–8.26 (m, 11 H, Ar-H).  $^{13}\text{C}$  NMR (75.47 MHz,  $\text{DMSO-d}_6$ );  $\delta$ : 20.4, 21.1, 55.3, 112.8, 125.0, 128.2, 130.4, 125.5, 129.8, 134.1, 135.2, 126.7, 134.3, 137.9, and 138.5 (Gök *et al.* 2014).

[1-(2-Diethylaminoethyl)-3-(2,3,5,6-tetramethylbenzyl)benzimidazol-2-ylidene]chlorosilver(I), SE-208

$^1\text{H}$  NMR (300.13 MHz,  $\text{DMSO-d}_6$ );  $\delta$ : 0.7–2.74 [m, 14 H,  $\text{NCH}_2\text{CH}_2\text{N}(\text{C}_2\text{H}_5)_2$ ]; 2.07 and 3.35 [s, 12 H,  $\text{NCH}_2\text{C}_6\text{H}(\text{CH}_3)_4$ -2,3,5,6]; 5.54 [s, 2 H,  $\text{NCH}_2\text{C}_6\text{H}(\text{CH}_3)_4$ -2,3,5,6]; 6.97–7.93 (m, 5 H, Ar-H).  $^{13}\text{C}$  NMR (75.47 MHz,  $\text{DMSO-d}_6$ );  $\delta$ : 12.1, 20.8, 46.5, 47.3, 16.4, 48.6, 52.8, 112.2, 112.6, 124.4, 131.9, 132.5, 133.6, 133.8, 134.4, and 134.5 (Akkoç *et al.* 2014).

1-(2-Diethylaminoethyl)-3-(2,3,4,5,6-pentamethylbenzyl)benzimidazole-2-ylidene]chlorosilver(I), SE-209

$^1\text{H}$  NMR (300.13 MHz,  $\text{DMSO-d}_6$ );  $\delta$ : 0.92 [t, 6 H,  $J$ : 7.16 Hz,  $\text{NCH}_2\text{CH}_2\text{N}(\text{CH}_2\text{CH}_3)_2$ ]; 2.21–2.35 [m, 15 H,  $\text{NCH}_2\text{C}_6(\text{CH}_3)_5$ ]; 2.52 [q, 4 H,  $J$ : 7.14 Hz,  $\text{N}(\text{CH}_2\text{CH}_3)_2$ ]; 2.84 and 4.39 (tt, 4 H,  $J$ : 6.61 and 6.59 Hz,  $\text{NCH}_2\text{CH}_2\text{NC}_4\text{H}_{10}$ ); 5.48 [s, 2 H,  $\text{NCH}_2\text{C}_6(\text{CH}_3)_5$ ]; 7.14–7.55 (m, 4 H, Ar-H).  $^{13}\text{C}$  NMR (75.47 MHz,  $\text{DMSO-d}_6$ );  $\delta$ : 12.1, 17.1, 17.2, 17.4, 47.6, 47.7, 49.0, 53.2, 111.3, 111.6, 123.9, 124.1, 126.6, 126.9, 132.9, 133.9, 134.2, and 137.3 (Akkoç *et al.* 2014).

#### Cell Culture and Evaluation of Compounds' Anticancer Effect

In the MTT assay, six doses of each drug candidate were added to the cells, with concentrations of 200, 100, 50, 25, 12.5, and 6.25  $\mu\text{M}$ . The absorbance data obtained from the MTT assay were evaluated using the GraphPad Prism software to determine the  $\text{IC}_{50}$  value for each cell line. The  $\text{IC}_{50}$  values for the cells are presented in Table 1.

According to the MTT results, SE-208 containing 2-diethylaminoethyl and 2,3,5,6-tetramethylbenzyl substituents on the nitrogen atoms in the benzimidazole ring is the most cytotoxic compound at  $\text{IC}_{50}$ , with a value of 3.08  $\mu\text{M}$ , against MCF7 cells. Overall, SE-208 was the most effective at the lowest dose for all cell lines.

According to the literature, silver compounds exhibit high cytotoxicity due to their metal complex content.

The apoptosis test's result graph was given in Fig.2. According to the results of the apoptosis test using Annexin V, all compounds statistically significantly affected the cells. The initial evaluation was performed by comparing silver compounds with each other. According to this comparison, silver compounds reduced the number of viable cells in A549 and CaCo2 cell lines compared to organic compounds.

For early apoptosis, the most effective cells for silver compounds were MCF7, PC3, and W138, respectively. The lowest early apoptosis values were observed in the CaCo2 cell line. An increase in late apoptosis values was observed in MCF7, CaCo2, and A549 cells. In the W138 cell line, the SE-208 compound primarily increased late apoptosis. CaCo2 and A549 cells had the highest number of dead cells.

When the results were evaluated cell-by-cell, the W138 epithelial lung line was the most affected by the compounds. The study included this line to test whether the compounds were specific to cancer cells. According to the apoptosis test, the SE209 compound containing 2-diethylaminoethyl and 2,3,4,5,6-pentamethylbenzyl substituents on the nitrogen atoms in the benzimidazole ring showed more cancer cell specificity than others.

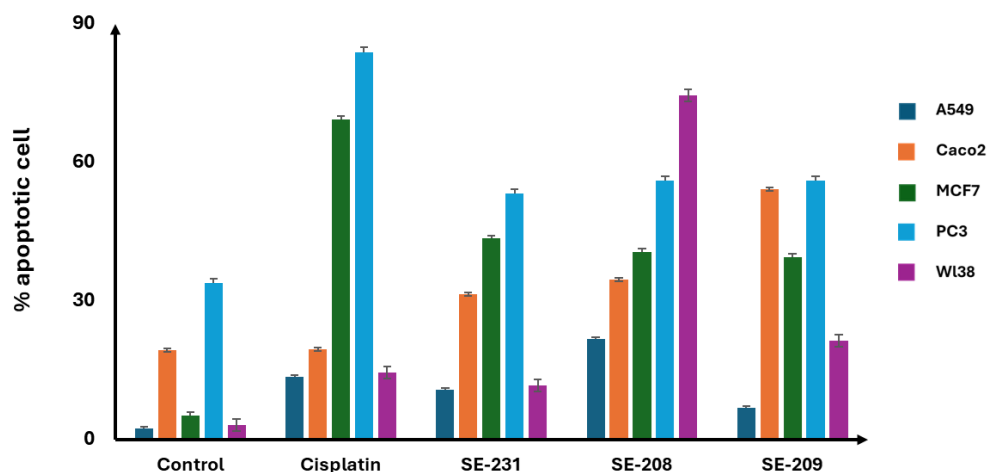
Regarding individual apoptosis test results for the produced compound, the SE209 compound was effective. SE209 significantly reduced viability in CaCo2 and A549 cells and increased apoptosis significantly in the same cell lines. Overall, CaCo2 and A549 cells were the most affected by the compounds and showed similar reactions.

The oxidative stress test results were given in Fig3. According to the oxidative stress test results, silver metal compounds increased the ROS activity more than Cis-platin on A549 (%ROS+ activity: Cis-platin56; SE23177; SE20864; SE20959), PC3 (%ROS+ activity: Cis-platin60; SE20961), and W138 (%ROS+ activity: Cis-platin17; SE23177; SE20819; SE20969) cell lines statistically significantly ( $p>0.05$ ). On CaCo2 and MCF7 cell lines, compounds affected the cells positively and reduced the ROS activity when compared to the control.

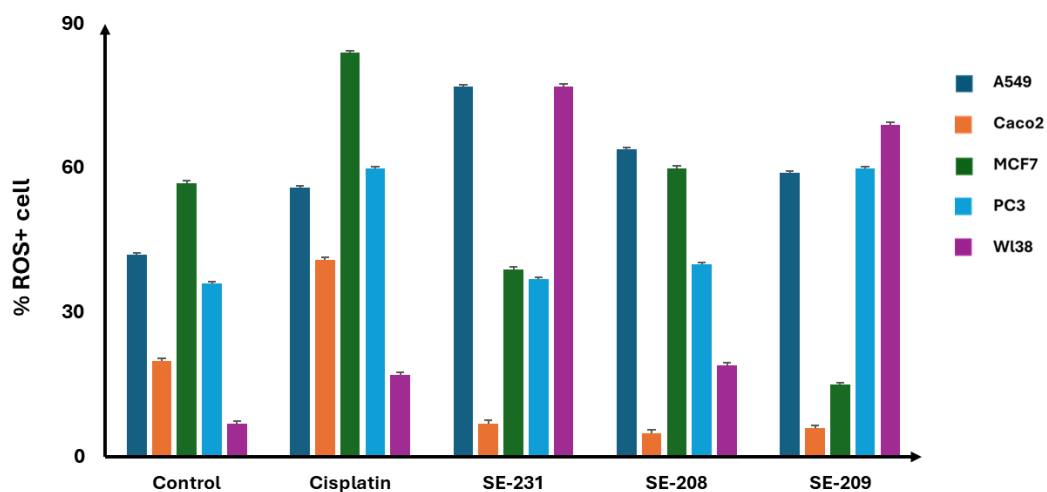
Based on the results obtained from PI-Hoechst double staining, PI staining was observed in the cells as a result of the compounds' apoptotic effects. The integrity of the cell membranes was maintained, and no disruption in cell integrity was observed (Figs 4-8).

Table 1.  $\text{IC}_{50}$  values of complexes.

Complexes	IC <sub>50</sub> (μM)				
	A549	CaCo2	MCF-7	PC3	W138
SE-231	38.95	22.22	49.62	163.90	6.83
SE-208	4.79	5.01	3.08	10.18	3.34
SE-209	14.49	9.60	17.74	45.48	40.34
Cisplatin	21.05	16.53	28.22	72.17	51.65



**Fig. 2.** Percentages of the cancer cell lines' apoptosis in the absence/presence of compounds SE-231, SE-208, SE-209.



**Fig. 3.** Percentages of the ROS+ cells in the absence/presence of compounds SE-231, SE-208, SE-209.

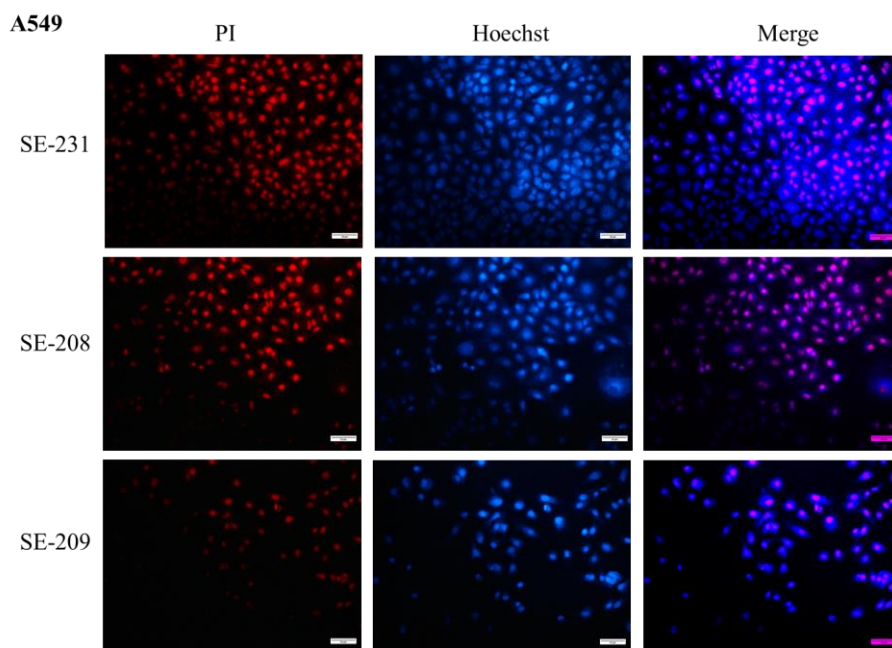


**Fig. 4.** The fluorescence microscopy images of A549 cell line in the presence of compounds SE-231, SE-208, and SE-209, scale bars=100μM.



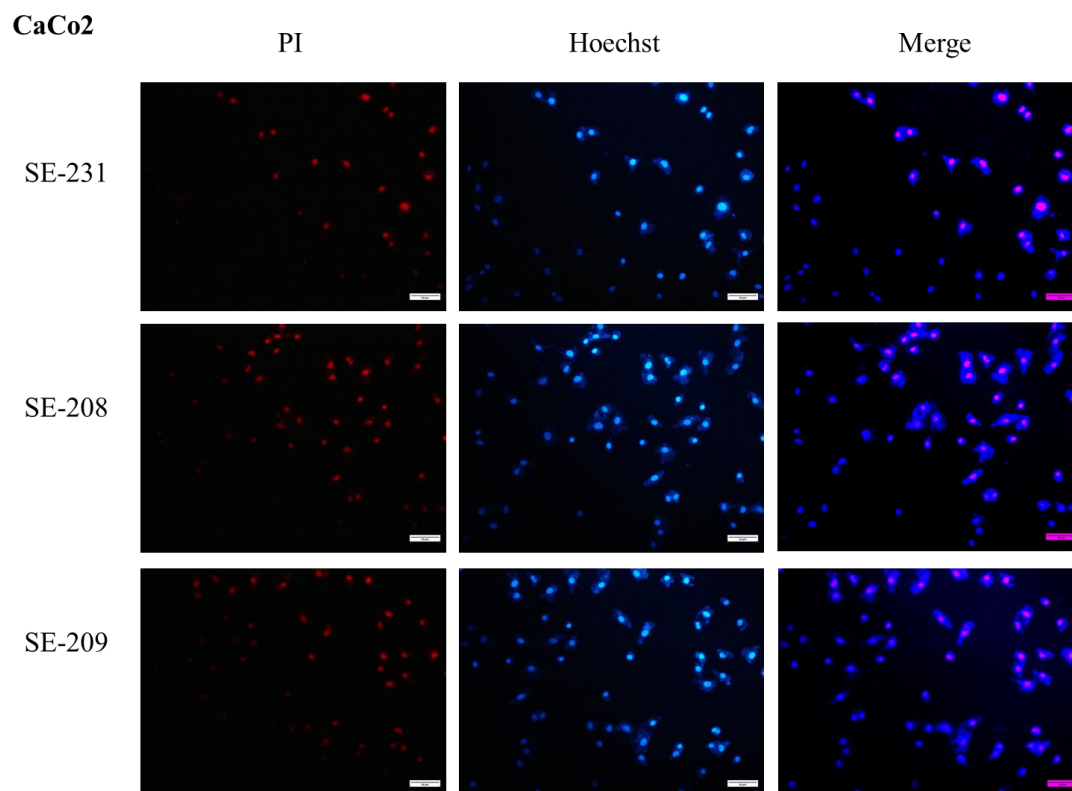


**Fig. 5.** The fluorescence microscopy images of the CaCo2 cell line in the presence of compounds SE-231, SE-208, and SE-209, scale bars=100 $\mu$ M.

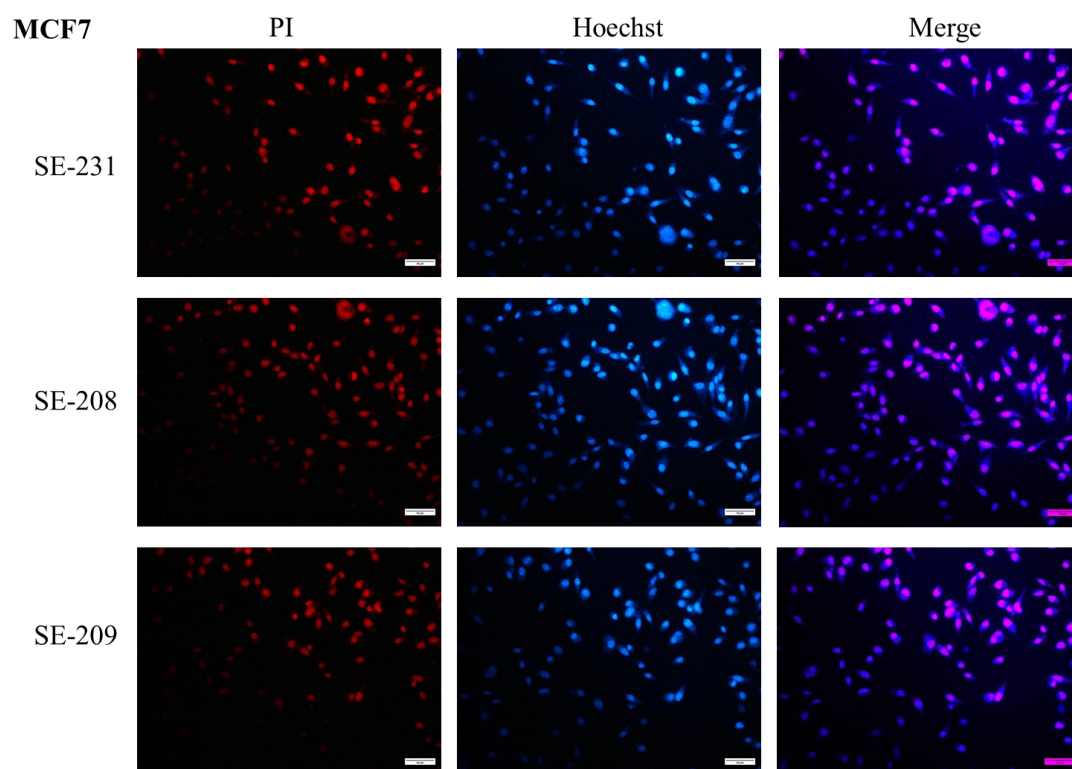


**Fig. 6.** The fluorescence microscopy images of the MCF-7 cell line in the presence of compounds SE-231, SE-208, and SE-209, scale bars=100 $\mu$ M.

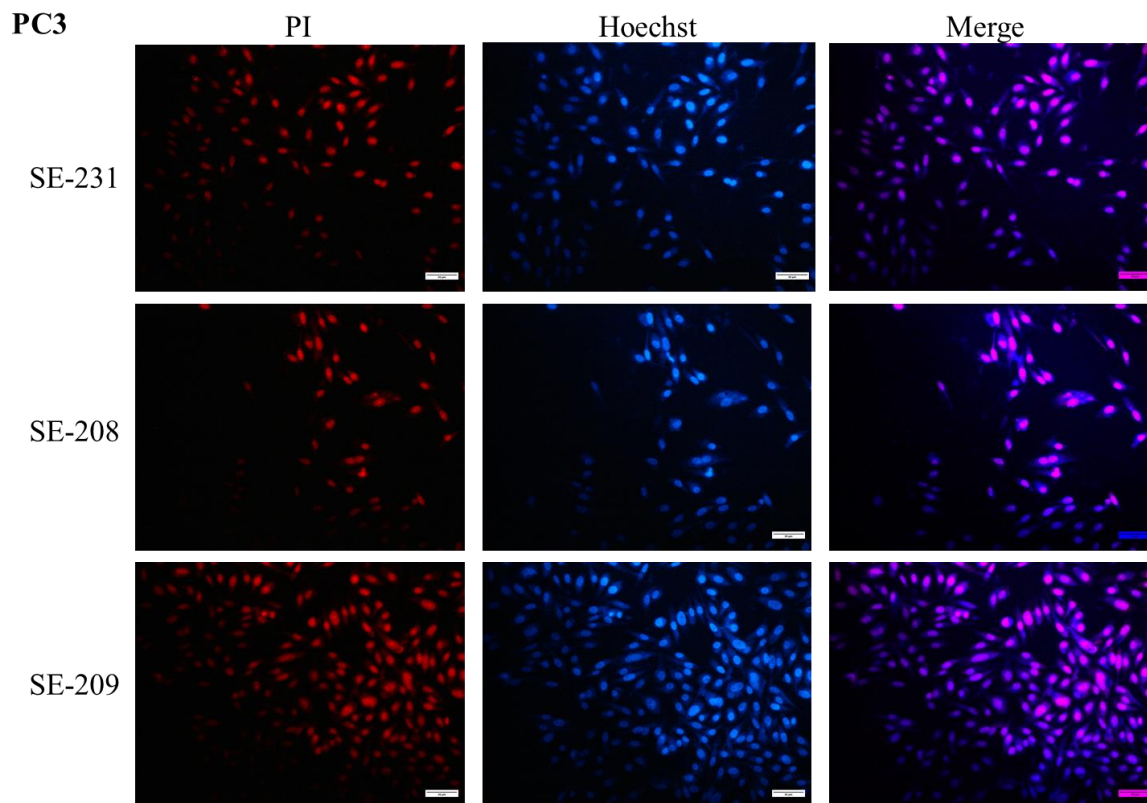


**Fig. 7.** The fluorescence microscopy images of the PC3 cell line in the presence of compounds SE-231, SE-208, and SE-209, scale bars=100 $\mu$ M.

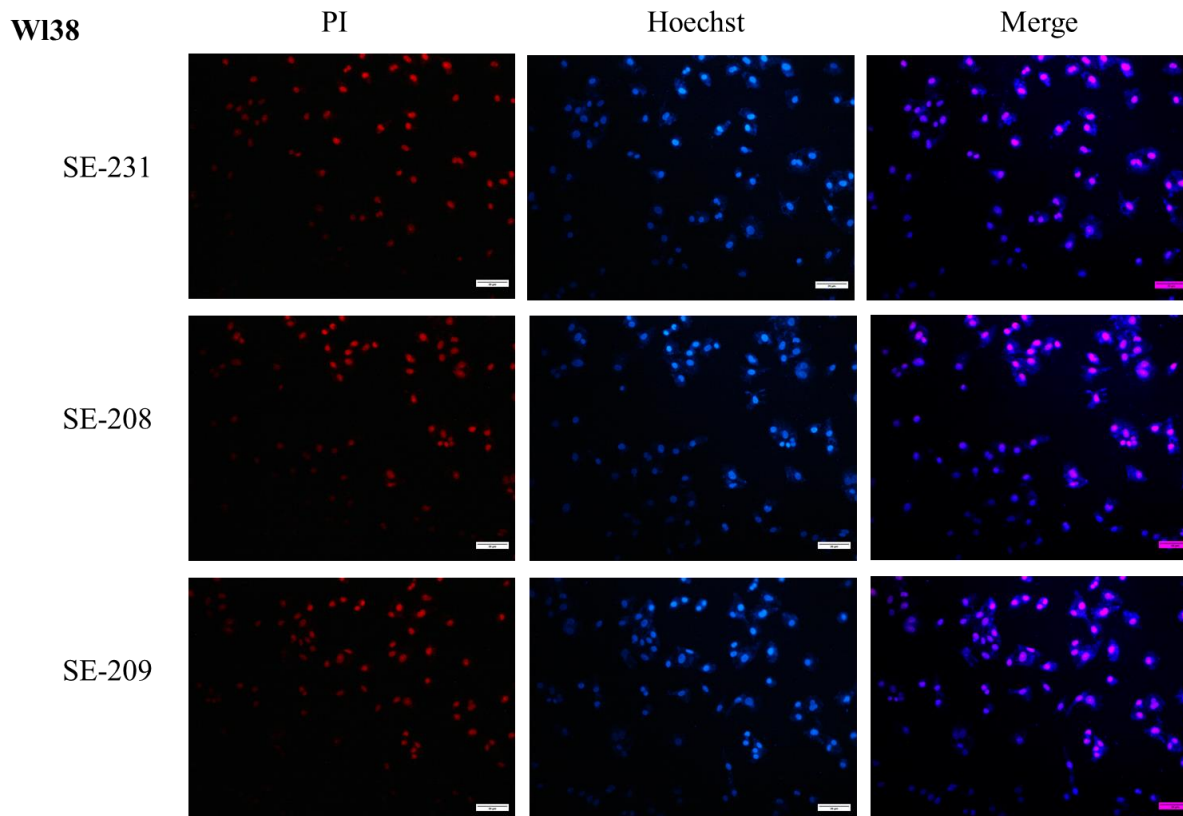


**Fig. 8.** The fluorescence microscopy images of the WI38 cell line in the presence of compounds SE-231, SE-208, and SE-209, scale bars=100 $\mu$ M.

## Discussion

Cancer is a threat to human life, with increasing mortality rates globally. The cancer drugs have toxic risks and resistance to cancer drugs is increasing. Because of this, the development of new drugs for disease treatment is urgent need. Benzimidazole containing drugs has cytotoxic effects on cancer cells (Bansal & Silakari 2012, Tonelli *et al.* 2014, Akkoç *et al.* 2016b, Gök *et al.* 2019). The benzimidazole ring's privileged skeletal structure has led to the development of many essential drugs used in various therapeutic areas, such as antihistamines, anthelmintics, proton pump inhibitors, and angiotensin receptor antagonists (Abdelgawad *et al.* 2019, Shingalapuri *et al.* 2010). Due to their various biological activity properties, benzimidazole-based heterocyclic compounds hold a significant place in chemistry (Taha *et al.* 2018, Özil *et al.* 2018).

With these underscores we investigated the silver metal complexes that contained benzimidazole nuclei on lung (A549), colon (CaCo2), breast (MCF7), and prostate (PC3) cancer cell lines and W138 healthy epithelial cell line. Our results show the three silver metal complexes SE-231, SE-208 and SE-209 have antiproliferative effects on cell lines. In some studies in the literature, are in line with our study.

Liu *et al.* (2012) investigated the anticancer effect of benzimidazole derivatives synthesized on A549, HCT116, A375, HepG2, and PC-9 cancer cell lines using the MTT method and reported that the synthesized compounds had high anticancer activity. Thimmegowda *et al.* (2008), who examined the effects of benzimidazole-like compounds on the MDA-MB-231 breast cancer cell line, stated that these compounds had a vigorous antiproliferative activity. Mavrova *et al.* (2013) used benzimidazole-containing compounds and HT-29, MDA-MB231, HeLa, HepG2, and Lep-3 cancer lines in their study, and found that the compounds they synthesized were more effective in a different cell line, and all compounds had particularly effective antiproliferative effects against Lep-3.

## References

1. Abdelgawad, M.A., Bakr, R.B., Ahmad, W., Al-Sanea, M.M. & Elshemy, H.A.H. 2019. New pyrimidine-benzoxazole/benzimidazole hybrids: Synthesis, antioxidant, cytotoxic activity, in vitro cyclooxygenase and phospholipase A2-V inhibition. *Bioorganic Chemistry*, 92: 1-6. <https://doi.org/10.1016/j.bioorg.2019.103218>
2. Akkoç, S. 2019. Derivatives of 1-(2-(Piperidin-1-yl) ethyl)-1H-benzo [d] imidazole: Synthesis, characterization, determining of electronic properties and cytotoxicity studies. *ChemistrySelect*, 4(17): 4938-4943. <https://doi.org/10.1002/slct.201900353>
3. Akkoç, S., Gök, Y., İlhan, İ.Ö. & Kayser, V. 2016a. N-Methylphthalimide-substituted benzimidazolium salts and PEPPSI-Pd-NHC complexes: synthesis, characterization and catalytic activity in carbon-carbon bond-forming reactions. *Beilstein Journal of Organic Chemistry*, 12(1): 81-88. <https://doi.org/10.3762/bjoc.12.9>
4. Akkoç, S., Gök, Y., Özdemir, İ. & Günel, S. 2014. N-Heterocyclic Carbene Silver Complexes: Synthesis, Characterization and in Vitro Antimicrobial Studies. *Journal of the Chinese Advanced Materials Society*, 2(1): 20-30. <https://doi.org/10.1080/22243682.2014.882795>
5. Akkoç, S., Kayser, V. & İlhan, İ.Ö. 2019. Synthesis and in vitro anticancer evaluation of some benzimidazolium salts. *Journal of Heterocyclic Chemistry*, 56(10): 2934-2944. <https://doi.org/10.1002/jhet.3687>
6. Akkoç, S., Kayser, V., İlhan, İ.Ö., Hibbs, D.E., Gök, Y., Williams, P.A., Hawkins, B. & Lai, F. 2017. New compounds based on a benzimidazole nucleus: synthesis, characterization and cytotoxic activity against breast and

In this study, three silver-containing compounds were produced. These compounds were compared regarding MTT, apoptosis, reactive oxygen species (ROS) activity, and cell membrane integrity in four cancers and one regular cell line. According to the apoptosis analysis, the most effective drug was SE209. CaCo2 and A549 cells were identified as the most affected cells by the drugs. According to the apoptosis data, again, the SE209 compound was more selective against cancer cells than cisplatin.

Regarding the oxidative stress analysis, cancer cells were more resistant to oxidative stress than normal cells. According to the fluorescent staining results, apoptosis markers were observed in the cells, and no disruption in cell membrane structures was observed. In conclusion, three benzimidazole containing silver metal complexes that may have anticancer properties were promising as anticancer drugs. *In vivo* animal studies may bring these compounds closer to clinical use.

## Acknowledgement

We would like to thank GENKOK, Erciyes University Research Fund (Eru BAP) and the Proofreading & Editing Office of the Dean for Research of Erciyes University for copyediting and proofreading service for an earlier version of the manuscript.

**Ethics Committee Approval:** Since the article does not contain any studies with human or animal subject, its approval to the ethics committee was not required.

**Data Sharing Statement:** All data are available within the study.

**Author Contributions:** Concept: D.H., S.A., B.B.O., Design: D.H., S.A., Execution: D.H., S.A., B.B.O., Material supplying: D.H., S.A., Data acquisition: D.H., S.A., B.B.O., Data analysis/interpretation: D.H., S.A., B.B.O., Writing: D.B., Critical review: D.B

**Conflict of Interest:** The authors have no conflicts of interest to declare.

**Funding:** The study was supported by the Erciyes University Research Fund with project number TKB-2020-10346.

- colon cancer cell lines. *Journal of Organometallic Chemistry*, 839: 98-107. <https://doi.org/10.1016/j.jorganchem.2017.03.037>
7. Akkoç, S., Özer İlhan, İ., Gök, Y., Upadhyay, P.J. & Kayser, V. 2016b. In vitro cytotoxic activities of new silver and PEPPSI palladium N-heterocyclic carbene complexes derived from benzimidazolium salts. *Inorganica Chimica Acta*, 449: 75-81. <https://doi.org/10.1016/j.ica.2016.05.001>
  8. Aslan, H. G., Akkoç, S. & Kökbudak, Z. 2020. Anticancer activities of various new metal complexes prepared from a Schiff base on A549 cell line. *Inorganic Chemistry Communications*, 111: 11-6. <https://doi.org/10.1016/j.inoche.2019.107645>
  9. Bansal, Y. & Silakari, O. 2012. The therapeutic journey of benzimidazoles: A review. *Bioorganic Medicinal Chemistry*, 20(21): 6208-6236. <https://doi.org/10.1016/j.bmc.2012.09.013>
  10. Block, K.I., Gyllenhaal, C., Lowe, L., Amedei, A., Amin, A.R., Amin, A., Ashraf, S.S. 2015. A broad-spectrum integrative design for cancer prevention and therapy. In *Seminars in Cancer Biology*, 35(Suppl): 276-304. <https://doi.org/10.1016/j.semcancer.2015.09.007>
  11. Chaicharoenaudomrung, N., Kunhorm, P. & Noisa, P. 2019. Three-dimensional cell culture systems as an in vitro platform for cancer and stem cell modeling. *World Journal of Stem Cells*, 11(12): 1065-1083. <https://doi.org/10.4252/wjsc.v11.i12.1065>
  12. Gök, Y., Akkoç, S., Albayrak, S., Akkurt, M. & Tahir, M.N. 2014. N-Phenyl-substituted carbene precursors and their silver complexes: synthesis, characterization and antimicrobial activities. *Applied Organometallic Chemistry*, 28(4): 244-251. <https://doi.org/10.1002/aoc.3116>
  13. Gök, Y., Akkoç, S., Çelikal, Ö.Ö., Özdemir, İ. & Günel, S. 2019. In vitro antimicrobial studies of naphthalen-1-ylmethyl substituted silver N-heterocyclic carbene complexes. *Arabian Journal of Chemistry*, 12(8): 2513-2518. <https://doi.org/10.1016/j.arabjc.2015.04.019>
  14. Siegel, R., Giaquinto A.N. & Jemal A. 2024. Cancer statistics. *CA: A Cancer Journal For Clinicians*, 60(5): 277-300. <https://doi.org/10.3322/caac.21820>
  15. Liu, T., Sun, C., Xing, X., Jing, L., Tan, R., Luo, Y. & Zhao, Y. 2012. Synthesis and evaluation of 2-[2-(phenylthiomethyl)-1H-benzimidazol-1-yl] acetohydrazide derivatives as antitumor agents. *Bioorganic & Medicinal Chemistry Letters*, 22(9): 3122-3125. <https://doi.org/10.1016/j.bmcl.2012.03.061>
  16. Mavrova, A.T., Wesselinova, D., Vassilev, N. & Tsenov, J.A. 2013. Design, synthesis and antiproliferative properties of some new 5-substituted-2-iminobenzimidazole derivatives. *European Journal of Medicinal Chemistry*, 63: 696-701. <https://doi.org/10.1016/j.ejmech.2013.03.010>
  17. Özil, M., Parlak, C. & Baltaş, N. 2018. A simple and efficient synthesis of benzimidazoles containing piperazine or morpholine skeleton at C-6 position as glucosidase inhibitors with antioxidant activity. *Bioorganic Chemistry*, 76: 468-477. <https://doi.org/10.1016/j.bioorg.2017.12.019>
  18. Shingalapuri, R.V., Hosamani, K.M., Keri, R.S. & Hugar, M.H. 2010. Derivatives of benzimidazole pharmacophore: Synthesis, anticonvulsant, antidiabetic and DNA cleavage studies. *European Journal of Medicinal Chemistry*, 45(5): 1753-1759. <https://doi.org/10.1016/j.ejmech.2010.01.007>
  19. Taha, M., Mosaddik, A., Rahim, F., Ali, S., Ibrahim, M. & Almandil, N.B., 2018. Synthesis, antilycation and antioxidant potentials of benzimidazole derivatives. *Journal of King Saud University -Science*, 32(1): 191-194. <https://doi.org/10.1016/j.jksus.2018.04.003>
  20. Thimmegowda, N.R., Swamy, S.N., Kumar, C.A., Kumar, Y.S., Chandrappa, S., Yip, G. W. & Rangappa, K.S. 2008. Synthesis, characterization and evaluation of benzimidazole derivative and its precursors as inhibitors of MDA-MB-231 human breast cancer cell proliferation. *Bioorganic & Medicinal Chemistry Letters*, 18(1): 432-435. <https://doi.org/10.1016/j.bmcl.2007.08.078>
  21. Tonelli, M., Novelli, F., Tasso, B., Vazzana, I., Sparatore, A., Boido, V., Sparatore, F., La Colla, P., Sanna, G., Giliberti, G., Busonera, B., Farci, P., Ibba, C. & Loddio, R. 2014. Antiviral activity of benzimidazole derivatives. III. Novel anti-CVB-5, anti-RSV and anti-Sb-1 agents. *Bioorganic Medicinal Chemistry*, 22(17): 4893-4909. <https://doi.org/10.1016/j.bmc.2014.06.043>



## *In silico* analysis of IL7RA missense mutations in lung, breast and skin cancers

Zeynep Tokcaer Keskin<sup>1,2,3</sup>

<sup>1</sup>Department of Molecular Biology and Genetics, Faculty of Engineering and Natural Sciences, Acibadem Mehmet Ali Aydınlar University, Istanbul, TÜRKİYE

<sup>2</sup>Department of Molecular Biology and Genetics, Institute of Natural and Applied Sciences, Acibadem Mehmet Ali Aydınlar University, Istanbul, TÜRKİYE

<sup>3</sup>Department of Molecular and Translational Biomedicine, Institute of Natural and Applied Sciences, Acibadem Mehmet Ali Aydınlar University, Istanbul, TÜRKİYE

e-mail: [zeynep.keskin@acibadem.edu.tr](mailto:zeynep.keskin@acibadem.edu.tr), ORCID: 0000-0001-7678-0590

### Cite this article as:

Tokcaer Keskin Z. 2025. *In silico* analysis of IL7RA missense mutations in lung, breast and skin cancers. *Trakya Univ J Nat Sci*, 26(1): 9-17, DOI: 10.23902/trkjinat.1545678

Received: 09 September 2024, Accepted: 02 January 2025, Online First: 11 February 2025, Published: 15 April 2025

**Abstract:** Interleukin 7 (IL7)-Interleukin 7 Receptor Alpha (IL7RA) signaling is well investigated in hematological cancers, but in solid cancers, its role needs to be investigated further. In a recent study, IL7R was identified as a key gene in leptomeningeal carcinoma. Unfortunately, there is limited patient data on leptomeningeal carcinoma from breast, lung and skin cancers. In this study, IL7RA missense mutations that could have pathologic importance in lung, breast and skin cancers were analyzed *in silico*. Using Genomic Data Commons (GDC) data portal, lung, breast and melanoma data from 3250 patients were filtered to list IL7RA missense mutations. Sorting Intolerant From Tolerant (SIFT), Polymorphism Phenotyping v2 (PolyPhen2), Universal Mutation Database Predictor (UMD-Predictor) and Single Nucleotide Polymorphisms & Gene Ontology (E-SNP&GO) servers were employed to reveal pathogenic variants. Conservation Surface Mapping (ConSurf) was used to analyze conservation scores. Domains were investigated by InterPro tool. Molecular docking of IL7-IL7RA was performed by ClusPro, Mutational Binding free energy change predictor 2 (Mutabind2) and Protein-Ligand Interaction Profiler (PLIP) servers. Stability of the mutations were analyzed by Impact-Mutant 2.0 (I-Mutant2), Mutation Protein Stability Prediction (MUpro) and Impact of Non-synonymous mutations on Protein Stability Multi Dimension (INPS-MD). Structural changes were determined using Dynamic Mutation predictor 2 (DynaMut2) and Have (y)Our Protein Explained (HOPE) servers. Out of 99 missense mutations identified, 6 (T56P, C57Y, K204I, S207F, G215V and W217C) were defined as pathogenic. All these mutations were primarily found in lung cancer and located in the extracellular domain of IL7RA. Although none were in the interaction interface of IL7, all were located at or next to conserved motifs. This proximity likely destabilizes IL7RA and drastically changes its bonding patterns. The IL7RA missense mutations may have a significant role in lung cancer, as they presumably change the protein's function.

### Edited by:

Melike Sapmaz Metin

### Key words:

Interleukin 7 Receptor Alpha

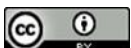
Missense mutation

Lung cancer

Computational biology

*In silico* simulation

**Özet:** İnterlökin 7 (IL7)-İnterlökin 7 Reseptör Alfa (IL7RA) sinyali hematolojik kanserlerde iyi araştırılmış, ancak, solid kanserlerdeki rolünün daha fazla araştırılması gerekmektedir. Son yapılan bir çalışmada, IL7R leptomeningeal karsinomda anahtar gen olarak tanımlanmıştır. Meme, akciğer ve deri kanserlerinden kaynaklanan leptomeningeal karsinomda, ne yazık ki sınırlı sayıda hasta verisi bulunmaktadır. Bu çalışmada, akciğer, meme ve deri kanserlerinde patolojik öneme sahip olabilecek IL7RA yanlış anlamalı mutasyonları bilgisayarlı olarak analiz edildi. GDC veri portalı kullanılarak, 3250 hastadan alınan akciğer, meme ve deri kanseri verileri filtrelenerek IL7RA yanlış anlamalı mutasyonları listelendi. Patojenik varyantları ortaya çıkarmak için Sorting Intolerant From Tolerant (SIFT), Polymorphism Phenotyping v2 (PolyPhen2), Universal Mutation Database Predictor (UMD-Predictor) ve Single Nucleotide Polymorphisms & Gene Ontology (E-SNP&GO) sunucuları kullanıldı. Korunma puanları analiz etmek için Conservation Surface Mapping (ConSurf) kullanıldı. Domain adları InterPro aracılığıyla araştırıldı. IL7-IL7RA'nın moleküler yerleştirilmesi ClusPro, Mutational Binding free energy change predictor 2 (Mutabind2) ve Protein-Ligand Interaction Profiler (PLIP) sunucuları tarafından gerçekleştirildi. Mutasyonların stabilitesi Impact-Mutant 2.0 (I-Mutant2), Mutation Protein Stability



OPEN ACCESS

Prediction (MUPro) ve Impact of Non-synonymous mutations on Protein Stability-Multi Dimension (INPS-MD) ile analiz edildi. Yapısal değişiklikler Dynamic Mutation predictor 2 (DynaMut2) ve Have (y)Our Protein Explained (HOPE) sunucuları kullanılarak belirlendi. Tanımlanan 99 yanlış anlamlı mutasyondan 6'sı (T56P, C57Y, K204I, S207F, G215V ve W217C) patojenik olarak belirlendi. Tüm mutasyonların öncelikli olarak akciğer kanserinde bulunduğu ve IL7RA'nın ekstraselüler alanında yerleştiği tespit edildi. Her ne kadar hiçbiri IL7 etkileşiminin ara yüzünde olmasa da, hepsi korunmuş motiflerin yanında veya yakınında konumlanmışlardı. Bu yakınlık IL7RA'yı istikrarsızlaştırmakta ve bağlanma paternini büyük ölçüde değiştirmektedir. IL7RA yanlış anlamlı mutasyonları muhtemelen proteinin işlevini değiştirdiği için akciğer kanserinde önemli bir role sahip olabilir.

## Introduction

Interleukin 7 (IL7) and IL7 Receptor Alpha (IL7RA) signaling is a widely studied pathway, whose role has been extensively defined in B and T cell development and differentiation (Mazzucchelli & Durum 2007, Winer *et al.* 2022). The signaling of IL7 starts upon binding to IL7RA extracellular domain. The receptor heterodimerization occurs after this binding and triggers the phosphorylation of cytoplasmic tyrosine residue on the IL7RA. This phosphorylation activates the Janus kinase/signal transducers and activators of transcription (JAK-STAT) signaling and results in cell survival and proliferation (Barros *et al.* 2021, Winer *et al.* 2022).

The signaling of IL7 is controlled through receptors as IL7 has constitutive expression. One of the control mechanisms is via receptor shedding and converting the membrane bound IL7RA into soluble IL7RA (sIL7RA) (Vranjkovic *et al.* 2007, Lundström *et al.* 2013). Another control mechanism is alternative splicing of the receptor transcript to generate the sIL7RA. The soluble version of the receptor competes with the membrane bound one for IL7 and reduces the amount of ligand that binds to it. However, sIL7RA suppresses the expression of negative controllers of the IL7 signaling and increases the bioactivity via membrane bound IL7RA (Vranjkovic *et al.* 2007, Mazzucchelli *et al.* 2012, Lundström *et al.* 2013, Barros *et al.* 2021, Wang *et al.* 2022).

There are many mutations of IL7RA causing different pathologies, of which those causing immunodeficiency and autoimmune diseases are well defined (Puel *et al.* 1998, Mazzucchelli *et al.* 2012, Campos *et al.* 2019, Yan *et al.* 2023). Alterations causing leukemia were also reported in many studies (Kim *et al.* 2013, Barata *et al.* 2019). In solid cancers, the effect of IL7 - IL7RA signaling was mostly investigated from the perspective of immune cell filtration or tumor microenvironment (Caushi *et al.* 2021, Wang *et al.* 2022). However, it is reported in the human protein atlas (proteinatlas.org) that tissues like the lung, breast, small intestine, skin and more also express IL7RA and studies reported the expression of the receptor in different cancer cell lines (Cosenza *et al.* 2002). One such study reported that in lung adenocarcinoma cell lines, IL7RA expression was significantly lower when compared with normal lung cell line (Wang *et al.* 2022). Although the expression was documented, there are few studies investigating the effects of IL7RA missense mutations in the context of solid tumors. One such study reported 3 intronic and 2 3'UTR variants in the Chinese-Han population increasing breast cancer susceptibility (Wang *et al.* 2020). Similarly,

T244I mutation was reported for susceptibility to breast cancer (Vitiello *et al.* 2018).

IL7R was reported as an important gene in brain metastasis from non-small cell lung cancer (Zu *et al.* 2023). In accordance with this finding, we have recently reported IL7R as an important role player in leptomeningeal carcinoma (Congur *et al.* 2023). This type of cancer is a metastatic form of lung, breast and skin cancer which localizes to the meninges of the brain. The patients after this metastasis unfortunately have a very short lifespan. That is why more investigation is required to understand this type of metastasis for developing better or targeted medications. The main focus of this study is to define and understand the effects of missense mutations of IL7RA in lung, breast and skin cancers by employing computational methods.

## Materials and Methods

### Data retrieval

The mutations of IL7R were retrieved from the National Institutes of Health Genomics Data Commons (GDC) Data Portal (<https://portal.gdc.cancer.gov>). The portal's last update was on March 29, 2024 at the time of the last analysis (July 4, 2024). Under the tab Cohort Builder, primary sites lung and bronchus, breast and skin were selected for analysis. Within the selected cohort, mutations of IL7R were searched by using mutation frequency app tool under the analysis tab. Then the mutations listed were filtered to show missense mutations.

### Mutation analysis

The pathogenicity of the mutations were analyzed by Sorting Intolerant From Tolerant (SIFT) (<https://sift.bii.a-star.edu.sg>) (Sim *et al.* 2012), Polymorphism Phenotyping v2 (PolyPhen2) (<http://genetics.bwh.harvard.edu/pph2/>) (Adzhubei *et al.* 2010), Universal Mutation Database Predictor (UMD-Predictor) (<https://umd-predictor.genomnis.com/mutation>) (Salgado *et al.* 2016) and Single Nucleotide Polymorphisms & Gene Ontology (E-SNP&GO) (<https://esnpsandgo.biocomp.unibo.it/>) (Manfredi *et al.* 2022) mutation analysis servers. UMD-Predictor was chosen considering it has high sensitivity (0.95) and accuracy (0.85) when compared with the tools available (Salgado *et al.* 2016). Similarly, E-SNP&GO determines the pathogenicity of the mutation, employing Gene Ontology (GO) functional annotations and has high precision (85.7%) when compared with the other methods (Manfredi *et al.* 2022). FASTA file of the protein sequence used in these tools listed above was obtained from Universal Protein Resource (UniProt) ID: P16871-1 and

the corresponding Ensembl ID ENST00000303115 was used in UMD-Predictor. The conservation analysis was performed by Conservation Surface Mapping (ConSurf) ([https://consurf.tau.ac.il/consurf\\_index.php](https://consurf.tau.ac.il/consurf_index.php)) (Ashkenazy *et al.* 2016) by using the UniProt ID: P16871. Disease association of the mutations was investigated by Clinical Variation (ClinVar) (<https://www.ncbi.nlm.nih.gov/clinvar/>).

#### Domain, Docking and Stability analysis

The domains where the mutations are located were analyzed by InterPro (<https://www.ebi.ac.uk/interpro/>) (Paysan-Lafosse *et al.* 2023). The stability of the mutated receptor was analyzed by using Impact-Mutant 2.0 (I-Mutant2) (<https://folding.biofold.org/cgi-bin/i-mutant2.0.cgi>) (Capriotti *et al.* 2005), Mutation Protein Stability Prediction (MUPRO) (<https://mupro.proteomics.ics.uci.edu/>) (Cheng *et al.* 2006) and Impact of Non-synonymous mutations on Protein Stability-Multi Dimension (INPS-MD) sequence based (<https://inps.biocomp.unibo.it/welcome/default/index>) (Fariselli *et al.* 2015) servers. The FASTA sequence of IL7RA protein was retrieved from UniProt ID: P16871.

For the docking of the IL7 to the mutated IL7RA, Cluspro (<https://cluspro.org/>) (Kozakov *et al.* 2013, Vajda *et al.* 2017, Kozakov *et al.* 2017, Desta *et al.* 2020), Mutational Binding free energy change predictor 2 (Mutabind2) (<https://lilab.jysw.suda.edu.cn/research/mutabind2/>) (Zhang *et al.* 2020) and Protein-Ligand Interaction Profiler (PLIP) (<https://plip-tool.biotec.tu-dresden.de/plip-web/plip/index>) servers (Salentin *et al.* 2015) were used. For the structural comparison analysis of wild type vs mutant receptors Dynamic Mutation predictor 2 (DynaMut2) (<https://biosig.lab.uq.edu.au/dynamut2/>, Pearson's correlation value 0.72) (Rodrigues *et al.* 2021) and Have (y)Our Protein Explained (HOPE) (<https://www3.cmbi.umcn.nl/hope/>) (Venselaar *et al.* 2010) servers were employed. The Protein Data Bank (PDB) files used in these analyses were obtained from UniProt available under the codes 7OPB, 3DI2, 3DI3 and 3UP1.

## Results

#### Data Mining and Evaluation of the Pathogenicity Risks

In GDC Data portal the primary sites lung and bronchus, breast and skin revealed 10382 cases. Among these cases 169 IL7RA somatic mutations were reported. Upon filtering for missense only mutations, 102 missense variants were listed, 2 of these mutations were synonymous and 1 was at the splice site. These 3 mutations were excluded and the pathogenicity risk analysis was performed over the remaining 99 mutations. (Supplementary Material 1).

Pathogenicity risks were computed by using SIFT and 40 of the mutations were found to be deleterious. Then these 40 mutations were further analyzed by PolyPhen2 tool which reduced the list to 24. These 24 mutations

annotated as “probably damaging” by PolyPhen2 were then run in UMD-Predictor and E-SNP&GO tools. UMD-Predictor scores the mutations for their pathogenicity over 100 where over 75 is categorized as pathogenic. Among these 24 variants 18 were found to be pathogenic and 11 variants were scored 100 for pathogenicity in UMD-Predictor (Supplementary Material 2). The variants that scored 100 were chosen. In E-SNP&GO the mutations were given a pathogenicity probability score over 1 annotating them as pathogenic or benign. Moreover, a reliability index over 9 was determined for the prediction of each variant, indicating 9 as the most reliable. For this purpose, upon the computation of E-SNP&GO tool, the mutations annotated as pathogenic which have a reliability score of 9 were chosen. 8 of the missense mutations were found to be reliably pathogenic according to this tool. As a result, the list of missense mutations was refined to 6 which were annotated as pathogenic in all 4 servers. These mutations were T56P, C57Y, K204I, S207F, G215V and W217C (Table 1).

#### Positions and Conservation Status of 6 Missense Mutations

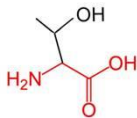
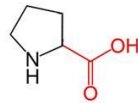
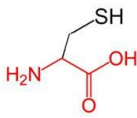
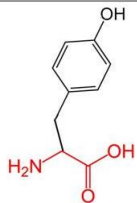
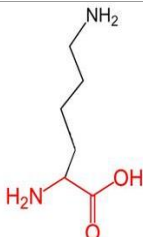
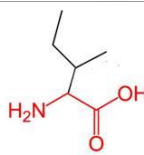
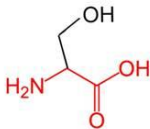
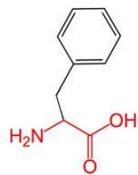
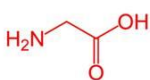
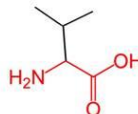
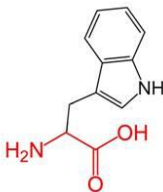
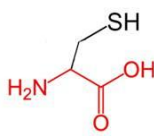
IL7RA missense mutations listed in Table 1 were further investigated in ClinVar. Except from G215V mutation, none of the others (T56P, C57Y, K204I, S207F, W217C) were reported in ClinVar. G215V variant was reported as likely pathogenic and was associated with immunodeficiency. The mutations were searched in GDC Data Portal specifically and 5 of the mutations, T56P, C57Y, S207F, G215V and W217C were detected in lung and bronchus but K204I variant was detected at skin as primary site. In this short list, no mutation was associated with breast cancer.

The 6 missense mutations were further analyzed according to the positions of the amino acids by using InterPro server (Supplementary Material 3). Interestingly all these mutations were located at the extracellular domain. T56P, C57Y were located at FN3\_7 domain specifically found in IL7RA (IL-7Ralpha, fibronectin type III domain). K204I, S207F, G215V and W217C were found in fibronectin type III (FN3) domain of IL7RA. Moreover, using Conservation Surface Mapping (ConSurf) tool the conservation scores of each amino acid at the IL7RA protein sequence were detected (Supplementary Material 4). The scoring ranges between 1-9, 9 being the most conserved. Regarding this tool, all the mutations were at conserved amino acids where for 5 of them (C57, K204, S207, G215 and W217), the score was 9 and T56 had a score of 7 (Table 2).

#### Comparing the Stability of the IL7RA mutants with the wild type

Since the ConSurf analysis revealed that the mutations were at conserved amino acids, the stability of the mutant proteins was investigated by using different tools (Table 3). When I-Mutant 2 tool was used, T56P, C57Y, K204I, G215V and W217C were found to decrease the stability of the protein while S207F alteration increased the stability.

**Table 1.** IL7RA mutations analyzed as pathogenic by 4 different tools.

Mutation	Wild type amino acid	Mutant amino acid
<b>T56P</b> (Thr56Pro)		
<b>C57Y</b> (Cys57Tyr)		
<b>K204I</b> (Lys204Ile)		
<b>S207F</b> (Ser207Phe)		
<b>G215V</b> (Gly215Val)		
<b>W217C</b> (Trp217Cys)		

**Table 2.** ConSurf conservation scores of the wild type IL7RA amino acids at the mutated sites.

AMINO ACID POSITION	T56 (THR56)	C57 (CYS57)	K204 (LYS204)	S207 (SER207)	G215 (GLY215)	W217 (TRP217)
SCORE	7	9	9	9	9	9

**Table 3.** Stability and  $\Delta\Delta G$  of the IL7RA mutants compared to wild type.

	T56P (Thr56Pro)	C57Y (Cys57Tyr)	K204I (Lys204Ile)	S207F (Ser207Phe)	G215V (Gly215Val)	W217C (Trp217Cys)
<b>I-Mutant2 (Stability)</b>	Decrease	Decrease	Decrease	Increase	Decrease	Decrease
<b>MUpro (Stability)</b>	Decrease	Decrease	Decrease	Decrease	Decrease	Decrease
<b>INPS-MD <math>\Delta\Delta G</math> (kcal/mol)</b>	-1.19	-2.06	0.56	-0.32	-1.71	-1.62



However, this latter change had a reliability index of 4 which was the lowest value among all 6 mutations tested. In addition to I-Mutant 2, the stabilities of the mutants were also investigated by MUPRO tool. MUPRO calculated the stability of all mutants as decreasing. These two algorithms were in consensus about the decreasing stability of all mutants except S207F. Additionally, the  $\Delta\Delta G$  (kcal/mol) scores of the mutated proteins were calculated with INPS-MD server by using the sequence as an input. The energy scores were negative for T56P, C57Y, S207F, G215V and W217C but positive for K204I. These algorithms calculate the free energy from folded structure towards unfolded structure (Pancotti *et al.* 2022, Benevenuta *et al.* 2023). In accordance with these results, most of the mutations might have a destabilizing effect on IL7RA.

#### Structural comparison of the IL7RA mutants with the wild type

After analyzing the stability of the mutations, the docking of IL7 was performed by using ClusPro,

Mutabind and PLIP tools, with PDB files obtained from UniProt. 3DI2, 3DI3 and 3UP1 files were analyzed in all 3 tools. 3DI2 and 3DI3 files contained, IL7 and IL7RA structural information, whereas 3UP1 file has the IL7RA homodimer interaction of the extracellular domain. However, although all the mutations were at the extracellular compartment of IL7RA, they were not at the IL7 or IL7RA interaction interface. Therefore, the structural comparison of the wild type versus mutant IL7RA was analyzed for each 6 of the mutations by both HOPE and DynaMut2 servers. These tools after computing the mutation, give graphical outputs of the mutated region of the protein by comparing mutated with the wild type. All 6 variants were analyzed in both tools. HOPE server requests UniProt ID as an input and recognizes the PDB file 7OPB, while DynaMut2 requires the PDB file of choice as an input. 7OPB file was used to standardize the PDB input and the visual figures were presented as the outputs of DynaMut2.

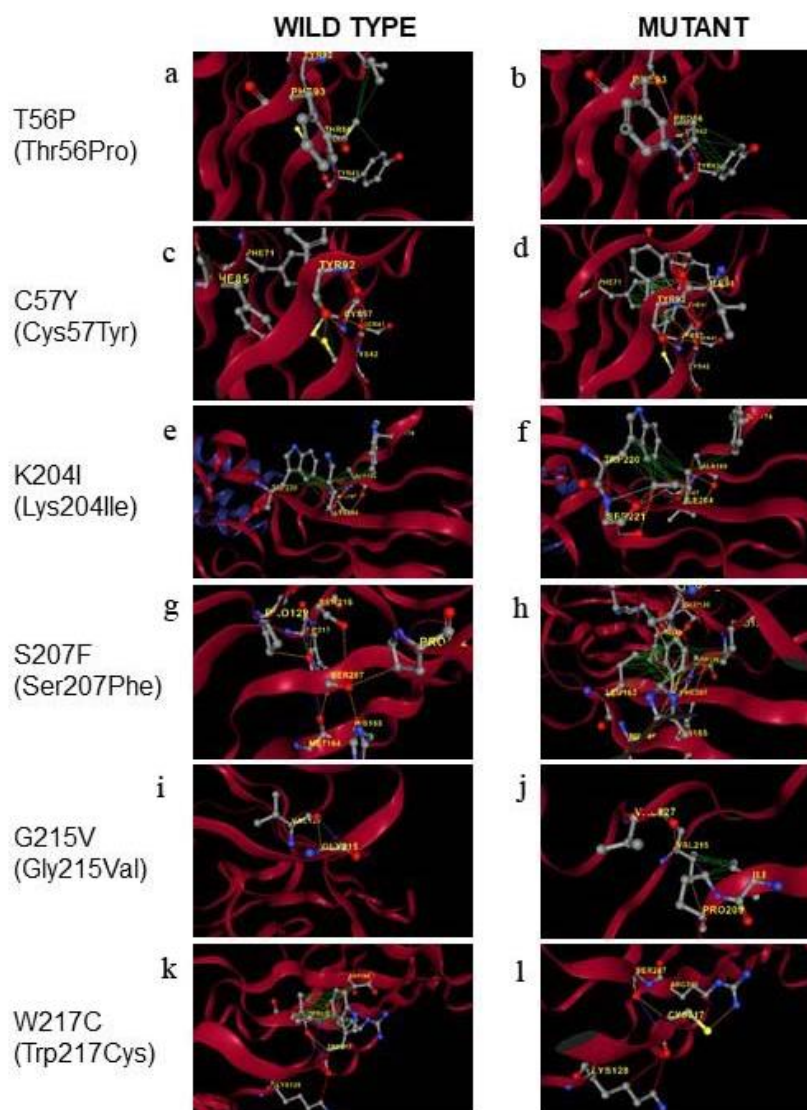


**Fig. 1.** Wild type versus mutant IL7RA structures executed by the DynaMut2 server. The differences were plotted by choosing single mutation analysis type. The colors of the interactions were annotated by the server as: light blue - Van der Waals attractions, green - hydrophobic bonds, red - hydrogen bonds, yellow - ionic bonds, light green - aromatic interactions, orange - polar bonds.

When each mutation was compared relative to its wild type, all mutations were found to disturb the sequence of FN3 domain, which was already confirmed by InterPro server. C57T mutation replaces cysteine, a small and –S containing amino acid, with a non –S and big amino acid, tyrosine, which also contains a ring. The cysteine at this position is associated with a sulfide bridge occurring between 2 cysteines (Campos *et al.* 2019) and this bridge should be lost at mutant protein, which probably would cause destabilization of IL7RA. Besides, the hydrophobicity of the wild type and mutant residues would be different affecting the hydrophobic interactions of the core protein. Tyrosine is a bigger amino acid by size, and it would not completely fit in the place of cysteine as well. As a result, the cysteine that is buried in wild type protein when altered into a tyrosine was assumed to be in a more exposed position (Fig. 1a-b).

Similar to C57T mutation T56P mutation is just before the cysteine bridge and it is also introducing a ring structure. Proline is known to be present more in beta turns and not compatible with beta strands (Li *et al.* 1996, Mir *et al.* 2023). Consequently, this structure change could disturb both the –S bridge and the beta sheet configurations in the wild type protein. Furthermore, their hydrophobicity differences would change hydrogen bonds in the core IL7RA protein disturbing the correct folding (Fig. 1c-d).

Mutation K204I was found to replace a positively charged amino acid, lysine with a neutral isoleucine. This change would be associated with the disruption of the salt bridge between lysine and glutamic acid at position 202 according to HOPE server. This charge change would affect the internal and external interactions of the receptor (Fig. 1e-f).

Variant S207F also introduced a ring structure to the IL7RA, changing the hydrogen bonds that were established in the wild type receptor. This assumption is also supported by the change in the hydrophobicity of the wild type amino acid. Moreover, serine in this position bears a buried confirmation while the mutant amino acid phenylalanine, would be exposed for being bigger than the wild type (Fig. 1g-h).

Glycine is a flexible amino acid (Senthil *et al.* 2019). G215V mutation for that reason could affect the flexibility of IL7RA protein which could cause functional changes. Additionally, the sizes of glycine in wild type and valine in the mutant differ and would result in an exposed amino acid in the backbone (Fig. 1i-j).

The last mutation W217C is located in a WSXWS motif. This motif is important for the receptor activation of the cytokine receptors (Campos *et al.* 2019). The mutant protein would have a disrupted motif and although the residue is not in the interface of IL7-IL7RA interaction, it could possibly affect the ligand receptor contacts by causing a change in the neighboring interactions (Fig. 1k-l).

## Discussion

IL7RA mutations were extensively studied in leukemia, T and B cell development. It is found both as homodimer and heterodimer but the dimerization depends on the type of the ligand bound (Mazzucchelli & Durum 2007, Winer *et al.* 2022). In our recent study, IL7R was proposed as one of the genes that could be important in leptomeningeal carcinoma (Congur *et al.* 2023). However, there are limited number of patient data on leptomeningeal carcinoma which is a deadly metastatic form of mostly breast, lung and skin cancers. Specifically, IL7RA downregulation was reported in lung cancer (Wang *et al.* 2022). Moreover, in non-small cell lung cancer, the knockdown of IL7RA leads to overexpression of multidrug resistance (Ke *et al.* 2019). However, the missense mutations were not very well investigated in these solid cancers. Therefore, a cohort of lung, breast and skin cancer as a primary site was selected to analyze the effects of mutations in IL7RA computationally.

In this study, 99 missense mutations from a cohort of 3250 patients were analyzed by 4 different servers (SIFT, PolyPhen2, UMD-Predictor and E-SNP&GO) to identify the pathogenic variants. SIFT and PolyPhen2 are widely employed servers which detect the pathogenicity score depending on the conservation of the amino acid between different species. UMD-Predictor uses the transcript information instead of the protein sequence as an input, but compares the conservation scores by taking biochemical properties of the proteins and the changes to the transcript into account. As a result of all these combined matrices, the server determines the pathogenicity score of the mutation. Suybeng *et al.* (2020) compared several different variant prediction tools and reported UMD-Predictor as the most accurate one among the tested. However, E-SNP&GO was developed in 2022 as another tool which also determines the pathogenicity by using the gene ontology annotations. As all these tools use different approaches for determining the pathogenicity, the list of missense mutations were analyzed sequentially in all 4 servers. Finally, the intersecting missense variants T56P, C57Y, K204I, S207F, G215V and W217C were selected for further investigation. Although all the tools used involved the conservation value for determining the pathogenicity, the conservation of the wild type residues were also checked by ConSurf tool as well to confirm the conservation of these residues one more time.

It was very interesting to see that all mutations were in the extracellular domain and were mostly very closely located to each other. IL7RA had 2 different fibronectin domains, FN3\_7 and FN3. Both domains are very important for the functioning of the IL7RA. These domains contain 2 important structural elements crucial for the normal folding and performance of the protein, disulfide bridge regions and WSXWS motifs (McElroy *et al.* 2009, Campos *et al.* 2019). C57Y, K204I and W217C variants are therefore directly related to the

proper formation of the IL7RA as they reside in these regions. The fibronectin domains as reported before have conserved beta strands in their structures (McElroy *et al.* 2009). C57Y alteration corresponds to one of the disulfide bonds, as a result probably disrupting the correct folding and beta strand configuration of the FN3\_7 domain. Similarly, K204I and W217C mutations were located at the WSXWS region of the IL7RA which is known as a conserved sequence for type I cytokine receptors (McElroy *et al.* 2009, Campos *et al.* 2019). Both variants replace the wild type amino acid in such a way that the bonding property of the region drastically changes. Although WSXWS motif is outside of the contact region of the ligand, this sequence was reported to be important for the correct folding of IL7RA which brings the receptor to a structure enabling IL7 binding (McElroy *et al.* 2009). Another mutation, W217X (rs104893893), was previously reported in ClinVar and was associated with immunodeficiency. This mutation was generating a stop codon with a G>A mutation and causing early termination. Whereas W217C mutation is G>T and not reported in ClinVar. A recent study performed with HEK293 cells indicated that cysteine tRNAs when overexpressed could act like a stop codon read-through (Valášek *et al.* 2023). Although this mutation does not replace a stop codon still it raises a possibility that the variant could have other consequences in IL7RA functions or expression that could be enlightened by further research studies.

Besides changing the intra bonding of the amino acids, these 6 mutations have a tendency towards an unfolded state energetically. This tendency presents a destabilized condition (Pancotti *et al.* 2022), that could possibly be interpreted by degradation or aggregation of the unfunctional receptor. Almost all these 6 mutations listed in this study were significantly changing the bonding, hence the folding of the protein. It was also proposed that the IL7RA on tumor cells could be a good prognosis marker for the capacity to regulate immune cell infiltration (Wang *et al.* 2022). Therefore, the structural integrity of IL7RA probably evokes a pivotal role for the survival of the cancer cell.

On the other hand, sequence-wise all 6 mutations are not a part of exon 6 and exon 6 skipping generates the soluble IL7RA (sIL7RA) (Barros *et al.* 2021). The soluble receptor competes with the membrane bound receptor for IL7. The decrease in IL7 concentration however can increase the bioactivity of the cytokine. Moreover, sIL7RA also suppresses the negative regulation of IL7 (Lundström *et al.* 2013, Barros *et al.* 2021). If any of these mutations do increase the contact time of IL7 with IL7R, then it is possible that the proliferative signal through JAK-STAT pathway could be enhanced. Increased proliferation could also contribute to the aggressiveness of the tumor. On the other hand, it was also demonstrated that IL7 binding to IL7RA could trigger membrane shedding and

desensitize the cell to IL7 signal (Vranjkovic *et al.* 2007). These mutations could reduce the shedding of the receptor keeping it active with a prolonged signal. Accordingly, the conformational changes that occur due to these missense mutations could have multiple different consequences.

The limitation of this current study is that the sequenced tumor tissue could also have immune cells infiltrated into the tissue. The consequence of tissue sequencing is not discriminating between different cell types in a heterogeneous tumor microenvironment. The second setback is the cohort of 3250 patients whose missense mutation list was obtained. If the number increases more potent mutations could be discovered. Moreover, all these mutations are found in 1 patient indicating that they are not hotspot mutations, which could also be the result of the limited patient number. Accordingly, with all the limitations of this study, the effect of the mutations should be validated before their pathogenicity is attributed to any solid cancer. To understand the nature of these mutations, it is necessary to perform fully controlled *in vitro* and *in vivo* experiments. In these experiments the potent mutations discovered with this research could be introduced into lung adenocarcinoma cell lines and the effects of the mutations could be investigated. Moreover, their tumorigenicity and metastatic capacities could be assessed with *in vivo* experiments. The results of this *in silico* study will help limit the number of mutations to be investigated by reverse genetics strategies.

## Conclusion

In this study the missense mutations of IL7RA were investigated and 6 mutations, T56P, C57Y, K204I, S207F, G215V and W217C were evaluated as pathogenic. These mutations were found to affect the structure of IL7RA by drastically changing the confirmation. The confirmation changes occur in important motifs of the protein and they could possibly cause a change in the proper functioning of the IL7RA. Understanding the molecular biology of such mutations with further *in vitro* and *in vivo* studies could elevate our understanding of IL7 signaling in solid cancers.

**Ethics Committee Approval:** Since the article does not contain any studies with human or animal subject, its approval to the ethics committee was not required.

**Data Sharing Statement:** All data are available within the study.

**Conflict of Interest:** The authors have no conflicts of interest to declare.

**Funding:** The author declared that this study has received no financial support.

## References

- Adzhubei, I.A., Schmidt, S., Peshkin, L., Ramensky, V.E., Gerasimova, A., Bork, P., Kondrashov, A.S. & Sunyaev, S.R. 2010. A method and server for predicting damaging missense mutations. *Nature Methods*, 7(4): 248-249. <https://doi.org/10.1038/nmeth0410-248>
- Ashkenazy, H., Abadi, S., Martz, E., Chay, O., Mayrose, I., Pupko, T. & Ben-Tal, N. 2016. ConSurf 2016: an improved methodology to estimate and visualize evolutionary conservation in macromolecules. *Nucleic Acids Research*, 44(W1): W344-50. <https://doi.org/10.1093/nar/gkw408>
- Barata, J.T., Durum, S.K. & Seddon, B. 2019. Flip the coin: IL-7 and IL-7R in health and disease. *Nature Immunology*, 20(12): 1584-1593. <https://doi.org/10.1038/s41590-019-0479-x>
- Barros, P.O., Berthoud, T.K., Aloufi, N. & Angel, J.B. 2021. Soluble IL-7R $\alpha$ /sCD127 in Health, Disease, and Its Potential Role as a Therapeutic Agent. *Immunotargets and Therapy*, 10: 47-62. <https://doi.org/10.2147/ITT.S264149>
- Benevenuta, S., Birolo, G., Sanavia, T., Capriotti, E. & Fariselli, P. 2023. Challenges in predicting stabilizing variations: An exploration. *Frontiers in Molecular Biosciences*, 9: 1075570. <https://doi.org/10.3389/fmolb.2022.1075570>
- Campos, L.W., Pissinato, L.G. & Yunes, J.A. 2019. Deleterious and Oncogenic Mutations in the IL7RA. *Cancers* (Basel). 11(12): 1952. <https://doi.org/10.3390/cancers11121952>
- Capriotti, E., Fariselli, P. & Casadio, R. 2005. I-Mutant2.0: predicting stability changes upon mutation from the protein sequence or structure. *Nucleic Acids Research*, 33(Web Server issue): W306-310. <https://doi.org/10.1093/nar/gki375>
- Caushi, J.X., Zhang, J., Ji, Z., Vaghasia, A., Zhang, B., Hsiue, E.H., Mog, B.J., Hou, W., Justesen, S., Blosser, R., Tam, A., Anagnostou, V., Cottrell, T.R., Guo, H., Chan, H.Y., Singh, D., Thapa S, Dykema, A.G., Burman, P., Choudhury, B., Aparicio, L., Cheung, L.S., Lanis, M., Belcaid, Z., El Asmar, M., Illei, P.B., Wang, R., Meyers, J., Schuebel, K., Gupta, A., Skaist A., Wheelan, S., Naidoo, J., Marrone, K.A., Brock, M., Ha J., Bush, E.L., Park, B.J., Bott, M., Jones, D.R., Reuss, J.E., Velculescu, V.E., Chافت, J.E., Kinzler, K.W., Zhou, S., Vogelstein, B., Taube J.M., Hellmann, M.D., Brahmer, J.R., Merghoub, T., Forde, P.M., Yegnasubramanian, S., Ji, H., Pardoll, D.M. & Smith, K.N. 2021. Transcriptional programs of neoantigen-specific TIL in anti-PD-1-treated lung cancers. *Nature*, 596(7870): 126-132. <https://doi.org/10.1038/s41586-021-03752-4>
- Cheng, J., Randall, A. & Baldi, P. 2006. Prediction of protein stability changes for single-site mutations using support vector machines. *Proteins*, 62(4): 1125-32. <https://doi.org/10.1002/prot.20810>
- Congur, I., Koni, E., Onat, O.E. & Tokcaer Keskin, Z. 2023. Meta-analysis of commonly mutated genes in leptomeningeal carcinomatosis. *PeerJ*. 11: e15250. <https://doi.org/10.7717/peerj.15250>
- Cosenza, L., Gorgun, G., Urbano, A. & Foss, F. 2002. Interleukin-7 receptor expression and activation in nonhaematopoietic neoplastic cell lines. *Cell Signal*, 14(4): 317-25. [https://doi.org/10.1016/S0898-6568\(01\)00245-5](https://doi.org/10.1016/S0898-6568(01)00245-5)
- Desta, I.T., Porter, K.A., Xia, B., Kozakov, D. & Vajda, S. 2020. Performance and its limits in rigid body protein-protein docking. *Structure*, 28(9): 1071-1081.e3. <https://doi.org/10.1016/j.str.2020.06.006>
- Fariselli, P., Martelli, P.L., Savojardo, C. & Casadio, R. 2015. INPS: predicting the impact of non-synonymous variations on protein stability from sequence. *Bioinformatics*, 31(17): 2816-2821. <https://doi.org/10.1093/bioinformatics/btv291>
- Ke, B., Wei, T., Huang, Y., Gong, Y., Wu, G., Liu, J., Chen, X. & Shi, L. 2019. Interleukin-7 resensitizes non-small-cell lung cancer to cisplatin via inhibition of ABCG2. *Mediators of Inflammation*. 2019: 7241418. <https://doi.org/10.1155/2019/7241418>
- Kim, M.S., Chung, N.G., Kim, M.S., Yoo, N.J. & Lee, S.H. 2013. Somatic mutation of IL7R exon 6 in acute leukemias and solid cancers. *Human Pathology*, 44(4): 551-555. <https://doi.org/10.1016/j.humpath.2012.06.017>
- Kozakov, D., Beglov, D., Bohnuud, T., Mottarella, S.E., Xia, B., Hall, D.R. & Vajda, S. 2013. How good is automated protein docking? *Proteins*, 81(12): 2159-2166. <https://doi.org/10.1002/prot.24403>
- Kozakov, D., Hall, D.R., Xia, B., Porter, K.A., Padhorny, D., Yueh, C., Beglov, D. & Vajda, S. 2017. The ClusPro web server for protein-protein docking. *Nature Protocols*, 12(2): 255-278. <https://doi.org/10.1038/nprot.2016.169>
- Li, S.C., Goto, N.K., Williams, K.A. & Deber, C.M. 1996. Alpha-helical, but not beta-sheet, propensity of proline is determined by peptide environment. *Proceedings of the National Academy of Sciences U S A*, 93(13): 6676-81. <https://doi.org/10.1073/pnas.93.13.6676>
- Lundström, W., Highfill, S., Walsh, S.T., Beq, S., Morse, E., Kockum, I., Alfredsson, L., Olsson, T., Hillert, J. & Mackall, C.L. 2013. Soluble IL7R $\alpha$  potentiates IL-7 bioactivity and promotes autoimmunity. *Proceedings of the National Academy of Sciences U S A*, 110(19): E1761-70. <https://doi.org/10.1073/pnas.1222303110>
- Manfredi, M., Savojardo, C., Martelli, P.L. & Casadio, R. 2022. E-SNPs&GO: embedding of protein sequence and function improves the annotation of human pathogenic variants. *Bioinformatics*, 38(23): 5168-5174. <https://doi.org/10.1093/bioinformatics/btac678>
- Mazzucchelli, R. & Durum, S.K. 2007. Interleukin-7 receptor expression: intelligent design. *Nature Reviews Immunology*, 7(2): 144-154. <https://doi.org/10.1038/nri2023>
- Mazzucchelli, R.I., Riva, A. & Durum, S.K. 2012. The human IL-7 receptor gene: deletions, polymorphisms and mutations. *Seminars in Immunology*, 24(3): 225-30. <https://doi.org/10.1016/j.smim.2012.02.007>
- McElroy, C.A., Dohm, J.A., Walsh, S.T. 2009. Structural and biophysical studies of the human IL-7/IL-7R $\alpha$  complex. *Structure*, 17(1): 54-65. <https://doi.org/10.1016/j.str.2008.10.019>



24. Mir, R.A., Shafi, S.M. & Zargar, S.M. 2023. Chapter 1 - Understanding the OMICS techniques: an introduction to genomics and proteomics. pp 1-28. In: Mir, R.A., Shafi, S.M. & Zargar, S.M. (eds). *Principles of Genomics and Proteomics*. Elsevier, New York. 274 pp.
25. Pancotti, C., Benevenuta, S., Birolo, G., Alberini, V., Repetto, V., Sanavia, T., Capriotti, E. & Fariselli, P. 2022. Predicting protein stability changes upon single-point mutation: a thorough comparison of the available tools on a new dataset. *Briefings in Bioinformatics*, 23(2): 555. <https://doi.org/10.1093/bib/bbab555>
26. Paysan-Lafosse, T., Blum, M., Chuguransky, S., Grego, T., Pinto, B.L., Salazar, G.A., Bileschi M.L., Bork, P., Bridge, A., Colwell, L., Gough, J., Haft, D.H., Letunić, I., Marchler-Bauer, A., Mi, H., Natale, D.A., Orengo, C.A., Pandurangan, A.P., Rivoire, C., Sigrist, C.J.A., Sillitoe, I., Thanki, N., Thomas, P.D., Tosatto, S.C.E., Wu, C.H. & Bateman, A. 2023. InterPro in 2022. *Nucleic Acids Research*, 51(D1): D418-D427. <https://doi.org/10.1093/nar/gkac993>.
27. Puel, A., Ziegler, S.F., Buckley, R.H. & Leonard, W.J. 1998. Defective IL7R expression in T(-)B(+)NK(+) severe combined immunodeficiency. *Nature Genetics*, 20(4): 394-397. <https://doi.org/10.1038/3877>
28. Rodrigues, C.H.M., Pires, D.E.V. & Ascher, D.B. 2021. DynaMut2: Assessing changes in stability and flexibility upon single and multiple point missense mutations. *Protein Science*, 30(1): 60-69. <https://doi.org/10.1002/pro.3942>
29. Salentin, S., Schreiber, S., Haupt, V.J., Adasme, M.F. & Schroeder, M. 2015. PLIP: fully automated protein-ligand interaction profiler. *Nucleic Acids Research*, 43(W1): W443-W447. <https://doi.org/10.1093/nar/gkv315>
30. Salgado, D., Desvignes, J.P., Rai, G., Blanchard, A., Miltgen, M., Pinard, A., Lévy, N., Collod-Bérout, G. & Bérout, C. 2016. UMD-Predictor: A high-throughput sequencing compliant system for pathogenicity prediction of any human cDNA Substitution. *Human Mutation*, 37(5): 439-46. <https://doi.org/10.1002/humu.22965>
31. Senthil, R., Usha, S. & Saravanan, K.M. 2019. Importance of fluctuating amino acid residues in folding and binding of proteins. *Avicenna Journal of Medical Biotechnology*, 11(4): 339-343.
32. Sim, N.L., Kumar, P., Hu, J., Henikoff, S., Schneider, G. & Ng, P.C. 2012. SIFT web server: predicting effects of amino acid substitutions on proteins. *Nucleic Acids Research*, 40(Web Server issue): W452-7. <https://doi.org/10.1093/nar/gks539>
33. Suybeng, V., Koeppl, F., Harlé, A. & Rouleau, E. 2020. Comparison of pathogenicity prediction tools on somatic variants. *The Journal of Molecular Diagnostics*, 22(12): 1383-1392. <https://doi.org/10.1016/j.jmoldx.2020.08.007>
34. Vajda, S., Yueh, C., Beglov, D., Bohnuud, T., Mottarella, S.E., Xia, B., Hall, D.R. & Kozakov, D. 2017. New additions to the ClusPro server motivated by CAPRI. *Proteins*, 85(3): 435-444. <https://doi.org/10.1002/prot.25219>
35. Valášek, L.S., Kučerová, M., Zeman, J. & Beznosková, P. 2023. Cysteine tRNA acts as a stop codon readthrough-inducing tRNA in the human HEK293T cell line. *RNA*, 29(9): 1379-1387. <https://doi.org/10.1261/rna.079688.123>
36. Venselaar, H., Te Beek, T.A., Kuipers, R.K., Hekkelman, M.L. & Vriend, G. 2010. Protein structure analysis of mutations causing inheritable diseases. An e-Science approach with life scientist friendly interfaces. *BMC Bioinformatics*, 11: 548. <https://doi.org/10.1186/1471-2105-11-548>
37. Vitiello, G.A.F., Losi Guembarovski, R., Amarante, M.K., Ceribelli, J.R., Carmelo, E.C.B. & Watanabe, M.A.E. 2018. Interleukin 7 receptor alpha Thr244Ile genetic polymorphism is associated with susceptibility and prognostic markers in breast cancer subgroups. *Cytokine*, 103: 121-126. <https://doi.org/10.1016/j.cyto.2017.09.019>
38. Vranjkovic, A., Crawley, A.M., Gee, K., Kumar, A. & Angel, J.B. 2007. IL-7 decreases IL-7 receptor alpha (CD127) expression and induces the shedding of CD127 by human CD8+ T cells. *International Immunology*, 19(12): 1329-1339. <https://doi.org/10.1093/intimm/dxm102>
39. Wang, C., Kong, L., Kim, S., Lee, S., Oh, S., Jo, S., Jang, I. & Kim, T.D. 2022. The role of IL-7 and IL-7R in cancer pathophysiology and immunotherapy. *International Journal of Molecular Sciences*, 23(18): 10412. <https://doi.org/10.3390/ijms231810412>
40. Wang, X., Chang, S., Wang, T., Wu, R., Huang, Z., Sun, J., Liu, J., Yu, Y., Mao, Y. 2022. IL7R is correlated with immune cell infiltration in the tumor microenvironment of lung adenocarcinoma. *Frontiers in Pharmacology*, 13: 857289. <https://doi.org/10.3389/fphar.2022.857289>
41. Wang, Z., Wang, X., Gao, Y., Wang, Y., Xu, M., Han, Q. & Zhao, X. 2020. IL-7R gene variants are associated with breast cancer susceptibility in Chinese Han women. *International Immunopharmacology*, 86: 106756. <https://doi.org/10.1016/j.intimp.2020.106756>
42. Winer, H., Rodrigues, G.O.L., Hixon, J.A., Aiello, F.B., Hsu, T.C., Wachter, B.T., Li, W. & Durum, S.K. 2022. IL-7: Comprehensive review. *Cytokine*, 160: 156049. <https://doi.org/10.1016/j.cyto.2022.156049>
43. Yan, L., He, Y., Zhang, Y., Liu, Y., Xu, L., Han, C., Zhao, Y. & Li, H. 2023. A novel 268 kb deletion combined with a splicing variant in IL7R causes of severe combined immunodeficiency in a Chinese family: a case report. *BMC Medical Genomics*, 16(1): 323. <https://doi.org/10.1186/s12920-023-01765-8>
44. Zhang, N., Chen, Y., Lu, H., Zhao, F., Alvarez, R.V., Goncarenco, A., Panchenko, A.R. & Li M. 2020. MutaBind2: Predicting the impacts of single and multiple mutations on protein-protein interactions. *iScience*, 23(3): 100939. <https://doi.org/10.1016/j.isci.2020.100939>
45. Zu, L., He, J., Zhou, N., Tang, Q., Liang, M. & Xu, S. 2023. Identification of multiple organ metastasis-associated hub mRNA/miRNA signatures in non-small cell lung cancer. *Cell Death and Disease*, 14(12): 798. <https://doi.org/10.1038/s41419-023-06286-x>



## *Eisenia foetida* (Sav.) coelomic fluid protect human umbilical vein endothelial cells against metformin-induced cell toxicity

Elif Kale Bakır<sup>1</sup>, Asuman Deveci Özkan<sup>\*2</sup>, Özlem Aksoy<sup>3</sup>, Yonca Yuzugullu Karakus<sup>3</sup>

<sup>1</sup> Department of Biology, Institute of Science, Kocaeli University, Kocaeli, TÜRKİYE

<sup>2</sup> Department of Medical Biology, Faculty of Medicine, Sakarya University, Sakarya, TÜRKİYE

<sup>3</sup> Department of Biology, Faculty of Science and Art, Kocaeli University, Kocaeli, TÜRKİYE

### Cite this article as:

Kale Bakır E., Deveci Özkan A. Aksoy A. & Yuzugullu Karakus. 2025. *Eisenia foetida* (Sav.) coelomic fluid protect human umbilical vein endothelial cells against metformin-induced cell toxicity. *Trakya Univ J Nat Sci*, 26(1): 19-27, DOI: 10.23902/trkjinat.1598922

Received: 09 December 2024, Accepted: 14 February 2025, Online First: 01 March 2025, Published: 15 April 2025

**Abstract:** The coelomic fluid of the red California earthworm *Eisenia foetida* (Sav.) includes a number of bioactive substances with antitumor and protective effects, thus making the fluid to also act as a defensive agent for the organism. *Eisenia foetida* coelomic fluid can be used as an alternative medication, for it is readily available and has few adverse effects. Metformin are widely used for managing type 2 diabetes mellitus by improving insulin sensitivity and reducing hepatic glucose production; however, therapeutic dose-related adverse effects have been reported. The present investigation aims to determine, for the first time, the protective effects of *E. foetida* coelomic fluid against possible metformin toxicity at the molecular and cellular levels. Metformin-induced cell toxicity was conducted following *E. foetida* coelomic fluid pre-treatment in Human Umbilical Vein Endothelial Cells (HUVEC). In addition to cell and nuclear morphology observation, a decrease in reactive oxygen species and apoptotic cell rate was determined. According to the obtained findings, the coelomic fluid of *E. foetida* preserved cell viability and morphology, reduced reactive oxygen species and apoptosis cell death, and enhanced anti-apoptotic mRNA expressions. When treating diseases, medical support and adjunct therapies should be taken into account. In this sense, our present preliminary *in vitro* findings showed that *E. foetida* coelomic fluid might has great additional treatment potential, and further molecular and animal studies to support this effect are needed.

### Edited by:

Yeşim Sağ Açıkel

### \*Corresponding Author:

Asuman Deveci Özkan  
[deveci@sakarya.edu.tr](mailto:deveci@sakarya.edu.tr)

### ORCID iDs of the authors:

EKB. 0000-0002-4266-9517  
ADO. 0000-0002-3248-4279  
OA. 0000-0003-0969-5171  
YYK. 0000-0003-0286-8711

### Key words:

Guanidine  
Type-2 Diabetes  
California worm  
HUVEC  
Cell viability

**Özet:** Kırmızı Kaliforniya solucanı *Eisenia foetida*'nın (Sav.) sölomik sıvısı, antitümör ve koruyucu etkilere sahip bir dizi biyoaktif maddeyi içerdiğinden, bu sıvının aynı zamanda organizma için bir savunma maddesi olarak da işlev görmesi sağlanmaktadır. *Eisenia foetida* sölomik sıvısı, kolayca bulunabilmesi ve yan etkilerinin az olması nedeniyle alternatif bir ilaç olarak kullanılabilir. Metformin, insülin duyarlılığını artırarak ve hepatik glukoz üretimini azaltarak tip 2 diyabetin tedavisinde yaygın olarak kullanılmaktadır; ancak terapötik doza bağlı yan etkiler bildirilmiştir. Bu araştırmanın amacı, *E. foetida* sölomik sıvısının olası metformin toksisitesine karşı moleküler ve hücre düzeyde koruyucu etkilerini ilk kez belirlemektir. Metformin kaynaklı hücre toksisitesi, *E. foetida* sölomik sıvısı ön muamelesinin ardından gerçekleştirildi. Hücre ve nükleer morfoloji gözlemine ek olarak, reaktif oksijen türleri ve hücre ölümü üzerindeki koruyucu etkisi belirlendi. Elde edilen bulgulara göre, *E. foetida* sölomik sıvısı hücre canlılığını ve morfolojisini korudu, reaktif oksijen türlerini ve apoptotik hücre ölümünü azalttı ve anti-apoptotik mRNA ekspresyonlarını artırdı. Hastalıkların tedavisi, destekleyici bakım ve yardımcı tedavilerin dikkate alınmasını içermelidir. Bu anlamda, bu *in vitro* ön bulgularımız *E. foetida* sölomik sıvısının büyük yardımcı tedavi potansiyeline sahip olduğunu gösterdi ve bu etkiyi desteklemek için daha fazla moleküler ve hayvan çalışmasına ihtiyaç vardır.

## Introduction

*Eisenia foetida* (Sav.) (the red California worm) is a red earthworm and since they are sensitive to light, they live in the dark and show hermaphrodite characteristics. Their body cavities are filled with a special fluid called coelom and they bear a unique natural defensive mechanism (Heredia Rivera *et al.* 2020). Production of a

wide range of bioactive compounds and the coelomic fluid, known to have antioxidant, hemolytic, antitumor, antibacterial, and protective effects, as a defense mechanism when animals are under stress is typical (Grdisa *et al.* 2001, Hua *et al.* 2011, Kilciler *et al.* 2022, Deveci Özkan *et al.* 2023). Although the ecological,



OPEN ACCESS

physiological, and other health-related consequences of *E. foetida* coelomic fluid (ECF) have been extensively studied, little is known about its therapeutic potential, pharmacological relevance, and cellular effects (Deng *et al.* 2018, Lin *et al.* 2018). Researchers claim that because ECF is widely accessible, reasonably priced, and has few side effects, it can be used as an alternative treatment agent (Dajem *et al.* 2020). More research on the capacity of ECF to protect against the side effects of various drugs is necessary, given its therapeutic utility, pharmacological relevance, and cellular impacts.

The plant *Galega officinalis* L. is the source of a class of chemicals called biguanides, which are based on the biguanidine molecule. The primary component of *G. officinalis*, guanidine, was shown to reduce blood glucose levels and used to make a number of anti-diabetic medications, including metformin (MET) (1,1 dimethylbiguanide) (Wang & Hoyte 2019, LaMoia & Shulman 2021). Although MET's label states that it treats type 2 diabetes mellitus, it is also used to treat other conditions such hyperinsular obesity, polycystic ovarian syndrome, and weight gain caused by antipsychotic drugs (Pfeiffer & Klein 2014, DeFronzo *et al.* 2016, Houston *et al.* 2021). Although MET is a widely used drug in many different conditions, therapeutic dose-related adverse events have been reported. Abdominal discomfort, nausea, diarrhea, and other gastrointestinal symptoms, and infrequently acute hepatitis and cholestasis are among the side effects connected to the therapeutic use of MET (Nammour *et al.* 2003, Kutoh 2005, Biyyani *et al.* 2009, Cone *et al.* 2010, Stanton 2015, Abutaleb & Kottlilil 2020). Patients who experience hyperlactatemia and metabolic acidosis when taking MET are susceptible to two primary types of toxicity: metformin-associated lactic acidosis (MALA) and metformin-induced lactic acidosis (MILA) (Blough *et al.* 2015). There is no specific treatment for MET toxicity. The foundation of its therapy is a supportive care, which includes the control of fluids, electrolytes, acid-base, respiratory, metabolic, renal, and hemodynamic abnormalities. Examples of adjunct therapy include metabolic rescue, extracorporeal techniques to reduce the body load of MET, serum alkalization, glucose and insulin, and intestinal decontamination (Abad *et al.* 2020).

It is thus important to search for different treatments and supportive options for MET's side effects, which is commonly used and even has a very tiring treatment for reducing side effects. In this study, we investigated the protective effects of ECF as a natural active component with a potential for protective effect, whose content was previously determined (Ozkan *et al.* 2022), on potential MET-toxicity.

## Materials and Methods

### Cell Culture Conditions

We investigated the protective effect of ECF against MET-induced cell toxicity *in vitro* using Uman Umbilical Vein Endothelial Cells (HUVEC). HUVECs

come from the umbilical cord's venous endothelium and are used as a model system for the function and pathophysiology of endothelial cells (Park *et al.* 2006). Commercial HUVECs were purchased from the American Type Culture Collection (ATCC) and cultured in Dulbecco's Modified Eagle Medium (DMEM) containing 10% FBS and 0.1% penicillin and streptomycin. The cells were grown at 37°C with 5% CO<sub>2</sub>. The details in Ozkan *et al.* (2022) was followed to obtain ECF of *E. foetida* (Ozkan *et al.* 2022).

### Cell Viability Assay

The cytotoxic effects of ECF and MET on HUVECs were determined by Water-Soluble Tetrazolium-1 (WST-1) cell viability assay. For this purpose, the cells were seeded in 96 well plates ( $2 \times 10^4$  cells/well) and incubated for 24 h. After incubation, the cells were treated with different concentrations of ECF (2, 4, 8, 16, 32, and 64 µg/mL) and MET (1.25, 2.5, 5, 10, and 20 mM) for 24 and 48 h at 37°C with 5% CO<sub>2</sub>. After the incubation times, WST-1 reagent (Biovision) was added to each well and optic density (OD) values were measured at 450 nm with a microplate reader (Thermo Fisher Scientific). For the MET-induced toxicity model, HUVECs were pre-treated with ECF and followed by exposure to MET. After treatments, cell viability was measured by the cell viability assay described below.

### Enzyme-Linked Immunosorbent Assay (ELISA)

To determine the cell death situation of cells after ECF pre-treatment against MET-induced cell toxicity, the free Annexin V (ANXA5) protein level in HUVECs were analyzed by the ELISA assay. For this purpose, the cells were seeded in 96 well plates ( $4 \times 10^6$  cells/well) and incubated for 24 h. Then, the cells were pre-treated with determined concentrations of ECF (2, 8, and 32 µg/mL) for 24h followed by exposure to MET (5 mM) for another 24h incubation. At the end of the incubation time, the cell culture media of each treatment group was collected and the free ANXA5 protein level was determined according to the Human ANXA5 ELISA kit (Abcam) procedure. The absorbance of each well was measured at 450 nm using a microplate reader (Benchmark Plus), and the ANXA5 levels of each group were calculated according to the standard curve.

### Reactive Oxygen Species (ROS) Microplate Assay

To determine the oxidative stress situation of the cells after ECF pre-treatment against MET-induced cell toxicity, the ROS generation levels of HUVECs were measured by the ROS microplate assay. For this purpose, HUVECs were seeded in 96 well plates ( $25 \times 10^3$  cells/well) and incubated for 24 h. Then, the cells were pre-treated with determined concentrations of ECF (2, 8, and 32 µg/mL) for 24h followed by exposure to MET (5 mM) for another 24 h incubation. After the incubation time, ROS level was determined according to the DCFDA/H2DCFDA-Cellular ROS Assay Kit (Abcam) procedure. The absorbance of each well was measured



using a microplate reader (Biotek), and ROS generation levels of each group were calculated as fold change.

#### Real-Time Polymerase Chain Reaction (RT-PCR) Analysis

To determine the gene expression level status of cells after ECF pre-treatment against MET-induced cell toxicity, the expression of *Bax* and *Bcl-2* mRNA levels were detected by RT-PCR in HUVECs. For this purpose, HUVECs were seeded in T<sub>25</sub> flasks ( $1 \times 10^6$  cells/flask) and incubated for 24 h. Then, the cells were pre-treated with determined concentrations of ECF (2, 8, and 32  $\mu\text{g/mL}$ ) for 24h followed by exposure to MET (5 mM) for another 24 h incubation. After the incubation, total RNA was isolated from the cells using the Trizol Reagent (Thermo Fisher) and the concentration of total RNA was measured by a Qubit 3 Fluorometer (Thermo Fisher Scientific). After RNA isolation, cDNA was synthesized with a cDNA Reverse Transcription Kit (Thermo Fisher Scientific) and the relative gene expression levels of *Bax* and *Bcl-2* were analyzed by using the CFX Connect Real-Time PCR Detection System from Bio-Rad. Additionally,  $\beta$ -Actin was used as an endogenous reference gene.

#### Acridine Orange (AO) and 4',6-diamidino-2-phenylindol (DAPI) Staining

To determine the morphological changes of cells after ECF pre-treatment against MET-induced cell toxicity, the changes in HUVECs and nucleus morphology were observed by AO and DAPI stainings, respectively. For this purpose, HUVECs were seeded in 6 well plates ( $1 \times 10^5$  cells/well) with slides and incubated for 24 h. Then, the cells were pre-treated with determined concentrations of ECF (2, 8, and 32  $\mu\text{g/mL}$ ) for 24h followed by exposure

to MET (5 mM) for another 24 h incubation. After incubation, the cells were fixed with 4% paraformaldehyde solution for 30 min. After fixation, the cells were washed twice and stained with AO and DAPI dyes (100 mg/mL) for 30 min, respectively. The slides were captured and analyzed with a fluorescence microscope (Olympus IX73, Japan).

#### Statistical Analysis

GraphPad Prism version 6.0 (La Jolla, CA) was used for statistical analyses, and a  $p < 0.05$  was recognized as a statistically significant threshold. Two-way ANOVA analysis with Dunnett's and Sidak's multiple comparisons test was employed for multiple comparisons. The Qiagen software (<https://www.qiagen.com/tr/shop/genes-andpathways/data-analysis-center-overviewpage/other-real-time-pcrprobes-orprimersdataanalysis-center/>) was used to analyze the gene expression results.

### Results

#### The Cytotoxic Effect of ECF and MET in HUVECs

The cytotoxic effects of ECF and MET on HUVECs were assessed using the WST-1 viability assay. The results indicated that ECF treatment reduced HUVEC viability in a dose- and time-dependent manner compared to the control group (Fig. 1, Table 1,  $p < 0.0001$ ). Specifically, all tested ECF concentrations, except for 2  $\mu\text{g/mL}$ , significantly decreased cell viability after 48 hours compared to the control (Fig. 1a,  $p < 0.05$ ). Based on these findings, we selected 2, 8, and 32  $\mu\text{g/mL}$  ECF concentrations as optimal for the pre-treatment procedure.

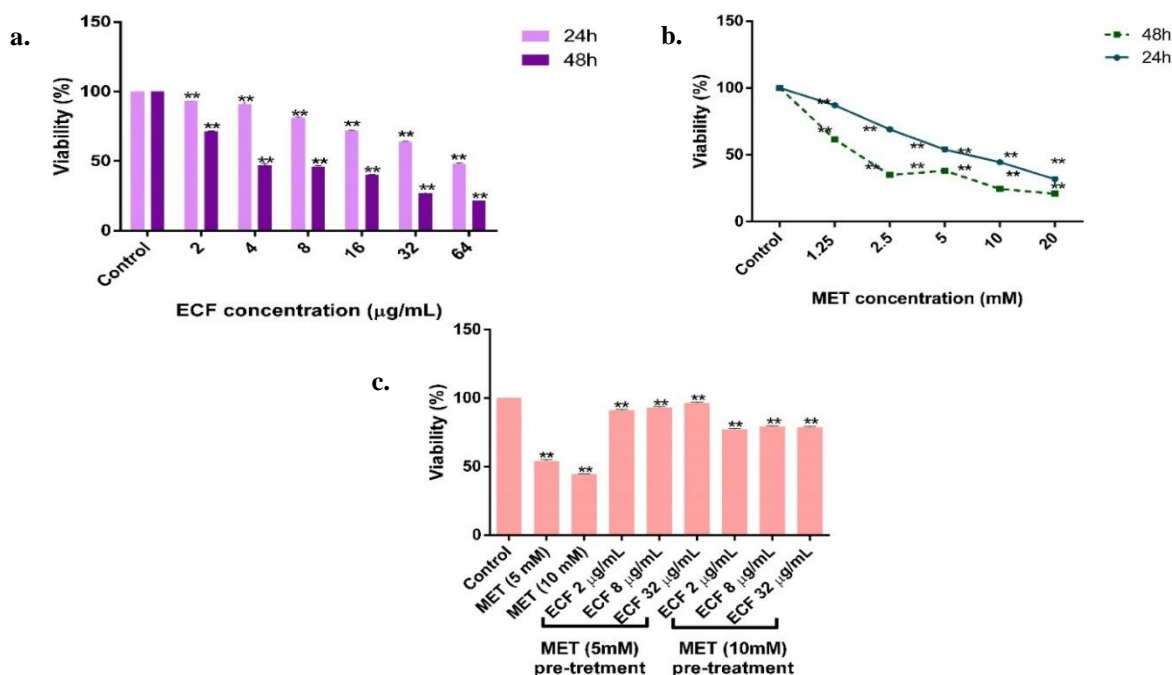


**Fig. 1.** Evaluation of HUVEC viability using the WST-1 assay. **a.** Effect of varying concentrations of ECF (2-64  $\mu\text{g/mL}$ ) on HUVEC viability, **b.** effect of MET at concentrations ranging from 1.25-20 mM on HUVEC viability, **c.** protective effects of ECF pre-treatment (2, 8, and 32  $\mu\text{g/mL}$  for 24 h) on HUVECs exposed to MET (5 mM) for an additional 24 h. Significant differences were observed at  $**p < 0.0001$ .

**Table 1.** Statistical analysis results of HUVEC viability assay. Two-way ANOVA analysis with Dunnett's and Sidak's multiple comparisons test was used for multiple comparisons.

ECF (µg/mL)	Mean Difference	95% CI of Difference	Significant?	Summary	Adjusted <i>p</i> Value
<b>24h</b>					
Control vs. 2	6.747	4.843 - 8.652	Yes	****	< 0.0001
Control vs. 4	8.968	7.063 - 10.87	Yes	****	< 0.0001
Control vs. 8	18.80	16.90 - 20.71	Yes	****	< 0.0001
Control vs. 16	28.05	26.15 - 29.96	Yes	****	< 0.0001
Control vs. 32	36.01	34.11 - 37.92	Yes	****	< 0.0001
Control vs. 64	51.83	49.92 - 53.73	Yes	****	< 0.0001
<b>48h</b>					
Control vs. 2	28.72	26.81 - 30.62	Yes	****	< 0.0001
Control vs. 4	52.99	51.09 - 54.90	Yes	****	< 0.0001
Control vs. 8	53.82	51.91 - 55.72	Yes	****	< 0.0001
Control vs. 16	59.97	58.06 - 61.87	Yes	****	< 0.0001
Control vs. 32	72.96	71.05 - 74.86	Yes	****	< 0.0001
Control vs. 64	78.49	76.59 - 80.40	Yes	****	< 0.0001
<b>MET (mM)</b>					
<b>24h</b>					
Control vs. 1.25	12.93	10.99 - 14.88	Yes	****	< 0.0001
Control vs. 2.5	30.92	28.98 - 32.87	Yes	****	< 0.0001
Control vs. 5	46.02	44.08 - 47.97	Yes	****	< 0.0001
Control vs. 10	55.42	53.47 - 57.36	Yes	****	< 0.0001
Control vs. 20	68.14	66.20 - 70.09	Yes	****	< 0.0001
<b>48h</b>					
Control vs. 1.25	38.26	36.32 - 40.21	Yes	****	< 0.0001
Control vs. 2.5	65.00	63.06 - 66.95	Yes	****	< 0.0001
Control vs. 5	61.83	59.88 - 63.77	Yes	****	< 0.0001
Control vs. 10	75.48	73.53 - 77.42	Yes	****	< 0.0001
Control vs. 20	79.10	77.15 - 81.04	Yes	****	< 0.0001
<b>ECF (µg/mL) pre-treatment + MET (mM)</b>					
Control vs. MET 5	23.01	21.85 - 24.18	Yes	****	< 0.0001
Control vs. MET 10	27.71	26.55 - 28.87	Yes	****	< 0.0001
Control vs. ECF 2+MET 5	4.385	3.221 - 5.550	Yes	****	< 0.0001
Control vs. ECF 8+MET 5	3.441	2.276 - 4.605	Yes	****	< 0.0001
Control vs. ECF 32+MET 5	1.753	0.5883 - 2.917	Yes	**	0.0019
Control vs. ECF 2+MET 10	11.39	10.23 - 12.55	Yes	****	< 0.0001
Control vs. ECF 8+MET 10	10.37	9.203 - 11.53	Yes	****	< 0.0001
Control vs. ECF 32+MET 10	10.63	9.466 - 11.79	Yes	****	< 0.0001

\* CI: confidence intervals.

Similarly, MET treatment (5 and 10 mM) exhibited a dose-dependent reduction in HUVEC viability (Fig. 1b,  $p < 0.0001$ ). For instance, treatment with 5 mM MET for 24 h resulted in a cell viability of approximately 45-53% (Fig. 1b,  $p < 0.0001$ ). This concentration was deemed sufficient to induce significant toxicity for further analysis. To evaluate the protective effects of ECF against MET-induced cytotoxicity in HUVECs, cells were pre-treated with 2, 8, or 32 µg/mL ECF for 24 h before exposure to 5 mM MET for an additional 24 h. As expected, MET-alone treatment significantly decreased cell viability compared to the control group. However, ECF pre-treatment notably improved cell viability compared to the MET-alone group (Fig. 1c,  $p < 0.0001$ ). In summary, these findings demonstrate that ECF pre-treatment mitigates MET-induced cytotoxicity in HUVECs, thereby preserving cell viability.

#### The Effect of ECF Pre-treatment after MET-induced Cell toxicity on ANXA5, ROS, and Gene Expression in HUVECs

The effects of ECF pre-treatment on MET-induced cell toxicity in HUVECs were assessed by ANXA5

ELISA, ROS production assays, and RT-PCR analysis (Fig. 2 and Table 2). The level of cell death following ECF pre-treatment was determined using ANXA5 ELISA (Fig. 2a). ANXA5 is a protein that binds phosphatidylserine (PS), a hallmark of apoptosis, making it a reliable marker for detecting apoptotic cells (Crowley et al. 2016). The ANXA5 ELISA results revealed that ANXA5 levels significantly decreased following MET (5 mM) treatment compared to the control group (Fig. 2a,  $p < 0.0001$ ). However, pre-treatment with ECF (2, 8, and 32 µg/mL) followed by MET exposure increased ANXA5 levels, with the most pronounced effect observed at the 2 µg/mL ECF concentration (Fig. 2a,  $p < 0.0001$ ). In terms of oxidative stress, MET treatment alone resulted in a significant 1.8-fold increase in ROS levels compared to the control group (Fig. 2b,  $p < 0.0001$ ). ECF pre-treatment at all concentrations (2, 8, and 32 µg/mL) significantly reduced ROS levels compared to the MET-alone treatment group (Fig. 2b,  $p < 0.0001$ ). RT-PCR analysis further demonstrated that ECF pre-treatment modulated the expression of apoptotic and anti-apoptotic genes. Specifically, Bax mRNA levels were significantly

decreased, while BCL-2 mRNA levels were significantly increased, particularly in the 2 µg/mL ECF pre-treatment group, compared to the MET-alone group (Fig. 2c,  $p < 0.0001$ ). These findings suggest that ECF exerts a protective effect against MET-induced cell death and oxidative stress in HUVECs by modulating apoptosis to related pathways and reducing ROS levels.

#### The Effect of ECF Pre-treatment After MET-induced Cell toxicity on Cell and Nuclear Morphology in HUVECs

The effects of ECF pre-treatment on MET-induced cell and nuclear morphology changes in HUVECs, AO and DAPI stainings were performed. The staining results revealed a slight increase in apoptotic cell morphology

characterized by cell shrinkage, nuclear condensation, and membrane blebbing following treatment with MET alone compared to the control group (Fig. 3). In contrast, pre-treatment with 2 and 8 µg/mL ECF followed by MET exposure reduced apoptotic morphology and improved overall cell morphology, resembling that of the control group. However, pre-treatment with 32 µg/mL ECF followed by MET exposure did not restore apoptotic cell morphology to the level observed in control cells (Fig. 3). These findings suggest that the lowest ECF concentration (2 µg/mL) is the most effective in protecting HUVECs from MET-induced cell toxicity and preserving normal cell morphology.

**Table 2.** Statistical analysis results of ANXA5, ROS and gene expression analysis. Two-way ANOVA analysis with Dunnett's and Sidak's multiple comparisons test was used for multiple comparisons.

ANXA5 level	Mean Difference	95% CI of Difference	Significant?	Summary	Adjusted p Value
<b>ECF (µg/mL) pre-treatment + MET (mM)</b>					
Control vs. MET 5	5.097	5.069 - 5.124	Yes	****	< 0.0001
Control vs. ECF 2+MET 5	-5.245	(-5.272) - (-5.217)	Yes	****	< 0.0001
Control vs. ECF 8+MET 5	-0.4276	(-0.4551) - (-0.4001)	Yes	****	< 0.0001
Control vs. ECF 32+MET 5	6.997	6.969 - 7.024	Yes	****	< 0.0001
<b>ROS level</b>					
<b>ECF (µg/mL) pre-treatment + MET (mM)</b>					
Control vs. MET 5	-0.3925	(-0.4540) - (-0.3310)	Yes	****	< 0.0001
Control vs. ECF 2+MET 5	-0.3125	(-0.3740) - (-0.2510)	Yes	****	< 0.0001
Control vs. ECF 8+MET 5	-0.1825	(-0.2440) - (-0.1210)	Yes	****	< 0.0001
Control vs. ECF 32+MET 5	-0.0650	(-0.1265) - (-0.003474)	Yes	*	0.0384
<b>Gene (mRNA) expression level</b>					
<b>ECF (µg/mL) pre-treatment + MET (mM)</b>					
<b>Bax</b>					
Control vs. MET 5	0.6350	0.5582 - 0.7118	Yes	****	< 0.0001
Control vs. ECF 2+MET 5	0.6650	0.5882 - 0.7418	Yes	****	< 0.0001
Control vs. ECF 8+MET 5	0.6500	0.5732 - 0.7268	Yes	****	< 0.0001
Control vs. ECF 32+MET 5	0.5350	0.4582 - 0.6118	Yes	****	< 0.0001
<b>BCL-2</b>					
Control vs. MET 5	0.7850	0.7082 - 0.8618	Yes	****	< 0.0001
Control vs. ECF 2+MET 5	-2.115	(-2.192) - (-2.038)	Yes	****	< 0.0001
Control vs. ECF 8+MET 5	-0.0600	-0.1368 - 0.01677	No	ns	0.1311
Control vs. ECF 32+MET 5	0.3900	0.3132 - 0.4668	Yes	****	< 0.0001

\* CI: confidence intervals.

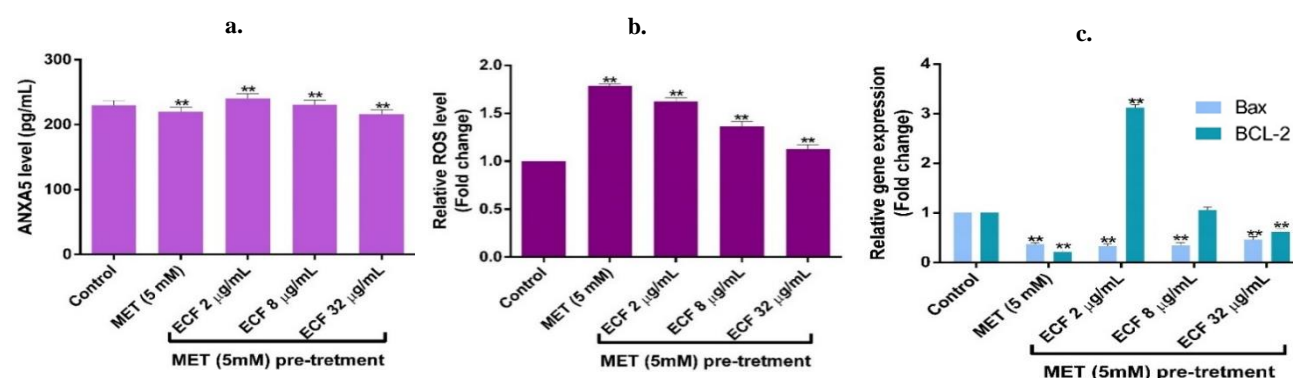


**Fig. 2.** Effects of ECF pre-treatment on MET-induced cell toxicity in HUVECs. **a.** ANXA5 levels, **b.** relative ROS levels and **c.** relative gene expression levels were evaluated, **c.** HUVECs were pre-treated with 2, 8, and 32 µg/mL ECF for 24 hours, followed by exposure to MET (5 mM) for an additional 24 hours. Significant differences were observed at \*\* $p < 0.0001$ .

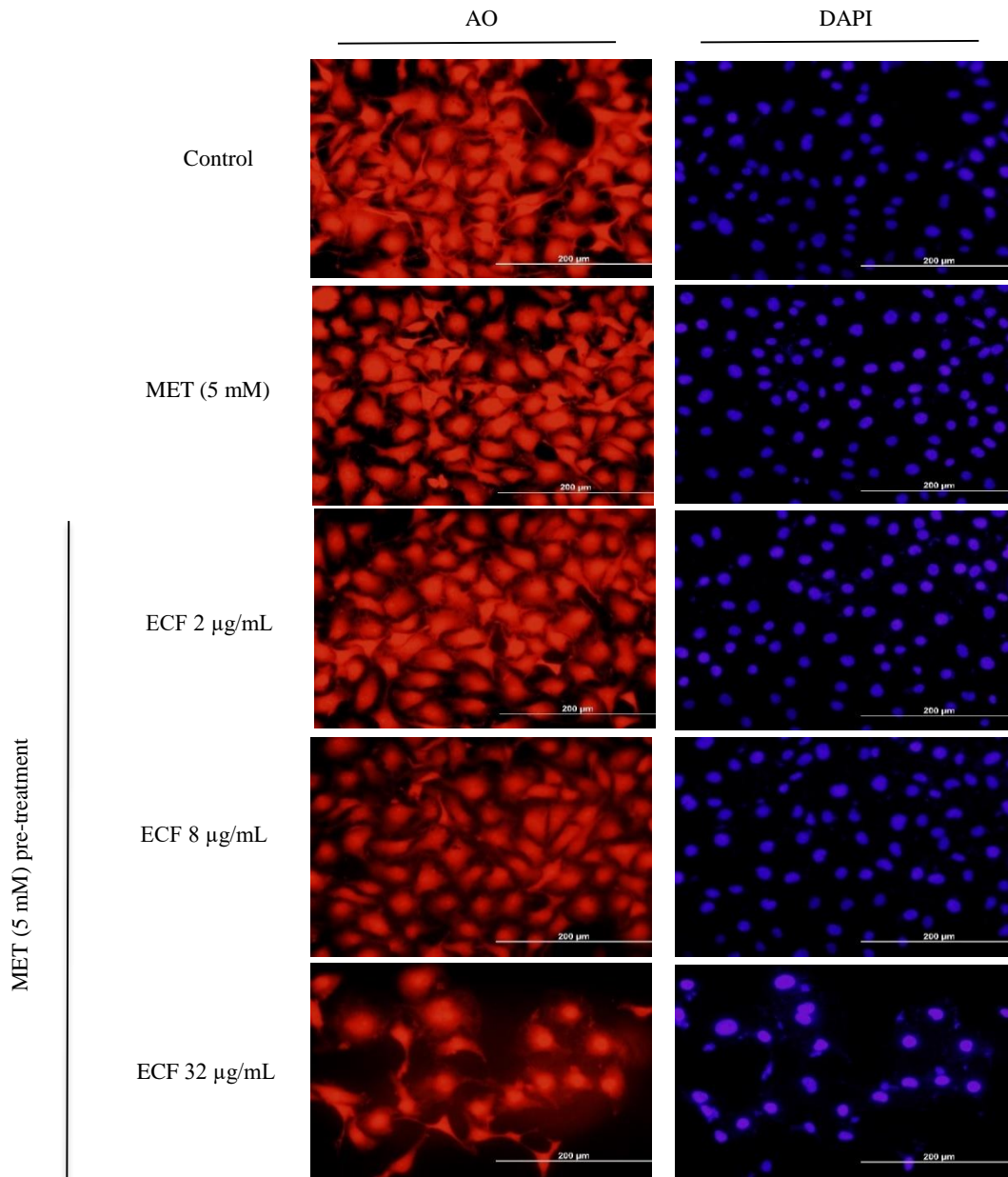


**Fig. 3.** Effects of ECF pre-treatment on cell and nuclear morphology in HUVECs following MET-induced cell toxicity, as assessed by AO and DAPI stainings. HUVECs were pre-treated with 2, 8, and 32  $\mu\text{g/mL}$  ECF for 24 h, followed by exposure to MET (5 mM) for an additional 24 h. The staining highlights changes in apoptotic morphology and nuclear integrity.

## Discussion

In this study, the *in vitro* protective effect of *E. foetida* coelomic fluid against MET-induced toxicity was determined in HUVECs. According to our findings, low ECF pre-treatment concentrations protect cell viability, preserve cell and nuclear morphology, reduce ROS production, and decrease apoptotic cell death against MET-induced toxicity.

The biguanide drug MET is commonly used to treat high blood sugar in people with type 2 diabetes mellitus, despite its well-known toxicity and side effects (Hasanvand *et al.* 2016). In addition to its beneficial effects on heart failure, MET therapy has positive effects on the organisms oxidative stress activities and lowers

endotoxemia and improves insulin signaling pathways in animals (Ghosh 2017). Furthermore, it exhibits a number of characteristics that make MET appealing for repurposing as an anti-cancer treatment, including melanoma and pancreatic cancer cells (Romero *et al.* 2017). Interestingly, our findings showed that ROS generation levels were particularly high in the MET alone treated group but were much lower in the cells pre-treated with the ECF group. Additionally, ANXA5 levels, as an apoptotic marker of the cells, did not exhibit higher differences among the ECF pre-treatment and MET alone treated groups. In one study, the preventive and curative effects of garlic and MET combination were evaluated on Gentamicin (GM) induced tubular toxicity in Wistar rats



and the results demonstrated that MET and garlic combination have curative and protective activity against GM nephrotoxicity (Rafieian-Kopaei *et al.* 2013). These results and studies referred so far demonstrate that MET maintains its own protective and beneficial features, although a cytotoxic dose damage model was created for MET in the current study. However, in our findings, it is very clear that ECF has the potential to exert a protective effect when MET has a therapeutic dose-related adverse event. In this case, the presence of MET suggests that the protective effect of ECF as a pre-treatment increases, although not very much.

MET side effects include gastrointestinal disorders, vitamin B12 deficiency, and hemolytic anemia. Although metformin offers many advantages such as being effective, affordable, and widely available, its use is often limited by kidney function issues commonly observed in individuals with type 2 diabetes mellitus. Decreased renal function increases the risk of lactic acidosis, a dangerous condition. Although MALA is the lowest, the probability of growth with MALA is high (Bennis *et al.* 2020). Excessive lactate production, inadequate lactate clearance, or both can cause lactic acidosis. The most common cause of excessive lactate production is the switch from aerobic to anaerobic glucose metabolism in hypoxic environments (Adeva-Andany *et al.* 2014). It is still unclear how MET may accelerate lactic acidosis, but one theory is that it may do so by inhibiting mitochondrial respiratory chain complex 1, the first enzyme in the mitochondrial electron transport chain (Fontaine 2018, Vial *et al.* 2019). MALA may also occur as a result of mitochondrial glycerophosphate dehydrogenase (mGPDH). Maintenance of toxicity should include additional therapies such as extracorporeal techniques and metabolic rescue to reduce MET body loss (Wang & Hoyte 2019). Considering the antioxidant and cytoprotective properties of ECF and the data obtained from the current study, ECF is thought to reduce MET-induced toxicity by alleviating the risk of lactic acidosis.

The literature states that many compounds with potential protective effects have been investigated in relation to various cell types (Vargas *et al.* 2014, Shi *et al.* 2021). Vargas *et al.* (2014) assessed how different amounts of vitamin E alpha-tocopherol ( $\alpha$ -T) isomer protected dental pulp cells from hydrogen peroxide ( $H_2O_2$ ) damage and they found that the pulp cells of the immortalized MDPC-23 were protected from the negative effects of  $H_2O_2$ . Shi *et al.* (2021) found that pre-treatment with Cryptotanshinone (CTS) may enhance cell survival and promote the expression of the *Bcl-2* anti-apoptotic gene in neonatal rat cardiomyocytes. Furthermore, CTS

may stop  $H_2O_2$ -induced NO synthesis and stop the production of ROS and MDA (Shi *et al.* 2021). Our findings are in line with previous research; as the concentration of ECF pre-treatment increased, oxidative damage from MET-induced toxicity decreased, free ANXA5 protein levels were reduced, and anti-apoptotic *Bcl-2* mRNA expression was enhanced. Additionally, AO and DAPI staining demonstrated that these findings were supported. In a previous study, we demonstrated how ECF impacted the molecular level of oxidative damage in MCFto7 cells produced by the chemotherapeutic agent NaBu, which is used to treat breast cancer (Ozkan *et al.* 2022). Our findings that ECF may be a potential therapeutic and supportive molecule with fewer side effects in cancer treatment and reduce the side effects of treatment in the future are consistent with this study's finding that ECF pre-treatment against NaBu-induced toxicity significantly reduced the amount of ROS production.

The findings of our study are preliminary and have limitations. More detailed molecular analyses are needed to show that MET toxicity is reduced by ECF. In particular, mitochondrial function and lactate production analysis should be performed by selecting cells that are sensitive to the effects of MET, such as liver or kidney cell lines. After cell culture experiments, the effect of ECF on MET-induced lactic acidosis should be tested in *in vivo* models. In conclusion, both the data we obtained and the methods we suggested can help us understand the potential protective effects of ECF on MET-induced lactic acidosis at the molecular, cellular and systemic levels. In this sense, these preliminary *in vitro* findings we obtained showed that ECF has great additional treatment potential. Considering the limitations of the study, future studies should focus more on *in vivo* validation, mechanistic analyses and long-term safety assessments.

**Ethics Committee Approval:** Since the article does not contain any studies with human or animal subject, its approval to the ethics committee was not required.

**Data Sharing Statement:** All data are available within the study.

**Author Contributions:** Concept: E.K.B., Design: E.K.B., A.D.O., Execution: E.K.B., A.D.O., O.K., Material supplying: E.K.B., Y.Y.K., Data acquisition: E.K.B., O.K., Data analysis/interpretation: E.K.B., A.D.O., O.K., Y.Y.K., Writing: E.K.B., A.D.O., O.K., Y.Y.K., Critical review: E.K.B., A.D.O.

**Conflict of Interest:** The authors have no conflicts of interest to declare.

**Funding:** The authors declared that this study has received no financial support.

## References

1. Abad, K., Kien, C. & Ganta, K. 2020. A Unique Case of Metformin-associated Severe Lactic Acidosis Without Preexisting Renal Disease: Perspectives on Prolonged Dialysis and Education for Prevention. *Cureus*, 12(4): e7564. <https://doi.org/10.7759/cureus.7564>
2. Abutaleb, A. & Kottiril, S. 2020. Hepatitis A. *Gastroenterology Clinics of North America*, 49(2): 191-199. <https://doi.org/10.1016/j.gtc.2020.01.002>

3. Adeva-Andany, M., López-Ojén, M., Funcasta-Calderón, R., Ameneiros-Rodríguez, E., Donapetry-García, C., Vila-Altesor, M. & Rodríguez-Seijas, J. 2014. Comprehensive review on lactate metabolism in human health. *Mitochondrion*, 17: 76-100. <https://doi.org/10.1016/j.mito.2014.05.007>
4. Bennis, Y., Bodeau, S., Batteux, B., Gras-Champel, V., Masmoudi, K., Maizel, J., De Broe, M. E., Lalau, J. D. & Lemaire-Hurtel, A. S. 2020. A Study of Associations Between Plasma Metformin Concentration, Lactic Acidosis, and Mortality in an Emergency Hospitalization Context. *Critical Care Medicine*, 48(12): e1194-e1202. <https://doi.org/10.1097/CCM.0000000000004589>
5. Biyyani, R.S.R.S., Battula, S., Erhardt, C.A. & Korkor, K. 2009. Metformin-induced cholangiohepatitis. *Case Reports*, 2009: bcr0920080950. <https://doi.org/10.1136/bcr.09.2008.0950>
6. Blough, B., Moreland, A. & Mora, A. 2015. Metformin-Induced Lactic Acidosis with Emphasis on the Anion Gap. *Baylor University Medical Center Proceedings*, 28(1): 31-33. <https://doi.org/10.1080/08998280.2015.11929178>
7. Cone, C.J., Bachyrycz, A.M. & Murata, G.H. 2010. Hepaticity associated with metformin therapy in treatment of type 2 diabetes mellitus with nonalcoholic fatty liver disease. *The Annals of Pharmacotherapy*, 44(10): 1655-1659. <https://doi.org/10.1345/aph.1P099>
8. Crowley, L.C., Marfell, B.J., Scott, A.P. & Waterhouse, N.J. 2016. Quantitation of Apoptosis and Necrosis by Annexin V Binding, Propidium Iodide Uptake, and Flow Cytometry. *Cold Spring Harbor Protocols*, 2016(11): pdb.prot087288. <https://doi.org/10.1101/pdb.prot087288>
9. Dajem, S., Ali, S., Abdelrady, O., Salahaldin, N., Soliman, A., Kamal, Y., Abdelazim, A., Mohamed, A., Morsy, K., Mohamed, A. & Fahmy, S. 2020. Allobophora caliginosa coelomic fluid ameliorates gentamicin-induced hepatorenal toxicity in rats. *Asian Pacific Journal of Tropical Biomedicine*, 10(9): 411. <https://doi.org/10.4103/2221-1691.290132>
10. DeFronzo, R., Fleming, G.A., Chen, K. & Bicsak, T.A. 2016. Metformin-associated lactic acidosis: Current perspectives on causes and risk. *Metabolism: Clinical and Experimental*, 65(2): 20-29. <https://doi.org/10.1016/j.metabol.2015.10.014>
11. Deng, Z., Yin, J., Luo, W., Kotian, R.N., Gao, S., Yi, Z., Xiao, W., Li, W. & Li, Y. 2018. The effect of earthworm extract on promoting skin wound healing. *Bioscience Reports*, 38(2): BSR20171366. <https://doi.org/10.1042/BSR20171366>
12. Deveci Özkan, A., Alimudin, J., Kilciler, Y., Yuksel, B., Aksoy, O. & Betts, Z. 2023. In vitro chemo-protective effect of *Eisenia foetida* coelomic fluid against histone deacetylase inhibitor-induced oxidative toxicity in breast cancer cells. *International Journal of Environmental Health Research*, 33(12): 1728-1737. <https://doi.org/10.1080/09603123.2022.2120970>
13. Fontaine, E. 2018. Metformin-Induced Mitochondrial Complex I Inhibition: Facts, Uncertainties, and Consequences. *Frontiers in Endocrinology*, 9: 753. <https://doi.org/10.3389/fendo.2018.00753>
14. Ghosh, P. 2017. The stress polarity pathway: AMPK 'GIV'-es protection against metabolic insults. *Aging*, 9(2): 303-314. <https://doi.org/10.18632/aging.101179>
15. Grdisa, M., Popovic, M. & Hrzenjak, T. 2001. Glycolipoprotein extract (G-90) from earthworm *Eisenia foetida* exerts some antioxidative activity. *Comparative Biochemistry and Physiology Part A: Molecular & Integrative Physiology*, 128(4): 821-825. [https://doi.org/10.1016/s1095-6433\(00\)00323-8](https://doi.org/10.1016/s1095-6433(00)00323-8)
16. Harrigan, R.A., Nathan, M.S. & Beattie, P. 2001. Oral agents for the treatment of type 2 diabetes mellitus: Pharmacology, toxicity, and treatment. *Annals of Emergency Medicine*, 38(1): 68-78. <https://doi.org/10.1067/mem.2001.114314>
17. Hasanvand, A., Abbaszadeh, A., Darabi, S., Nazari, A., Gholami, M. & Kharazmkia, A. 2016. Evaluation of selenium on kidney function following ischemic injury in rats; protective effects and antioxidant activity. *Journal of Renal Injury Prevention*, 6(2): 93-98. <https://doi.org/10.15171/jrip.2017.18>
18. Heredia Rivera, B., Rodríguez, M.G., Rodríguez-Heredia, M., Rodríguez-Heredia, B., Barois, I. & González Segovia, R. 2020. Characterisation by Excitation-Emission Matrix Fluorescence Spectroscopy of Pigments in Mucus Secreted of Earthworm *Eisenia foetida* Exposed to Lead. *Journal of Fluorescence*, 30(3): 725-733. <https://doi.org/10.1007/s10895-020-02533-y>
19. Houston, R., Sekine, Y., Larsen, M.B., Murakami, K., Mullett, S.J., Wendell, S.G., Narendra, D.P., Chen, B.B. & Sekine, S. 2021. Discovery of bactericides as an acute mitochondrial membrane damage inducer. *Molecular Biology of The Cell*, 32(21): ar32. <https://doi.org/10.1091/mbc.E21-04-0191>
20. Hua, Z., Wang, Y.-H., Cao, H.-W., Pu, L.-J. & Cui, Y.-D. 2011. Purification of a protein from coelomic fluid of the earthworm *Eisenia foetida* and evaluation of its hemolytic, antibacterial, and antitumor activities. *Pharmaceutical Biology*, 49(3): 269-275. <https://doi.org/10.3109/13880209.2010.508498>
21. Kilciler, Y., Deveci Ozkan, A. & Betts, Z. 2022. Protective effect of *Eisenia foetida* coelomic fluid against oxidative damage in human endothelial cells. *Toxicological & Environmental Chemistry*, 104(2): 307-320. <https://doi.org/10.1080/02772248.2022.2137165>
22. Kutoh, E. 2005. Possible metformin-induced hepatotoxicity. *The American Journal of Geriatric Pharmacotherapy*, 3(4): 270-273.
23. LaMoia, T. E. & Shulman, G. I. 2021. Cellular and Molecular Mechanisms of Metformin Action. *Endocrine Reviews*, 42(1): 77-96. <https://doi.org/10.1210/endrev/bnaa023>
24. Lin, Z., Zhen, Z., Ren, L., Yang, J., Luo, C., Zhong, L., Hu, H., Liang, Y., Li, Y. & Zhang, D. 2018. Effects of two ecological earthworm species on atrazine degradation performance and bacterial community structure in red soil. *Chemosphere*, 196: 467-475. <https://doi.org/10.1016/j.chemosphere.2017.12.177>
25. Nammour, F.E., Fayad, N.F. & Peikin, S.R. 2003. Metformin-Induced Cholestatic Hepatitis. *Endocrine Practice*, 9(4): 307-309. <https://doi.org/10.4158/EP.9.4.307>
26. Ozkan, A.D., Eskiler, G.G., Sarihan, M., Kazan, N., Aksoy, O., Yuksel, B. & Betts, Z. 2022. Anticancer Properties of *Eisenia Foetida* Proteins in Prostate Cancer Cells In Vitro. *International Journal of Peptide Research and Therapeutics*, 28(4): 119. <https://doi.org/10.1007/s10989-022-10428-8>



27. Park, H.J., Zhang, Y., Georgescu, S.P., Johnson, K.L., Kong, D. & Galper, J.B. 2006. Human umbilical vein endothelial cells and human dermal microvascular endothelial cells offer new insights into the relationship between lipid metabolism and angiogenesis. *Stem Cell Reviews*, 2(2): 93-102. <https://doi.org/10.1007/s12015-006-0015-x>
28. Pfeiffer, A.F. & Klein, H.H. 2014. The treatment of type 2 diabetes. *Deutsches Arzteblatt International*, 111(5): 69-82. <https://doi.org/10.3238/arztebl.2014.0069>
29. Rafieian-Kopaei, M., Baradaran, A., Merrikhi, A., Nematbakhsh, M., Madihi, Y. & Nasri, H. 2013. Efficacy of Co-administration of Garlic Extract and Metformin for Prevention of Gentamicin-Renal toxicity in Wistar Rats: A Biochemical Study. *International Journal of Preventive Medicine*, 4(3): 258-264.
30. Romero, R., Erez, O., Hüttemann, M., Maymon, E., Panaitescu, B., Conde-Agudelo, A., Pacora, P., Yoon, B. H. & Grossman, L. I. 2017. Metformin, the aspirin of the 21st century: its role in gestational diabetes mellitus, prevention of preeclampsia and cancer, and the promotion of longevity. *American Journal of Obstetrics and Gynecology*, 217(3): 282-302. <https://doi.org/10.1016/j.ajog.2017.06.003>
31. Shi, G., Wang, Y., Yang, J., Liu, T., Luo, F., Jin, G., Ma, Y. & Zhang, Y. 2021. Effect of Cryptotanshinone on Measures of Rat Cardiomyocyte Oxidative Stress and Gene Activation Associated with Apoptosis. *Cardiorenal Medicine*, 11(1): 18-26. <https://doi.org/10.1159/000507184>
32. Stanton, R.C. 2015. Metformin Use in Type 2 Diabetes Mellitus With CKD: Is It Time to Liberalize Dosing Recommendations? *American Journal of Kidney Diseases*, 66(2): 193-195. <https://doi.org/10.1053/j.ajkd.2015.04.001>
33. Vargas, F. da S., Soares, D.G., Ribeiro, A.P.D., Hebling, J. & De Souza Costa, C.A. 2014. Protective Effect of Alpha-tocopherol Isomer from Vitamin E against the H<sub>2</sub>O<sub>2</sub> Induced toxicity on Dental Pulp Cells. *BioMed Research International*, 2014: 1-5. <https://doi.org/10.1155/2014/895049>
34. Vial, G., Demaille, D. & Guigas, B. 2019. Role of Mitochondria in the Mechanism(s) of Action of Metformin. *Frontiers in Endocrinology*, 10: 294. <https://doi.org/10.3389/fendo.2019.00294>
35. Wang, G.S. & Hoyte, C. 2019. Review of Biguanide (Metformin) toxicity. *Journal of Intensive Care Medicine*, 34(11-12): 863-876. <https://doi.org/10.1177/0885066618793385>



## Brominated flame retardant BDE-99 promotes apoptosis by intrinsic mitochondrial pathway in rat liver

Aysegül Cerkezkayabekir<sup>1\*</sup>, Elvan Bakar<sup>2</sup>, Deniz Yüksel Yence<sup>1</sup>

<sup>1</sup> Department of Biology, Faculty of Science, Trakya University, Edirne, TÜRKİYE

<sup>2</sup> Department of Basic Sciences of Pharmacy, Trakya University, Faculty of Pharmaceutical, Edirne, TÜRKİYE

### Cite this article as:

Cerkezkayabekir A., Bakar E. & Yüksel Yence D. 2025. Brominated flame retardant BDE-99 promotes apoptosis by intrinsic mitochondrial pathway in rat liver. *Trakya Univ J Nat Sci*, 26(1): 29-37, DOI: 10.23902/trkjinat.1366842

Received: 16 October 2024, Accepted: 30 January 2025, Online First: 05 March 2025, Published: 15 April 2025

**Abstract:** This study examined *in vivo* effects of 2,2',4,4',5-pentabromodiphenyl ether (BDE-99) on the liver of Wistar Albino rats (250-300 gr) in doses of 0.05 mg/kg and 0.1 mg/kg for ten days by gavage. Our objective was to investigate the effects of BDE-99 on the apoptotic process in the liver. Previous studies have shown that BDE-99 causes accumulation and oxidative damage in various tissues, especially the liver. Although the primary mechanism of BDE-99 toxicity is known to involve oxidative stress, limited information is available on its specific impact on apoptosis. Therefore, immunoreactivity of *Proliferating Cell Nuclear Antigen* (PCNA), Vimentin and Topoisomerase 2A (TOP2A) and Topoisomerase 2B (TOP2B) and Terminal deoxynucleotidyl transferase dUTP Nick End Labeling (TUNEL) were determined in the liver. Superoxide dismutase (SOD), Glutathione peroxidase (GPX) and Catalase (CAT) activities were measured in the liver. qRT-PCR analyses for the p53, Bax, Bcl-2, PCNA and Vimentin genes were carried out from paraffin-embedded liver tissues. Cell membrane damage, hypertrophy, endothelial injury, mononuclear cell infiltration in the liver were determined by Hematoxylin & Eosin. Immunoreactivity of TUNEL, Vimentin, TOP2A and TOP2B increased in both doses, but immunoreactivity of PCNA significantly increased only 0.1 mg/kg BDE-99 dose ( $p < 0.05$ ). SOD and GPX activities increased but CAT activity decreased significantly ( $p < 0.05$ ) in the liver. Bax, Bcl-2, PCNA, Vimentin gene expressions increased in a dose-dependent manner and p53 expression increased only in 0.1 mg/kg BDE-99. In conclusion, our results point out BDE-99 inducing apoptosis of the intrinsic mitochondrial pathway in rat liver and indicate that exposure to BDE-99 is possible to be a potential risk factor for liver diseases.

**Özet:** Bu çalışmada 2,2',4,4',5-pentabromodifenil eter (BDE-99), 0,05 mg/kg ve 0,1 mg/kg dozlarıyla Wistar Albino (250-300 gr) sıçanlara on gün boyunca gavaj yoluyla uygulandı ve karaciğer üzerine *in vivo* etkileri araştırıldı. Amacımız BDE-99'un karaciğerdeki apoptotik süreç üzerindeki etkilerini araştırmaktır. Önceki çalışmalar BDE-99'un çeşitli dokularda birikime ve oksidatif hasara neden olduğunu göstermiştir. BDE-99 toksisitesinin birincil mekanizmasının oksidatif stresi içerdiği bilinse de apoptozis üzerindeki spesifik etkisi hakkında sınırlı bilgi mevcuttur. Bu nedenle, karaciğerde *Proliferating Cell Nuclear Antigen* (PCNA), Vimentin ve Topoizomerase 2A (TOP2A) ve Topoizomerase 2B (TOP2B)'nin ve Terminal deoxynucleotidyl transferase dUTP Nick End Labeling (TUNEL) ile immünoreaktivitesi belirlendi. Karaciğerde Süperoksit dismutaz (SOD), Glutasyon peroksidaz (GPX) ve Katalaz (CAT) aktivitesi ölçüldü. Parafin gömülmüş karaciğer dokularından izole edilen total RNA kullanılarak sentezlenen cDNA örneklerinde, p53, Bax, Bcl-2, PCNA ve Vimentin genlerine yönelik qRT-PCR analizleri yapıldı. Karaciğerde hücre zarı hasarı, hipertrofi, endotel hasarı, mononükleer hücre infiltrasyonu Hematoksilen & Eozin boyama ile belirlendi. TUNEL, Vimentin, TOP2A ve TOP2B'nin immünreaktivitesi her iki dozda da arttı, ancak PCNA'nın immünreaktivitesi yalnızca 0,1 mg/kg BDE-99 dozunda anlamlı düzeyde arttı ( $p < 0.05$ ). Karaciğerde SOD ve GPX aktiviteleri arttı ancak CAT aktivitesi anlamlı düzeyde azaldı ( $p < 0.05$ ). Bax, Bcl-2, PCNA, Vimentin gen ekspresyonu doza bağlı olarak artarken, p53 ekspresyonu sadece 0,1 mg/kg BDE-99 dozunda arttı. Sonuç olarak, bulgularımız sıçan karaciğerinde BDE-99'un intrinsik mitokondriyal yolda apoptozu indüklediğine işaret etmekte ve BDE-99'a maruz kalmanın karaciğer hastalıkları için potansiyel bir risk faktörü olabileceğini göstermektedir.

**Edited by:**  
Reşat Ünal

**\*Corresponding Author:**  
Aysegül Cerkezkayabekir  
[aysegulckb@trakya.edu.tr](mailto:aysegulckb@trakya.edu.tr)

**ORCID iDs of the authors:**  
AC. 0000-0001-5537-1042  
EB. 0000-0001-5703-3469  
DYY. 0000-0001-8696-9725

**Key words:**  
BDE-99  
Apoptosis  
TUNEL  
Immunohistochemistry  
Antioxidant enzymes  
qRT-PCR



OPEN ACCESS

## Introduction

Polybrominated diphenyl ethers (PBDEs) have been used commercially as a flame retardant on a global scale since 1970 (Alaee *et al.* 2003, Albina *et al.* 2010). While the main source of PBDEs is exposure to seafood, air, water, household waste and domestic dust, the most important way of intake is nutrition (Hooper & McDonald 2000, Bakker *et al.* 2008). Accumulation of 2,2',4,4',5-pentabromodiphenyl ether (BDE-99), a derivative of PBDE, is more common in liver and adipose tissues compared to other PBDEs (Guenius *et al.* 2001). The deposition sites of BDE-99, a well-absorbed brominated flame retardant species and the second most abundant congener, were reported to be the lipophilic tissues (Birnbaum & Staskal 2004, Johnson-Restrepo *et al.* 2005). In a study with mouse and human preadipocyte, BDE-99 administration was shown to lead to increased lipid accumulation. BDE-99 induced differentiation and lipid accumulation in undifferentiated preadipocytes (Armstrong *et al.* 2020). In a study on rats where a mixture of BDE-47 and BDE-99 was used, isoproterenol-induced lipolysis increased and altered insulin signaling (Hoppe & Carey 2007). Furthermore, tissue disposition and toxicokinetics of PBDEs, especially BDE-99 and BDE-47, were pointed out as risk factors for human health (Darnierud *et al.* 2001, Hakk *et al.* 2002, Staskal *et al.* 2006).

PBDE-induced hypertrophy and vacuolization in hepatocytes and increased liver weight were reported to occur in rats and mice after oral exposure (Dunnick & Nyska 2009). Histological examination of kidneys of adult mice showed that BDE-99 caused phagolysosomes in kidney (Chen *et al.* 2006, Albina *et al.* 2010). BDE-99 decreased Catalase (CAT) activity significantly but Superoxide dismutase (SOD) and Glutathione peroxidase (GPX) activities increased in liver of adult male mice after exposure for 45 days by gavage (Albina *et al.* 2010). BDE-99 decreased glutathione (GSH) and increased oxidized glutathione (GSSG) and GSSG/GSH levels in liver and radicalic damage was described as potential mechanism for hepatotoxicity by acute oral administration of BDE-99 (Albina *et al.* 2010). BDE-99 decreased testicular weight and sperm count at high doses in male rats (Kuriyama *et al.* 2005). Wang *et al.* (2015) reported, in their study investigating tumorigenesis, that BDE-99 may cause metastasis in cancer cell line via the PI3K/AKT/Snail pathway.

The consideration of results of the available studies shows that little is known about the mechanism of toxicity of BDE-99. One of the suggested toxicity mechanisms is the increase of reactive oxygen species (ROS) that can affect liver and kidney (Albina *et al.* 2010). There are limited published studies on the effect of BDE-99 on the apoptotic process, and all these studies are *in vitro* studies. Madia *et al.* (2004) defined the apoptotic properties of BDE-99 at immunohistochemical level through Terminal deoxynucleotidyl transferase dUTP Nick End Labeling (TUNEL) Hoechst 33258 and p53. Souza *et al.* (2013) showed that a high dose (25  $\mu$ M) of BDE-99 caused

apoptosis in HepG2 cells. Wu *et al.* (2023) reported that BDE-99 induced spermatogenic cell apoptosis in GC-1 spg cell line. In the studies investigating the toxic effects of BDE-99, the main focus has been on the mechanism of this effect without sufficient explanation, especially on the triggering of the apoptotic process and the expression of related genes. The fact that the apoptotic properties of BDE-99 have not been demonstrated by *in vivo* studies also points to a gap in this regard. For this reason, this is the first *in vivo* study explaining the toxic effect mechanism of BDE-99 on apoptotic markers in rat liver. We aimed to reveal the effect of BDE-99 *in vivo* on the apoptotic process and expression of the related genes p53, Bax, Bcl-2, Proliferating Cell Nuclear Antigen (PCNA), Topoisomerase 2A (TOP2A), Topoisomerase 2B (TOP2B) and Vimentin in liver as a main detoxification organ.

## Materials and Methods

### Animals and the experimental protocol

Twenty-four adult male Wistar albino rats (250-300 g) obtained from the Trakya University Experimental Animal Research Unit were used in the study. The rats were kept under controlled conditions (22 $\pm$ 10°C, 12 h light/dark cycle) during the experimental period and fed with drinking water and pellet feed containing 21% crude protein. Animals were divided into three random groups ( $n=8$  for each). The animals of one of the two experimental groups were fed with 0.05 mg/kg body weight BDE-99 (Cas No: 60348-60-9 Sigma-Aldrich) dissolved in corn oil by gavage, and those of the other group was fed 0.1 mg/kg body weight BDE-99 dissolved in corn oil by gavage (1-1.5 ml dose volume). These doses are lower than the 0.6 and 1.2 mg/kg body weight doses used by Albina *et al.* (2010), which are the lowest *in vivo* doses previously tested. The control group was given only the same volume of corn oil orally. The design of the study and the experimental procedures were approved by the Ethical Committee of Trakya University (Protocol number: 2016/48).

### Histopathological examination

After 10 days of the experiment, liver tissue samples were harvested by anaesthesia with Rompun (2%, Bayer) and Ketazol (10%, Richterpharma) for histopathological examination. The samples were fixed with formalin (10%) for 24 hours for light microscopy and embedded in paraffin. Sections (5  $\mu$ m) were stained with Hematoxylin & Eosin (H&E).

### Immunohistochemistry (IHC)

For avidin and biotinylated enzyme complex (ABC) method, firstly, liver sections (5 $\mu$ m) were kept in xylene for deparaffinization and rehydrated by series of ethanol. Then antigen retrieval was performed in citrate buffer (pH: 6.0) for 45 min using an IHC evaporating bath (IHC World, Woodstock, MD). After cooling to room temperature for 20 min, they were applied in 3% hydrogen peroxide (H<sub>2</sub>O<sub>2</sub>) and methanol for 5 min and treated twice

with phosphate-buffered saline (PBS) and once with PBS that contained 0.1% Tween-20 (PBS-T). Ultra V block (Thermo Scientific, Waltham, MA) was applied to each slide for 5 min in a humidified chamber (Bakar *et al.* 2015b). The sections were treated with anti-PCNA (1:500) (NB500-106/Novus), anti-Vimentin (1:100) (NBP1-31327/Novus), anti-TOP2A (1:100) (NBP2-67442/Novus) and anti-TOP2B (1:100) (NBP1-89527/Novus) as a primary antibody at room temperature for 1 hour and overnight at +4°C. After washing three times for 5 min each time with PBS, they were treated with biotinylated goat anti-polyvalent (ab7481, Abcam) for 10 min and washed four times in buffer. Streptavidin peroxidase was then applied for 10 min at room temperature. The slides were washed with PBS and with PBS-T. After washing, the sections were stained with DAB (Vector SK-4100, Vector Laboratories, Peterborough, UK) and then Mayer's Hematoxylin (Sigma, Aldrich). Immunohistochemical analysis was performed by systematic random samplings in each group using ten cross-sectional areas and five slides. For the evaluation of immunoreactivity of PCNA, the proliferation index was calculated by counting the (+) cells in an average of 1000 cells in 5 different areas in the sections of 8 subjects belonging to each group. Positive cells of Vimentin, TOP2A and TOP2B were counted in 5 different fields and their immunoreactivity was scored between 1 (+) and 5 (+) at most. All scoring was done by a randomized selection of microscopic fields and a double-blind by two researchers, the mean of which was used for statistical analysis.

#### In situ detection of apoptotic cells (TUNEL)

Liver sections (5 µm) were taken on poly-L-lysine-coated slides (Sigma, PO425-72EA). Apoptotic liver cells were detected with the TUNEL method (ApopTaqPeroxidase In Situ Apoptosis Detection Kit; S7101-KIT, Millipore) following the manufacturer's instructions. Rodent mammary gland sections and distilled water were used as the positive and the negative controls, respectively. Ten randomly selected fields under the light microscope were evaluated for each animal of the groups and the apoptotic cells were determined by their intense brown nuclear staining. The average of apoptotic cell numbers per liver sample and standard deviation (SD) were expressed as the score of TUNEL (Bakar *et al.* 2015a).

#### Quantitative Real Time Polymerase Chain Reaction (qRT-PCR)

Changes in expression levels of p53, Bax, Bcl-2, PCNA and Vimentin genes were determined by using qRT-PCR. For this purpose, firstly total RNA was isolated from paraffin embedded tissue samples using the High Pure FFPE RNA Isolation Kit (Roche, Cat No: 06 650775001) as recommended by the manufacturer. Complementary DNA (cDNA) synthesis was performed using the Transcriptor First Strand cDNA synthesis Kit (Roche, Cat No. 04896866001) using random hexamers according to the manufacturer's instructions. The obtained cDNA samples were stored at -20°C until the time to be

used as a template in qRT-PCR. qRT-PCR was performed with ABI Step One Plus (Thermo Pico) thermal cycler. The sequences of the primers used in the study are shown in Table 1. Amplifications of the PCR products were monitored via SYBR Green I dye which is an intercalator-based method. qRT-PCR mix was prepared with 5 µl cDNA, 12.5 µl SYBR Green 2X master mix, 1 µl forward and reverse primers (10 pmol/µl) and 6.5 µl ddH<sub>2</sub>O in 25 µl total reaction volume. The cycling program consisted of an initial denaturation at 95°C for 10 min, followed by 50 cycles of 95°C for 15 s, 60°C for 1 min, 60°C for 1 min for all genes. The specificity of the primers used in PCR was confirmed by melting curve analysis during qRT-PCR as well as optimization studies. Expression levels of the target genes were normalized using the internal gene GAPDH and compared with the data obtained from the control group according to the 2-ΔΔCT method (Livak & Schmittgen 2001).

#### Antioxidant enzyme assay (SOD, GPX and CAT)

The liver samples were washed with saline and placed in deep freezer for storage at -80°C for the biochemical parameters by the time the assay is performed. The liver samples (0.5 g) were homogenized with phosphate buffer [0.05 M, pH: 7.0, containing 1% (g/mL) Triton X-100]. The extracted volume was centrifuged at 12,000 g at +4°C for 20 min and the supernatant was assayed for SOD, GPX and CAT activities. The SOD and GPX activities were monitored by a spectrophotometer (Schimadzu UV-VIS) at 37°C by the Ransod SD 125 kit (Randox) (Arthur & Boyne 1985, Bakar *et al.* 2015b) and Ransel RS 505 kit (Randox), respectively (Kraus & Ganther 1980, Topcu-Tarlacalisir *et al.* 2013, Bakar *et al.* 2015b). CAT activity was determined by measuring decomposed 1 µmol H<sub>2</sub>O<sub>2</sub> per minute at 37°C according to Aebi (1974) (Aebi 1974) One-unit SOD activity was defined as the amount of enzyme that causes a 50% inhibition of the rate of reduction of 2-(4-iodophenyl)-3-(nitrophenol)-5-phenyltetrazolium chloride. One-unit GPX activity was defined as the amount of enzyme that oxidized 1 µmol NADPH to NADP in 1 min.

**Table 1.** Primary sequences of the target genes and the internal gene.

Target genes	Primary sequences (5' → 3')	References
p53	CACAGTCGGATATGAGCATC GTCGTCCAGATACTCAGCAT	(Zaragoza <i>et al.</i> 2003)
Bax	GACACCTGAGCTGACCTTGG GAGGAAGTCCAGTGTCCAGC	(Die <i>et al.</i> 2019)
Bcl2	GGGATGCCTTTGTGGAACCTA CTCACTTGTGGCCAGGTAT	(Die <i>et al.</i> 2019)
Vimentin	CGTACGTCAGCAATATGAAAG TGTGTCAGAGAGGTCAGCAAA CTTGGA	(Dong <i>et al.</i> 2014)
PCNA	GGTGCTTGGCGGGAGC ATCGCTTGAGCCCAGAAGT	(Moldovan <i>et al.</i> 2007)
GAPDH	GCATCTTCTTGTGCAGTGCC GATGGTGATGGGTTTCCCGT	(Potmesil <i>et al.</i> 1988)



One-unit CAT was defined as the amount of enzyme that decomposed 1  $\mu\text{mol}$   $\text{H}_2\text{O}_2$  per minute at 37°C and pH: 7.0. The amount of total protein was measured according to Lowry (Lowry *et al.* 1951). All enzyme activities were presented as U/mg protein.

#### Statistical analysis

All data from body weight, immunohistochemical analysis, antioxidant enzyme activities, TUNEL assay and relative expression levels of target genes are expressed as the mean $\pm$ standard deviation (SD). Non-normally distributed groups (body weights, all immunohistochemical scoring) were tested with the Kruskal-Wallis test and enzyme activities was tested Mann-Whitney U test for comparison between two groups. Student-t test was performed to determine changes in relative expression levels of target genes between the experimental groups and the control group. SPSS 16 for Windows (IBM SPSS Inc., Chicago, IL, USA) software was used for statistical analyses. The results were considered statistically significant when  $p < 0.05$ .

#### **Results**

The conditions of the animals were checked every day during the experiment period before the administration. No injuries to the bodies of the animals or any deterioration in their general condition were observed during the experiment. The initial number of subjects was maintained because there was no animal death. The body weights of the animals before and after the experiment are presented in Table 2 as mean $\pm$  SD in all groups ( $n=8$ ). Body weight increased significantly in both the 0.05 mg/kg and the 0.1 mg/kg BDE-99 groups compared to the control group.

#### Histopathology of the liver

The general histological structure of the tissue was preserved in the liver of the control group (Fig. 1a) and the degenerative changes consisted in the liver of the experimental groups (0.05 mg/kg BDE-99 and 0.1 mg/kg BDE-99).

**Table 2.** The body weights of the animals before and after the experiment are presented as mean $\pm$ SD in all groups ( $n=8$ ).

	Body weight (before) $\pm$ SD	Body weight (after) $\pm$ SD
<b>Control group</b>	265.20 $\pm$ 9.23	266.50 $\pm$ 12.10
<b>0.05 mg/kg BDE-99</b>	265.11 $\pm$ 16.22	283.12 $\pm$ 14.21 <sup>a</sup>
<b>0.10 mg/kg BDE-99</b>	266.50 $\pm$ 14.84	287.00 $\pm$ 10.12 <sup>a</sup>

<sup>a</sup> indicates statistical significance compared with the control group,  $p < 0.05$ .

Irregularity in hepatocyte cords was observed in the 0.05 mg/kg BDE-99 group. Loss of integrity as a result of endothelial damage in the veins and mononuclear cell infiltration around the veins in small areas were determined (Fig. 1b). Hypertrophic hepatocytes and cytoplasm loss in hepatocytes were observed throughout the liver tissue in the 0.1 mg/kg BDE-99 group. Damaged hepatocyte membranes and cytoplasm loss around the nucleus of hepatocytes occurred. In addition, mononuclear cell infiltration around the veins more than the low dose of BDE-99 was determined (Fig. 1c).

#### In situ detection of apoptotic cells (TUNEL)

TUNEL results showed that apoptosis increased significantly in a dose-dependent manner in both doses of BDE-99 in the liver (Fig. 2).

#### Immunohistochemistry of the liver (IHC)

IHC staining was performed and scored to determine PCNA, Vimentin, TOP2A and TOP2B for immunoreactivity in the liver (Figs 3-4). Immunoreactivity of PCNA and TOP2B increased significantly only 0.1 mg/kg BDE-99 group when compared with the control group. Vimentin and TOP2A increased significantly in a dose-dependent manner in both doses of BDE-99 (Fig. 4).

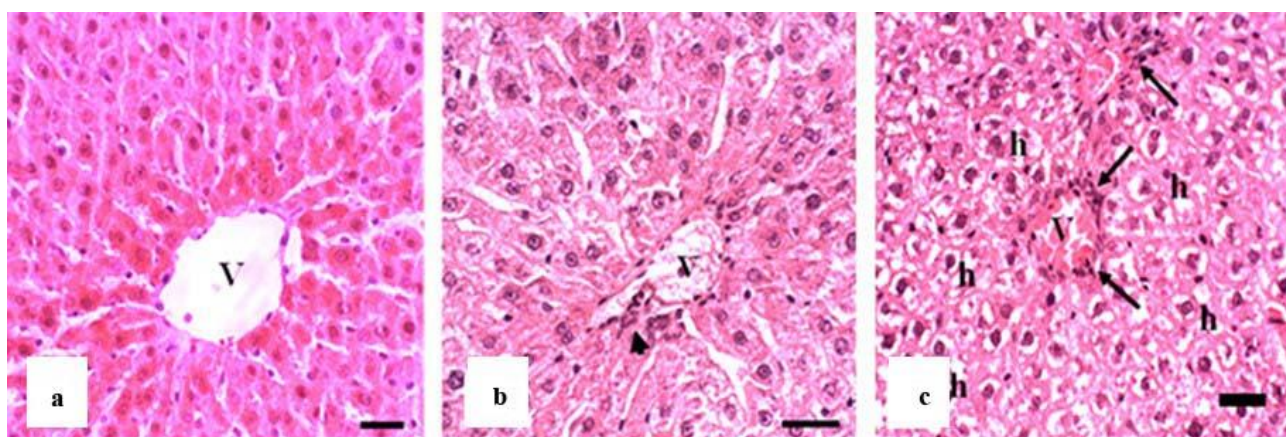


**Fig. 1.** Histopathology of liver (H&E staining) **a.** Control group; V: central vein, **b.** 0.05 mg/kg BDE-99 group; V: central vein, loss of integrity around central vein, arrow: irregularity in hepatocyte cords, and endothelial damage in the vein, **c.** 0.1 mg/kg BDE-99 group, h: hypertrophic hepatocytes and cytoplasm loss around the nucleus, arrows: mononuclear cell infiltration around the vein and loss of integrity in hepatocyte cords. Scale bar represents 40  $\mu\text{m}$ .



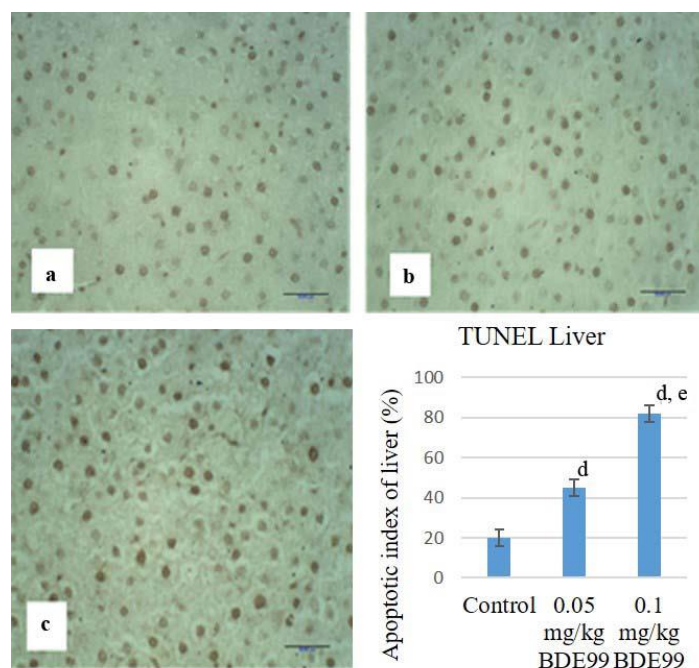


**Fig. 2.** TUNEL of liver. **a.** Control group, **b.** 0.05 mg/kg BDE-99 group, brown stained nuclei are indication of apoptotic cells, **c.** 0.1 mg/kg BDE-99 group, brown stained nuclei are indication of apoptotic cells. Scale bar represents 40  $\mu$ m. Apoptotic index of liver (%) by TUNEL. Values are presented as the mean $\pm$ SD, and  $n=8$  for all groups.

<sup>d</sup> indicates statistical significance compared with the control group. <sup>e</sup> indicates significance compared with the 0.5 mg/kg BDE-99 group,  $p < 0.05$ .

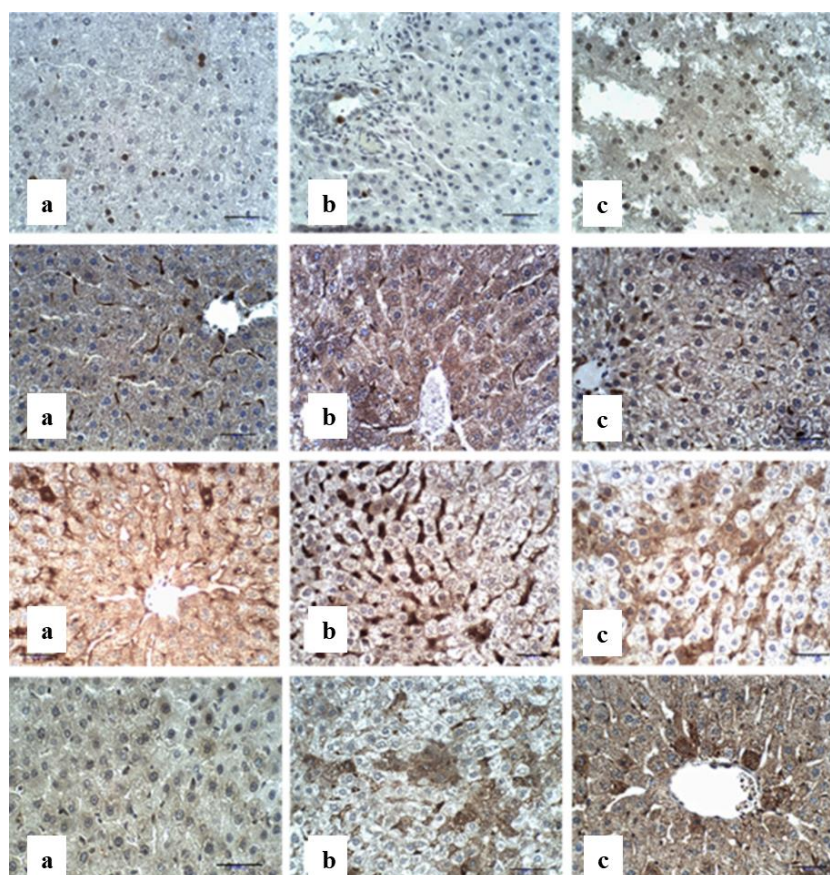


**Fig. 3.** Immunohistochemical (IHC) evaluation of liver. **a.** Control group, **b.** 0.05 mg/kg BDE-99 group, **c.** 0.1 mg/kg BDE-99 group. Line 1: PCNA, brown stained nuclei are indication of PCNA+ cells. Line 2: Vimentin, brown stained nuclei are indication of Vimentin+ cells. Line 3: TOP2A, brown stained nuclei are indication of TOP2A+ cells. Line 4: TOP2B, brown stained nuclei are indication of TOP2B+ cells. Scale bar represents 40  $\mu$ m.

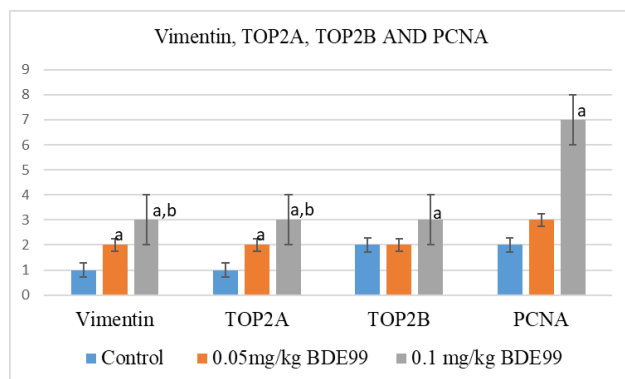


**Fig. 4.** IHC scores of Vimentin, TOP2A, TOP2B and PCNA in the liver. Values are presented as the mean±SD, and  $n=8$  for all groups.

<sup>a</sup> indicates statistical significance compared with the control group. <sup>b</sup> indicates significance compared with the 0.5 mg/kg BDE-99 group,  $p < 0.05$ .

#### Quantitative Real Time Polymerase Chain Reaction (qRT-PCR)

Gene expressions of Bax (6.3 fold), Bcl2 (5.7 fold), PCNA (6.95 fold) and Vimentin (34.35 fold) significantly increased in 0.05 mg/kg and Bax (4.33 fold), Bcl2 (6.25 fold), PCNA (25 fold) and Vimentin (48.95 fold) in 0.1 mg/kg BDE-99 groups, but p53 gene expression significantly increased (4.74 fold) only in the 0.1 mg/kg group (Fig. 5).

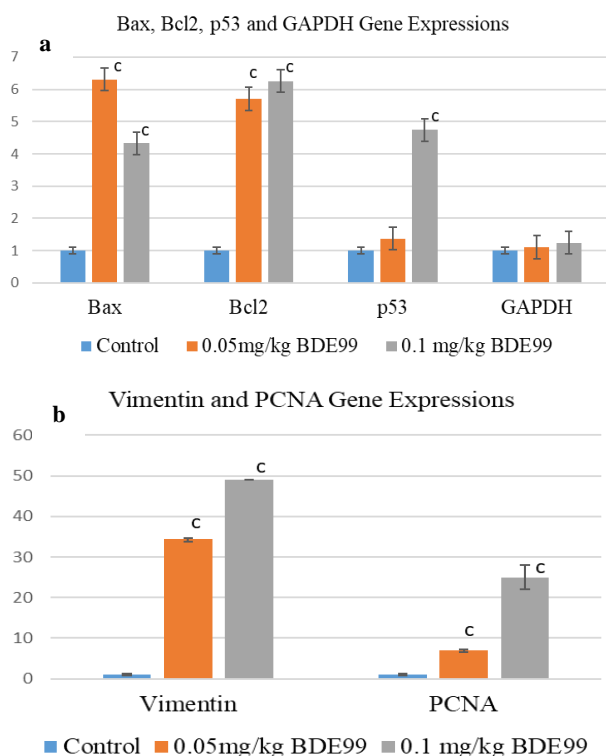


**Fig. 5.** Gene expressions in the liver. **a.** Bax, Bcl2, p53, GAPDH, **b.** vimentin and PCNA. Columns represent relative fold changes in mRNA expression of target genes normalized by GAPDH and mean±SD.

<sup>c</sup> represents statistically significant compared with the control group ( $p < 0.05$ ).

#### Antioxidant enzyme assay (SOD, GPX and CAT)

SOD and GPX activity increased significantly in both the 0.05 mg/kg and the 0.1 mg/kg BDE-99 groups but CAT activity decreased significantly only in 0.1 mg/kg BDE-99 group compared to the control group (Fig. 6).

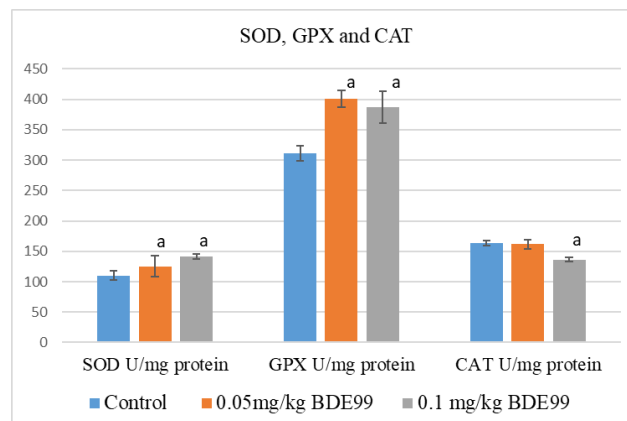


**Fig. 6.** SOD, GPX and CAT activities in the liver. Results were expressed as mean±SD.

<sup>a</sup> represents statistically significant compared with the control group ( $p < 0.05$ ).

#### **Discussion**

BDE-99 toxicity is important in human health because of its widespread use in many areas. In a risk assessment study, it was stated that long-term exposure to BDE-99 is significant in terms of reproductive toxicity (Bakker *et al.* 2008). Die *et al.* (2019) reported that PBDE emissions and risks are lower in modern, recycling facilities but pointed out that the effectiveness of pollution controls in other areas needs to be investigated further (Die *et al.* 2019). Dong *et al.* (2014) showed that waste of electrical and electronic equipment recycling contributed 52% of the PBDEs concentration in the surrounding agricultural soils (Dong *et al.* 2014). Although significant accumulation of BDE in lipophilic tissues and toxic effects in many tissues such as liver, kidney and reproductive systems have been described (Kuriyama *et al.* 2005, Bakker *et al.* 2008, Albina *et al.* 2010, Armstrong *et al.* 2020), the knowledge about the toxicity mechanism of BDE-99 is limited. In previous studies, ROS formation and related cellular degenerations were defined as the main toxicity mechanism for BDE-99, but there are also recent studies showing that apoptosis is induced by BDE-99. However, these are all *in vitro* studies and there is no study investigating the effect of BDE-99 on apoptosis *in vivo* in rats. Therefore, in the present study, we aimed to reveal the effect of BDE-99 primarily on the apoptotic process in the liver in addition to its histopathological examination and the presence of ROS with changes in key antioxidant enzyme activities.

BDE-99 damaged the general integrity of the liver tissue of the experimental animals, and significant lacking of cytoplasm and hypertrophy were observed in hepatocytes in liver as revealed by staining with H&E (Fig. 1). Similarly, it was reported that histopathological

effects occurred in the liver in the acute oral administration of BDE-99 (Albina *et al.* 2010) increase liver weights and lesions were observed in the liver after treatment of BDE-99 (Dunnick & Nyska 2009). We believe that the increase in animal weights observed in this study is consistent with widespread hypertrophic change in the liver.

We determined that apoptosis increased in a dose-dependent manner in liver by TUNEL immunoreactivity (Fig. 2). Madia *et al.* (2004) defined the apoptotic properties of BDE-99 at immunohistochemical level via TUNEL, Hoechst 33258 and p53. Similarly, Souza *et al.* (2013) showed that a high dose (25  $\mu$ M) of BDE-99 caused apoptosis in HepG2 cells. Wu *et al.* (2023) reported that BDE-99 induced spermatogenic cell apoptosis in GC-1 spg cell line by staining with Annexin V and count by flow cytometry. Our TUNEL results confirm that apoptosis is triggered in liver by the effect of BDE-99 in line with the *in vitro* studies mentioned above.

In the present study, PCNA immunoreactivity (Figs 3-4) and gene expression (Fig. 5) increased significantly in a dose-dependent manner in liver. PCNA, an important moderator of many functions in the DNA replication fork (Moldovan *et al.* 2007) indicates preparation for the increased mitotic activity for the repair of damaged liver tissue. We have not found any studies on how PCNA changes with the effect of BDE-99. Therefore, we think that this change is an adaptive response to the toxic effect of BDE-99.

Topoisomerase 2 is an enzyme that cuts two strands of DNA simultaneously and catalyses their reconnection, reducing the tension of the double strand of DNA. In this way, the effect of the rotation created by the helicase on DNA is prevented (Potmesil *et al.* 1988). Therefore, in cases where gene expression is increased, it is a normal physiological state to increase Topoisomerase 2 expression. In our study, TOP2A immunoreactivity increased significantly in the liver at both doses, but TOP2B immunoreactivity increased only at the dose of 0.1 mg/kg (Figs 3-4). These changes observed in TOP2A and TOP2B immunoreactivity are also consistent with increased PCNA and TUNEL immunoreactivity in the liver. It is possible that the increased PCNA, TOP2A, and TOP2B immunoreactivity signifies an adaptive proliferative response to BDE-99-induced cellular damage. It seems that while cellular damage occurs by induced apoptosis, the markers of the restoration process are activated in the liver tissue.

Expression of p53 in the liver increased only at the dose of 0.1 mg/kg, and the expressions of Bax and Bcl-2 increased significantly at both doses (Fig. 5). p53 is a central protein that responds to numerous cellular stress signals (Vaseva *et al.* 2012) and can be activated by hypoxia and oxidative stress. Activation of p53 results in cell cycle arrest, followed by DNA repair or induced apoptosis in various ways (Gudkov & Komarova 2010, Pflaum *et al.* 2014). One of these pathways to apoptosis is

the intrinsic mitochondrial pathway and proceeds via the Bcl-2 family, cytochrome c and caspases. In our study, we believe that the accumulation of p53 in the cytosol triggers the pro-apoptotic Bcl-2 proteins and the Bax protein directly, stimulating the cell to apoptosis. Consistent with the TUNEL results, the parallel increase in expressions of p53, Bax and Bcl-2 shows that the apoptotic process was triggered by the effect of BDE-99 in the liver (Fig. 5). Similarly, Wu *et al.* (2023) reported that PBDE-99 caused the formation of ROS, triggered autophagy and spermatogenic apoptosis in their studies examining the long-term effects of prenatal exposure on spermatogenic injuries. They showed that Bax, a pro-apoptotic protein, expression increased while Bcl-2 protein, anti-apoptotic protein, was slightly reduced due to BDE-99 toxicity with the other related genes. Our study determined that Bax gene expression and Bcl2 gene expression increased simultaneously. We observed that Bcl2 increased in a way contrary to Wu *et al.* (2023). When this increase in Bcl2 was evaluated with the increase in the p53 gene and TUNEL findings, we think that it occurs competitively with Bax and liver cells enter the intrinsic mitochondrial apoptotic pathway depending on the Bax/Bcl2 ratio. Yang *et al.* (2022) reported that induced oxidative stress, histopathological changes, DNA fragmentation, cell proliferation and apoptosis were observed in their study investigating the toxicity of BDE-47, the second most common type of PBDEs.

Wang *et al.* (2018) reported that apoptotic cells increased significantly in the brain of zebrafish (*Danio rerio*) embryos by early life exposure to BDE-47. Hou *et al.* (2019) showed that BDE-209, another toxic flame retardant, can induce apoptosis of vascular endothelial cells by increasing ROS production and induced ER stress. Consistently, the findings of our study are in line with other studies in which BDE-99 and/or some of its congeners have been reported to induce apoptosis.

Vimentin immunoreactivity and gene expression increased in the liver at both doses (Figs 4-5). The increase in both gene expression and the cytoplasmic amount of Vimentin protein in the liver, which is an essential component of the cytoskeleton, can be considered a sign of intracellular rearrangements. In light of these findings, it seems that this is accompanied by a rearrangement of the cytoskeleton, which is a cellular part of both the apoptotic process and the process of restoration by mitosis.

When we examine the changes in the activities of SOD, GPX and CAT, which are the key antioxidant enzymes (Fig. 6), we think that ROS-induced stress occurs in the liver, as indicated by the increase in SOD and GPX activities. The decrease in CAT activity also suggests that there may be a deficiency in the removal of H<sub>2</sub>O<sub>2</sub> via peroxisomes, but a cellular response is effectuated with GPX to H<sub>2</sub>O<sub>2</sub> in the cytosol. It has been stated in previous studies that BDE-99 causes oxidative damage (Albina *et al.* 2010) and it has been accepted as the main toxicity mechanism.



In conclusion, our findings display BDE-99 inducing apoptosis via the intrinsic mitochondrial pathway in the rat liver. We think that this study, in which we have shown *in vivo* that this pathway is triggered in the p53, Bax and Bcl-2 axis, will contribute to regarding studies on the subject in detail. We report that BDE-99, as a flame retardant species which humans are increasingly exposed to, is a potential risk factor for liver diseases.

#### Acknowledgement

The authors would like to thank Dr. Pelin Türker (Edirne, Türkiye), from Technology Research and Development Application and Research Center (TÜTAGEM) of Trakya University, Edirne, Türkiye for her support in the performing of the qRT-PCR.

**Ethics Committee Approval:** Ethics committee approval was received for this study from the Ethics Committee of Trakya University by the number TUHADYEK 2016/48.

#### References

1. Aebi, H. 1974. Catalase, 673-684. In H. U. Bergmeyer (Ed.), *Methods of Enzymatic Analysis (Second Edition)*, Academic Press, 673-684 pp.
2. Alaei, M., Arias, P., Sjödin, A. & Bergman, A. 2003. An overview of commercially used brominated flame retardants, their applications, their use patterns in different countries/regions and possible modes of release. *Environment International*, 29(6): 683-689. [https://doi.org/10.1016/S0160-4120\(03\)00121-1](https://doi.org/10.1016/S0160-4120(03)00121-1)
3. Albina, M.L., Alonso, V., Linares, V., Belles, M., Sirvent, J.J., Domingo, J.L. & Sanchez, D.J. 2010. Effects of exposure to BDE-99 on oxidative status of liver and kidney in adult rats. *Toxicology*, 271(1-2): 51-56. <https://doi.org/10.1016/j.tox.2010.03.006>
4. Armstrong, L.E., Akinbo, S. & Slitt, A.L. 2020. 2,2',4,4',5-Pentabromodiphenyl ether induces lipid accumulation throughout differentiation in 3T3-L1 and human preadipocytes *in vitro*. *Journal of Biochemical And Molecular Toxicology*, 34(6): e22485. <https://doi.org/10.1002/jbt.22485>
5. Arthur, J.R. & Boyne, R. 1985. Superoxide dismutase and glutathione peroxidase activities in neutrophils from selenium deficient and copper deficient cattle. *Life Science*, 36(16): 1569-1575. [https://doi.org/10.1016/0024-3205\(85\)90381-9](https://doi.org/10.1016/0024-3205(85)90381-9)
6. Bakar, E., Ulucam, E. & Cerkez kayabekir, A. 2015a. Investigation of the protective effects of proanthocyanidin and vitamin E against the toxic effect caused by formaldehyde on the liver tissue. *Environmental Toxicology*, 30(12): 1406-1415. <https://doi.org/10.1002/tox.22010>
7. Bakar, E., Ulucam, E. & Cerkez kayabekir, A. 2015b. Protective effects of proanthocyanidin and vitamin E against toxic effects of formaldehyde in kidney tissue. *Biotechnic & Histochemistry*, 90(1): 69-78. <https://doi.org/10.3109/10520295.2014.954620>
8. Bakker, M.I., de Winter-Sorkina, R., de Mul, A., Boon, P.E., van Donkersgoed, G., van Klaveren, J.D., Baumann, B.A., Hijman, W.C., van Leeuwen, S.P., de Boer, J. & Zeilmaker, M.J. 2008. Dietary intake and risk evaluation of polybrominated diphenyl ethers in The Netherlands. *Molecular Nutrition & Food Research*, 52(2): 204-216. <https://doi.org/10.1002/mnfr.200700112>
9. Birnbaum, L.S. & Staskal, D.F. 2004. Brominated flame retardants: cause for concern? *Environmental Health Perspectives*, 112(1): 9-17. <https://doi.org/10.1289/ehp.6559>
10. Chen, L.J., Lebetkin, E.H., Sanders, J.M. & Burka, L.T. 2006. Metabolism and disposition of 2,2',4,4',5-pentabromodiphenyl ether (BDE99) following a single or repeated administration to rats or mice. *Xenobiotica*, 36(6): 515-534. <https://doi.org/10.1080/00498250600674477>
11. Darnerud, P.O., Eriksen, G.S., Johannesson, T., Larsen, P.B. & Viluksela, M. 2001. Polybrominated diphenyl ethers: occurrence, dietary exposure, and toxicology. *Environmental Health Perspectives*, 109 Suppl 1: 49-68. <https://doi.org/10.1289/ehp.01109s149>
12. Die, Q., Nie, Z., Huang, Q., Yang, Y., Fang, Y., Yang, J. & He, J. 2019. Concentrations and occupational exposure assessment of polybrominated diphenyl ethers in modern Chinese e-waste dismantling workshops. *Chemosphere*, 214: 379-388. <https://doi.org/10.1016/j.chemosphere.2018.09.130>
13. Dong, Y., Li, L., Bie, P., Jia, S., Wang, Q., Huang, Z., Qiu, X., Zhang, J. & Hu, J. 2014. Polybrominated diphenyl ethers in farmland soils: Source characterization, deposition contribution and apportionment. *Science of The Total Environment*, 466-467: 524-532. <https://doi.org/10.1016/j.scitotenv.2013.07.058>
14. Dunnick, J.K. & Nyska, A. 2009. Characterization of liver toxicity in F344/N rats and B6C3F1 mice after exposure to a flame retardant containing lower molecular weight polybrominated diphenyl ethers. *Experimental and Toxicologic Pathology*, 61(1): 1-12. <https://doi.org/10.1016/j.etp.2008.06.008>
15. Gudkov, A.V. & Komarova, E.A. 2010. Pathologies associated with the p53 response. *Cold Spring Harbor Perspectives in Biology*, 2(7): a001180. <https://doi.org/10.1101/cshperspect.a001180>
16. Guvenius, D., Bergman, A. & Norén, K. 2001. Polybrominated Diphenyl Ethers in Swedish Human Liver

**Data Sharing Statement:** All data are available within the study.

**Author Contributions:** Concept: A.C., E.B., Design: A.C., E.B., Execution: A.C., E.B., D.Y.Y., Material supplying: A.C., E.B., Data acquisition: A.C., E.B., D.Y.Y., Data analysis/interpretation: A.C., E.B., D.Y.Y., Writing: A.C., Critical review: E.B., D.Y.Y.

**Conflict of Interest:** The authors have no conflicts of interest to declare.

**Funding:** The study was supported by the Trakya University Scientific Research Committee with project number 2017/85.

**Editor-in-Chief note:** Aysegül Cerkez kayabekir is a member of Editorial Board of Trakya University Journal of Natural Sciences. However, she wasn't involved in the decision process during manuscript evaluation.

- and Adipose Tissue. *Archives Of Environmental Contamination And Toxicology*, 40: 564-570. <https://doi.org/10.1007/s002440010211>
17. Hakk, H., Larsen, G. & Klasson-Wehler, E. 2002. Tissue disposition, excretion and metabolism of 2,2',4,4',5-pentabromodiphenyl ether (BDE-99) in the male Sprague-Dawley rat. *Xenobiotica*, 32(5): 369-382. <https://doi.org/10.1080/00498250110119117>
  18. Hooper, K. & McDonald, T.A. 2000. The PBDEs: an emerging environmental challenge and another reason for breast-milk monitoring programs. *Environmental Health Perspectives*, 108(5): 387-392. <https://doi.org/10.1289/ehp.00108387>
  19. Hoppe, A.A. & Carey, G.B. 2007. Polybrominated diphenyl ethers as endocrine disruptors of adipocyte metabolism. *Obesity (Silver Spring)*, 15(12): 2942-2950. <https://doi.org/10.1038/oby.2007.351>
  20. Hou, Y., Fu, J., Sun, S., Jin, Y., Wang, X. & Zhang, L. 2019. BDE-209 induces autophagy and apoptosis via IRE1 $\alpha$ /Akt/mTOR signaling pathway in human umbilical vein endothelial cells. *Environmental Pollution*, 253: 429-438. <https://doi.org/10.1016/j.envpol.2019.07.030>
  21. Johnson-Restrepo, B., Kannan, K., Rapaport, D.P. & Rodan, B.D. 2005. Polybrominated diphenyl ethers and polychlorinated biphenyls in human adipose tissue from New York. *Environmental Science & Technology*, 39(14): 5177-5182. <https://doi.org/10.1021/es050399x>
  22. Kraus, R.J. & Ganther, H.E. 1980. Reaction of cyanide with glutathione peroxidase. *Biochemical And Biophysical Research Communications*, 96(3): 1116-1122. [https://doi.org/10.1016/0006-291x\(80\)90067-4](https://doi.org/10.1016/0006-291x(80)90067-4)
  23. Kuriyama, S.N., Talsness, C.E., Grote, K. & Chahoud, I. 2005. Developmental exposure to low dose PBDE 99: effects on male fertility and neurobehavior in rat offspring. *Environmental Health Perspectives*, 113(2): 149-154. <https://doi.org/10.1289/ehp.7421>
  24. Livak, K.J. & Schmittgen, T.D. 2001. Analysis of relative gene expression data using real-time quantitative PCR and the 2<sup>(-Delta Delta C(T))</sup> Method. *Methods*, 25(4): 402-408. <https://doi.org/10.1006/meth.2001.1262>
  25. Lowry, O.H., Rosebrough, N.J., Farr, A.L. & Randall, R.J. 1951. Protein measurement with the Folin phenol reagent. *The Journal of Biological Chemistry*, 193(1): 265-275. [https://doi.org/10.1016/S0021-9258\(19\)52451-6](https://doi.org/10.1016/S0021-9258(19)52451-6)
  26. Madia, F., Giordano, G., Fattori, V., Vitalone, A., Branchi, I., Capone, F. & Costa, L.G. 2004. Differential in vitro neurotoxicity of the flame retardant PBDE-99 and of the PCB Aroclor 1254 in human astrocytoma cells. *Toxicol Lett*, 154(1-2): 11-21. <https://doi.org/10.1016/j.toxlet.2004.06.013>
  27. Moldovan, G.L., Pfander, B. & Jentsch, S. 2007. PCNA, the maestro of the replication fork. *Cell*, 129(4): 665-679. <https://doi.org/10.1016/j.cell.2007.05.003>
  28. Pflaum, J., Schlosser, S. & Muller, M. 2014. p53 Family and Cellular Stress Responses in Cancer. *Frontiers in Oncology*, 4: 285. <https://doi.org/10.3389/fonc.2014.00285>
  29. Potmesil, M., Hsiang, Y.H., Liu, L.F., Bank, B., Grossberg, H., Kirschenbaum, S., Forlenza, T.J., Penziner, A., Kanganis, D. & et al. 1988. Resistance of human leukemic and normal lymphocytes to drug-induced DNA cleavage and low levels of DNA topoisomerase II. *Cancer Research*, 48(12): 3537-3543.
  30. Souza, A.O., Pereira, L.C., Oliveira, D.P. & Dorta, D.J. 2013. BDE-99 congener induces cell death by apoptosis of human hepatoblastoma cell line - HepG2. *Toxicology In Vitro*, 27(2): 580-587. <https://doi.org/10.1016/j.tiv.2012.09.022>
  31. Staskal, D.F., Hakk, H., Bauer, D., Diliberto, J.J. & Birnbaum, L.S. 2006. Toxicokinetics of polybrominated diphenyl ether congeners 47, 99, 100, and 153 in mice. *Toxicological Sciences*, 94(1): 28-37. <https://doi.org/10.1093/toxsci/kfl091>
  32. Topcu-Tarlacalisir, Y., Akpolat, M., Uz, Y.H., Kizilay, G., Sapmaz-Metin, M., Cerkezayabekir, A. & Omurlu, I.K. 2013. Effects of curcumin on apoptosis and oxidoinflammatory regulation in a rat model of acetic acid-induced colitis: the roles of c-Jun N-terminal kinase and p38 mitogen-activated protein kinase. *Journal of Medicinal Food*, 16(4): 296-305. <https://doi.org/10.1089/jmf.2012.2550>
  33. Vaseva, A.V., Marchenko, N.D., Ji, K., Tsirka, S.E., Holzmann, S. & Moll, U.M. 2012. p53 opens the mitochondrial permeability transition pore to trigger necrosis. *Cell*, 149(7): 1536-1548. <https://doi.org/10.1016/j.cell.2012.05.014>
  34. Wang, F., Fang, M., Hinton, D.E., Chernick, M., Jia, S., Zhang, Y., Xie, L., Dong, W. & Dong, W. 2018. Increased coiling frequency linked to apoptosis in the brain and altered thyroid signaling in zebrafish embryos (Danio rerio) exposed to the PBDE metabolite 6-OH-BDE-47. *Chemosphere*, 198: 342-350. <https://doi.org/10.1016/j.chemosphere.2018.01.081>
  35. Wang, F., Ruan, X.J. & Zhang, H.Y. 2015. BDE-99 (2,2',4,4',5-pentabromodiphenyl ether) triggers epithelial-mesenchymal transition in colorectal cancer cells via PI3K/Akt/Snail signaling pathway. *Tumori*, 101(2): 238-245. <https://doi.org/10.5301/tj.5000229>
  36. Wu, J., Deng, F., Tang, X., Chen, W., Zhou, R., Zhao, T., Mao, X. & Shu, F. 2023. Long-term effect of PBDE-99 prenatal exposure on spermatogenic injuries via the dysregulation of autophagy. *Journal of Hazardous Materials*, 452: 131234. <https://doi.org/10.1016/j.jhazmat.2023.131234>
  37. Yang, Y., Wang, L., Zhao, Y., Ma, F., Lin, Z., Liu, Y., Dong, Z., Chen, G. & Liu, D. 2022. PBDEs disrupt homeostasis maintenance and regeneration of planarians due to DNA damage, proliferation and apoptosis anomaly. *Ecotoxicology and Environmental Safety*, 248: 114287. <https://doi.org/10.1016/j.ecoenv.2022.114287>
  38. Zaragoza, R., Garcia, C., Rus, A.D., Pallardo, F.V., Barber, T., Torres, L., Miralles, V.J. & Vina, J.R. 2003. Inhibition of liver trans-sulphuration pathway by propargylglycine mimics gene expression changes found in the mammary gland of weaned lactating rats: role of glutathione. *The Biochemical Journal*, 373 (Pt 3): 825-834. <https://doi.org/10.1042/BJ20030387>





## 6,3'-dimethoxy flavonol: Evidence-based insights into anti-proliferative and apoptotic effect on osteosarcoma cells

Kaniga Pandi<sup>1\*</sup>, Binoy Varghese Cheriyan<sup>1</sup>, Srinithi Manikandan<sup>1</sup>, Jayavarthini Jayaraman<sup>1</sup>, Lokesh Kumar Harikrishnan<sup>1</sup>, Vijaykumar Sayeli<sup>2</sup>, Elumalai Perumal<sup>3</sup>

<sup>1</sup> Department of Pharmaceutical Chemistry, Saveetha College of Pharmacy, SIMATS, Chennai, 600077, Tamil Nadu, INDIA

<sup>2</sup> Department of Pharmacology, Mamata Medical College, Khammam, 507002, Telangana, INDIA

<sup>3</sup> Department of Pharmacology, Cancer Genomics Lab, Saveetha Dental College and Hospital, Saveetha Institute of Medical and Technical Sciences, SIMATS, Chennai, 600077, Tamil Nadu, INDIA

### Cite this article as:

Pandi K., Cheriyan B.V., Manikandan S., Jayaraman J., Harikrishnan L.K., Sayeli V. & Perumal E. 2025. 6,3'-dimethoxy flavonol: Evidence-based insights into anti-proliferative and apoptotic effect on osteosarcoma cells. *Trakya Univ J Nat Sci*, 26(1): 39-47, DOI: 10.23902/trkijnat.1615568

Received: 08 January 2025, Accepted: 23 March 2025, Published: 15 April 2025

Edited by:  
İpek Süntar

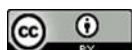
\*Corresponding Author:  
Kaniga Pandi  
[kanigapharma@gmail.com](mailto:kanigapharma@gmail.com)

ORCID iDs of the authors:  
KP. 0009-0001-0846-5246  
BVC. 0000-0003-0830-6816  
SM. 0009-0002-5281-5546  
JJ. 0009-0005-1353-3003  
LKH. 0009-0001-3792-4122  
VS. 0000-0002-6846-1829  
EP. 0000-0001-7205-7389

Key words:  
6,3'-dimethoxy flavonol  
Cell viability  
Metastasis inhibition

**Abstract:** Osteosarcoma, a cancer predominantly affecting children and teenagers, has shown limited improvements in long-term survival rates despite advances in treatment, necessitating new therapeutic approaches. Natural compounds, particularly flavonoids, are being investigated for their anti-cancer properties due to their ability to modulate signaling pathways and induce apoptosis in cancer cells. This study evaluates the anti-carcinogenic effects of 6,3'-dimethoxy flavonol on MG-63 osteosarcoma cells, a *p53*-null model suitable for testing novel therapies, using various assays. Cell viability and proliferation were measured via MTT assay, showing dose dependent inhibition with an IC<sub>50</sub> of 221.017 µg/ml at 48 hours. Phase-contrast microscopy revealed morphological changes consistent with apoptosis, including cell shrinkage, reduced density and cytoplasmic blebbing. Wound healing assays demonstrated significant inhibition of cell migration at 100 µg/ml and 234.12 µg/ml, highlighting its anti-metastatic potential. Acridine orange/ethidium bromide (AO/EB) staining confirmed apoptotic cell death. Real-time PCR analysis revealed an increased (Bax/Bcl-2) ratio and upregulation of *p53* expression, indicating activation of the intrinsic apoptotic pathway. These findings demonstrate that 6,3'-dimethoxy flavonol effectively induces apoptosis and inhibits migration in MG-63 cells by modulating apoptotic markers and signaling pathways. The results suggest its potential as a therapeutic agent for osteosarcoma. Future studies should explore its *in vivo* efficacy, possible synergistic effects in combination therapies, and its mechanisms in *p53*-positive cell lines. This evidence underscores the promise of flavonoid based interventions in cancer treatment.

**Özet:** Çoğunlukla çocukları ve gençleri etkileyen bir kanser türü olan osteosarkom, tedavi alanındaki gelişmelere rağmen uzun süreli sağkalım oranlarında sınırlı iyileşmeler göstermiş, bu durum da yeni tedavi yaklaşımlarını gerekli kılmıştır. Doğal bileşikler, özellikle de flavonoidler, kanser hücrelerinde sinyal yollarını düzenleme ve apoptozu başlatma kabiliyetlerine bağlı olarak kanser karşıtı özellikleri açısından araştırılmaktadır. Bu çalışmada, 6,3'-dimetoksi flavonolün yeni tedavilerin test edilmesine uygun bir model olan MG-63 osteosarkom hücreleri üzerindeki antikarsinojenik etkileri çeşitli analizler kullanılarak değerlendirilmiştir. MTT testi ile hücre canlılığı ve çoğalması ölçülmüş ve 48 saatte 221.017 µg/ml'lik bir IC<sub>50</sub> ile doza bağlı bir inhibisyon tespit edilmiştir. Faz-kontrast mikroskopisi incelemesi, hücre büzülmesi, yoğunluğun azalması ve sitoplazmik kabarcıklanma gibi apoptozla uyumlu morfolojik değişiklikleri ortaya koymuştur. Yara iyileşme deneyleri, 100 µg/ml ve 234,12 µg/ml'de hücre göçünün önemli ölçüde inhibe edildiğini göstererek 6,3'-dimethoxy flavonolün anti-metastatik potansiyelini öne çıkarmıştır. Uygulanan Akridin turuncusu/etidyum bromür (AT/EB) boyaması apoptotik hücre ölümünü doğrulamıştır. Bax/Bcl-2 oranında artış ve *p53* ekspresyonunda artış olduğunu ortaya koyan gerçek zamanlı PCR analizi, intrinsik apoptotik yolağın aktive olduğunu göstermiştir. Bu bulgular, 6,3'-dimetoksi flavonolün apoptotik belirteçleri ve sinyal yollarını düzenleyerek MG-63 hücrelerinde apoptozu etkili bir şekilde indüklediğini ve hücre göçünü engellediğini göstermektedir. Sonuçlar, 6,3'-dimetoksi flavonolün osteosarkom için tedavi edici bir ajan olarak potansiyeli olduğunu da göstermektedir. Gelecek çalışmalarda 6,3'-dimetoksi flavonolün *in vivo* etkinliği, kombinasyon tedavilerindeki olası sinerjik etkileri ve *p53* pozitif hücre hatlarındaki mekanizmaları araştırılmalıdır. Çalışmada sunulan kanıtlar, kanser tedavisinde flavonoid bazlı müdahalelerin umut verici olduğunun altını çizmektedir.



OPEN ACCESS

## Introduction

Cancer remains a major global health concern due to its high rate of morbidity and mortality (Singh *et al.* 2024, Bushi *et al.* 2025). Osteosarcoma, also known as osteogenic sarcoma (Joshy *et al.* 2023, Gavarraju *et al.* 2024), is a type of cancer that arises in the bones and originates from primitive bone-forming cells (Kannan *et al.* 2024, Zuvairiya *et al.* 2024, Nautiyal *et al.* 2024). Osteosarcoma, sometimes called osteogenic sarcoma that arises in the bones (Joshy *et al.* 2023, Gavarraju *et al.* 2024). It is considered as a rare malignant disease, and mainly affects children and teenagers (Gavarraju *et al.* 2024). It is an uncommon and dangerous form of bone cancer that mostly affects the body's long bones, such the arms and legs (Prithiksha & Priyadharshini *et al.* 2024, Sekar *et al.* 2025). Treatment for osteosarcoma, including radiation, chemotherapy and possibly surgery, has advanced significantly in the modern period. Individuals with osteosarcoma are currently evaluated to have a 5-year survival rate of 60 to 70%. Among the chemotherapeutic medications used, methotrexate and ifosfamide are the most common ones, but a number of combinations and additional cytotoxic compounds, such as etoposide, have also been reported in related literature (Kansara *et al.* 2014). However, using these drugs may result in a number of problems and side effects including emesis, nausea, mouth fissures, fatigue, severe diarrhea and neutropenia. Among the acute reactions, anthracyclines may be the most notorious perpetrators, causing shortness of breath and chest pain, highlighting how these serious side effects constitute a major drawback of chemotherapy (Broder *et al.* 2008). Another problem with modern treatments is chemoresistance (Broder *et al.* 2008). In order to uncover innovative treatments for a range of malignancies, including osteosarcoma, researchers have been motivated by these therapeutic limits to start exploring new directions, such as identifying novel targets and comprehending their mechanisms. The most widely used cell lines for osteosarcoma are MG-63, which were produced from the fibroblastic or epithelial origins of young, white patients. MG-63 cells exhibit a phenotype characterized by high proliferation, rapid growth rate, and moderate differentiation, making them a widely used in vitro model for studying osteosarcoma biology and anticancer drug screening (Czekanska *et al.* 2012). This particular cell line was chosen because it is accessible, reasonably priced and useful for experimental study. Due to their aggressive proliferative nature, MG-63 cells serve as an ideal model to evaluate the anticancer potential of various therapeutic agents, including natural compounds like flavonoids, which have shown promising cytotoxic and apoptotic effects against osteosarcoma cells, which have interesting properties such as the activation of epigenetic changes and the Ubiquitin-proteasome pathway (Nabavi *et al.* 2018, Barreca *et al.* 2021, Khan *et al.* 2021, Gervasi *et al.* 2022). Because flavonols selectively engage with specific intercellular signaling pathways to promote different activities inside the cells, they have shown anti-cancer

properties in numerous *invitro* and *invivo* studies. 6,3'-dimethoxy flavonol is a naturally occurring flavonoid derivative that belongs to the larger class of flavonols, which have a number of pharmacological characteristics, including anti-inflammatory, anti-cancer, and antioxidant effects. The structure of flavonols is characterized by a hydroxyl group on the 3<sup>rd</sup> carbon of the flavone backbone, while 6,3'-dimethoxy flavonol features methoxy groups at the 6 and 3' positions, which may influence its biological activity by affecting its solubility, cell permeability, and interaction with biomolecules (Fig. 1).

Like other flavonoids, flavonols are known to have anticancer properties through a number of ways, including apoptosis induction, cell growth suppression and disruption of cell signaling pathways implicated in the development of cancer. Specifically, compounds with methoxy substitutions often show enhanced bioactivity, as methylation can improve cell uptake and metabolic stability compared to their hydroxylated counterparts. The study suggests that flavonoids with methoxy groups, such as 6,3'-dimethoxy flavonol, have the potential to modulate cellular oxidative stress, induce cell cycle arrest, and inhibit key enzymes involved in tumor progression. Flavonoids with methoxy groups, such as 6,3'-dimethoxy flavonol, have the potential to modulate cellular oxidative stress, induce cell cycle arrest, and inhibit key enzymes involved in tumor progression. These actions make them promising candidates for cancer therapy (López-Lázaro *et al.* 2009). Also, Studies showed its antioxidant activities, and role in neuropathy pain and inflammation (Nadipelly *et al.* 2018, Sayeli *et al.* 2019).

This study aims to investigate the anticancer effects of 6,3'-dimethoxy flavonol on human cancer cell lines, with a particular emphasis on how it affects gene expression, migration, and cell viability. To evaluate cytotoxicity, the MTT assay was employed, providing insights into 6,3'-dimethoxy flavonol's dose-dependent effects on cell survival. The scratch migration assay was conducted to assess the influence of 6,3'-dimethoxy flavonol (DMF) on cellular movement, a critical factor in cancer metastasis. We also analyzed gene expression changes in key regulatory genes to understand the molecular mechanisms underlying 6,3'-dimethoxy flavonol's anticancer activity.

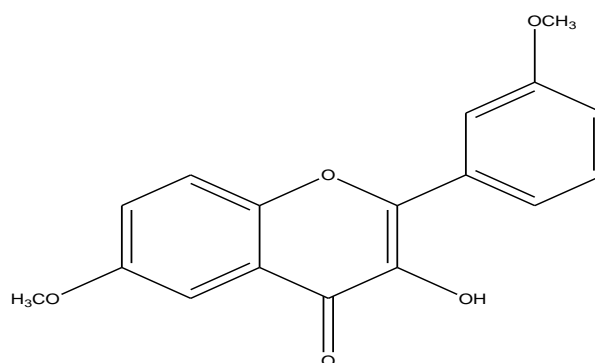


**Fig. 1.** The chemical structure of 6,3'-dimethoxy flavonol.

By exploring the effects of 6,3'-dimethoxy flavonol on cancer cells through multiple assays, this study sheds light on its potential as a therapeutic candidate, advancing our understanding of naturally derived compounds in cancer treatment.

## Materials and Methods

### Chemicals

The 6,3'-dimethoxy flavonol used in the study was procured from Research Organics, Chennai, India.

### Cell line maintenance

We obtained MG-63 Cell lines from the NCCS in Pune. The cells were cultivated in DMEM and RPMI in T25 culture flasks supplemented with 10% FBS and 1% antibiotics. The cells were kept in a humidified environment with 5% CO<sub>2</sub> at 37°C, and were trypsinised and passaged once they had reached confluency.

### Cell viability (MTT) assay

A common colorimetric method for assessing a drug's detrimental effects is the MTT assay, which measures mitochondrial activity in living cells (Fig. 2). NAD(P)H-dependent oxidoreductase enzymes, the basis of this assay, are only active in metabolically active cells. Spectrophotometry is used to assay the colour intensity, when these enzymes convert the yellow MTT dye (3-(4,5-dimethylthiazol-2-yl)-2,5-diphenyl tetrazolium bromide) into soluble insoluble purple formazan crystals (Ahn *et al.* 2010). This reduction mechanism only takes place in living cells since it is dependent on continuous mitochondrial activity. The MTT assay is a trustworthy technique for determining cell viability and the cytotoxic effect of a test item since the absorbance is directly proportional to the number of viable cells. The MTT assay (Van Meerloo *et al.* 2011) was used to evaluate the cell viability of the MG-63 Cell line treated with 6,3'-dimethoxy flavonol. The assay relies on metabolically active cells reducing soluble yellow tetrazolium salt to insoluble purple formazan crystals. The osteosarcoma cell line was plated at a density of  $5 \times 10^3$  cells/well in 96-well plates, and then cultured for 3 h at 37°C in serum-free medium to starve them. Then, two washes were performed using 100µl of serum-free media. Following a 24 h fast, cells were exposed to varying doses of 6,3'-dimethoxy flavonol (50-350 µg/ml). Following the treatment, 100µl of MTT containing DMEM (0.5 mg/ml) was added to each well after the media from the control and Rutin-treated cells had been removed.

### Morphology study

We identified the ideal dosages for additional research based on the MTT experiment (IC<sub>50</sub>: 234.12 µg/ml for osteosarcoma cell line and 100 and 234.12 µg/ml for MG-63 cell system) using a phase contrast microscope to evaluate changes in cell morphology. After being grown on 6 well plates,  $2 \times 10^5$  cells were exposed to 6,3'-dimethoxy flavonol for a full day. Cells were given a single wash with phosphate buffer saline (PBS pH 7.4) following the removal of the medium at the end of the

incubation period. A phase contrast microscope was used to view the plates (Perumal *et.al.* 2023).

### Scratch wound healing assay

In six-well culture plates, osteosarcoma cells ( $2 \times 10^5$  cells/well) were cultivated. After making a wound with a 200µl tip, the cell monolayer was cleaned with PBS and captured on camera using an inverted microscope. Following a 24 h treatment with the IC<sub>50</sub> dose and the administration of serum-free growth media to control cells, images of the damaged area were captured using the same microscope. The experiments were carried out three times for each treatment group (Felice *et al.* 2015).

### Using acridine orange (AO)/ethidium bromide (EtBr) dual labelling to identify the mode of cell demise

By using the previously published AO/EtBr dual staining, the effects of 6,3'-dimethoxy flavonol (100 & 234.12 µg/ml) on osteosarcoma cell mortality were ascertained. Following a 24 h treatment with 6,3'-dimethoxy flavonol, after being collected, Ice-cold PBS was used to wash the cells. 5 µl of acridine orange (1 mg/ml) and 5 µl of EtBr (1 mg/ml) were used to re-suspend the pellets. A fluorescent microscope was then used to view the apoptotic alterations in the designated cells (Ezhilarasan *et al.* 2019).

### Real Time PCR

Real-time PCR was used to measure the gene expression of apoptotic signaling molecules. Trizol Reagent (Sigma) was used in the standardized procedure to isolate total RNA. A Prime Script first strand cDNA synthesis kit (TakaRa, Japan) was used to synthesize reverse transcription cDNA from two µg of RNA. Certain primers were used to amplify the pertinent genes (Table 1). The GoTaq® qPCR Master Mix (Promega), which includes SYBR green dye and all the PCR components, was used to conduct the PCR reaction. The CFX96 PCR system (Biorad) was used to perform the real-time PCR. The comparative CT method was used to assess the results and Schmittgen & Livak's 2-ΔΔCT method was used to compute the fold change (Morrison *et al.* 1998).

**Table 1.** List of the primers used. Tm corresponds to Melting Temperature

Gene	Forward Primer	Reverse Primer	Tm
p53	AGGCCTTGGAAC CAAGGAT	TGAGTCAGGCCCTT CTGTCT	60
Bax	TACCTCTTCCCTTC CTTTCTCC	TCCTGGATGAAAC TAGAGTGGG	58
Bcl-2	CATGTGTGTGGAG AGCGTCAAC	CAGATAGGCACCC AGGGTGAT	58
Bad	GCTGGACATTGGA CTTCCTC	CTCAGCCCATCTTC TTCCAG	60
Caspase-3	GCTATTGTAGGCG GTTGT	TGTTTCCCTGAGGT TTGC	55
GAPDH	CGACCACTTTGTCA AGCTCA	CCCTCTTCAAGGG GTCTAC	58

### Statistical analysis

The collected data were analyzed using SPSS software, employing One-Way ANOVA and Student's t-test, and compared between the control and treated groups at various concentrations (100 µg/ml, 150 µg/ml, 200 µg/ml, 250 µg/ml, 300 µg/ml, and 350 µg/ml). A threshold of  $p < 0.05$  was set for statistical significance, and the results were presented in triplicate as mean  $\pm$  standard deviation (SD).

### Abbreviations

**AO/Et Br** - Acridine Orange / Ethidium Bromide

**Bad** - Bcl-2-associated death promoter

**Bax** - Bcl-2-Associated X Protein

**DMEM** - Dulbecco's Modified Eagle Medium

**FBS** - Fetal Bovine Serum

**IC** - Inhibitory Concentration

**MTT** - 3-(4,3-Dimethylthiazol-2-yl)-2,5-diphenyl tetrazolium bromide Assay

**MOMP** - Mitochondrial Outer Membrane Permeabilization

**NCCS** - National Centre for Cell Sciences

**PBS** - Phosphate Buffered Saline

**p53** - Tumor Protein

**PCR** - Polymerase Chain Reaction

**SAR** - Structural Activity Relationship

### Results

#### 6,3'-dimethoxy flavonol significantly reduces MG-63 cell viability

The cytotoxic effects of 6,3'-dimethoxy flavonol were evaluated at varying concentrations (50-350 µg/ml) using the MTT assay, with absorbance values used to calculate percentage cell viability. Following a 24 h incubation period, the outcomes were contrasted with untreated control cells (Fig. 2). In Table 2, the cytotoxicity was expressed as mean  $\pm$  SD, and indicate a dose-dependent cytotoxic effect of 6,3'-dimethoxy flavonol. The control showed 100% viability, while at 50 µg/ml, viability was  $95.3\% \pm 2.9$  with minimal variability. As the concentration increased, viability decreased:  $80.5\% \pm 2.8$  (100 µg/ml),  $73.9\% \pm 5$  (150 µg/ml),  $56.7\% \pm 9.8$  (200 µg/ml),  $36.1\% \pm 5.4$  (250 µg/ml),  $21.3\% \pm 4.5$  (300 µg/ml), and  $15.7\% \pm 3.8$  (350 µg/ml). The increasing SD at higher concentrations suggests greater variability in cellular response.

**Table 2.** Dose-dependent cytotoxic effect of 6,3'-dimethoxy flavonol.

Test Compound	Percentage Viability
Control	100
6,3'-dimethoxy flavonol (50 µg/ml)	$95.3 \pm 2.9$
6,3'-dimethoxy flavonol (100 µg/ml)	$80.5 \pm 2.8$
6,3'-dimethoxy flavonol (150 µg/ml)	$73.9 \pm 5$
6,3'-dimethoxy flavonol (200 µg/ml)	$56.7 \pm 9.8$
6,3'-dimethoxy flavonol (250 µg/ml)	$36.1 \pm 5.4$
6,3'-dimethoxy flavonol (300 µg/ml)	$21.3 \pm 4.5$
6,3'-dimethoxy flavonol (350 µg/ml)	$15.7 \pm 3.8$

The data shown as mean  $\pm$  SD ( $n = 3$ ).

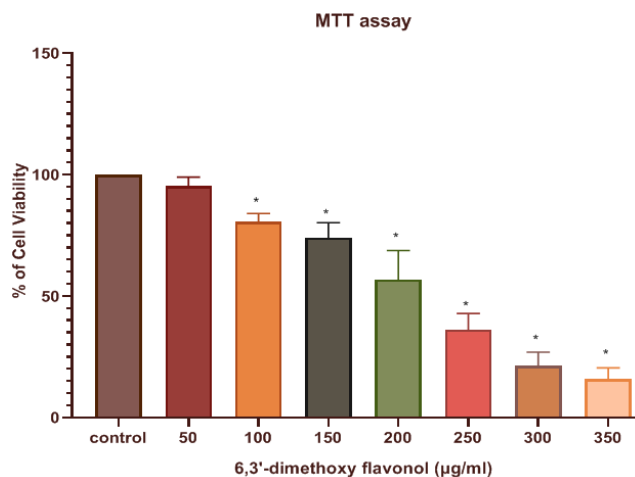


**Fig. 2.** The cytotoxic effects of 6,3'-dimethoxy flavonol on osteosarcoma (MG-63) cells. Cells were treated with 6,3'-dimethoxy flavonol (50-350 µg/ml) for 24 hours.

#### Morphological study of 6,3'-dimethoxy flavonol

Cells were treated with 6,3'-dimethoxy flavonol (100 µg/ml, 234.12 µg/ml & 300 µg/ml) for 24 hours. The cell population significantly decreased after treatment, indicating strong cytotoxic effects. The cells showed signs of apoptosis, including cell shrinkage and blebbing of the cytoplasmic membrane. These alterations indicate cellular damage and stress. An inverted phase-contrast microscope set to  $\times 10$  magnification was used to monitor and record these changes (Fig. 3).

#### 6,3'-dimethoxy flavonol decreases wound closure in MG-63 cells

Using the scratch wound healing assay, the effect of 6,3'-dimethoxy flavonol on migration was assessed. Following injury to a cell, migration experiment was conducted 24 h later with and without the administration of 6,3'-dimethoxy flavonol (100 and 234.12 µg/ml).

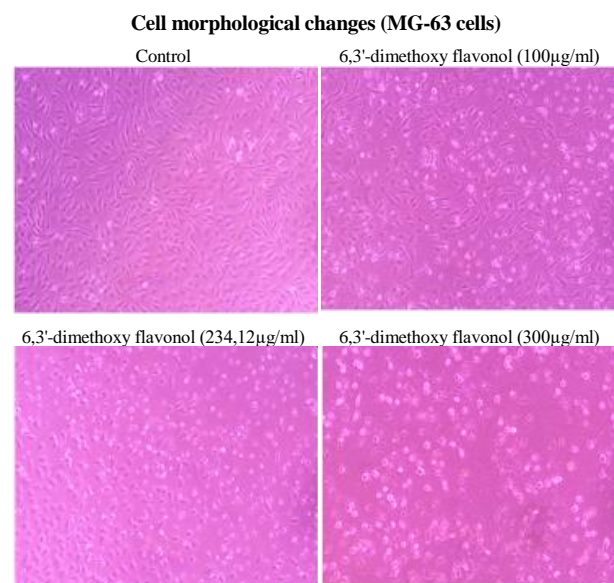


**Fig. 3.** Effect of 6,3'-dimethoxy flavonol (100 µg/ml, 234.12 µg/ml & 300 µg/ml) on cell morphology.



A uniform scratch was introduced into a confluent cell monolayer, and the wound closure was monitored after treatment. In comparison to the untreated control, both doses markedly reduced cell migration, and a dose-dependent delay in wound closure was noted. These results indicate that 6,3'-dimethoxy flavonol effectively impairs the migratory ability of MG-63 cells, highlighting its potential to suppress metastatic behavior in osteosarcoma (Felice *et al.* 2015) (Fig. 4).

#### Acridine Orange/Ethidium bromide (AO/EB) staining

Ethidium Bromide (EB) only stains dead cells with compromised membrane integrity, whereas Acridine Orange (AO) stains both living and dead cells. When using this technique to identify apoptosis, the nuclei of live cells show consistent green fluorescence, whereas the nuclei of early apoptotic cells display bright green patches due to chromatin condensation. On the other hand, late apoptotic cells with broken or constricted nuclei and lost membrane integrity appear orange due to EB binding. Different stages of cell death can be easily distinguished. Red-stained necrotic cells have a nucleus structure similar to that of living cells, but they lack condensed chromatin.

Following treatment with 6,3'-dimethoxy flavonol (100 and 234.12  $\mu\text{g/ml}$ ), the quantity of green-fluorescent cells, which indicates a reduction in viable cells, decreased in a dose-dependent manner. The presence of early apoptotic cells with fragmented DNA was indicated by the emergence of high-intensity green spots on nuclei. Compared to the control group, the percentage of orange-stained necrotic or late apoptotic cells was significantly higher ( $X\% \pm \text{SD}$ ,  $p < 0.05$ ) in the 6,3'-dimethoxy flavonol-treated group (Fig. 5).

#### Gene expression profiles induced by 6,3'-dimethoxy flavonol

Gene expression analysis of MG-63 cells treated with 6,3'-dimethoxy flavonol at 100  $\mu\text{g/ml}$  and 234.12  $\mu\text{g/ml}$  revealed significant modulation of key apoptotic markers. The treatment downregulated Bcl-2, an anti-apoptotic gene, while upregulating Bax, a pro-apoptotic gene, thereby increasing the Bax/Bcl-2 ratio and promoting apoptosis. Additionally, the expression of *p53*, a tumor suppressor, was enhanced, indicating its role in regulating apoptotic pathways.

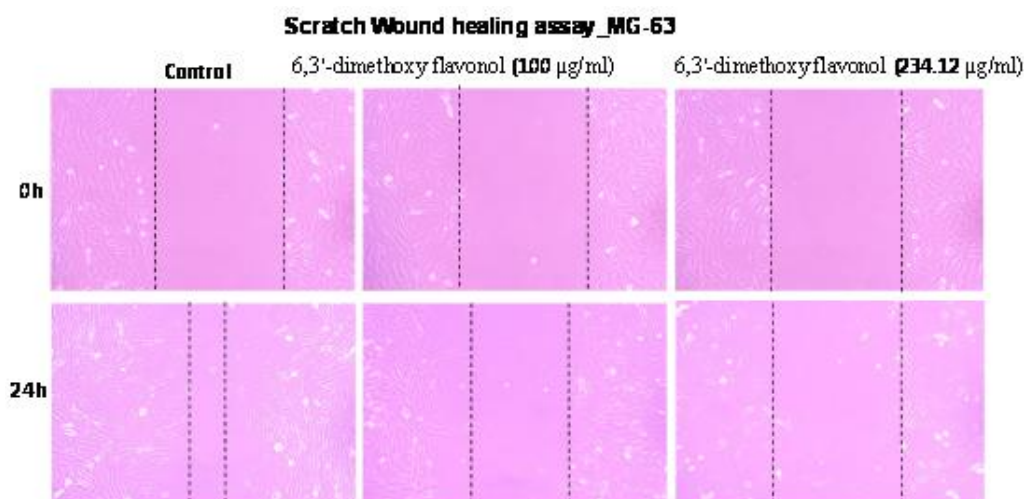


**Fig. 4.** MG-63 Cells were injured and cell migration assay with and without treatment of 6,3'-dimethoxy flavonol (100 and 234.12  $\mu\text{g/ml}$ ) was performed at 24 h. Images were obtained using an inverted phase contrast microscope.

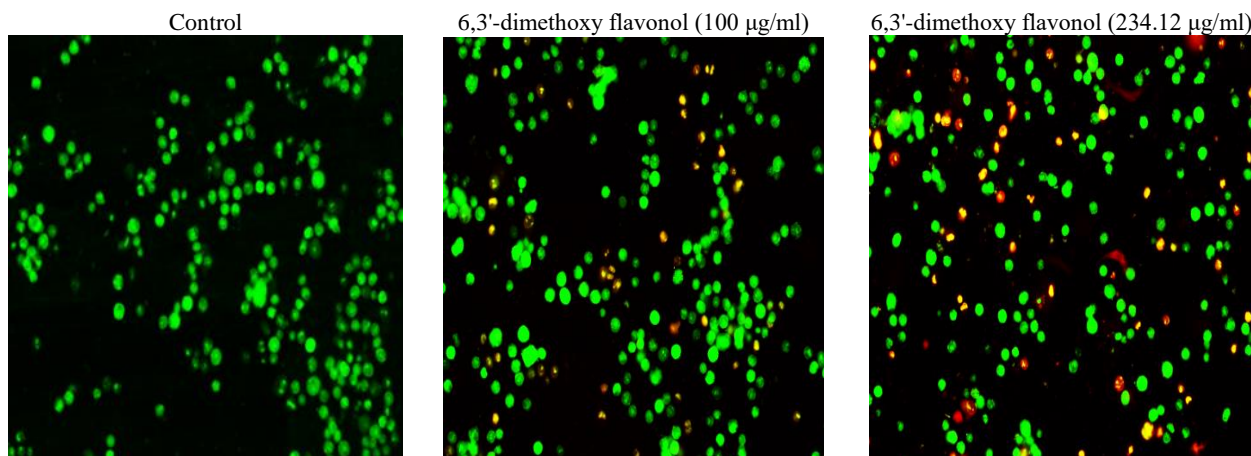


**Fig. 5.** Effect of 6,3'-dimethoxy flavonol (100 $\mu\text{g/ml}$  & 234.12  $\mu\text{g/ml}$ ) on nuclear morphology of MG-63 Cell line.

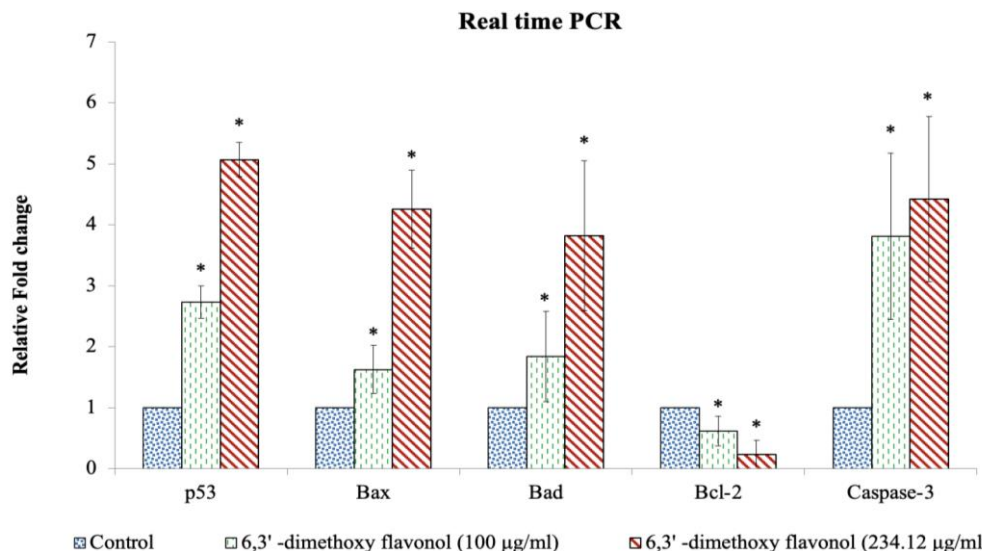


**Fig. 6.** Effect of 6,3'-dimethoxy flavonol (100 and 234.12 µg/ml) on pro-apoptotic gene (Bax, Bad, Bcl-2, and Caspase-3) expressions in osteosarcoma cell line. Target gene expression is normalized to GAPDH mRNA expression and the results are expressed as fold change from the control.

These findings align with the growing body of evidence that flavonoids, including flavonols, exhibit anti-cancer properties by targeting key signaling pathways involved in cell survival and apoptosis. The specificity of 6,3'-dimethoxy flavonol in modulating these pathways at effective concentrations (100 µg/ml and 234.12 µg/ml) highlights its potential therapeutic application. Furthermore, the dose-dependent response observed suggests that higher concentrations may elicit a stronger apoptotic response, providing insights into its pharmacological activity (Fig. 6). Table 3 illustrates apoptotic marker expression (*p53*, Bax, Bad, Bcl-2, Caspase-3) under different conditions. In the experimental setup, *p53* increased (2.728 to 5.068), accompanied by elevated Bax, Bad, and Caspase-3 levels, while Bcl-2 decreased (0.6182 to 0.2377), indicating apoptosis. The control showed minimal marker expression, with slight increases under experimental conditions. Overall, *p53* activation enhanced pro-apoptotic markers and suppressed Bcl-2, reinforcing an apoptosis-driven response.

**Table 3.** Apoptotic marker expressions.

Gene	6,3'-dimethoxy flavonol (100 µg/ml)	6,3'-dimethoxy flavonol (234.12 µg/ml)
<i>p53</i>	2.728 ± 0.26	5.06 ± 0.27
Bax	1.62 ± 0.39	4.25 ± 0.63
Bad	1.84 ± 0.74	3.82 ± 1.23
Bcl-2	0.61 ± 0.24	0.237 ± 0.232
Caspase-3	3.80 ± 1.36	4.41 ± 1.35

## Discussion

Osteosarcoma, a rare cancer worldwide, primarily affects children and teenagers. Even though new treatment approaches for osteosarcoma have improved the prognosis, the long-term survival rate for the disease has

remained stagnant. The development of new, creative treatments is necessary to improve the long-term prognosis for patients with osteosarcoma. Common cancer therapies include chemotherapy, surgery, and radiation therapy, each of which has a number of disadvantages. Nowadays, the majority of anticancer medications come from natural sources. Natural compounds inhibit cell signaling pathways and trigger cellular apoptosis (Baskar *et al.* 2012) to produce their anticancer effects. In this study, we examined the anti-carcinogenic properties of 6,3'-dimethoxy flavonol on human osteosarcoma cell line. MG-63 cells make a great model cell line for developing novel therapeutic treatments for patients with osteosarcoma (Hashem *et al.* 2022). The current study's findings are consistent with other research showing flavonol has a variety of biological effects, like anti-inflammatory, anti-oxidative, anti-proliferative, and anticoagulative properties (Lee *et al.* 2019, Kim *et al.* 2008). No research has so far evaluated for 6,3'-dimethoxy flavonol's *in vitro* anti-cancer activities in osteosarcoma. Thus, the current study's goal was to look into 6,3'-dimethoxy flavonol's anti-cancer effects in osteosarcoma. In order to do this, the impact of 6,3'-dimethoxy flavonol on osteosarcoma cell viability and proliferation was assessed, and the signaling pathways that mediate these effects were examined.

6,3'-dimethoxy flavonol decreased cell proliferation in the MG-63 cell line in a dose-dependent way in our experiments. After 24 and 48 h of treatment, the IC<sub>50</sub> was reported to be 221.017 µg/ml (Fig. 2). This finding suggests that 6,3'-dimethoxy flavonol is primarily cytotoxic to cancerous cells. Following the cytotoxicity assessment of 6,3'-dimethoxy flavonol, its effect on MG-63 cell morphology was analyzed using an inverted phase-contrast microscope. The impact of 6,3'-dimethoxy flavonol on cell morphology is thoroughly analysed by using different concentrations (100 µg/ml, 234.12 µg/ml,



and 300 µg/ml). The findings showed that cells treated with 6,3'-dimethoxy flavonol showed significant morphological changes in comparison to untreated cells. These alterations included shrinkage, reduced cell density, and dose-dependent cytoplasmic blebbing all of which are traits of apoptotic cells (Fig. 3).

The observed inhibition of MG-63 cell migration at both concentrations (100 and 234.12 µg/ml) suggests that this compound significantly impairs the migratory ability of cancer cells, which is a critical step in the metastatic cascade (Van *et al.* 2011). Cell migration plays a pivotal role in cancer progression and metastasis, enabling tumor cells to invade surrounding tissues and establish secondary tumors. The dose-dependent inhibition of wound closure indicates that 6,3'-dimethoxy flavonol interferes with cellular processes essential for migration. The delayed wound closure observed in treated groups further underscores the compound's potential to suppress osteosarcoma metastasis. The dose-dependent nature of inhibition indicates that the higher concentration of 6,3'-dimethoxy flavonol (234.12 µg/ml) exerts a stronger inhibitory effect, aligning with the compound's bioactivity profile. These results are particularly significant as osteosarcoma is known for its aggressive nature and high propensity for metastasis, especially to the bone cells. By targeting the migratory capacity of MG-63 cells, 6,3'-dimethoxy flavonol could serve as a valuable therapeutic agent in reducing metastatic risk. 6,3'-dimethoxy flavonol demonstrates a strong anti-migratory effect on MG-63 cells, supporting its potential role in managing metastatic osteosarcoma (Fig. 4).

Apoptotic cell death is characterized by nuclear fragmentation and cell shrinkage. Using dyes that bind fluorescent DNA, like AO/EB, morphological alterations and apoptosis-induced cell death were detected. Acridine orange is a necessary dye that can be used to stain both living and dead cells. The fluorescent intercalating chemical ethidium bromide, which creates linkages between DNA bases, only stains cells with damaged cytoplasmic membranes, giving their nucleus a red hue when exposed to UV light.

While late apoptotic cells contain contracted and broken orange chromatin (Renvoize *et al.* 1988, Liu *et al.* 2015), early apoptotic cells have condensed or fragmented chromatin with a bright green nucleus. In our study, green cells were uniformly distributed throughout the control group or untreated cells. According to the applied stainings, cells treated with 6,3'-dimethoxy flavonol exhibited more orange to red nuclei and perinuclear bright green patches than the control group. This suggests that 6,3'-dimethoxy flavonol increases both early and late apoptotic cells at doses of 100 and 234.12 µg/ml. Furthermore, the treatment enhances apoptosis by increasing the levels of active cleaved caspase-3 and cleaved poly-ADP ribose polymerase (PARP), both of which are key markers of programmed cell death. Additionally, it elevates the Bax/Bcl-2 ratio, promoting a

pro-apoptotic balance that favors cell death in cancerous cells. (Fig. 5)

The gene expression of pro-apoptotic and anti-apoptotic cells were evaluated with the help of real-time PCR. The results showed that 6,3'-dimethoxy flavonol can cause MG-63 osteosarcoma cells to undergo apoptosis by altering important apoptotic indicators. A disruption of mitochondrial membrane integrity is suggested by the observed downregulation of the anti-apoptotic protein Bcl-2 and the overexpression of the pro-apoptotic protein Bax, a characteristic of the intrinsic apoptotic pathway (Fig. 6). The elevated Bax/Bcl-2 ratio, which is generally acknowledged as a crucial element of mitochondrial outer MOMP, which results in the release of cytochrome c and the subsequent activation of caspases, lends additional credence to this. The intrinsic pathway's involvement is further shown by the overexpression of *p53*, a tumor suppressor gene that is essential for controlling cell cycle arrest and apoptosis. It is known that *p53* represses anti-apoptotic genes like Bcl-2 while transcriptionally activating pro-apoptotic genes like Bax. It may function, at least in part, by activating *p53*-dependent apoptotic signaling, as evidenced by its enhanced expression in response to therapy. The enhanced expression of *p53* may also indicate the ability of 6,3'-dimethoxy flavonol to induce DNA damage or stress responses, triggering apoptosis as a protective mechanism against malignant transformation. These results are consistent with the increasing amount of data showing that flavonoids, notably flavonols, have anti-cancer effects by focusing on important signaling pathways that are involved in apoptosis and cell survival. The specificity of 6,3'-dimethoxy flavonol in modulating these pathways at effective concentrations (100 µg/ml and 234.12 µg/ml) highlights its potential therapeutic application. Furthermore, the dose-dependent response observed suggests that higher concentrations may elicit a stronger apoptotic response, providing insights into its pharmacological activity. Further exploration of its therapeutic applications could provide new avenues for combating this aggressive cancer.

Future research should expand the investigation of 6,3'-dimethoxy flavonol to other osteosarcoma cell lines, such as SaOS-2 and U2OS, to validate its broad anticancer efficacy. To evaluate its pharmacokinetics, biodistribution, and capacity to impede tumor growth and metastasis in a physiological setting, *in vivo* research employing animal models is crucial. Exploring combination therapy with standard chemotherapeutic agents like doxorubicin could enhance efficacy while minimizing toxicity. Elucidating molecular mechanisms beyond *p53*-dependent pathways, particularly in *p53*-positive cell lines, will provide a deeper understanding of its anticancer action. Structure-activity relationship (SAR) studies could optimize its bioactivity, while developing nanoparticle-based delivery systems may improve its bioavailability and reduce systemic toxicity. Additionally, the exploration of its immunomodulatory

effects on the tumor microenvironment, such as modulating immune cell infiltration and cytokine production, may reveal synergistic therapeutic potential. Clinical translational studies, including early-phase clinical trials, will be crucial to establish its safety and efficacy in osteosarcoma patients. High-throughput genomic and proteomic profiling could further identify biomarkers for patient stratification, enabling personalized treatment approaches. These future directions could position 6,3'-dimethoxy flavonol as a promising candidate in the development of innovative osteosarcoma therapies.

## Conclusion

This study highlights the therapeutic potential of 6,3'-dimethoxy flavonol, a bioactive molecule with strong antiproliferative effects on MG-63 osteosarcoma cells. Morphological analysis post-treatment revealed hallmark signs of apoptosis, such as decreased density and cell shrinkage, indicating a successful interference with cancer cell survival. In a wound-healing study, the molecule also demonstrated anti-migratory qualities, suggesting that it may prevent metastasis. The Bax/Bcl-2 ratio shifted towards apoptosis at the molecular level, as demonstrated by RT-PCR analysis, which revealed elevated (anti-apoptotic) expression. Its potential as a selective anticancer drug is highlighted by this dual

mechanism. The study does, however, admit many limitations, such as its exclusive emphasis on a particular cell line. To confirm efficacy and safety, further osteosarcoma models and *in vivo* investigations are essential for future study. In summary, 6,3'-dimethoxy flavonol exhibits strong anticancer properties, providing a potentially effective therapy option for osteosarcoma.

## Acknowledgement

The authors express their thanks to Saveetha College of Pharmacy – SIMATS for providing the necessary facilities to carry out this work.

**Ethics Committee Approval:** Since the article does not contain any studies with human or animal subject, its approval to the ethics committee was not required.

**Data Sharing Statement:** All data are available within the study.

**Author Contributions:** Concept: B.V.C., Design: K.G., B.V.C., Material supplying: S.M., Data acquisition: J.J., L.K.H., Data analysis/interpretation: V.S., Writing: B.V.C., K.P., S.M., Critical review: E.P.

**Conflict of Interest:** The authors have no conflicts of interest to declare.

**Funding:** The authors declared that this study has received no financial support.

## References

- Ahn, J.Y., Choi, S.E., Jeong, M.S., Park, K.H., Moon, N.J., Joo, S.S. & Seo, S.J. 2010. Effect of taxifolin glycoside on atopic dermatitis-like skin lesions in NC/Nga mice. *Phytotherapy Research*, 24(7): 1071-1077. <https://doi.org/10.1002/ptr.3084>
- Barreca, D., Trombetta, D., Smeriglio, A., Mandalari, G., Romeo, O., Felice, M.R. & Nabavi, S. M. (2021). Food flavonols: Nutraceuticals with complex health benefits and functionalities. *Trends in Food Science & Technology*, 117: 194-204.
- Baskar, R., Lee, K.A., Yeo, R. & Yeoh, K.W. 2012. Cancer and radiation therapy: current advances and future directions. *International journal of medical sciences*, 9(3): 193. <https://doi.org/10.7150/ijms.3635>
- Broder, H., Gottlieb, R.A. & Lepor, N.E. 2008. Chemotherapy and cardiotoxicity. *Reviews in cardiovascular medicine*, 9(2): 75-83.
- Bushi, G., Gaidhane, S., Balaraman, A.K., Padmapriya, G., Kaur, I., Lal, M., Iqbal, S., Prasad, G.V.S., Pramanik, A., Vishwakarma, T., Malik, P., Sharma, P., Punia, A., Jagga, M., Singh, M.P., Lingamaiah, D., Shabil, M., Mehta, R., Sah, S. & Zahiruddin, Q.S. 2025. Global prevalence of falls among older adults with cancer: A systematic review and meta-analysis. *Journal of geriatric oncology*, 16(3): 102202. Advance online publication. <https://doi.org/10.1016/j.jgo.2025.102202>
- Czekanska, E.M., Stoddart, M.J., Richards, R.G. & Hayes, J. S. 2012. In search of an osteoblast cell model for *in vitro* research. *European cells & materials*, 24(4): 1-17. <https://doi.org/10.22203/ecm.v024a01>
- Ezhilarasan, D., Apoorva, V.S. & Ashok Vardhan, N. 2019. Syzygiumcumini extract induced reactive oxygen species-mediated apoptosis in human oral squamous carcinoma cells. *Journal of Oral Pathology & Medicine*, 48(2): 115-121. <https://doi.org/10.1111/jop.12806>
- Felice, F., Zambito, Y., Belardinelli, E., Fabiano, A., Santoni, T. & Di Stefano, R. 2015. Effect of different chitosan derivatives on *in vitro* scratch wound assay: A comparative study. *International journal of biological macromolecules*, 76: 236-241. <http://doi.org/10.1016/j.ijbiomac.2015.02.041>
- Gavarraju, L.N.J., Rao, A.S., Anusha, R., Reddy, D.N., Anantula, J. & Surendra, D. 2024. Integrating Multimodal Medical Imaging Data for Enhanced Bone Cancer Detection: A Deep Learning-Based Feature Fusion Approach. *Journal of Theoretical and Applied Information Technology*. 102(18): 6761-6773.
- Gervasi, T., Calderaro, A., Barreca, D., Tellone, E., Trombetta, D., Ficarra, S. & Gattuso, G. 2022. Biotechnological applications and health-promoting properties of flavonols: An updated view. *International Journal of Molecular Sciences*, 23(3): 1710. <https://doi.org/10.3390/ijms23031710>
- Hashem, S., Ali, T. A., Akhtar, S., Nisar, S., Sageena, G., Ali, S. & Bhat, A.A. 2022. Targeting cancer signaling pathways by natural products: Exploring promising anti-cancer agents. *Biomedicine & Pharmacotherapy*, 150: 113054. <https://doi.org/10.1016/j.biopha.2022.113054>
- Joshy, M.R., Lakshmi Thangavelu, M.J.R. & Perumal, E. 2023. *In vitro* Anti-proliferative and Pro-apoptotic Activities of Cinnamomum cassia Bark Extract on osteosarcoma

- cells. *Journal of Survey in Fisheries Sciences*, 10(1S): 233-242.
13. Kannan, N., Ramalingam, K., Ramani, P. & Krishnan, M. 2024. Exploring Prevalence Trends of Jaw Bone Pathologies: A Three-Year Institutional Study. *Cureus*, 16(5): e60574. <https://doi.org/10.7759/cureus.60574>
  14. Kansara, M., Teng, M.W., Smyth, M.J. & Thomas, D.M. 2014. Translational biology of osteosarcoma. *Nature Reviews Cancer*, 14(11): 722-735. <https://doi.org/10.1038/nrc3838>
  15. Khan, H., Belwal, T., Efferth, T., Farooqi, A.A., Sanches-Silva, A., Vacca, R.A. & Nabavi, S.M. 2021. Targeting epigenetics in cancer: therapeutic potential of flavonoids. *Critical reviews in food science and nutrition*, 61(10): 1616-1639. <https://doi.org/10.1080/10408398.2020.1763910>
  16. Kim, Y.J., Choi, S.E., Lee, M.W. & Lee, C.S. 2008. Taxifolin glycoside inhibits dendritic cell responses stimulated by lipopolysaccharide and lipoteichoic acid. *Journal of Pharmacy and Pharmacology*, 60(11): 1465-1472. <https://doi.org/10.1211/jpp/60.11.0007>
  17. Lee, C.M., Lee, J., Nam, M.J., Choi, Y.S. & Park, S.H. 2019. Tomentosin displays anti-carcinogenic effect in human osteosarcoma MG-63 cells via the induction of intracellular reactive oxygen species. *International journal of molecular sciences*. 20(6): 1508. <https://doi.org/10.3390/ijms20061508>
  18. Liu, K., Liu, P.C., Liu, R. & Wu, X. 2015. Dual AO/EB staining to detect apoptosis in osteosarcoma cells compared with flow cytometry. *Medical science monitor basic research*, 21: 15. <https://doi.org/10.12659/msmbr.893327>
  19. López-Lázaro, M. 2009. Distribution and biological activities of the flavonoid luteolin. *Mini reviews in medicinal chemistry*, 9(1): 31-59. <https://doi.org/10.2174/138955709787001712>
  20. Morrison, T.B., Weis, J.J. & Wittwer, C.T. 1998. Quantification of low-copy transcripts by continuous SYBR Green I monitoring during amplification. *Biotechniques*, 24(6): 954-958.
  21. Nabavi, S.F., Atanasov, A.G., Khan, H., Barreca, D., Trombetta, D., Testai, L. & Nabavi, S.M. 2018. Targeting ubiquitin-proteasome pathway by natural, in particular polyphenols, anticancer agents: Lessons learned from clinical trials. *Cancer letters*, 434: 101-113. <https://doi.org/10.1016/j.canlet.2018.07.018>
  22. Nadipelly, J., Sayeli, V., Kadhivelu, P., Shanmugasundaram, J., Cheriyan, B.V. & Subramanian, V. 2018. Effect of certain trimethoxy flavones on paclitaxel-induced peripheral neuropathy in mice. *Integrative Medicine Research*, 7(2): 159-167. <https://doi.org/10.1016/j.imr.2018.03.006>
  23. Nautiyal, M., Ganapathy, D., Ameya, K.P. & Sekar, D. 2024. Analysis of Carboplatin and STAT3 in the Breast Cancer MCF7 Cell Line. *Texila International Journal of Public Health*, 12: 1-7.
  24. Perumal, E. 2023. Anti-proliferative and antimigratory potential of cinnamomum cassia bark extract on breast cancer cells. *Journal of Survey in Fisheries Sciences*, 10(1S): 382-391. <https://doi.org/10.17762/sfs.v10i1S.184>
  25. Prithiksha, N. & Priyadharshini, R. 2024. *In vitro* Molecular Mechanisms of Anticancer Activity of Stevioside in Human Osteosarcoma Cell Lines (Sarcoma Osteogenic). *Contemporary Clinical Dentistry*, 15(3): 198-201. [https://doi.org/10.4103/ccd.ccd\\_429\\_23](https://doi.org/10.4103/ccd.ccd_429_23)
  26. Renvoize, C., Biola, A., Pallardy, M. & Breard, J. 1998. Apoptosis: identification of dying cells. *Cell biology and toxicology*, 14: 111-120. <https://doi.org/10.1023/A:1007429904664>
  27. Sayeli, V., Nadipelly, J., Kadhivelu, P., Cheriyan, B.V., Shanmugasundaram, J. & Subramanian, V. 2019. Antinociceptive effect of flavonol and a few structurally related dimethoxyflavonols in mice. *Inflammopharmacology*, 27: 1155-1167. <https://doi.org/10.1007/s10787-019-00579-4>
  28. Sekar, K., Ramanathan, A., Khalid, R., Mun, K.S., Valliappan, V. & Ismail, S.M. 2025. An unusual case of multiple primary tumours involving the long bone and oral cavity. *Oral and maxillofacial surgery*, 29(1): 62. <https://doi.org/10.1007/s10006-025-01356-0>
  29. Singh, O., Sah, U.K., Chandra, J. & Patel, S. 2024. The Impact of ctDNA on Metastatic Cancer Management: Current Trends and Future Directions. *Oral Oncology Reports*, 13: 100705. <https://doi.org/10.1016/j.oor.2024.100705>
  30. Van Meerloo, J., Kaspers, G.J. & Cloos, J. 2011. Cell sensitivity assays: the MTT assay. *Cancer cell culture: methods and protocols*, 237-245. [https://doi.org/10.1007/978-1-61779-080-5\\_20](https://doi.org/10.1007/978-1-61779-080-5_20)
  31. Zuvairiya, U., Menaka, S., Jayaraman, S. & Suresh, V. 2024. The Oncolytic Effect of Aervalanata on Osteosarcoma Cell Lines via the Apoptotic Signaling Pathway. *Cureus*, 16(4): e58091. <https://doi.org/10.7759/cureus.58091>



## Comparison of dCas9-activator complexes for the activation of *PDX1* and *NGN3* pancreatic genes using the CRISPR system

Fatma Akçakale Kaba, Ersin Akıncı, Mehmet Fatih Cengiz, Adem Kaba\*

Department of Agricultural Biotechnology, Faculty of Agriculture, Akdeniz University, Antalya, TÜRKİYE

### Cite this article as:

Akçakale Kaba F., Akıncı E., Cengiz M.F. & Kaba A. 2025. Comparison of dCas9-activator complexes for the activation of *PDX1* and *NGN3* pancreatic genes using the CRISPR system. *Trakya Univ J Nat Sci*, 26(1): 49-59, DOI: 10.23902/trkjinat.1622077

Received: 17 January 2025, Accepted: 25 March 2025, Published: 15 April 2025

**Abstract:** *Diabetes mellitus* is a prevalent metabolic disorder characterized by persistently high blood glucose levels due to insufficient insulin production or response. Although significant progress has been made in symptom management, a definitive cure remains unavailable. This study presents a novel approach to generate insulin-producing  $\beta$  cells from non- $\beta$  cell sources using the CRISPR/dCas9 gene activation system. We focused on enhancing  $\beta$ -cell differentiation by activating *PDX1* and *NGN3*, two key transcription factors in pancreatic development. To optimize this process, we compared three activator domains (VP64, VPR, and p300) and found VPR to be the most effective. Specifically, the VPR activator led to a 19-fold increase in *PDX1* expression and a 256-fold increase in *NGN3* expression when combined with four gRNAs. This superiority is likely due to its stronger transcriptional activation capability, which enhances gene expression more efficiently than VP64 and p300. Gene and protein expression were confirmed through RT-qPCR and immunostaining, respectively. Our findings demonstrate that CRISPR/dCas9-mediated gene activation can effectively induce  $\beta$ -cell differentiation, offering a promising approach for type 1 diabetes therapy, where  $\beta$ -cell loss is a major challenge. Future studies should explore the long-term functionality and stability of these  $\beta$ -like cells in preclinical models to further assess their therapeutic potential. By optimizing transcription factor activation, our study provides new insights into  $\beta$ -cell regeneration, advancing the field of gene-based diabetes treatments.

**Edited by:**  
Reşat Ünal

**\*Corresponding Author:**  
Adem Kaba  
[admbdm7@gmail.com](mailto:admbdm7@gmail.com)

**ORCID iDs of the authors:**  
AKB. 0000-0003-0680-7406  
EA. 0000-0003-1463-2255  
MFC. 0000-0002-6836-2708  
AK. 0000-0003-3362-0997

**Key words:**  
CRISPR/dCas9Activation  
Insulin-Producing  $\beta$ -like Cells  
*PDX1* and *NGN3* Gene Regulation  
 $\beta$ -cell Differentiation and Regeneration  
Diabetes Gene Therapy

**Özet:** Türkçe *Diabetes mellitus*, yetersiz insülin üretimi veya yanıtı nedeniyle kalıcı olarak yüksek kan glukoz seviyeleriyle karakterize edilen yaygın bir metabolik bozukluktur. Belirtilerin yönetimi konusunda önemli ilerlemeler kaydedilmiş olsa da kesin bir tedavi halen mevcut değildir. Bu çalışma, CRISPR/dCas9 gen aktivasyon sistemini kullanarak insülin üreten  $\beta$ -benzeri hücrelerin  $\beta$  hücresi olmayan kaynaklardan elde edilmesine yönelik yeni bir stratejiyi araştırmaktadır. Pankreas gelişiminde kilit rol oynayan iki transkripsiyon faktörü olan *PDX1* ve *NGN3*'ün aktivasyonu yoluyla  $\beta$  hücre farklılaşmasını artırmaya odaklandık. Bu süreci optimize etmek için üç farklı aktivatör bölgesini (VP64, VPR ve p300) karşılaştırdık ve VPR'nin en etkili aktivatör olduğunu belirledik. Özellikle VPR aktivatörü, dört gRNA ile birlikte kullanıldığında *PDX1* ekspresyonunda 19 kat, *NGN3* ekspresyonunda ise 256 kat artış sağladı. Bu üstünlüğün, VPR'nin VP64 ve p300'e kıyasla daha güçlü transkripsiyon aktivasyonu sağlamasından kaynaklandığını düşünüyoruz. Gen ve protein ekspresyonu sırasıyla RT-qPCR ve immün boyama teknikleriyle doğrulandı. Bulgularımız, CRISPR/dCas9 aracılı gen aktivasyonunun  $\beta$  hücre farklılaşmasını etkili bir şekilde indükleyebileceğini ve  $\beta$  hücre kaybının büyük bir sorun olduğu tip 1 diyabet tedavisi için umut vadeden bir yaklaşım sunduğunu göstermektedir. Gelecekteki çalışmalar, bu  $\beta$ -benzeri hücrelerin uzun vadeli fonksiyonelliğini ve stabilitesini prelinik modellerde inceleyerek terapötik potansiyellerini daha kapsamlı bir şekilde değerlendirmelidir. Transkripsiyon faktörü aktivasyonunu optimize eden bu çalışma,  $\beta$  hücre rejenerasyonu hakkında yeni içgörüler sunarak gen temelli diyabet tedavileri alanına önemli bir katkı sağlamaktadır.

### Introduction

The CRISPR (Clustered Regularly Interspaced Short Palindromic Repeats) system is a precise genome-editing tool derived from bacterial immune defense, utilizing the Cas9 nuclease and a guide RNA (gRNA) to target specific

DNA sequences. Due to its efficiency, specificity, and simplicity, CRISPR/Cas9 has become the predominant genome-editing method, enabling applications such as gene silencing and regulation. The discovery of Cas9



OPEN ACCESS

orthologs and variants with different protospacer adjacent motif (PAM) specificities has further expanded its targeting capabilities. To adapt CRISPR for gene regulation, (Qi *et al.* 2013) engineered a catalytically inactive Cas9 (dCas9) by mutating its HNH and RuvC-like nuclease domains. dCas9 can bind to DNA without cleaving it, allowing precise transcriptional modulation when fused to effector domains. CRISPR activation facilitates gene regulation by linking dCas9 with transcriptional activation domains, enabling targeted gene upregulation or downregulation without altering the DNA sequence (Casas-Mollano *et al.* 2020, Razavi *et al.* 2024). In the CRISPR-Cas9 system, dCas9 is preferred over Cas9 in gene regulation studies because it allows transcriptional or epigenetic control of target genes without DNA cleavage. This approach offers significant advantages for modulating gene expression without introducing permanent genomic modifications. Due to mutations in the RuvC and HNH nuclease domains (D10A/H840A), dCas9 lacks endonuclease activity but retains the ability to bind target DNA, facilitating the recruitment of transcription factors or epigenetic regulators to specific genomic loci. This property eliminates the risk of genomic instability and unintended mutations (Richter *et al.* 2020). Additionally, when fused with effector proteins such as VP64 or KRAB, dCas9 can either enhance or repress gene expression, making it ideal for dynamic control of cellular functions (Nuñez *et al.* 2021). In epigenetic regulation, dCas9 can be fused with DNA methyltransferases (e.g., DNMT3A) or histone-modifying enzymes (e.g., p300) to alter chromatin structure and achieve long-term gene expression control without permanent mutations (Dominguez *et al.* 2022). While its DNA-cleaving ability can lead to unintended mutations at off-target sites, dCas9 significantly reduces off-target effects, making it a safer option for therapeutic applications (Seo *et al.* 2023). These advantages establish dCas9 as an essential tool for gene regulation, epigenetic engineering, and therapeutic development. The CRISPR-dCas9 system utilizes effector proteins such as VPR, VP64, and p300 to regulate gene expression through transcriptional activation or epigenetic modification. These proteins, when fused with dCas9, manipulate the expression of target genes by binding to specific DNA regions. VP64 is a fusion of four VP16 transcriptional activation domains derived from the human herpesvirus and activates transcription by binding to the promoter region of the target gene. It is preferred for achieving high levels of gene expression, although its activation power is limited. VPR, a combination of VP64, human p65 (NF- $\kappa$ B), and Rta (from the Epstein-Barr virus), provides stronger transcriptional activation compared to VP64. This system is particularly effective for activating genes that are difficult to express, such as those located in silent chromatin regions. p300, an epigenetic regulator with histone acetyltransferase (HAT) activity, works by acetylating histones in the target gene region. This modification opens the chromatin structure, facilitating transcriptional activation. p300 is used for long-term

regulation of gene expression without permanently altering the DNA sequence. These activation domains offer distinct advantages: VP64 is an efficient and straightforward tool for basic gene activation, VPR is suitable for genes requiring higher levels of activation, and p300 enables sustainable activation without permanent DNA changes (Chavez *et al.* 2015, Dominguez *et al.* 2022, Riedmayr *et al.* 2022).

Synthetic transcription factors including those used in the CRISPR-dCas9 system, play crucial roles in regulating gene expression, stimulating tissue regeneration, compensating for genetic defects, activating silenced tumor suppressors, controlling stem cell differentiation, performing genetic screening, and generating synthetic genes. These factors typically target enhancers or promoters of both endogenous genes and transgenes (Beerli *et al.* 2000, Kunii *et al.* 2018). In mammals, gRNA activation is usually moderate; however, using multiple gRNAs can help enhance activation by targeting distinct locations upstream of the transcription start site (Gilbert *et al.* 2013, Maeder *et al.* 2013). Several CRISPR activation systems, such as dCas9-VP64, dCas9-VPR, dCas9-SunTag, the gRNA-activation domain system, the SAM (Synergistic Activation Mediator) system, and the dCas9-p300 core system, employ various strategies to promote gene expression through targeted activation mechanisms. The dCas9-VP64, dCas9-VPR, and dCas9-p300 systems are distinct CRISPR activation platforms, each offering specific mechanisms for gene activation. dCas9-VP64 is the first-generation CRISPR activation system, in which dCas9 is fused with the VP64 transactivation domain (Balboa *et al.* 2015). This system can activate targeted endogenous genes using a single gRNA while minimizing off-target effects (Maeder *et al.* 2013). The use of multiple gRNAs can lead to the synergistic activation of various genes, such as *IL1RN* and *VEGFA* (Cheng *et al.* 2013, Maeder *et al.* 2013, Pablo Perez-Pinera *et al.* 2013). dCas9-VPR system enhances the activation capabilities of dCas9 by incorporating a tripartite activator domain. Compared to dCas9-VP64, the dCas9-VPR system achieves significantly higher gene expression, with up to a 320-fold increase in expression level (Chavez *et al.* 2015). This system is particularly effective when multiple gRNAs are used to activate genes related to cellular reprogramming and development (Chavez *et al.* 2015). Lastly, the dCas9-p300 system fuses dCas9 with the catalytic core of p300 acetyltransferase, which directly catalyzes histone acetylation at target sites, leading to robust transcriptional activation of genes from both promoters and enhancers. The dCas9-p300 system has been demonstrated to activate genes like *IL1RN* and *OCT4*, showcasing its ability to directly modify the epigenetic landscape (Hilton *et al.* 2015, Chen & Qi 2017). In summary, dCas9-VP64 is a foundational system for gene activation, dCas9-VPR offers enhanced activation capabilities, and dCas9-p300 provides a mechanism for direct epigenetic modification to achieve gene activation (Chen & Qi 2017, Hsu *et al.* 2019).



Recent advancements in pancreatic gene activation and  $\beta$  cell differentiation for diabetes treatment have achieved significant progress, particularly in stem cell-based approaches, transdifferentiation, gene therapy, and epigenetic modulation. Human pluripotent stem cells (iPSCs) have been successfully converted into functional  $\beta$  cells through the use of key transcription factors such as *PDX1*, *NGN3*, *MAFA*, and *NKX6.1* (Dadheech & James Shapiro 2019). Moreover, 3D organoid culture systems have further enhanced this process by enabling the maturation of these cells through matrix interactions and signaling molecules like Wnt and TGF- $\beta$  (Pollock *et al.* 2023). Additionally, CRISPR-Cas9-based gene editing has proven effective in correcting genetic defects in monogenic diabetes models (Maxwell *et al.* 2020), while the dCas9-VPR system has emerged as a powerful tool for activating pancreatic genes. Studies have demonstrated that coexpressing dCas9-VPR with gRNAs targeting key transcription factors such as *PDX1*, *NGN3*, *NKX6.1*, and *MAFA* results in the substantial activation of these genes, indicating the potential of CRISPR systems in enhancing gene expression for  $\beta$  cell differentiation (Lee *et al.* 2023). Transdifferentiation, the process of converting non- $\beta$  cells into insulin-producing cells, has also been a focus of recent research. The reprogramming of acinar cells into  $\beta$ -like cells has been successfully achieved through the viral delivery of transcription factors like *NGN3*, *PDX1*, and *MAFA* in mouse models (Cavelti-Weder *et al.* 2017). Further, the use of the dCas9-VP160 and dCas9-P300 systems has shown promise in activating pancreatic genes like *INS*, *PDX1*, *NGN3*, and *PAX4*, both *in vitro* and *in vivo*, indicating the potential of CRISPR-based gene activation for treating complex diseases like type 1 diabetes (Giménez *et al.* 2016). Gene therapy has also made strides, with the delivery of *PDX1* and *MAFA* genes to pancreatic cells via AAV vectors improving glucose homeostasis in mice (Guo *et al.* 2023). These findings emphasize the growing potential of gene activation and reprogramming strategies in the development of new therapeutic options for diabetes treatment. Although significant progress has been made, challenges remain in achieving a true  $\beta$  cell phenotype, as external genes introduced during cell reprogramming can activate both endogenous and target genes, which may continue to drive cellular programming processes even after the exogenous genes are removed (Soria 2001, Akinci *et al.* 2012, Elhanani *et al.* 2020). Nevertheless, these approaches hold great promise for future advances in regenerative medicine and diabetes treatment.

One of the main challenges in  $\beta$  cell reprogramming is the limited activity of endogenous genes, which often leads to inefficient reprogramming outcomes. In this study, we utilized the CRISPR-dCas9 system incorporating the VPR, VP64, and P300 activation domains to enhance the expression of *PDX1* and *NGN3*, two crucial transcription factors for pancreatic development. By targeting the promoter regions of these genes, we observed significant upregulation of both gene

and protein levels, as confirmed through immunostaining and RT-qPCR analyses. Unlike previous studies that have focused on the isolated roles of *PDX1* and *NGN3*, our approach employed a multi-faceted strategy using three different dCas9 activators and multiple gRNA constructs to optimize gene expression across the -250 to +1 promoter region. Notably, our results demonstrate a synergistic effect of the VPR domain, leading to a remarkable 19- and 256-fold increase in *PDX1* and *NGN3* expression, respectively, compared to conventional methods. These findings represent a significant advancement in  $\beta$  cell reprogramming, providing a more efficient platform for generating insulin-producing  $\beta$ -like cells from non- $\beta$  cell sources.

## Materials and Methods

### Design and cloning of gRNA expression plasmids

The PAM required for gRNA targeting was selected as the *Streptococcus pyogenes* NGG. Ten gRNA sequences for the *PDX1* gene and eight gRNA sequences for the *NGN3* gene were determined using the online CRISPR-ERA tool (CRISPR-ERA 2025). DNA oligonucleotides encoding 20-nt long gRNAs were synthesized (Supplementary Material Tables S1, S2). The synthesized DNA oligonucleotides were ligated to the *BbsI* site in the gRNA expression vector. The gRNA expression vector plasmid was obtained from Addgene pSPgRNA (# 47108) (Pablo Perez-Pinera *et al.* 2013).

### Selection of dCas9-activator expression plasmids

For the activation of target genes, we used dCas9-based transcriptional activators. The following expression plasmids were obtained from Addgene (<https://www.addgene.org/>): dCas9-VP64 (#47107) (P. Perez-Pinera *et al.* 2013), dCas9-VP64-GFP (#61422) (Koneremann *et al.* 2015), dCas9-VPR (#63798) (Chavez *et al.* 2015), and dCas9-p300 core (#61357) (Hilton *et al.* 2015). These constructs were selected based on their distinct transcriptional activation mechanisms, allowing for a comparative evaluation of their efficiency in upregulating endogenous *PDX1* and *NGN3* expression.

### HEK293 cell culture and transfection

HEK293 cells (Thermo Fisher Scientific, USA) were cultured in Dulbecco's modified Eagle's medium (DMEM) (Capricorn, Germany) supplemented with 10% fetal bovine serum (FBS) (Biological Industries, Israel), 1X non-essential amino acids (Gibco, USA) and 1X Antibiotic-Antimycotic (Biowest, France). HEK293 cells were seeded into 12-well plates at a density of 25000 cells per well 1 day before transfection. The cells were cultured in medium without antibiotics prior to transfection. Twenty ng of *NGN3* or *PDX1* gRNA plasmids were transfected using Lipofectamine 2000 (Life Technologies, USA), along with 200 ng of dCas9-VP64, dCas9-VPR or dCas9-P300, according to the manufacturer's instructions. The medium was refreshed 24 h after transfection. RNA isolation was performed with TRIzol (Invitrogen, USA) 48 h after transfection, according to the manufacturer's instructions. Cells were grown for an

additional 48 h before they were harvested for immunostaining. The estimated transfection efficiency was approximately 70% using 200 ng dCas9-VP64-GFP plasmid (Fig. S1). Transformation trials were conducted using various concentrations of dCas9-VPR, dCas9-p300, and dCas9-VP64 plasmids (10, 20, 50, 75, 100, 150, and 200 ng). The highest transfection efficiency was observed at 200 ng (data not shown). Control experiments were performed using HEK293 cells that were cultured under the same conditions but without transfection.

#### Real-Time Quantitative PCR (RT-qPCR)

Total RNA was extracted from cell samples using TRIzol reagent and reverse-transcribed into cDNA using the iScript cDNA Synthesis Kit (Bio-Rad Laboratories, USA). For each quantitative RT-qPCR reaction, 200 ng cDNA were used as a template in a 10 µl reaction system with iTaq™ Universal SYBR® Green Supermix (Bio-Rad Laboratories, USA). Quantitative RT-PCR was performed with the LightCycler® 96 thermal cycler (Roche Applied Science, Germany), using the following conditions: initial denaturation at 95°C for 10 min, followed by 45 cycles of 95°C for 15 s, and 60°C for 60 s with fluorescence acquisition, followed by a standard melting curve stage. The measured transcript levels were normalized to GAPDH levels, and all samples were analyzed in triplicate. The primers used for RT-qPCR analysis are listed in Supplementary Material Table S3. RT-qPCR was performed as described above. As a negative control, HEK293 cells were used without any transfection. The data are presented as Log<sub>2</sub> (relative expression to GAPDH), which allows for a clearer representation of fold changes in gene expression relative to the control group. This approach simplifies the visualization of gene expression changes, particularly in cases of increased or decreased expression compared to the negative control.

#### Immunostaining

The cell culture medium was removed 48 h after plasmid transfection. HEK293 cells were washed three times with 1X PBS. The cells were fixed with 10% (v/v) formalin for 20 min at room temperature. After incubation, the formalin was removed, and the cells were washed three times with 1X PBS, each wash lasting 5 min. Next, the cells were permeabilized by adding 0.2% (v/v) PBS-TritonX-100 and incubating for 15 min at room temperature. After incubation, the cells were washed three times with 0.1% (v/v) PBS-Tween 20, each wash lasting 5 min. Following the washing, 5% (w/v) PBS-Tween 20-BSA was added, and the cells were incubated for 2 h at room temperature. After incubation, the cells were washed three times with 0.1% (v/v) PBS-Tween 20 for 5 min each. The primary antibodies Rabbit polyclonal anti-PDX1 (1: 2000 dilution; Abcam, UK), Rabbit polyclonal anti-NGN3 (1: 200 dilutions; Abcam, UK), and Rabbit monoclonal anti-Insulin (1: 300 dilution; Abcam, UK) were used. The antibodies were incubated overnight at 4°C. Following incubation, the primary antibodies were removed by washing the cells three times with 0.1% (v/v)

PBS-Tween 20 (v/v) for 5 min each. The secondary goat anti-rabbit IgG antibody was prepared in 1% PBS-Tween 20-BSA solution at a 1:400 dilution and added to each well. The nucleic acid stain, antibodies, and their dilution ratios used in immunofluorescence staining are listed in Table S4. The cells were incubated for 1 h at room temperature. After incubation, the secondary antibody was removed by washing the cells three times with 0.1% (v/v) PBS-Tween 20 for 5 min each. Hoechst dye was prepared at a 1:400 dilution in 1% PBS-Tween 20-BSA solution, added to each well, and incubated for 20 min at room temperature. After incubation, the cells were washed three times with 1X PBS. Finally, 1X PBS was added to the cells, and images were captured using a Leica DMi8 inverted microscope (Leica DMi8, LASX Software).

#### Statistical analysis

In the transfection experiments, HEK293 cells were transfected at three different time points to assess experimental conditions. For each time point, three independent biological replicates were performed, each with three technical replicates. Biological replicates represent separate experiments using distinct samples, while technical replicates are repeated measurements from the same sample to assess precision. This design accounted for both technical and biological variability, ensuring reliable results. Statistical analyses were performed on the averages of independent experiments. An unpaired two-tailed Student's t-test was used for comparisons between two groups, with significance set at  $p < 0.05$ . Data are presented as mean  $\pm$  SEM ( $n=3$ ).

### **Results**

#### dCas9-Transactivator and gRNA Optimization for PDX1 gene activation

Each of the ten gRNAs specific to *PDX1* was introduced separately into the cells, along with the dCas9-VP64, dCas9-VPR, and Cas9-p300. The effects of each gRNA on gene expression were assessed using RT-qPCR. Fig. 1 shows that the *PDX1* gene is active in compared to the control group. Among the 10 gRNAs tested, gRNA1, gRNA2, gRNA7, and gRNA9 were most effective in activating the *PDX1*. These gRNAs also meet the criteria established in the gRNA optimization and design experiments conducted (Graf et al. 2019, Wang et al. 2019).

The four optimal gRNAs were selected for activation experiments of the *PDX1* using dCas9 activator complexes. Among these complexes, the VPR activator showed the highest activation level compared to the control group, as shown in Fig. 1d. The simultaneous application of the four gRNAs targeting *PDX1* resulted in a 19-fold increase in gene expression with VPR and a 3.9-fold increase with VP64.

The transfections were performed using 200 ng of the dCas9-activator plasmid and 20 ng of each gRNA (\*\* $p < 0.005$ , \*\*\*\* $p < 0.0001$ ).

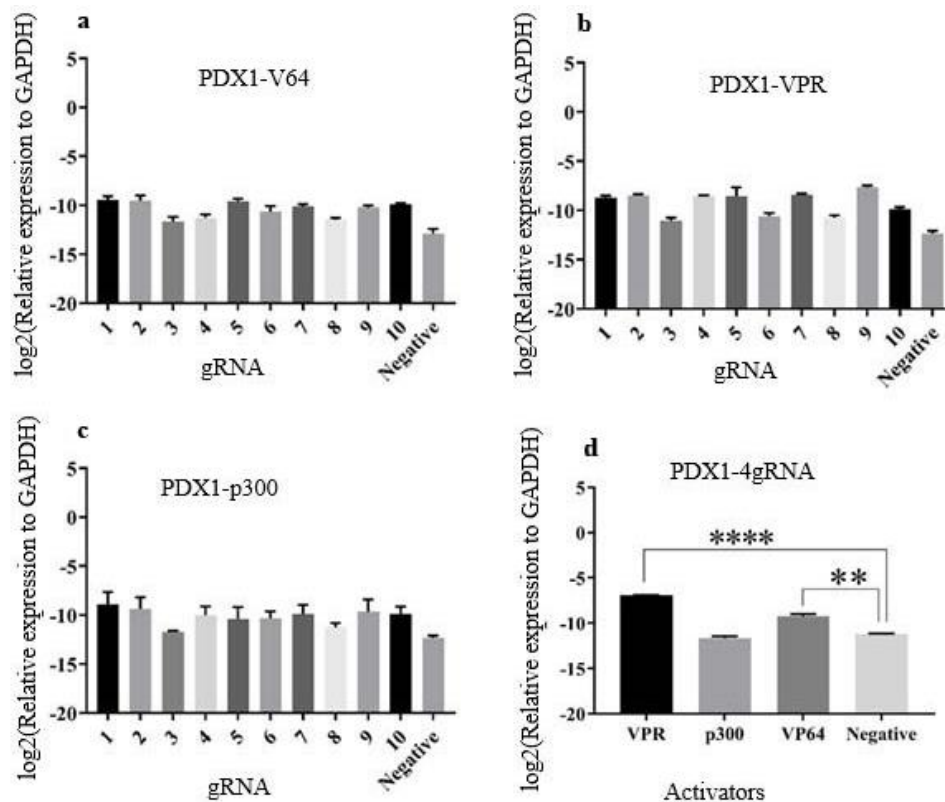


**Fig. 1.** Upregulation of the *PDX1* expression in HEK293 cells by **a.** dCas9-VP64, **b.** dCas9-VPR, **c.** dCas9-p300, and **d.** optimal 4 gRNA activators. The relative expression levels were measured by RT-qPCR 48 h after transfection. Data represents mean  $\pm$  SEM,  $n=3$  independent transfections.

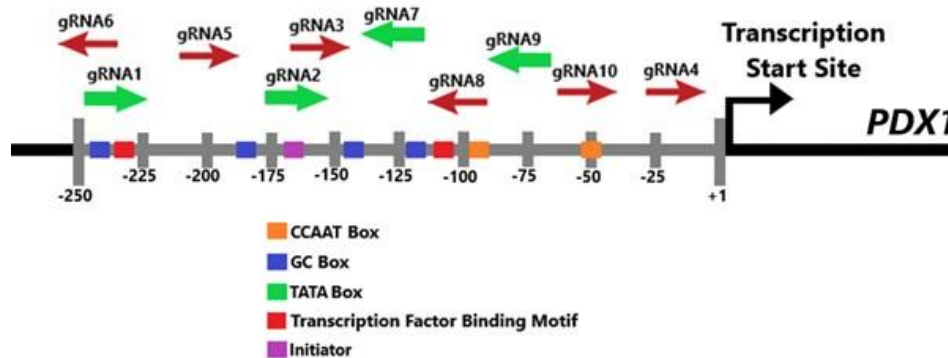


**Fig. 2.** The promoter region of *PDX1*, which spans from -250 to +1 base pairs, is considered crucial for the regulation of gene expression.

Once the optimal gRNAs were identified, an examination was conducted using the Eukaryotic Promoter Database (Dreos *et al.* 2017, Database 2025) to determine if any regulatory regions influencing gene activity were present near the locations of these gRNAs. Based on this investigation, we found that gRNA1 is associated with a region containing a transcription factor motif, GC box, and transcription factor binding motif. Similarly, gRNA2 is linked to a region containing the initiator motif. Furthermore, RNA7 binds to a region containing the GC box. Fig. 2 illustrates that no discernible motif or specific region was identified for gRNA9.

#### dCas9-Transactivator and gRNA Optimization for *NGN3* gene activation

Each of the 8 gRNAs identified for the *NGN3* gene was separately introduced into the cells using dCas9-VP64, dCas9-VPR, and Cas9-p300. The effect of each gRNA on gene expression were assessed using RT-qPCR. Fig. 3 demonstrates that the *NGN3* gene is active in compared to the control group. Out of the 8 gRNAs, gRNA1, gRNA2, gRNA4, and gRNA7 were optimal for activating the *NGN3*. The simultaneous application of these four *NGN3*-targeting gRNAs resulted in a 256-fold increase in gene expression with VPR, a 35-fold increase with p300, and a 3-fold increase with VP64. The gRNAs

also met the criteria established in the gRNA optimization and design experiments conducted by Graf *et al.* (2019) and Wang *et al.* (2019). Activation assays were conducted using dCas9 activator complexes with the four optimal gRNA sequences identified to activate the *NGN3*. The results showed that the VPR activator exhibited the highest level of activation compared with the control group (Fig. 3d). The VPR activator enhanced the affinity of transcription factors for the promoter regions of *NGN3*, which is specifically recognized by four gRNAs. As a result, transcription is initiated and, gene expression is enhanced.

The absence of statistically significant activation observed for individual gRNAs implies that these gRNAs may not precisely bind to the promoter region of the target gene, or even if they do bind, they may not effectively recruit transcription factors and activate transcription. The presence of four gRNAs causing excessive activation indicates that these gRNAs have the potential to bind to distinct sections of the promoter region of their target genes.

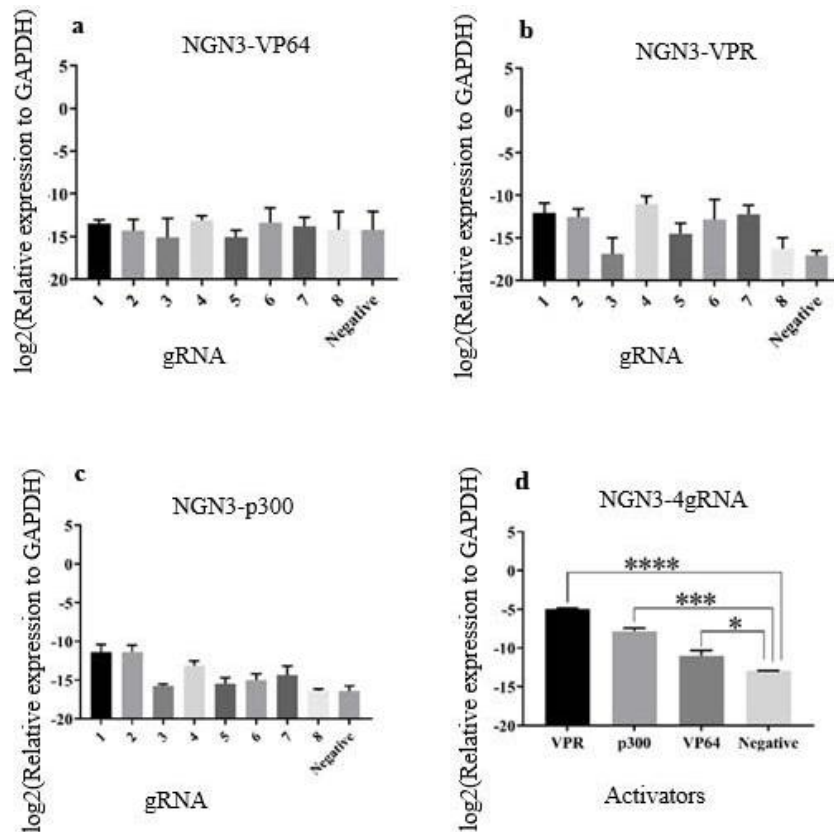


**Fig. 3.** Upregulation of the *NGN3* gene in HEK293 cells by **a.** dCas9-VP64, **b.** dCas9-VPR, **c.** dCas9-p300, and **d.** optimal 4 gRNA activators. The relative expression levels were measured by RT-qPCR 48 h after transfection. Data represents mean  $\pm$  SEM, n=3 independent transfections. The transfections were performed using 200 ng of the dCas9-activator plasmid and 20 ng of each gRNA (\* $p$  < 0.05, \*\*\* $p$  < 0.0005, \*\*\*\* $p$  < 0.0001).

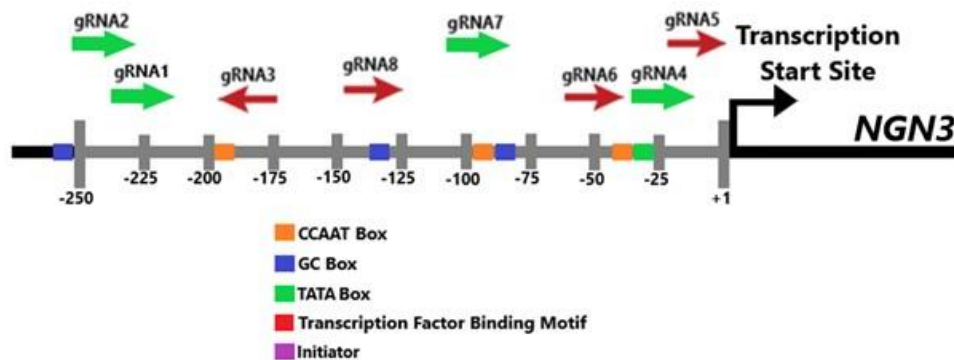


**Fig. 4.** The regulatory elements within the promoter region of *NGN3*, specifically spanning from -250 to +1 base pairs, are considered to play a critical role in the modulation of gene expression.



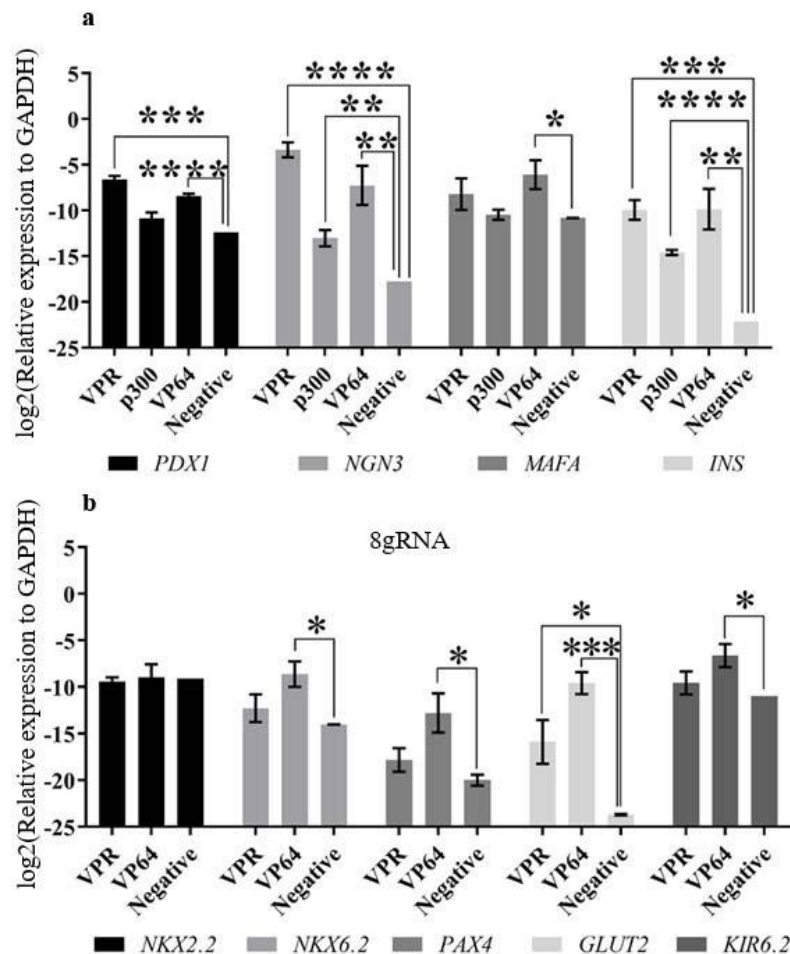


**Fig. 5.** Activation results of important pancreatic genes. **a.** Expression of the *PDX1*, *NGN3*, *MAFA*, and *INS* genes, **b.** activation of the *NKX2.2*, *NKX6.2*, *PAX4*, *GLUT2*, and *KIR6.2* genes from important pancreatic genes. Data represents mean  $\pm$  SEM,  $n = 3$  independent transfections. The transfections were performed using 200 ng of the dCas9-activator and 20 ng of each gRNA (\* $p < 0.05$ , \*\* $p < 0.005$ , \*\*\* $p < 0.0005$ , \*\*\*\* $p < 0.0001$ ).

This leads to more efficient recruitment of transcription factors and the initiation of transcription.

Once the optimal gRNAs were identified, an examination was conducted using The Eukaryotic Promoter Database (Dreos *et al.* 2017, Database 2025) to discover if there were any regulatory areas influencing gene activity in the vicinity of the gRNAs. The results revealed that gRNA4 attaches to the region encompassing the TATA box and CCAAT box, and is located near the regions where gRNA2 binds to the GC box. Additionally, gRNA7 binds to both the CCAAT box and GC box regions (Fig. 4).

#### Synergistic Activation of PDX1 and NGN3 Genes Using CRISPR-dCas9 System with Optimized gRNAs

Four gRNA sequences were identified for the activation of *PDX1* and *NGN3*. These gRNA sequences were then introduced into cells along with the dCas9-VPR, dCas9-p300, and dCas9 VP64 activators. The expression levels of crucial cellular genes were subsequently analyzed. Co-transfecting these 8 gRNAs demonstrated a synergistic effect on gene activation. The

combination of 8 gRNA with the VP64 activator for *PDX1*, and the VPR activator for *NGN3* yielded the highest level of activation, as shown in Fig. 5a. The *INS* gene exhibited the greatest significant activation when using 8 gRNAs and p300 activators. Activation of the *PDX1* and *NGN3* genes using 8 gRNA and VP64 activators resulted in the highest level of activation of the *MAFA*, *NKX6.2*, *PAX4*, *GLUT2*, and *KIR6.2* genes, as shown in Fig. 5b. These genes are responsible for the distinctive characteristics of pancreatic  $\beta$  cells. The upregulation of these genes enhances the process of cell differentiation into  $\beta$  cells. Fig. 5 shows a substantial increase in the expression of these genes compared with the control cells.

#### Immunostaining

Gene expression was demonstrated by transfecting HEK293 cells with 20 ng of gRNA plasmid and 200 ng of dCas9-activator plasmid using anti-PDX1, anti-NGN3, and anti-Insulin antibodies. The CRISPR/dCas9 activation mechanism induced the expression of endogenous PDX1 and NGN3, resulting in the localization of endogenic proteins in the nucleus (Figs 6, 7).



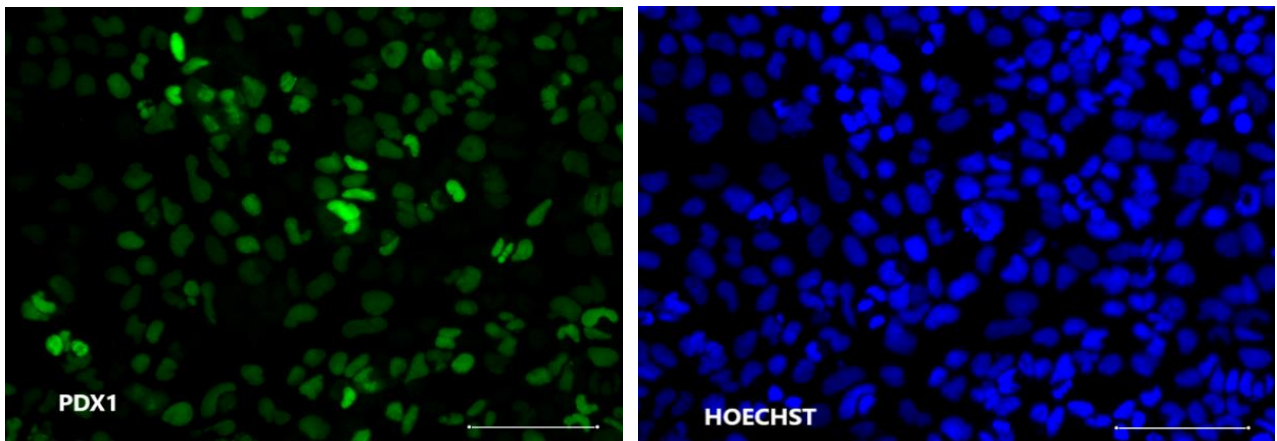


**Fig. 6.** Anti-PDX1 (green) and Hoechst (blue) immunostaining results after activation of the *PDX1* gene using 4 gRNA and the dCas9-VPR plasmid. Scale bars represent 100  $\mu$ m.

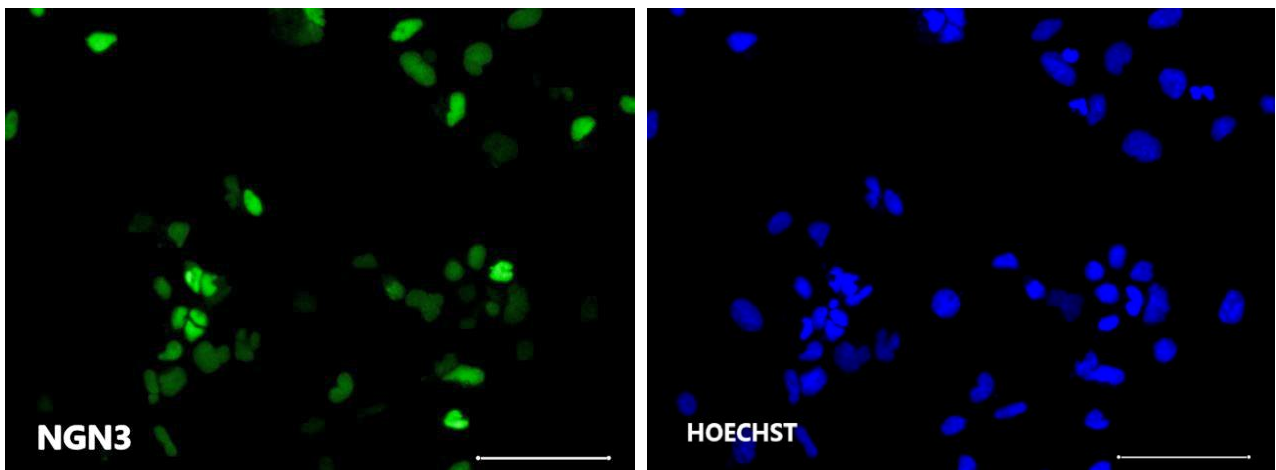


**Fig. 7.** Immunocytochemical analysis of NGN3 in HEK293 cells 72 h after transfection with dCas9-VPR activator and *NGN3* targeting 4 gRNAs. Anti-NGN3 (green), Hoechst (blue). Scale bars represent 100  $\mu$ m.

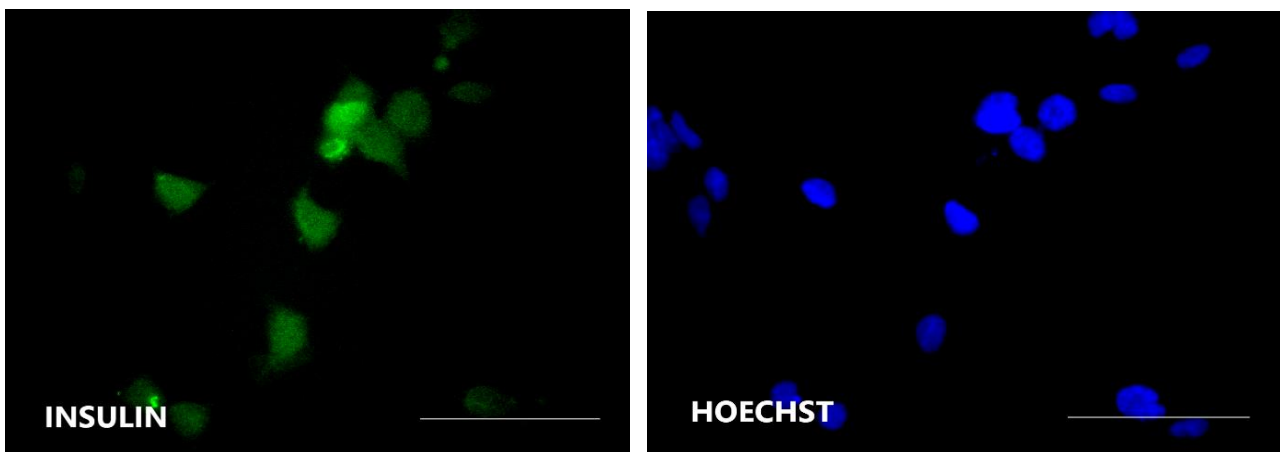


**Fig. 8.** Immunocytochemical analysis of INS in HEK293 cells 72 h after transfection with dCas9-VPR activator and 8 gRNAs targeting *PDX1* and *NGN3*. Insulin (green), Hoechst (blue), and scale bars represent 100  $\mu$ m.

Immunocytochemical staining for insulin in HEK293 cells 72 h post-transfection using the dCas9-VPR activator system and 8 gRNAs designed to target the *PDX1* and *NGN3* genes. The cells were stained with an anti-Insulin antibody to visualize the expression of insulin. The results show significant insulin expression in cells transfected with the dCas9-VPR activator and gRNAs targeting *PDX1* and *NGN3*, compared with the control group, which exhibits minimal to no insulin expression. This indicates that the activation of the *PDX1* and *NGN3* genes via the dCas9-VPR system effectively induces insulin (INS) expression in HEK293 cells, highlighting the potential of this approach for gene activation studies aimed at generating pancreatic  $\beta$  cell-like cells.

## Discussion

In this study, dCas9-based activator complexes were used to evaluate the activation of the *NGN3* gene using different gRNAs. The HEK293 cell line is an ideal model for CRISPR/dCas9-based gene activation due to its high transfection efficiency and sensitivity to genetic modifications. Its rapid proliferation and ease of culture ensure a stable environment for long-term experiments, allowing for effective evaluation of gene activation. Low basal expression levels facilitate clear observation of transcription factor activation, such as *PDX1* and *NGN3*, while supporting reliable results in immunofluorescence and RT-qPCR analyses. These features make HEK293 a robust model for optimizing gene regulation strategies that induce  $\beta$ -cell differentiation. Our findings emphasize the critical role of gRNA selection, transcription factor recruitment, and promoter structure in gene activation. Among the eight gRNAs tested, gRNA1, gRNA2, gRNA4, and gRNA7 were identified as the most effective. Activity was assessed by measuring *NGN3* gene expression levels using RT-qPCR and comparing transcriptional increases achieved with activator complexes. Additionally, the binding sites within the promoter region and transcription factor recruitment were also analyzed. When used alone, gRNAs did not result in significant transcriptional activation, but the combination of these four gRNAs, particularly when used with the VPR activator, led to a 256-fold increase in *NGN3* expression. A 35-fold increase was observed with the p300 activator, and a 3-fold increase was observed with VP64. Analysis of the binding sites within the promoter region revealed that gRNA4 was located near the TATA box and CCAAT box. These elements are critical for initiating transcription, and gRNAs binding near these regions are thought to effectively recruit transcription factors, increasing RNA polymerase II binding. In contrast, gRNA1 and gRNA2, which bind to the GC box, exhibited relatively lower activation potential. This suggests that while the GC box can initiate transcription, TATA and CCAAT boxes offer higher activation efficiency.

In studies evaluating the activation of the *PDX1* gene, the effectiveness of various gRNAs and their binding regions to transcription factors were analyzed. RT-qPCR results showed that gRNA1, gRNA2, gRNA7, and

gRNA9 achieved the highest activation of *PDX1* expression. Notably, gRNA1 and gRNA2 were associated with motifs like the GC box and the promoter motif, which play significant roles in transcriptional regulation. The presence of these motifs indicates that the corresponding gRNAs can enhance transcriptional efficiency by recruiting transcription factors to the target region. On the other hand, the effect of gRNA7, which includes a GC box but lacks a notable motif, is likely mediated through chromatin structure modulation or indirect mechanisms. When dCas9 activator complexes were tested, the highest activation of *PDX1* expression was achieved by the VPR system, resulting in a 19-fold increase. The VP64 activator also provided significant activation, although at a lower level (3.9-fold) compared to VPR. However, a combination of multiple gRNAs with the dCas9-p300 activator complex did not lead to a significant improvement in *PDX1* expression. This may be due to the more limited transcriptional activation capacity of p300 compared to VPR.

The concurrent activation of *PDX1* and *NGN3* genes resulted in the upregulation of pancreatic  $\beta$ -cell-related genes, suggesting that CRISPR-based gene activation could promote  $\beta$ -cell differentiation. Our findings indicate that the use of multiple gRNAs produces a synergistic effect in enhancing gene activation. The combination of VP64 for *PDX1* and VPR for *NGN3* provided the strongest gene expression, highlighting the critical role of activator selection in optimizing gene expression. Additionally, p300 was observed to be particularly effective in enhancing the expression of the *INS* gene, which is thought to be related to its role in histone acetylation and chromatin remodeling. These results support the idea that targeted epigenetic modifications can significantly improve the transcriptional environment in somatic cells. Furthermore, the upregulation of key  $\beta$ -cell markers such as *MAFA*, *NKX6.2*, *PAX4*, *GLUT2*, and *KIR6.2* indicates that CRISPR activation not only activates *PDX1* and *NGN3* genes but also triggers critical genetic programs essential for pancreatic  $\beta$ -cell development.

Immunohistochemistry analysis confirmed that the combination of dCas9-VPR and the target gRNAs successfully increased *PDX1* and *NGN3* protein expression in HEK293 cells, leading to a significant rise in insulin expression. These findings validate the specificity of cellular reprogramming and suggest that CRISPR/dCas9 activation could be an effective method for acquiring pancreatic  $\beta$ -cell features. However, functional evaluations of the  $\beta$ -cell-like cells are required. For these evaluations, it is recommended to validate the insulin production levels using Western blot analysis, assess cellular glucose sensitivity through static glucose stimulation tests, and analyze cellular response mechanisms such as calcium flux. Additionally, evaluating the phenotypic stability of the cells under long-term culture conditions will be critical to understanding the functional continuity of the generated  $\beta$ -cell-like cells.

Future studies should include validation of insulin production using Western blot analysis, assessment of glucose sensitivity, and investigation of long-term stability. Moreover, conducting similar experiments in other cell lines like INS-1, HP62, and HP74 will help ensure the broader biological relevance of these findings. The gRNAs identified in our study, along with the dCas9 activators we compared, make significant contributions to gene activation and cell differentiation studies. In conclusion, CRISPR/dCas9-based approaches hold great potential for cellular reprogramming and  $\beta$ -cell regeneration, and these methods could provide valuable insights for future biomedical applications.

**Ethics Committee Approval:** Since the article does not contain any studies with human or animal subject, its approval to the ethics committee was not required.

## References

1. Akinci, E., Banga, A., Greder, L.V., Dutton, J.R. & Slack, J.M. 2012. Reprogramming of pancreatic exocrine cells towards a beta ( $\beta$ ) cell character using Pdx1, Ngn3 and MafA. *Biochemistry Journal*, 442(3): 539-550. <https://doi.org/10.1042/bj20111678>
2. Balboa, D., Weltner, J., Eurola, S., Trokovic, R., Wartiovaara, K. & Otonkoski, T. 2015. Conditionally Stabilized dCas9 Activator for Controlling Gene Expression in Human Cell Reprogramming and Differentiation. *Stem Cell Reports*, 5(3): 448-459. <https://doi.org/10.1016/j.stemcr.2015.08.001>
3. Beerli, R.R., Dreier, B. & Barbas, C.F., 3rd. 2000. Positive and negative regulation of endogenous genes by designed transcription factors. *Proceedings of the National Academy of Sciences of the United States of America*, 97(4): 1495-1500. <https://doi.org/10.1073/pnas.040552697>
4. Casas-Mollano, J.A., Zinselmeier, M.H., Erickson, S.E. & Smanski, M.J. 2020. CRISPR-Cas Activators for Engineering Gene Expression in Higher Eukaryotes. *The CRISPR Journal* 3(5): 350-364. <https://doi.org/10.1089/crispr.2020.0064>
5. Cavelti-Weder, C., Zumsteg, A., Li, W. & Zhou, Q. 2017. Reprogramming of Pancreatic Acinar Cells to Functional Beta Cells by In Vivo Transduction of a Polycistronic Construct Containing Pdx1, Ngn3, MafA in Mice. *Current Protocols in Stem Cell Biology*, 40: 4a.10.11-14a.10.12. <https://doi.org/10.1002/cpsc.21>
6. Chavez, A., Scheiman, J., Vora, S., Pruitt, B.W., Tuttle, M., P R Iyer, E., Lin, S., Kiani, S., Guzman, C.D., Wiegand, D.J., Ter-Ovanesyan, D., Braff, J.L., Davidsohn, N., Housden, B.E., Perrimon, N., Weiss, R., Aach, J., Collins, J.J. & Church, G.M. 2015. Highly efficient Cas9-mediated transcriptional programming. *Nature Methods*, 12(4): 326-328. <https://doi.org/10.1038/nmeth.3312>
7. Chen, M. & Qi, L.S. 2017. Repurposing CRISPR System for Transcriptional Activation. *Advances in experimental medicine and biology*, 983, 147-157. [https://doi.org/10.1007/978-981-10-4310-9\\_10](https://doi.org/10.1007/978-981-10-4310-9_10)
8. Cheng, A.W., Wang, H., Yang, H., Shi, L., Katz, Y., Theunissen, T.W., Rangarajan, S., Shivalila, C.S., Dadon, D.B. & Jaenisch, R. 2013. Multiplexed activation of endogenous genes by CRISPR-on, an RNA-guided transcriptional activator system. *Cell Research*, 23(10): 1163-1171. <https://doi.org/10.1038/cr.2013.122>
9. CRISPR-ERA. 2025. gRNA design tool for CRISPR-mediated gene editing. <http://CRISPR-ERA.stanford.edu> (Date accessed: 23.03.2025).
10. Dadheech, N. & James Shapiro, A.M. 2019. Human Induced Pluripotent Stem Cells in the Curative Treatment of Diabetes and Potential Impediments Ahead, pp. 25-35. In K. Turksen (Ed.), *Cell Biology and Translational Medicine, Volume 5: Stem Cells: Translational Science to Therapy*, Springer International Publishing, Cham.
11. Database, E.P. 2025. Eukaryotic Promoter Database. <http://epd.vital-it.ch> (Date accessed: 23.03.2025).
12. Dominguez, A., Chavez, M.G., Urke, A., Gao, Y., Wang, L. & Qi, L.S. 2022. CRISPR-Mediated Synergistic Epigenetic and Transcriptional Control. *The CRISPR Journal*, 5(2): 264-275. <https://doi.org/10.1089/crispr.2021.0099>
13. Dreos, R., Ambrosini, G., Groux, R., Cavin P  rier, R. & Bucher, P. 2017. The eukaryotic promoter database in its 30th year: focus on non-vertebrate organisms. *Nucleic Acids Research*, 45(D1): D51-d55. <https://doi.org/10.1093/nar/gkw1069>
14. Elhanani, O., Salame, T.M., Sobel, J., Leshkowitz, D., Povodovski, L., Vaknin, I., Kolodkin-Gal, D. & Walker, M.D. 2020. REST Inhibits Direct Reprogramming of Pancreatic Exocrine to Endocrine Cells by Preventing PDX1-Mediated Activation of Endocrine Genes. *Cell Reports*, 31(5): 107591. <https://doi.org/10.1016/j.celrep.2020.107591>
15. Gilbert, L.A., Larson, M.H., Morsut, L., Liu, Z., Brar, G.A., Torres, S.E., Stern-Ginossar, N., Brandman, O., Whitehead, E.H., Doudna, J.A., Lim, W.A., Weissman, J.S. & Qi, L.S. 2013. CRISPR-mediated modular RNA-guided regulation of transcription in eukaryotes. *Cell*, 154(2): 442-451. <https://doi.org/10.1016/j.cell.2013.06.044>
16. Gim  nez, C.A., Ielpi, M., Mutto, A., Grosembacher, L., Argibay, P. & Pereyra-Bonnet, F. 2016. CRISPR-on system for the activation of the endogenous human INS gene. *Gene Therapy*, 23(6): 543-547. <https://doi.org/10.1038/gt.2016.28>

17. Graf, R., Li, X., Chu, V.T. & Rajewsky, K. 2019. sgRNA Sequence Motifs Blocking Efficient CRISPR/Cas9-Mediated Gene Editing. *Cell Reports*, 26(5): 1098-1103. <https://doi.org/10.1016/j.celrep.2019.01.024>
18. Guo, P., Zhang, T., Lu, A., Shiota, C., Huard, M., Whitney, K.E. & Huard, J. 2023. Specific reprogramming of alpha cells to insulin-producing cells by short glucagon promoter-driven Pdx1 and MafA. *Molecular Therapy Methods & Clinical Development*, 28: 355-365. <https://doi.org/10.1016/j.omtm.2023.02.003>
19. Hilton, I.B., D'Ippolito, A.M., Vockley, C.M., Thakore, P.I., Crawford, G.E., Reddy, T.E. & Gersbach, C.A. 2015. Epigenome editing by a CRISPR-Cas9-based acetyltransferase activates genes from promoters and enhancers. *Nature Biotechnology*, 33(5): 510-517. <https://doi.org/10.1038/nbt.3199>
20. Hsu, M.N., Chang, Y.H., Truong, V.A., Lai, P.L., Nguyen, T.K.N. & Hu, Y.C. 2019. CRISPR technologies for stem cell engineering and regenerative medicine. *Biotechnology Advances*, 37(8): 107447. <https://doi.org/10.1016/j.biotechadv.2019.107447>
21. Konermann, S., Brigham, M.D., Trevino, A.E., Joung, J., Abudayyeh, O.O., Barcena, C., Hsu, P.D., Habib, N., Gootenberg, J.S., Nishimasu, H., Nureki, O. & Zhang, F. 2015. Genome-scale transcriptional activation by an engineered CRISPR-Cas9 complex. *Nature*, 517(7536): 583-588. <https://doi.org/10.1038/nature14136>
22. Kunii, A., Hara, Y., Takenaga, M., Hattori, N., Fukazawa, T., Ushijima, T., Yamamoto, T. & Sakuma, T. 2018. Three-Component Repurposed Technology for Enhanced Expression: Highly Accumulable Transcriptional Activators via Branched Tag Arrays. *The CRISPR Journal* 1(5): 337-347. <https://doi.org/10.1089/crispr.2018.0009>
23. Lee, M.-H., Thomas, J.L., Lin, C.-Y., Li, Y.-C.E. & Lin, H.-Y. 2023. Nanoparticle-mediated CRISPR/dCas9a activation of multiple transcription factors to engineer insulin-producing cells. *Journal of Materials Chemistry B*, 11(9): 1866-1870. <https://doi.org/10.1039/D2TB02431D>
24. Maeder, M.L., Linder, S.J., Cascio, V.M., Fu, Y., Ho, Q.H. & Joung, J.K. 2013. CRISPR RNA-guided activation of endogenous human genes. *Nature Methods*, 10(10): 977-979. <https://doi.org/10.1038/nmeth.2598>
25. Maxwell, K.G., Augsornworawat, P., Velazco-Cruz, L., Kim, M.H., Asada, R., Hoglebe, N.J., Morikawa, S., Urano, F. & Millman, J.R. 2020. Gene-edited human stem cell-derived  $\beta$  cells from a patient with monogenic diabetes reverse preexisting diabetes in mice. *Science Translational Medicine*, 12(540): eaax9106. <https://doi.org/doi:10.1126/scitranslmed.aax9106>
26. Nuñez, J.K., Chen, J., Pommier, G.C., Cogan, J.Z., Replogle, J.M., Adriaens, C., Ramadoss, G.N., Shi, Q., Hung, K.L., Samelson, A.J., Pogson, A.N., Kim, J.Y.S., Chung, A., Leonetti, M.D., Chang, H.Y., Kampmann, M., Bernstein, B.E., Hovestadt, V., Gilbert, L.A. & Weissman, J.S. 2021. Genome-wide programmable transcriptional memory by CRISPR-based epigenome editing. *Cell*, 184(9): 2503-2519.e2517. <https://doi.org/10.1016/j.cell.2021.03.025>
27. Perez-Pinera, P., Kocak, D.D., Vockley, C.M., Adler, A.F., Kabadi, A.M., Polstein, L.R., Thakore, P.I., Glass, K.A., Ousterout, D.G., Leong, K.W., Guilak, F., Crawford, G.E., Reddy, T.E. & Gersbach, C.A. 2013. RNA-guided gene activation by CRISPR-Cas9-based transcription factors. *Nature Methods*, 10(10): 973-976. <https://doi.org/10.1038/nmeth.2600>
28. Pollock, S.D., Galicia-Silva, I.M., Liu, M., Gruskin, Z.L. & Alvarez-Dominguez, J.R. 2023. Scalable generation of 3D pancreatic islet organoids from human pluripotent stem cells in suspension bioreactors. *STAR Protocols*, 4(4): 102580. <https://doi.org/10.1016/j.xpro.2023.102580>
29. Qi, L.S., Larson, M.H., Gilbert, L.A., Doudna, J.A., Weissman, J.S., Arkin, A.P. & Lim, W.A. 2013. Repurposing CRISPR as an RNA-guided platform for sequence-specific control of gene expression. *Cell*, 152(5): 1173-1183. <https://doi.org/10.1016/j.cell.2013.02.022>
30. Razavi, Z., Soltani, M., Souri, M. & van Wijnen, A.J. 2024. CRISPR innovations in tissue engineering and gene editing. *Life Sciences*, 358: 123120. <https://doi.org/10.1016/j.lfs.2024.123120>
31. Richter, M.F., Zhao, K.T., Eton, E., Lapinaite, A., Newby, G.A., Thuronyi, B.W., Wilson, C., Koblan, L.W., Zeng, J., Bauer, D.E., Doudna, J.A. & Liu, D.R. 2020. Phage-assisted evolution of an adenine base editor with improved Cas domain compatibility and activity. *Nature Biotechnology*, 38(7): 883-891. <https://doi.org/10.1038/s41587-020-0453-z>
32. Riedmayr, L.M., Hinrichsmeyer, K.S., Karguth, N., Böhm, S., Splith, V., Michalakakis, S. & Becirovic, E. 2022. dCas9-VPR-mediated transcriptional activation of functionally equivalent genes for gene therapy. *Nature Protocols*, 17(3): 781-818. <https://doi.org/10.1038/s41596-021-00666-3>
33. Seo, J.H., Shin, J.H., Lee, J., Kim, D., Hwang, H.-Y., Nam, B.-G., Lee, J., Kim, H.H. & Cho, S.-R. 2023. DNA double-strand break-free CRISPR interference delays Huntington's disease progression in mice. *Communications Biology*, 6(1): 466. <https://doi.org/10.1038/s42003-023-04829-8>
34. Soria, B. 2001. In-vitro differentiation of pancreatic  $\beta$ -cells. *Differentiation*, 68(4-5): 205-219. <https://doi.org/10.1046/j.1432-0436.2001.680408.x>
35. Wang, D., Zhang, C., Wang, B., Li, B., Wang, Q., Liu, D., Wang, H., Zhou, Y., Shi, L., Lan, F. & Wang, Y. 2019. Optimized CRISPR guide RNA design for two high-fidelity Cas9 variants by deep learning. *Nature Communications*, 10(1): 4284. <https://doi.org/10.1038/s41467-019-12281-8>





## Fungal contamination in residential water systems: A comparative study between hot and cold water samples

Esra Merve Dizge<sup>1</sup>, Duygu Göksay Kadaifçiler<sup>2\*</sup>

<sup>1</sup> Institute of Graduate Studies in Sciences, Istanbul University, 34134, Istanbul, TÜRKİYE

<sup>2</sup> Department of Biology, Faculty of Science, Istanbul University, 34134, Istanbul, TÜRKİYE

### Cite this article as:

Dizge E.M. & Göksay Kadaifçiler D. 2025. Fungal contamination in residential water systems: A comparative study between hot and cold water samples. *Trakya Univ J Nat Sci*, 26(1): 61-72, DOI: 10.23902/trkjinat.1576675

Received: 13 December 2024, Accepted: 07 April 2025, Published: 15 April 2025

**Abstract:** Some fungal species are known to have adverse health effects for humans and their presence in water systems may lead to alterations in the taste and odour of the water they occupy. Although a few country-based regulations are known, no universal legal restriction on the presence of fungi in drinking or utility water is present currently. Waterborne fungi have been a neglected part of microbial studies worldwide, and more studies are needed in the current era of global warming. This study was performed to evaluate (i) the fungal load in randomly selected residential water systems connected to the municipal water supply in Istanbul, Türkiye, and (ii) the possible impact of water temperature on the number and biodiversity of fungi. Additionally, the relationship between bacterial loads, some water parameters and the determined fungi were investigated. Cold and hot water samples were taken from 20 randomly selected buildings in Istanbul and inoculated into SDA using the membrane filtration method for fungal isolation, and onto R2A and *Candida* Agar using the spread plate method for bacterial and *Candida* isolation, respectively. More microorganisms were detected in cold water samples than in hot water. The mean fungal and bacterial numbers in cold and hot water samples were 2.4, 1.47, 702.3 and 79.5 cfu/100 mL, respectively. No *Candida* was found. It was determined that temperature affected the biodiversity and frequency of fungi. *Penicillium* (41%) and *Aspergillus* (43.75%) were the dominant fungal genera in cold and hot water, respectively. *Aspergillus versicolor* was the most common fungal species found in both water samples. 9 of fungi were identified that are known to have the potential to cause allergies and/or opportunistic infections. No relationship was detected between fungal growth and pH and chlorine.

### Edited by:

İskender Karlatlı

### \*Corresponding Author:

Duygu Göksay Kadaifçiler  
[dgoksay@istanbul.edu.tr](mailto:dgoksay@istanbul.edu.tr)

### ORCID iDs of the authors:

EMD. 0000-0003-2272-6956  
DGK. 0000-0002-4825-243X

### Key words:

Fungi  
Biodiversity  
Tap water  
Hot and cold water  
Temperature

**Özet:** Bazı mantar türlerinin insanlar için olumsuz sağlık etkileri olduğu bilinmektedir ve su sistemlerinde bulunmaları, bulundukları suyun tadında ve kokusunda değişikliklere yol açabilir. Birkaç ülke bazlı yasal düzenleme bilinmesine rağmen, şu anda içme veya kullanma suyuyla mantar varlığına ilişkin evrensel bir yasal kısıtlama bulunmamaktadır. Su kaynaklı mantarlar, dünya çapında mikrobiyal çalışmaların ihmal edilmiş bir parçasıdır ve küresel ısınmanın yaşandığı günümüzde daha fazla çalışmaya ihtiyaç duyulmaktadır. Bu çalışma, (i) İstanbul, Türkiye'deki belediye su şebekesine bağlı rastgele seçilmiş konut su sistemlerindeki mantar yükünü ve (ii) su sıcaklığının mantar sayısı ve biyolojik çeşitliliği üzerindeki olası etkisini değerlendirmek için gerçekleştirilmiştir. Ek olarak, bakteri yükleri, bazı su parametreleri ve belirlenen mantarlar arasındaki ilişki araştırılmıştır. İstanbul'da rastgele seçilmiş 20 binadan soğuk ve sıcak su örnekleri alınmış ve mantar izolasyonu için membran filtrasyon yöntemi kullanılarak SDA'ya, bakteri ve *Candida* izolasyonu için sırasıyla yayılmış plaka yöntemi kullanılarak R2A ve *Candida* Agar'a ekimleri yapılmıştır. Soğuk su örneklerinde sıcak sudan daha fazla mikroorganizma tespit edilmiştir. Soğuk ve sıcak su örneklerindeki ortalama mantar ve bakteri sayıları sırasıyla 2,4, 1,47, 702,3 ve 79,5 cfu/100 mL olarak bulundu. *Candida* bulunmadı. Sıcaklığın mantarların biyoçeşitliliğini ve sıklığını etkilediği belirlendi. Soğuk ve sıcak suda sırasıyla baskın mantar cinsleri *Penicillium* (%41) ve *Aspergillus* (%43,75) idi. Her iki su örneğinde de en sık bulunan mantar türü *Aspergillus versicolor* idi. Alerji ve/veya fırsatçı enfeksiyonlara neden olma potansiyeli olduğu bilinen 9 mantar türü tanımlanmıştır. Mantar üremesi ile pH ve klor arasında bir ilişki saptanmamıştır.

### Introduction

Mains water, also known as tap or municipal water, is supplied to homes, hospitals, and schools, through a network of pipes and treatment plants maintained by city

managements. It is a prerequisite to treat and process this type of water supply to make it biologically safe for various usage purposes including drinking, cooking, bathing and



OPEN ACCESS

cleaning (Provincial Health Directorate of Istanbul, 2022). Studies addressing the microbial load of man-made water systems showed the presence of various bacteria and fungi of health concern in high numbers in these systems connected to the mains water supply (Hageskal *et al.* 2006, Kadaifçiler & Çotuk 2014). It is therefore crucial to monitor the mains water to prevent microbial contamination, particularly for presence of agents with the potential to have adverse effects on human health. The direct or indirect use of contaminated water in various ways, and inhalation of aerosols causes serious health problems and may even result in death over time (Babič *et al.* 2017). For this reason, it is essential to determine presence of a contamination in the mains water and microorganism responsible for the contamination. Although studies conducted on water systems have mainly focused on bacterial contamination (Zacheus & Martikainen 1995), the importance of fungal biocontamination has also been reported (Anaissie *et al.* 2002).

Fungi naturally live in soil and air environments, but they can also grow in aquatic systems. Some fungal species have developed an adaptation to grow in man-made water systems. In these systems, fungi can either be found in planktonic status in the water body, or they can be sessile in the biofilm layer. After increasing their colony number in the biofilm, they can break off from the biofilm layer and mix with the water (Kadaifçiler & Çotuk 2014, Babič *et al.* 2017). The initial contamination problems caused by fungi in mains water were identified in the 1960s and 1970s, and many fungal genera, mainly *Aspergillus*, *Penicillium*, *Fusarium*, *Acremonium*, *Arthroderma*, *Candida*, *Cladosporium*, *Chaetomium* and *Phialophora* have been detected in water systems (Hapçioğlu *et al.* 2005, Hageskal *et al.* 2006, Kanzler *et al.* 2007, Kadaifçiler & Çotuk 2014, Babič *et al.* 2017, Kadaifçiler & Demirel 2018). The water contaminated with fungi can lead to adverse human health and environmental effects (Burman 1965, Bays *et al.* 1970). Fungi in water systems can cause various diseases, including invasive infections (i.e. aspergillosis and endocarditis) as well as superficial diseases (i.e. keratitis and otomycosis). Besides their potential health risks, some microfungi such as *Chaetomium globosum* can cause taste and odor problems in water (Alangaden 2011).

Studies on water supply systems have mainly focused on cold water systems (Hapçioğlu *et al.* 2005, Hageskal *et al.* 2006, Kanzler *et al.* 2007, Kadaifçiler & Çotuk 2014, Kadaifçiler & Demirel 2018). There are only a limited number of studies that have investigated fungal loads in both cold and hot water systems simultaneously (Anaissie *et al.* 2002, Figueiredo Fonseca *et al.* 2010, Hayette *et al.* 2010). It is worth to mention that the water safety is traditionally monitored mainly by bacterial parameters that indicate faecal contamination. Therefore, the number of studies investigating fungal contamination is comparatively lower than that of bacterial contamination (Ma *et al.* 2015).

Temperature is an important parameter that affects the presence, diversity and distribution of microorganisms in water environments. With the climate changes affecting all ecosystems due to global warming, studies on fungi in freshwater have also accelerated. Global warming is expected to significantly affect nutrient and carbon cycles in ecosystems by changing the diversity, structure and activities of fungal communities (Hyde *et al.* 2016). Studies on fungal metabolism to temperature change often reach contradictory and location-specific results (Canhoto *et al.* 2016). Preciado *et al.* (2021) observed that temperature caused more dramatic changes in the fungal community in biofilm compared to tap water, such as loss of fungal diversity. However, certain fungal genera have been reported to become dominant and the number of opportunistic pathogenic bacteria increased with high temperatures. It has been concluded that the increased abundance of these microorganisms in water due to high temperatures is an undesirable situation as it may lead to health problems (Zacheus & Martikainen 1995).

The aim of this study is to investigate (i) the presence and concentration of fungi in residential water systems linked to a municipal water supply and (ii) the effect of water temperature variation on the quantity and biodiversity of fungi. In addition, the relationship between the presence of aerobic bacteria, water parameters, buildings' properties and the presence of fungi were also investigated. The findings of this research could be contribute to our understanding of the microbial composition and potential risks associated with water quality in residential water systems.

## Materials and Methods

### Water Sampling

A total of 40 water samples, 20 hot water and 20 cold water, were collected from 20 randomly selected residences in Istanbul, Türkiye. Samples were collected in 1 L sterile polypropylene bottles and were transferred to the laboratory in an insulated bag. Microbiological analyses were performed on the same day. The temperature, pH and free chlorine values of the samples were measured during samplings. The residences were multi-storey apartment buildings that are independent of each other, and only one flat in each apartment was sampled. 7 residences were on the Anatolian side and 13 residences are on the European side of the city. Building information including the age of the residences, districts, pipe material, presence of water tank were also noted.

The samples were taken from 15 different districts with the highest population density in Istanbul. There was no green area around the residences, and all of these residences were multi-story apartment buildings. The mean age of 20 randomly selected houses in Istanbul is 24.6 years. In 85% of the residences, polyvinyl chloride (PVC) was used as the pipe (surface) material, while in the remaining residences, galvanized steel (GS) was used. Only 15% of the buildings had water tanks and it was reported that there was no regular disinfection for them (Table 1).

**Table 1.** The general information of 20 residences.

Building Code	District	Building Age (Year)	Pipe Material	Presence of Water Tank
A	Kartal	15	GS	Yes
B	Esenler	22	PVC	No
C	Beylikdüzü	9	PVC	Yes
D	Zeytinburnu	22	PVC	No
E	Eyüpsultan	10	PVC	No
F	Bahçelievler	22	PVC	No
G	Eyüpsultan	7	PVC	No
H	Şişli	55	GS	No
I	Bahçelievler	20	PVC	No
J	Küçükçekmece	14	PVC	No
K	Avcılar	30	PVC	No
L	Ümraniye	20	PVC	No
M	Kartal	20	PVC	Yes
N	Maltepe	33	PVC	No
O	Şişli	20	PVC	No
P	Pendik	29	PVC	No
R	Kadıköy	45	GS	No
S	Fatih	50	PVC	No
T	Tuzla	27	PVC	No
U	Zeytinburnu	22	PVC	No

#### Isolation and Counting of Microorganisms

The membrane filtration method was performed for isolation and enumeration of fungi in the samples. Dilution series up to  $10^{-3}$  were prepared for each sample. 100 mL of water samples were taken directly from the sampling bottles and dilution series were filtered through nitrocellulose membrane filters (47 mm diameter, 0.45 µm pore size, Millipore, UK) using membrane filtration device (Millipore, UK) in triplicates. Membrane filters were placed onto petri dishes containing Sabouraud Dextrose Agar (SDA) medium (Merck, Germany) supplemented with 500 mg streptomycin (Sammon *et al.* 2011). The petri dishes of cold and hot water were incubated at  $25 \pm 2^\circ\text{C}$  for 14 days and at  $37^\circ\text{C}$  for 30 days, respectively (Hapçioğlu *et al.* 2005, Figueiredo Fonseca *et al.* 2010). At the end of the incubation period, the fungal counts in the water samples were determined and expressed as colony-forming unit per 100 ml of the water (cfu/100 mL). Fungal isolates with different macromorphological characteristics were determined to be pure and transferred to SDA media and after 7 days of incubation cultures were stored at  $+4^\circ\text{C}$ . In addition, cryotubes containing pure fungal spores were frozen at  $-86^\circ\text{C}$  for the long-term storage of fungal isolates.

For *Candida* yeast isolation and enumeration steps, concentrated samples were prepared. For this purpose, water samples (500 mL) were filtered separately through nylon membrane filters (47 mm diameter, 0.22 µm pore

size) using the membrane filtration device (Millipore, UK). The concentrated samples were obtained after shaking the filters with 10 mL of sterile tap water for 1 min in the stomacher device (IUL Instruments S.A.). Dilution series up to  $10^{-3}$  were prepared for each sample. 1 mL of original and diluted water samples were spread plated in triplicate onto *Candida* Agar plates. Petri dishes used for cold and hot water samples were incubated at  $30^\circ\text{C}$  and  $37^\circ\text{C}$ , respectively, for 2 days. The growth in petri dishes was controlled at the end of the incubation period. Incubation was extended to 30 days in case of no growth was observed (Hi-Media 2003, Kadaifçiler & Çotuk 2014).

Bacterial plating was performed using R2A agar medium to determine the number of aerobic bacterial counts. Petri dishes of cold and hot water samples were incubated at  $28^\circ\text{C}$  and  $37^\circ\text{C}$ , respectively, for 7-14 days and then the counts were obtained (Leginowicz *et al.* 2018).

#### Fungal Identification

Pure fungal isolates were first identified at genus level. Fresh fungal cultures were inoculated into Malt Extract Agar (MEA) medium and incubated at  $25 \pm 2^\circ\text{C}$  for 14 days. Macroscopic properties of the colonies were examined under a stereo microscope and microscopic properties were examined using a light microscope (Barnett & Hunter 1999).

For species-level identification of isolates of the genus *Aspergillus*, fresh cultures were inoculated into petri dishes containing Czapek Dox Agar (CDA), Czapek Yeast Extract Agar with 20% Sucrose (CY20S), Czapek Yeast Extract Agar (CYA) and MEA media. All petri dishes were incubated at  $25^\circ\text{C}$  for 7 days. Additional petri dishes containing CYA medium were incubated at  $37^\circ\text{C}$  for 7 days (Klich 2002, Sammon *et al.* 2010). At the end of the incubation period, colony properties (colony diameter, colony texture, colony/ colony reverse color, pigmentation, exudates, sclerotia) of the isolates were first determined. Then, preparates were prepared with lactophenol cotton blue dye from fungal cultures. Micromorphological properties (spore size, spore color, vesicle shape, stipe size, Hülle cell, ascospore, cleistothecia) were examined under light microscope. Identification of the isolates was carried out by comparing the defined characteristics of the fungi with the accepted identification key (Klich 2002).

In order to identify isolates of the genus *Penicillium* at species level, fresh cultures were inoculated into petri dishes containing CYA, MEA, 25% Glycerol Nitrate Agar (G25N), Yeast Extract Sucrose Agar (YES) and Creatine Sucrose Agar (CREA) media. Petri dishes were incubated at  $25^\circ\text{C}$  7 days. Additional petri dishes containing CYA medium were incubated at  $5^\circ\text{C}$  and  $37^\circ\text{C}$  for 7 days (Pitt 1979, Sammon *et al.* 2010). At the end of the incubation period, macromorphological characteristics of the isolates were observed. Then, fungal preparates stained with lactophenol cotton blue dye were examined under light microscope and

micromorphological characteristics (conidiophore branching patterns, metulae length, phialide shape, cleistothecium, spore size, spore color) were determined. Identification of the isolates was carried out by comparing the defined characteristics of the fungi with the universally accepted standards (Pitt 1979).

For species-level identification of fungal isolates including Dematiaceous Hyphomycetes, fresh cultures were inoculated into Potato Dextrose Agar (PDA) plates. Petri dishes were incubated at 25°C for 14 days. The macro- and micromorphological characteristics were examined, and identifications were performed according to Ellis (1971).

Current names of fungi identified at genus or/and species level, as well as fungal authors, were standardized according to the “Index Fungorum Partnership” website (Hawksworth *et al.* 2011). The phyla of the identified fungi were updated according to the Mycobank website (<http://www.mycobank.org/quicksearch.aspx>).

#### Statistical Analysis

Statistical data were obtained using IBM SPSS Statistics software (version 29.0.0.0). The normal distribution of the arithmetic means was determined by the normality test and the confidence interval was accepted as  $p < 0.05$ . Since the number of subjects in both hot and cold water samples was below 30, the normality test was evaluated according to the Shapiro-Wilk method. It was determined that it did not show a normal distribution. Therefore, Non-parametric Mann-Whitney U test (among independent groups) was used to evaluate the difference in the mean numbers of fungi, aerobic bacteria in cold and hot water sample. Spearman correlation coefficients test was used to evaluate the relationship between fungi numbers in water samples, bacterial counts, water temperature, pH, free chlorine, age of residences, type of water systems and water tank. Significance level was accepted as  $p < 0.05$ .

### **Results**

#### Water Parameters

It has been determined that the temperatures of the cold water samples randomly collected from 20 residences varied between 20°C and 25°C (the mean value was 21°C). The temperatures of the hot water samples were in the range of 40°C and 55°C (the mean value was 46.7°C). The mean pH values of the cold and hot water samples were 6 and 7, respectively. Free chlorine values in cold water samples were determined to be in the range of 0.1-1 ppm (the mean value was 0.73), and free chlorine values in the hot water samples were determined to be in the range of 0.3-1 ppm (the mean value was 0.74).

#### Microbial Enumeration

Fungal growth was observed in 85% of cold and 45% of hot water samples (Table 2). The mean fungal counts in cold and hot water samples were 2.4 cfu/100 mL and 1.47 cfu/100 mL, respectively. The highest fungal counts

in cold and hot water samples were detected in residences A and B, respectively.

**Table 2.** The mean microbiological counts in water samples of 20 residences.

Building Code	Fungi		Bacteria	
	Cold Water (cfu/100 mL)	Hot Water (cfu/100 mL)	Cold Water (cfu/100 mL)	Hot Water (cfu/100 mL)
A	7.5 ± 6.36	2 ± 0	3340 ± 0.56	260 ± 1.13
B	5 ± 1.41	9 ± 2	0 ± 0	0 ± 0
C	2 ± 1.41	1.5 ± 0.71	420 ± 1.97	0 ± 0
D	2 ± 0	6 ± 0	0 ± 0	0 ± 0
E	6.5 ± 0.71	0 ± 0	106.6 ± 0.56	0 ± 0
F	2 ± 0	0 ± 0	0 ± 0	600 ± 0.56
G	1.5 ± 0.71	1 ± 0	40 ± 0	150 ± 0.42
H	1 ± 0	0 ± 0	330 ± 1.27	0 ± 0
I	0 ± 0	1 ± 0	0 ± 0	0 ± 0
J	1 ± 0	6 ± 1.41	60 ± 0.28	60 ± 0.28
K	2.66 ± 0.58	0 ± 0	70 ± 0.14	50 ± 0.4
L	6 ± 0	0 ± 0	150 ± 0.89	0 ± 0
M	3.5 ± 2.12	2 ± 0	7920 ± 1.13	0 ± 0
N	0 ± 0	0 ± 0	140 ± 0.28	0 ± 0
O	1 ± 0	0 ± 0	0 ± 0	0 ± 0
P	3.5 ± 0.71	1 ± 0	390 ± 0.98	0 ± 0
R	1 ± 0	0 ± 0	0 ± 0	0 ± 0
S	0 ± 0	0 ± 0	0 ± 0	0 ± 0
T	1 ± 0	0 ± 0	640 ± 11.3	240 ± 0.7
U	1 ± 0	0 ± 0	440 ± 0.28	230 ± 0.7

Since the number of subjects in both cold and hot water samples was 20, the normality test was run according to the Shapiro-Wilk method ( $W = 0.803$ ,  $p = 0.001$  for cold water), ( $W = 0.645$ ,  $p = 0.001$  for hot water), and no normal distribution was determined. According to Mann-Whitney U test, a difference was found between the mean numbers of fungi in cold and hot water samples ( $U = 120.000$ ,  $p = 0.26$ ). Fungal counts were found to be higher in cold water samples than in hot water ones ( $p < 0.05$ ). No *Candida* growth was observed in any of the water samples.

Bacterial growth was observed in 65% of cold and 35% of hot water samples (Table 2). The mean bacterial counts in cold and hot water samples were 702.33 cfu/100 mL and 79.5 cfu/100 mL, respectively. The highest bacterial counts in cold and hot water samples were detected in residence M and F, respectively. Since the number of subjects in both cold and hot water samples was 20, the normality test was run according to the Shapiro-Wilk method ( $W = 0.415$ ,  $p = 0.001$  for cold water), ( $W = 0.603$ ,  $p = 0.001$  for hot water), and no normal distribution was found. According to Mann-Whitney U test, a difference was found between the mean numbers of bacteria in cold and hot water ( $U = 130.500$ ,  $p = 0.44$ ). Bacterial counts were found to be higher in cold water samples than in hot water samples ( $p < 0.05$ ).

According to the Spearman correlation coefficients test, no significant correlation was detected between the fungal and bacterial numbers detected in cold ( $r = 0.313$ ,

$p = 0.180$ ) and hot ( $r = -0.50$ ,  $p = 0.833$ ) water samples (Tables 3, 4).

In addition, a positive correlation was detected between the number of fungi in cold water samples and the presence of tanks ( $r = 0.482$ ,  $p = 0.032$ ). A negative correlation was determined between the number of fungi in hot water samples and the buildings' age ( $r = -0.460$ ,  $p = 0.041$ ). No correlation was found between fungi and other parameters (pH, chlorine, pipe material) in both cold and hot water samples.

#### Fungal Isolates

A total of 60 fungal isolates were obtained, 44 from cold water and 16 from hot water samples (Fig. 1). The highest total isolate number in cold and hot water was in building B with 8. The highest numbers of fungal isolates (with 5 each) were determined in cold water samples of residences A, B, and K. The highest number of fungal isolates (3 each) in hot water samples were detected in residences B, C, and J.

**Table 3.** Results of Spearman correlation analysis on the correlation between fungi in cold water and other parameters.

Fungi in cold water		Bacterial counts	pH	Chlorine	Temperature	Water Tank	Building age	Pipe material
Spearman's rho	Correlation Coefficient	0.313	0.243	-0.334	-0.014	0.482*	-0.441	0.012
	Sig. (2-tailed)	0.180	0.302	0.151	0.955	0.032	0.052	0.959
	N	20	20	20	20	20	20	20

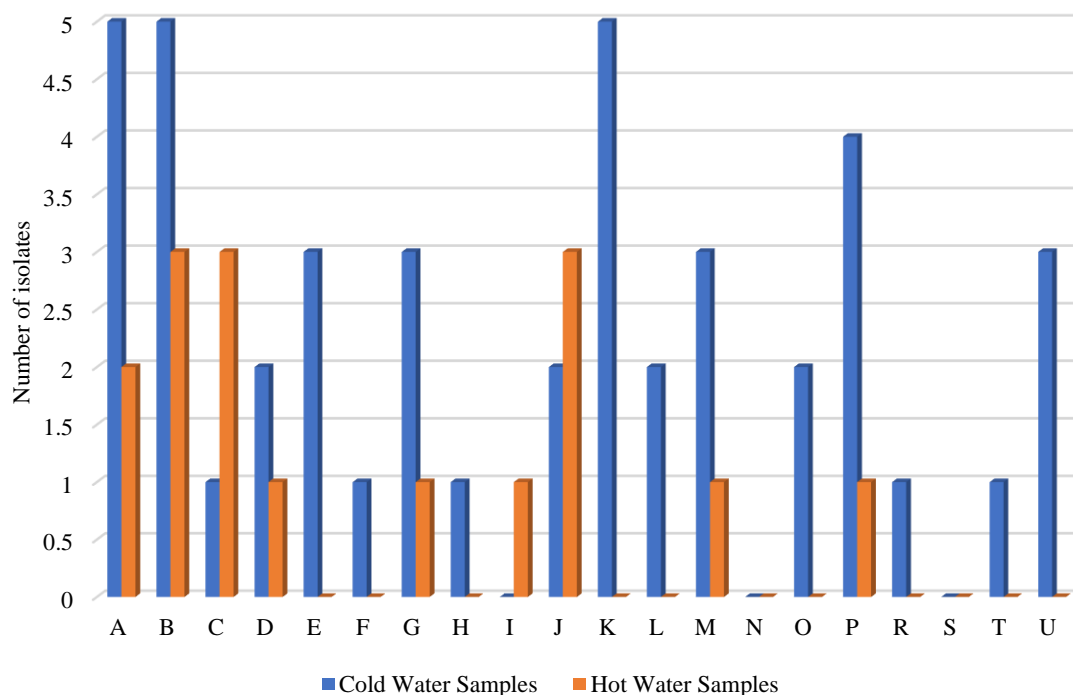


**Fig. 1.** Number of microfungus isolates in cold and hot waters sampled in the residences.



**Table 4.** Results of Spearman correlation analysis on the correlation between fungi in hot water and other parameters

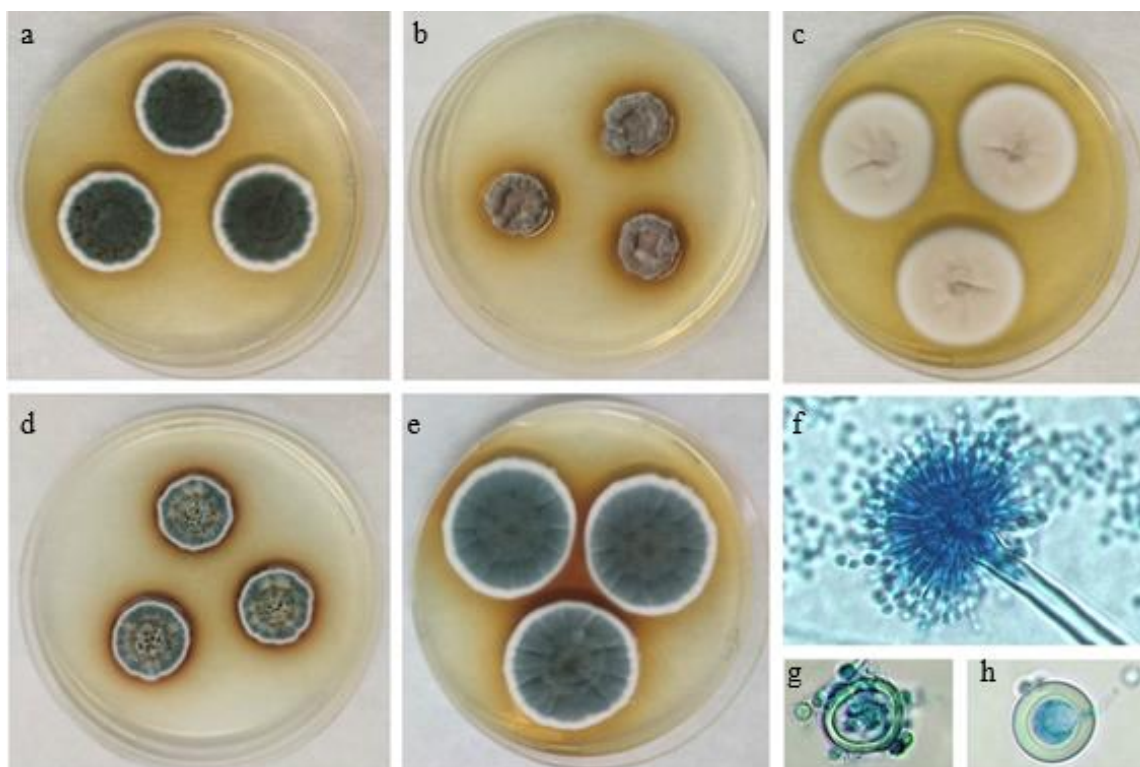
Fungi in hot water		Bacterial counts	pH	Chlorine	Temperature	Water Tank	Building age	Pipe material
Spearman's rho	Correlation Coefficient	-0.50	0.114	-0.259	0.082	0.000	-0.460*	-0.080
	Sig. (2-tailed)	0.833	0.632	0.270	0.730	1.000	0.041	0.738
	N	20	20	20	20	20	20	20

**Table 5.** The identified microfungi in all water samples.

Building code	Isolate Code	Water	Genus/Species
A	F1	Cold	<i>Penicillium chrysogenum</i> Thom 1910
	F2	Cold	<i>Acremonium kiliense</i> Current: <i>Sarocladium kiliense</i> (Grütz) Summerb, 2011
	F3	Cold	<i>Scopulariopsis asperula</i> (Sacc.) S. Hughes 1958
	F4	Cold	<i>Penicillium aurantiogriseum</i> Dierckx 1901
	F5	Cold	Non-spore forming fungi
	F6	Hot	Non-spore forming fungi
	F7	Hot	Non-spore forming fungi
B	F8	Cold	<i>Penicillium chrysogenum</i> Thom 1910
	F9	Cold	<i>Chaetomium globosum</i> Kunze 1817
	F10	Cold	Yeast
	F11	Cold	<i>Penicillium citrinum</i> Thom 1910
	F12	Cold	<i>Eurotium amstelodami</i> Current: <i>Aspergillus amstelodami</i> (L. Mangin) Thom&Church 1926
	F13	Hot	<i>Penicillium citrinum</i> Thom 1910
	F14	Hot	<i>Penicillium raistrickii</i> G. Sm. 1933
C	F15	Hot	<i>Aspergillus versicolor</i> (Vuill.) Tirab. 1908
	F16	Cold	<i>Eurotium amstelodami</i> Current: <i>Aspergillus amstelodami</i> (L. Mangin) Thom&Church 1926
	F17	Hot	<i>Aspergillus versicolor</i> (Vuill.) Tirab. 1908
	F18	Hot	Non-spore forming fungi
D	F19	Hot	Non-spore forming fungi
	F20	Cold	<i>Penicillium expansum</i> Link 1809
	F21	Cold	Yeast
	F22	Hot	<i>Eurotium amstelodami</i> Current: <i>Aspergillus amstelodami</i> (L. Mangin) Thom&Church 1926
E	F23	Cold	<i>Penicillium brevicompactum</i> Dierckx 1901
	F24	Cold	<i>Aspergillus versicolor</i> (Vuill.) Tirab. 1908
	F25	Cold	<i>Arthroderma</i> sp. Curr. 1860
F	F26	Cold	<i>Penicillium brevicompactum</i> Dierckx 1901
G	F27	Cold	<i>Aspergillus flavus</i> Link 1809
	F28	Cold	<i>Chaetomium globosporum</i> Rikhy & Mukerji 1974
	F29	Cold	<i>Chrysosporium inops</i> J.W. Carmich. 1962
	F30	Hot	<i>Phialophora</i> sp. Medlar 1915
H	F31	Cold	<i>Penicillium olsonii</i> Bainier & Sartory 1912
I	F32	Hot	<i>Aspergillus niveus</i> Current: <i>Aspergillus neoniveus</i> Samson, S.W. Peterson, Frisvad & Varga 2011
J	F33	Cold	<i>Penicillium chrysogenum</i> Thom 1910
	F34	Cold	<i>Penicillium aurantiogriseum</i> Dierckx 1901
	F35	Hot	<i>Aspergillus versicolor</i> (Vuill.) Tirab. 1908
	F36	Hot	Non-spore forming fungi
	F37	Hot	Non-spore forming fungi
K	F38	Cold	<i>Penicillium expansum</i> Link 1809
	F39	Cold	<i>Chaetomium globosum</i> Kunze 1817
	F40	Cold	Non-spore forming fungi
	F41	Cold	<i>Aspergillus versicolor</i> (Vuill.) Tirab. 1908
	F42	Cold	Non-spore forming fungi
L	F43	Cold	<i>Aspergillus versicolor</i> (Vuill.) Tirab. 1908
	F44	Cold	<i>Penicillium expansum</i> Link 1809
M	F45	Cold	<i>Aspergillus versicolor</i> (Vuill.) Tirab. 1908
	F46	Cold	Non-spore forming fungi
	F47	Cold	<i>Penicillium chrysogenum</i> Thom 1910
	F48	Hot	<i>Aspergillus versicolor</i> (Vuill.) Tirab. 1908

**Table 5.** The identified microfungi in all water samples (Continued).

Building code	Isolate Code	Water	Genus/Species
O	F49	Cold	<i>Botrytis</i> sp. <i>Botrytis</i> P. Micheli ex Pers. 1794
	F50	Cold	<i>Penicillium brevicompactum</i> Dierckx 1901
P	F51	Cold	Non-spore forming fungi
	F52	Cold	<i>Arthroderma flavescens</i> R. G. Rees 1967
	F53	Cold	<i>Penicillium</i> sp. Link 1809
	F54	Cold	Non-spore forming fungi
	F55	Hot	<i>Aspergillus versicolor</i> (Vuill.) Tirab. 1908
R	F56	Cold	<i>Monocillium humicola</i> Current: <i>Penicillium lagena</i> (Delitsch) Stolk & Samson 1983
T	F57	Cold	<i>Penicillium restrictum</i> J.C. Gilman & E.V. Abbott 1927
U	F58	Cold	<i>Penicillium brevicompactum</i> Dierckx 1901
	F59	Cold	<i>Penicillium griseofulvum</i> Dierckx 1901
	F60	Cold	Non-spore forming fungi

**Fig. 2.** *Aspergillus versicolor* a-e. Colony morphology after 7 days on CYA (25°C), CYA (37°C), MEA, CDA, and CY20S media, respectively, f. microscopic image of the conidial head at  $\times 500$  magnification, g-h. microscopic images of the hülle cells at  $\times 1000$  magnification.

Of the 60 fungal isolates obtained from the water samples, 96.6% were filamentous fungi and the others were yeasts. 21.6% of the fungal isolates were non-spore forming fungi. 45 filamentous fungal isolates belonged to 11 different genera (Table 5).

*Penicillium* was the most frequently isolated fungal genus in all water samples, constituting  $\sim 33.3\%$ . *Penicillium* (41%) and *Aspergillus* (43.75%) were the most dominant fungal isolates in cold and hot water samples, respectively. *Aspergillus versicolor* was the most frequently isolated fungal species in all water samples (Fig. 2).

Among the cold water samples, the most frequently isolated fungal species were *Aspergillus versicolor*

(9.1%), *Penicillium brevicompactum* (9.1%), and *Penicillium chrysogenum* (9.1%). However, in hot water samples, *Aspergillus versicolor* (31.25%) was the most frequently isolated fungal species.

Other fungi detected in water samples, according to their frequencies, were *Eurotium amstelodami* (current: *Aspergillus amstelodami*), *Chaetomium globosum*, *Penicillium aurantiogriseum*, *Penicillium citrinum*, *Acremonium kiliense* (current: *Sarocladium kiliense*), *Aspergillus flavus*, *Aspergillus niveus* (current: *Aspergillus neoniveus*), *Arthroderma* sp., *Arthroderma flavescens*, *Botrytis* sp., *Chaetomium globosporum*, *Chrysosporium inops*, *Monocillium humicola* (current: *Penicillium lagena*), *Penicillium* sp., *Phialophora* sp., *Scopulariopsis asperula*.

## Discussion

Water is of paramount importance in human daily life. Tap water should be free from any microorganism or substance, both likely to constitute a potential danger to human health. There is no standardization regarding fungi in the mains water in Türkiye. The World Health Organisation (WHO) states that pathogenic or allergenic microorganisms should not be present in tap water, but does not specifically address microfungi in water standards (WHO 2022). However, Czech Republic and Sweden are the two countries that included microfungi in their drinking water quality standards. According to the water quality standards of the Czech Republic, the mains waters may contain 50 individuals/mL of microorganisms (bacteria and fungi) (Czech Republic Ministry of Health, 2004). Sweden has included fungi specifically in its water quality standards, allowing for 100 cfu/100 mL in mains waters (Swedish National Food Agency, 2001). However, the water quality standard is zero for fungi, 0 individuals/L in Hungary (Ministry of Health Hungary, 2001). Although fungi may not be specifically mentioned in water system standards of many countries, their presence should not be ignored due to their potential as opportunistic pathogens. In the present study, fungal numbers obtained in water samples of 20 residences included in the analysis were found to meet standards of both Czech Republic and Sweden. A general evaluation of data reported in former similar studies showed that our fungal counts are not high in comparison (Hapçioğlu *et al.* 2005, Hayette *et al.* 2010, Kadaifçiler & Demirel 2018). This suggests that routine processes carried out by the Istanbul Water and Sewerage Administration (IWSA), such as ozonation and sand filtration in the municipal water supply systems before chlorine application, may contribute to the prevention of fungal growth along with disinfection.

According to the monthly water quality reports published by IWSA during our study period, the presence of enterococcus, *Escherichia coli*, *Clostridium perfringens* and coliform bacteria, which are pollution indicators in tap waters, was investigated in determining water quality, and no bacterial contamination caused by these bacteria was detected in water samples (IWSA, 2022). Considering the bacteria counts in our study, it is thought that there may be a contamination in various ways in tap water systems known to have chlorine disinfection, as well as possible detachments from pipe surfaces, water tanks and also possible biofilm layers on shower heads. Bacteria and fungi passing into the water with these breaks may have caused the number and diversity of microorganisms in the water to be determined higher than they actually are during the collection of water samples. Chlorine is the most used disinfectant in water supply systems; it is effective against planktonic microbes but cannot penetrate biofilms (Kim *et al.* 2002). According to the monthly water quality reports of IWSA, there is quite high levels of chloride (28.76-170.18 ppm) in the mains water given from the facilities. Free chlorine levels in our water samples were low. Since chlorine is a volatile gas

by its structure, the free chlorine in the mains water may decrease by being lost throughout the water system until it reaches the tap. Additionally, the presence of biofilms that may have formed along the pipeline of the water system can also trap chlorine in the water, leading to lower free chlorine levels being detected. The reduction in chlorine concentration caused by these factors might have been responsible for microbial growth in water samples. On the other hand, many microorganisms sensitive to chlorine can be easily eliminated from water even if the chlorine level is low. Although fungi were detected more than bacteria in both hot and cold water samples, fungal colony numbers were lower than bacterial colony numbers. This may suggest that bacteria are better adapted to oligotrophic water environments than fungi, and that the biofilm layer helps them in this adaptation by hosting them. As a matter of fact, it has been reported that fungi require longer time to take part in biofilms than bacteria and that they settle in the biofilm layer in a non-homogeneous and loose manner (Göksay Kadaifçiler *et al.* 2024). The biofilm works as a reservoir, and fungus may be transported intermittently to the water. Although no correlation was detected between fungi and bacteria in our study, it is suggested that there may be synergistic or antagonistic effects, depending on the species, between fungi and bacteria in settling in biofilms in water systems (Göksay Kadaifçiler *et al.* 2024). In a biofilm investigation using fungi and bacteria species, researchers reported that bacteria with high growth rates and metabolic activity reduced fungal spore germination, potentially due to nutrient competition (Barros Afonso *et al.* 2020, 2021). Different studies found relationships between fungi and bacteria with different results. It has been suggested that fungi usually colonize pre-established bacterial biofilms and their different ecological requirements may lead to a positive relationship between these microorganisms. In cultivation processes, negative relationships have been reported due to direct competition between both fungi and bacteria for resources. These findings may be a result of several factors such as differences in the composition of microorganisms isolated from water systems or differences in methodologies (Barros Afonso *et al.* 2020, 2021).

Cold water samples have a higher incidence of fungus than hot water samples, as shown in previous studies by Zacheus and Martikainen (1995) and Hayette *et al.* (2010). This finding can be attributed to the decrease in dissolved oxygen levels in water as the temperature increases (Xing *et al.* 2014), creating an environment unfavorable for the existence of aerobic microorganisms. This situation can also be explained by the fact that the microorganisms in the water are sensitive to temperature and cannot increase their growth or survive. Microorganisms generally grow by feeding on organic matter that adheres to pipe surfaces in water systems in the presence of appropriate temperature and pH values. The type of the pipe materials can affect the ability of microorganisms to adhere depending on the roughness of their surfaces and the chemical components in their structure. Plastic pipes such

as PVC generally hold more water, and microorganism growth may be more common on such surfaces. The limited moisture retention capacity of metal surfaces and the fact that some metals may have antimicrobial properties may limit microorganism growth. However, it has been determined that microbial communities obtained from cast iron pipes are more stable than microbial communities obtained from non-ferrous pipe materials (Doggett 2000, Makris *et al.* 2014). Studies have stated that the type of pipe material may be associated with differences in the composition of microbial communities (Makris *et al.* 2014, Lee *et al.* 2021). It has been reported that fungi can also be present in water systems and can be included in the biofilm structure by interacting with the pipe surface material. These interactions may vary depending on the type of pipe surface material, environmental conditions (temperature, pH, etc.) and fungal species (Doggett 2000, Marangoni *et al.* 2013, Goksay Kadaifçiler *et al.* 2024). For this reason, the relationship between these parameters mentioned above and fungi in water systems may differ for each study. Residence A, where the highest number of fungi were detected in cold water samples, has a water tank. The tank surface material is galvanized steel coated with zinc, and it is known that fungal biofilms form despite the toxic effect of zinc. It is known that sessile fungi can leave the biofilm over time and pass into water, causing the number of planktonic fungi to increase (Goksay Kadaifçiler *et al.* 2024). In addition, the low amount of free chlorine in both the cold water sample of residence A and the hot water sample of residence B may have caused the fungal disinfection to be insufficient, causing the number of fungi to be detected high.

In water systems, filamentous fungi are more commonly encountered than yeasts. Yeasts require an optimum pH value of 4.5-5 that supports their growth and a high nutrient content, and they are more sensitive to chlorine than filamentous fungi. Mains water do not provide suitable environmental conditions for the growth of yeasts, as they have low nutrient content and pH values that fluctuate between 6-7 (Rosenzweig *et al.* 1983, Barnett & Hunter 1999). For these reasons, yeasts may be less isolated than filamentous fungi in all water samples. The genus *Penicillium* was found to be dominant in cold water samples. It has been reported that fungal spores are more resistant to chlorination compared to bacteria and yeasts (Rosenzweig *et al.* 1983). Also, *Penicillium* spores are more resistant to chlorination than other fungal genera and are frequently detected in water environments (Pereira *et al.* 2013). On the other hand, the genus *Aspergillus* was found to be dominant in hot water samples. *Aspergillus* has the ability to survive under various challenging environmental conditions such as high temperature and low oxygen content (Babič *et al.* 2017), making *Aspergillus* spores to be commonly found in water systems (Richardson & Rautemaa-Richardson 2019). *Penicillium* and *Aspergillus* are known to be commonly found in hot water samples. These fungi are able to adapt to high temperatures by developing heat-

resistant structures such as thick cell walls, which protect them from heat stress. Significantly these fungi have the ability to produce heat shock proteins, which help to protect them from the harmful effects of high temperatures (Tiwari *et al.* 2015). *Aspergillus*, *Penicillium*, *Candida*, and *Fusarium* that have been identified as pathogens, opportunistic pathogens, allergens, and toxigenic species have been found in man-made water system (Warris *et al.* 2001, Alangaden 2011). Opportunistic pathogenic fungi are known to thrive in warm and humid environments. Several studies showed that high temperatures can increase the growth rate and virulence of these fungi, making them more pathogenic to humans and animals (Klich 2002). The presence of opportunistic pathogens in hot water samples have been linked to an increased risk of infections, such as respiratory infections, skin infections, and systemic infections, particularly in immunocompromised individuals (Anaissie *et al.* 2001, 2002).

In the studies conducted on drinking and utility water connected to the mains water system in Türkiye, the focus has been on total and fecal coliform bacteria and pathogenic bacteria, which are important from a health standpoint. However, there are limited studies that investigate microbial load and diversity, including fungi. In one of these studies, which use the membrane filtration method, *Penicillium* spp., *Aspergillus* spp., and *Acremonium* spp. were detected in a hospital water system in Istanbul (Hapçioğlu *et al.* 2005). *Penicillium*, *Aspergillus*, *Cladosporium*, and *Paecilomyces* were reported as dominant fungi in dental unit water systems connected to the mains water system in Istanbul (Kadaifçiler & Çotuk 2014). Similarly, in our study, it is noteworthy that *Aspergillus* and *Penicillium*, which are frequently detected in water samples, were also dominant in previous studies. *Penicillium* and *Aspergillus* spp. were identified as the predominant species among the 32 different species found in a study investigating the fungal diversity in water samples obtained from houses, hospitals, and shopping centers connected to the municipal water supply system in Istanbul. Furthermore, *Aspergillus* species with mycotoxigenic properties were also reported (Kadaifçiler & Demirel 2018). The comparison of findings of our present study with the fungal diversity of water based samples reported in relevant literature showed the results obtained were similar in general. Hageskal *et al.* (2006) investigated the presence of fungi in drinking and mains waters in Norway using the membrane filtration method. They detected 30 different fungal taxa, predominantly belonging to the *Penicillium* and *Aspergillus* genera. The fungi identified in our study, such as *Acremonium* sp., *Botrytis* sp., *Chaetomium* sp., *Chaetomium globosum*, *Penicillium brevicompactum*, *Penicillium chrysogenum*, *Penicillium citrinum*, *Penicillium expansum*, *Penicillium olsonii*, *Penicillium raistrickii*, *Penicillium restrictum*, *Phialophora* sp., and *Scopulariopsis* sp. were also present in the study of Hageskal *et al.* (2006). Kanzler *et al.* (2007) investigated the presence of filamentous fungi and yeasts

in drinking and main waters and groundwater in Austria. They identified 32 different taxa of fungi, predominantly *Cladosporium* spp. and *Penicillium* spp. which were also the dominant fungi in our study. Additionally, the identified species, including *Aspergillus* sp., *Acremonium* sp., and a small number of yeasts, were also present in our study. In this study, the identified fungi such as *Acremonium kiliense*, *Arthroderma* sp., *Aspergillus amstelodami*, *Aspergillus flavus*, *Aspergillus versicolor*, *Aspergillus niger*, *Botrytis* sp., *Chaetomium globosum*, *Penicillium chrysogenum*, *Penicillium citrinum*, *Phialophora* sp., and *Scopulariopsis asperula* are known to have allergenic and opportunistic pathogenic properties. *Acremonium kiliense*, in particular, has gained clinical significance as it can cause systemic fungal diseases in immunocompromised individuals. *Arthroderma* sp. can lead to fungal infections on the skin. *Aspergillus amstelodami*, *A. flavus*, *A. versicolor*, and *A. niger* can cause invasive aspergillosis. *Botrytis* sp., also known as a plant pathogen, is an allergen. *Chaetomium globosum* can cause respiratory tract infections, rhinocerebral infections, and infections on the skin and nails. *Penicillium chrysogenum* and *P. citrinum* can cause invasive infections (Babič *et al.* 2017). *Phialophora* sp. can lead to systemic infections such as endocarditis and keratitis, particularly in immunocompromised patients (Migrino *et al.* 1995). *Scopulariopsis* sp. can cause fungal infections on the nails and keratitis.

## References

- Alangaden, G.J. 2011. Nosocomial fungal infections: Epidemiology, infection control, and prevention. *Infectious Disease Clinics*, 25(1): 201-225. <https://doi.org/10.1016/j.idc.2010.11.003>
- Anaissie, E.J., Kuchar, R.T., Rex, J.H., Francesconi, A., Kasai, M., Muller, F.C., Lozano Chiu, M., Summerbell, R.C., Dignani, M.C., Chanock, S.J. & Walsh, T.J. 2001. Fusariosis associated with pathogenic *Fusarium* species colonization of a hospital water system: A new paradigm for the epidemiology of opportunistic mold infections. *Clinical Infectious Diseases*, 33(11): 1871-1878. <https://doi.org/10.1086/324501>
- Anaissie, E.J., Stratton, S.L., Dignani, M.C., Summerbell, R.C., Rex, J.H., Monson, T.P., Spencer, T., Kasai, M., Francesconi, A. & Walsh, T.J. 2002. Pathogenic *Aspergillus* species recovered from a hospital water system: A 3-year prospective study. *Clinical Infectious Diseases*, 34(6): 780-789. <https://doi.org/10.1086/338958>
- Babič, M., Gunde-Cimerman, N., Vargha, M., Tischner, Z., Magyar, D., Verissimo, C., Sabino, R., Viegas, C., Meyer, W. & Brandao, J. 2017. Fungal contaminants in drinking water regulation? A tale of ecology, exposure, purification and clinical relevance. *International Journal of Environmental Research and Public Health*, 14(6): 636. <https://doi.org/10.3390/ijerph14060636>
- Barnett, H. L. & Hunter, B. B. 1999. *Illustrated genera of imperfect fungi*, 4<sup>th</sup> ed., APS Press, St. Paul, Minnesota, USA, 0-89054-192-2.
- Barros Afonso, T., Simoes, L. C. & Lima, N. 2019. *In vitro* assessment of inter-kingdom biofilm formation by bacteria and filamentous fungi isolated from a drinking water distribution system. *Biofouling*, 35(10): 1041-1054. <https://doi.org/10.1080/08927014.2019.1688793>
- Barros Afonso, T., Simoes, L. C. & Lima, N. 2020. Effect of quorum sensing and quenching molecules on inter-kingdom biofilm formation by *Penicillium expansum* and bacteria. *Biofouling*, 36(8): 965-976. <https://doi.org/10.1080/08927014.2020.1836162>
- Barros Afonso, T., Simoes, L. C. & Lima, N. 2021. Occurrence of filamentous fungi in drinking water: their role on fungal-bacterial biofilm formation. *Research in Microbiology*, 172(1): 103791. <https://doi.org/10.1016/j.resmic.2020.11.002>
- Bays, L.R., Burman N.P. & Lewis W.M. 1970. Taste and odor in water supplies in Great Britain: A survey of the present position and problems for the future. *Water Treatment and Examination*, 19(2): 136-160.
- Burman, N.P. 1965. Taste and odour due to stagnation and local warming in long lengths of piping. *Proceedings of the Society for Water Treatment and Examination*, 14: 125-131.
- Canhoto, C., Goncalves, A.L. & Baerlocher, F. 2016. Biology and ecological functions of aquatic hyphomycetes in a warming climate. *Fungal Ecology*, 19: 201-218. <https://doi.org/10.1016/j.funeco.2015.09.011>

The study shows that fungi, especially filamentous fungi, can be present in variable concentrations in building water systems and that temperature can change the number and diversity of fungi. In conclusion, analysis of water samples from building systems can reveal significant information about the microbial load, microbial community, and their effects on human health. Given the limited global research on waterborne fungi, especially in the context of climate change, further studies are necessary to understand the full scope of fungal contamination in water and its potential health impacts.

**Ethics Committee Approval:** Since the article does not contain any studies with human or animal subject, its approval to the ethics committee was not required.

**Data Sharing Statement:** All data are available within the study.

**Author Contributions:** Concept: D.G.K., Design: D.G.K., Execution: E.M.D., D.G.K., Material supplying: E.M.D., D.G.K., Data acquisition: E.M.D., D.G.K., Data analysis/interpretation D.G.K., Writing: E.M.D., D.G.K., Critical review: D.G.K.

**Conflict of Interest:** The authors have no conflicts of interest to declare.

**Funding:** This study was funded by Scientific Research Project Coordination Unit of Istanbul University. Project number: FYL-2020-36872.



12. Czech Republic Ministry of Health. 2004. ČVyhlaška č. 252/2004 Sb., kterou se stanoví hygienické požadavky na pitnou a teplou vodu a četnost a rozsah kontroly pitné vody. Praha: Ministerstvo zdravotnictví.
13. Doggett, M.S. 2000. Characterization of fungal biofilms within a municipal water distribution system. *Applied And Environmental Microbiology*, 66(3): 1249-1251 <https://doi.org/10.1128/aem.66.3.1249-1251.2000>
14. Ellis, M.B. 1971. *Dematiaceous Hyphomycetes*, The Eastern Press, London, 608 pp. 85198027-9.
15. Figueiredo Fonseca, J.C., Bouakline, A., Claisse, J.P., Feuilhade, M., Baruchel, A., Dombret, H., Pavie, J., Andrade Moreira, E.S., Derouin, F. & Lacroix, C. 2010. Fungal contamination of water and water-related surfaces in three hospital wards with immunocompromised patients at risk for invasive fungal infections. *Journal of Infection Prevention*, 11(2): 36-41. <https://doi.org/10.1177/1757177409358416>
16. Goksay Kadaifçiler, D., Unsal, T. & İlhan-Sungur, E. 2024. Long-term evaluation of culturable fungi in a natural aging biofilm on galvanised steel surface: Fungi in aging biofilm on galvanised steel surfaces. *Johnson Matthey Technology Review*, 68(1): 60-70. <https://doi.org/10.1595/205651323X16748145957998>
17. Hageskal, G., Knutsen, A.K., Gaustad, P., de Hoog, G.S. & Skaar, I. 2006. Diversity and significance of mold species in Norwegian drinking water. *Applied and Environmental Microbiology*, 72(12): 7586-7593. <https://doi.org/10.1128/AEM.01628-06>
18. Hapçioğlu, B., Yegenoglu, Y., Erturan, Z., Nakipoglu, Y. & Issever, H. 2005. Heterotrophic bacteria and filamentous fungi isolated from a hospital water distribution system. *Indoor and Built Environment*, 14(6): 487-493. <https://doi.org/10.1177/1420326X05060039>
19. Hawksworth, D.L., Crous, P.W. & Redhead, S.A. 2011. The Amsterdam declaration on fungal nomenclature. *IMA Fungus*, 2: 105-112. <https://doi.org/10.5598/ima fungus.2011.02.01.14>
20. Hayette, M.P., Christiaens, G., Mutsers, J., Barbier, C., Huynen, P., Melin, P. & de Mol, P. 2010. Filamentous fungi recovered from the water distribution system of a Belgian university hospital. *Medical Mycology*, 48(7): 969-974. <https://doi.org/10.3109/13693781003639601>
21. Hi-Media. 2003. *The Hi-Media manual for microbiology and cell culture laboratory practice*, Hi-Media Laboratories Pvt. Limited, India, 19.
22. Hyde, K.D., Fryar, S., Tan, Q., Bahkali, A. H. & Xu, J. 2016. Lignicolous freshwater fungi along a north south latitudinal gradient in the Asian/Australian region; Can we predict the impact of global warming on biodiversity and function? *Fungal Ecology*, 19: 19-200. <https://doi.org/10.1016/j.funeco.2015.07.002>
23. Index Fungorum Partnership, 2008, ISF search index fungorum, <http://www.indexfungorum.org/Names/Names.asp>. (Date accessed: 20.11.2022).
24. Istanbul Water and Sewerage Administration (IWSA), <https://www.iski.istanbul/web/tr-TR/su-kalite-raporlari>, (Date Accessed: 22.12.2022).
25. Kadaifçiler, D.G. & Çotuk, A. 2014. Microbial contamination of dental unit waterlines and effect on quality of indoor air. *Environmental Monitoring and Assessment*, 186: 3431-3444. <https://doi.org/10.1007/s10661-014-3628-6>
26. Kadaifçiler, D.G. & Demirel, R. 2018. Fungal contaminants in man-made water systems connected to municipal water. *Journal of Water and Health*, 16(2): 244-252. <https://doi.org/10.2166/wh.2018.272>
27. Kanzler, D., Buzina, W., Paulitsch, A., Haas, D., Platzer, S., Marth, E. & Mascher, F. 2007. Occurrence and hygienic relevance of fungi in drinking water. *Mycoses*, 51(2): 165-169. <https://doi.org/10.1111/j.1439-0507.2007.01454.x>
28. Kim, B. R., Anderson, J. E., Mueller, S. A., Gaines, W. A. & Kendall, A. M. 2002. Literature review – Efficacy of various disinfectants against *Legionella* in water systems, *Water Research*, 36: 4433-4444. [https://doi.org/10.1016/S0043-1354\(02\)00188-4](https://doi.org/10.1016/S0043-1354(02)00188-4)
29. Klich, M.A. 2002. *Identification of common Aspergillus species*, Utrecht, The Netherlands, VI + 116 pp. ISBN 90-70351-46-3
30. Lee, D., Calendo, G., Kopec, K., Henry, R., Coutts, S., McCarthy, D. & Murphy, H.M. 2021. The impact of pipe material on the diversity of microbial communities in drinking water distribution systems. *Frontiers in Microbiology*, 12: 779016. <https://doi.org/10.3389/fmicb.2021.779016>
31. Leginowicz, M., Siedlecka, A. & Piekarska, K. 2018. Biodiversity and antibiotic resistance of bacteria isolated from tap water in Wrocław, Poland. *Environment Protection Engineering*, 44 (4): 85-98. <https://doi.org/10.5277/epe180406>
32. Ma, X., Baron, J.L., Vikram, A., Stout, J.E. & Bibby, K. 2015. Fungal diversity and presence of potentially pathogenic fungi in a hospital hot water system treated with on-site monochloramine. *Water Research*, 71: 197-206. <https://doi.org/10.1016/j.watres.2014.12.052>
33. Makris, K.C., Andra, S.S & Botsaris, G. 2014. Pipe scales and biofilms in drinking-water distribution systems: Undermining finished water quality. *Critical Reviews in Environmental Science and Technology*, 44(13): 1477-1523. <https://doi.org/10.1080/10643389.2013.790746>
34. Marangoni, P.R.D., Robl, D., Dalzoto, P.R., Berton, M.A.C., Vicente, V.A., Pimentel, I.C. 2013. Microbial diversity of biofilms on metallic surfaces in natural waters case study in a hydropower plant on amazon forest. *Journal of Water Resource and Hydraulic Engineering*, 2(4):140-148. <http://JWRHE10027-20131224-145001-9003-39180.pdf>
35. Migrino, R.Q., Hall, G.S. & Longworth, D.L. 1995. Deep tissue infections caused by *Scopulariopsis brevicaulis*: report of a case of prosthetic valve endocarditis and review. *Clinical Infectious Diseases*, 21(3): 672-674. <https://doi.org/10.1093/clinids/21.3.672>
36. Ministry of Health of Hungary. Government Decree 201/2001 on the Quality and Monitoring Requirements of Drinking Water. 1st ed. Ministry of Health; Budapest, Hungary: 2001.
37. MycoBank, 2008, International Mycological Association, <http://www.mycobank.org/quicksearch.aspx>, (Date Accessed: 21.11.2022).

38. Pereira, V.J., Marques, R., Marques, M., Benoliel, M.J. & Crespo, M.B. 2013. Free chlorine inactivation of fungi in drinking water sources. *Water Research*, 47(2): 517-523. <https://doi.org/10.1016/j.watres.2012.09.052>
39. Pitt, J.I. 1979. *The genus Penicillium and its telemorphic states Eupenicillium and Talaromyces*, 3<sup>th</sup> ed., Academic Press Inc., London, 0-12-557750-7.
40. Preciado C.C., Boxall, J., Carrasco V.S., Martinez, S. & Douterelo, I. 2021. Implications of climate change: How does increased water temperature influence biofilm and water quality of chlorinated drinking water distribution systems? *Frontiers in Microbiology*, 12: 658927. <https://doi.org/10.3389/fmicb.2021.658927>
41. Provincial Health Directorate of Istanbul. <https://istanbulism.saglik.gov.tr/TR,109716/icme-kullanma-sulari-sehir-sebeke-suyu.html> (Date Accessed: 14.12.2022).
42. Richardson, M. & Rautemaa-Richardson, R. 2019. Exposure to *Aspergillus* in home and healthcare facilities' water environments: Focus on biofilms. *Microorganisms*, 7(1): 7. <https://doi.org/10.3390/microorganisms7010007>
43. Rosenzweig, W.D., Minnigh, H.A. & Pipes, W.O. 1983. Chlorine demand and inactivation of fungal propagules. *Applied and Environmental Microbiology*, 45(1): 182-186. <https://doi.org/10.1128/aem.45.1.182-186.1983>
44. Sammon, N.B., Harrower, K.M., Fabbro, L.D. & Reed, R.H. 2010. Incidence and distribution of microfungi in a treated municipal water supply system in sub-tropical Australia. *International Journal of Environmental Research and Public Health*, 7(4): 1597-1611. <https://doi.org/10.3390/ijerph7041597>
45. Sammon, N.B., Harrower, K.M., Fabbro, L.D. & Reed, R.H. 2011. Three potential sources of microfungi in a treated municipal water supply system in Sub-Tropical Australia. *International Journal of Environmental Research and Public Health*, 8(3): 713-732. <https://doi.org/10.3390/ijerph8030713>
46. Swedish National Food Agency, Livsmedelsverkets Föreskrifter om Dricksvatten, SLVFS 2001:30, 1<sup>st</sup> ed., National Food Administration: Uppsala, 33 pp.
47. Tiwari, S., Thakur, R. & Shankar, J. 2015. Role of heat-shock proteins in cellular function and in the biology of fungi. *Biotechnology Research International*, 2015: 132635. <https://doi.org/10.1155/2015/132635>
48. Warris, A., Gaustad, P., Meis, J.F., Voss, A., Verweij, P.E. & Abrahamsen, T.G. 2001. Recovery of filamentous fungi from water in a paediatric bone marrow transplantation unit. *Journal of Hospital Infection*, 47(2): 143-148. <https://doi.org/10.1053/jhin.2000.0876>
49. World Health Organization, (WHO) 2022. Guidelines Guidelines for drinking-water quality: fourth edition incorporating the first and second addenda. ISBN 978-92-4-004506-4.
50. Xing, W., Yin, M., Lv, Q., Hu, Y., Liu, C. & Zhang, J. 2014. *Oxygen solubility, diffusion coefficient, and solution viscosity*, pp.1-31. In: Xing, W., Yin, G. & Zhang, J. (eds). *Rotating electrode methods and oxygen reduction electrocatalysts*. Elsevier, Amsterdam, 306 pp.
51. Zacheus, O.M. & Martikainen, P.J. 1995. Occurrence of heterotrophic bacteria and fungi in cold and hot water distribution systems using water of different quality, *Canadian Journal of Microbiology*, 41(12): 1088-1094. <https://doi.org/10.1139/m95-152>

## Astaxanthin: Unveiling biochemical mysteries, expanding horizons, and therapeutic opportunities in health science and biomedical research

Moh Aijaz, Arun Kumar\*

School of Pharmacy, Graphic Era Hill University, Dehradun, Uttarakhand, INDIA

### Cite this article as:

Aijaz M. & Kumar A. 2025. Astaxanthin: Unveiling biochemical mysteries, expanding horizons, and therapeutic opportunities in health science and biomedical research. *Trakya Univ J Nat Sci*, 26(1): 73-91, DOI: 10.23902/trkjinat.1604014

Received: 19 December 2024, Accepted: 21 February 2025, Online First: 18 March 2025, Published: 15 April 2025

**Abstract:** This systemic study surveys the multifaceted nature of Astaxanthin (AXT), a member of carotenoid pigments broadly used in nutraceuticals and pharmaceuticals. Starting with an insight into its biological origin, the review proceeds to detail the complex chemical structure of AXT followed by considerations on its bioavailability, pharmacokinetics and safety as a dietary supplement. Foremost among these is the biological activities of AXT, especially its strong antioxidant activity which plays an important role in reducing oxidative stress (OS) damage to cells. The description of AXT as an anti-apoptotic and anti-inflammatory cytokine indicates its important role in cell protection and chronic inflammation improvement. Additional studies emphasize positive anti-obesity and anti-diabetic activities that could be exploited as therapy for metabolic disease. The review goes on to describe the immunomodulatory and neuroprotective effects of AXT, its role in cardiovascular protection, as well as hepatic health. The discussion of the anti-cancer activity of AXT is important, since it is related with its mechanisms for preventing and treating cancer. The broad perspective ends with an overview of the diverse biological activities of AXT, suggesting future research directions and its ability to be a multi-target ameliorator. Data compiled here aims to significantly help to improve knowledge on AXT, thus facilitating health and biomedical research progression.

### Edited by:

Etıl Güzelmeriç

### \*Corresponding Author:

Arun Kumar

[arun\\_pharma1@rediffmail.com](mailto:arun_pharma1@rediffmail.com)

### ORCID iDs of the authors:

MA. 0000-0002-0526-1854

AK. 0000-0002-7940-4096

### Key words:

Astaxanthin

Anticancer activity

Anti-inflammatory activity

Neuroprotective activity

Cardioprotective activity

**Özet:** Bu sistematik çalışma, geniş çapta nutrasötiklerde ve farmasötiklerde kullanılan karotenoid pigmentlerinin bir üyesi olan Astaksantin (AXT) çok yönlü doğasını incelemektedir. İncelemede, öncelikle AXT'nin biyolojik kökenine dair bilgiler sunulmakta, ardından karmaşık kimyasal yapısı detaylandırılmakta ve diyet takviyesi olarak biyoyararlanımı, farmakokinetiği ve güvenliği ele alınmaktadır. Bunların başında AXT'nin biyolojik aktiviteleri, özellikle oksidatif stresin hücrelere verdiği hasarı azaltmada önemli rol oynayan güçlü antioksidan aktivitesi gelmektedir. AXT'nin anti-apoptoz ve anti-enflamatuvar sitokin olarak tanımlanması, hücre koruma ve kronik iltihaplanmanın iyileştirilmesindeki önemli rolünü göstermektedir. Ek çalışmalar, AXT'nin metabolik hastalıkların tedavisinde kullanılabilecek olumlu anti-obezite ve anti-diyabetik aktivitelerini vurgulamaktadır. Çalışma ayrıca AXT'nin immünomodülatör ve nöroprotektif etkilerini, kardiyovasküler korumadaki rolünü ve karaciğer sağlığı üzerindeki etkilerini ele almaktadır. AXT'nin anti-kanser aktivitesinin tartışılması önemlidir, çünkü bu, kanseri önleme ve tedavi etme mekanizmaları ile ilgilidir. Geniş kapsamlı perspektif, AXT'nin çeşitli biyolojik aktivitelerine genel bir bakış sunarak gelecekteki araştırma yönlerini ve çok hedefli bir iyileştirici olarak potansiyelini önermektedir. Bu derleme, AXT hakkındaki bilgileri önemli ölçüde geliştirmeyi, böylece sağlık ve biyomedikal araştırmaların ilerlemesine katkıda bulunmayı amaçlamaktadır.

### Introduction

Astaxanthin (AXT) is a lipid-soluble red-orange oxycarotenoid pigment belonging to the xanthophylls group of carotenoids, which also contains  $\beta$ -cryptoxanthin, canthaxanthin, lutein, and zeaxanthin.

AXT was first developed for aquaculture pigmentation purposes, and was approved as a food supplement in 1991 due to the strength of its antioxidant properties, physiological effects and vitamin A precursor ability



OPEN ACCESS

shown in both rats and fish. The increasing need for natural AXT has attracted research interest particularly for human nutrition (Fakhri *et al.* 2018). Various sources like microorganisms, phytoplankton, marine animals, and seafood are natural providers of AXT. While wild salmon acquire AXT through the food chain, farmed salmon obtain their characteristic color from AXT feed supplements. *Haematococcus pluvialis* (Flotow), a green microalgae, is a prominent natural source of AXT for human consumption. Under stress conditions such as nitrogen deprivation, elevated salinity, and temperature fluctuations, *Haematococcus pluvialis* exhibits enhanced AXT accumulation. Other sources include the yeast *Xanthophyllomyces dendrorhous* (Phaff, Carmo Souza & Starmer), certain plants, fungi, microalgae, i.e. *Chlorococcum* (Geyler) species and *Chlorella zofingiensis* (Dönn), and the marine bacteria *Agrobacterium aurantiacum* (Sahin, Ladha & Young) (Sajilata & Singhal 2008). AXT shares structural similarities with  $\beta$ -carotene, having oxygen groups distinguishing it from other carotenoids. Its extended structure features polar ends and a nonpolar middle, with 13 conjugated double bonds-unique properties contributing to its antioxidant efficacy and light absorption. AXT's hydroxyl and keto groups enhance its polarity and membrane functionality. This polar-nonpolar-polar structure enables precise integration into cell membranes (Martínez-Cámara *et al.* 2021). AXT exhibits common carotenoid-related physiological and metabolic activities. It is present in micro-organisms and marine life as a xanthophyll carotenoid. It is a red, lipid-soluble pigment that lacks pro-Vitamin A functionality within the human body. Nevertheless, certain studies have indicated that AXT exhibits greater biological efficacy compared to other carotenoids (Pérez-Rodríguez *et al.* 2020). United States (US) Food and Drug Administration (FDA) has approved AXT as an animal feed colorant, while the European Commission categorized it as a food dye. *Haematococcus pluvialis*, who accumulates AXT under stress conditions, is a primary human consumption source and also used for pigmentation in salmon, trout, and shrimp feed. AXT consumption offers preventive and therapeutic benefits for diverse disorders in humans and animals (Fig. 1). Its use as a supplement is burgeoning across various sectors including food industry, feeds, nutraceuticals, and pharmaceuticals (Ambati *et al.* 2014). In the present review, various biological sources, chemical profile and various pharmacological aspects of AXT are summarized.

#### Biological Sources of AXT

The sources of AXT found in nature encompass algae, yeast, aquatic organisms such as salmon, trout, krill, shrimp, and crayfish. Predominantly, commercially available AXT is obtained from the *Phaffia* yeast, *Haematococcus* microalgae, or synthesized chemically.

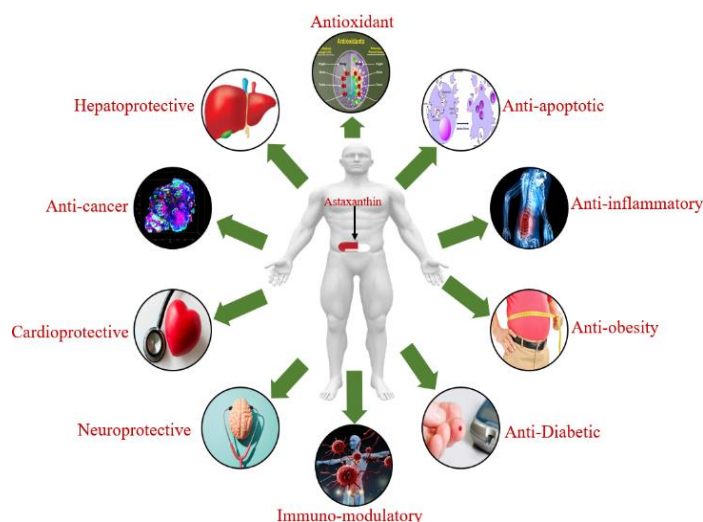


**Fig. 1.** Graphical representation showing pharmacological activities of AXT.

Among these, *H. pluvialis* stands out as a best natural source of AXT (Capelli *et al.* 2019). Among various species of wild salmon, the highest levels of AXT content have been recorded in sockeye salmon, ranging from 26 to 38 mg/kg of flesh, while comparatively lower content has been observed in chum salmon. Farmed Atlantic salmon has been noted to contain around 6 to 8 mg/kg of flesh (Torrissen *et al.* 1995). Sizable trout derived source produce 6 mg/kg of flesh in the European market while 25 mg/kg of flesh in the Japanese market. Dietary reservoirs of AXT encompass shrimp, crab, and salmon, with wild-caught salmon standing out as a noteworthy natural source. Consuming 165 grams of salmon per day would yield approximately 3.6 mg of AXT. Alternatively, a daily supplement of 3.6 mg of AXT could potentially confer health benefits (Shah *et al.* 2023). The diversification of microorganism-derived AXT sources is outlined in Table 1 and percentage content of AXT present in various biological sources are summarized in Fig. 2 (Ambati *et al.* 2014).

#### Chemical structure of AXT

AXT possesses a distinct planar structure, featuring two terminal cyclic rings designated as ring A and ring B. Ring A, known as the  $\beta$ -ionone ring, forms a hexagonal framework accommodating asymmetrical carbon atoms at positions 3 and 3', each bonded to hydroxyl groups (-OH) (Fig. 3). These groups contribute to molecular reactivity and stereochemistry of AXT (Brotosudarmo *et al.* 2020). A polyene chain, composed of alternating single and double bonds, links the terminal rings. This chain contains conjugated double bonds, creating interconnected p-orbitals responsible for AXT's light absorption and crimson coloration. The presence of additional functional groups in AXT depends on its molecular form, whether esterified or free. This intricate planar arrangement influences AXT's behavior in optics, chemistry, and biology. AXT's structural distinctiveness aligns with its classification as a xanthophyll. Its composition includes carbon, hydrogen, and oxygen (Seabra & Pedrosa 2010).



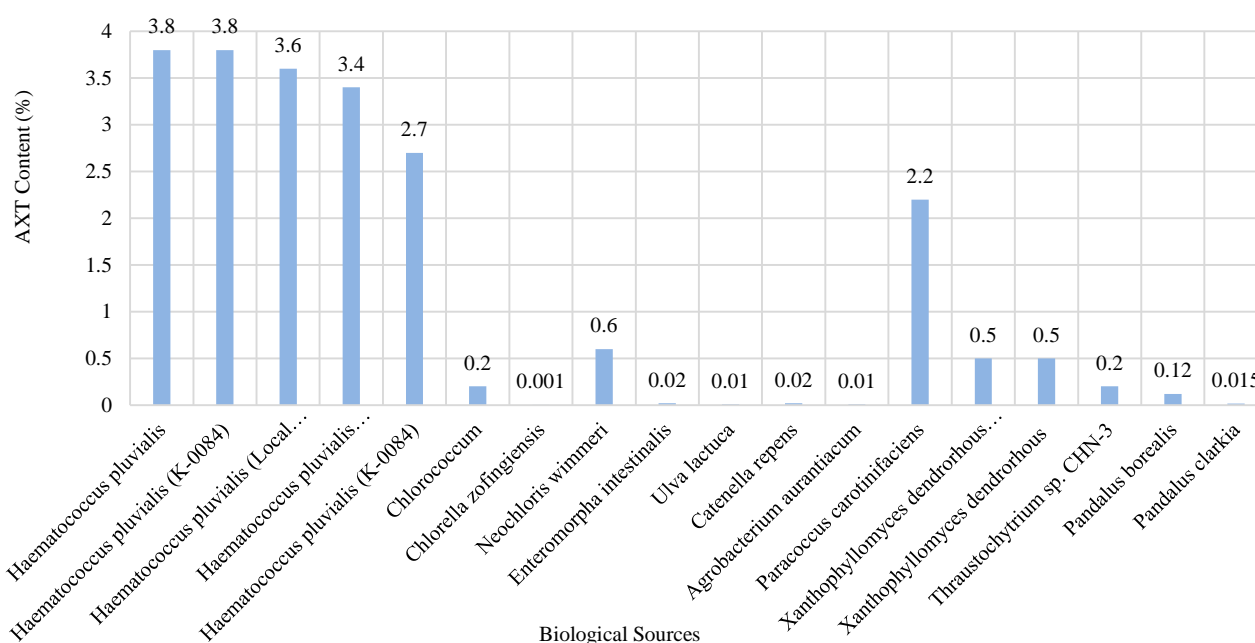
**Table 1.** Biological sources of AXT.

Source	Scientific/Common Name	AXT Content	Notes	Reference
Algae	<i>Haematococcus pluvialis</i>	High	Microalgae known for producing high levels of AXT.	(Boussiba & Vonshak 1991)
Algae	<i>Chlorella zofingiensis</i>	Moderate	Green microalgae capable of synthesizing AXT.	(Ip & Chen 2005)
Algae	<i>Nannochloropsis</i> sp.	Low to Moderate	Microalgae that can produce AXT under specific conditions.	(Fithriani <i>et al.</i> 2019)
Algae	<i>Isochrysis</i> sp.	Low to Moderate	Microalgae capable of AXT production, often used in aquaculture.	(Crupi <i>et al.</i> 2013)
Algae	<i>Tetraselmis</i> sp.	Low	Microalgae that can produce small amounts of AXT.	(Binti Ibnu Rasid <i>et al.</i> 2014)
Algae	<i>Dunaliella salina</i>	Low	Contains a mixture of carotenoids including AXT.	(Chen <i>et al.</i> 2020)
Algae	<i>Chlorococcum</i> sp.	Moderate	Green microalgae containing AXT pigment.	(Liu & Lee 1999)
Bacteria	<i>Agrobacterium aurantiacum</i>	Low	Certain bacteria can be engineered to produce AXT.	(Yokoyama & Miki 1995)
Crustaceans	Shrimp	Moderate	Shrimp accumulate AXT from their diet.	(Yaqoob <i>et al.</i> 2022)
Crustaceans	<i>Brachyura</i>	Moderate	Certain crab species contain AXT due to their diet.	(Ribeiro <i>et al.</i> 2001)
Crustaceans	<i>Cambarus</i> sp.	Moderate	Crayfish can possess AXT based on their food intake.	(Song <i>et al.</i> 2024)
Crustaceans	Lobster	Low to Moderate	Some lobster species can contain AXT due to their diet.	(Wade <i>et al.</i> 2005)
Crustaceans	Prawn	Low to Moderate	Prawns can accumulate AXT from their food sources.	(Zhang <i>et al.</i> 2021)
Fish	<i>Salmo salar</i>	Variable (high in sockeye)	Wild salmonids, especially the sockeye salmon, acquire AXT from their diet.	(Ytrestøyl & Bjerkeng 2007)
Fish	<i>Oncorhynchus mykiss</i>	High	Large trout species are noted for their AXT content.	(Pulcini <i>et al.</i> 2021)
Fish	<i>Euphausiacea</i>	High	Krill are an abundant source of AXT due to their diet.	(Ibrahim <i>et al.</i> 1984)
Fish	Chum Salmon	Low	Chum salmon exhibit lower AXT content compared to other species.	(Kitahara 1983)
Fish	Atlantic Salmon (farmed)	Moderate	Farmed salmon's AXT levels are influenced by their diet.	(Storebakken <i>et al.</i> 1987)
Fish	Rainbow Trout	Moderate	Rainbow trout can accumulate AXT, especially when fed AXT-rich diets.	(Foss <i>et al.</i> 1987)
Fish	Mackerel	Low	Certain fish species like mackerel can possess AXT.	(Roy <i>et al.</i> 2020)
Fish	Herring	Low	AXT content varies in different fish species.	(Bjerkeng <i>et al.</i> 1999)
Fungi	<i>Penaeus monodon baculovirus</i>	Low	Used in genetic engineering for AXT synthesis.	(Supamattaya <i>et al.</i> 2005)
Fungi	<i>Xanthophyllomyces dendrorhous</i>	High	Yeast-like fungus used for commercial AXT production.	(Rodríguez-Sáiz <i>et al.</i> 2010)
Fungi	<i>Phaffia rhodozyma</i>	High	Anamorphic yeast known for its AXT-rich pigment.	(Mussagy <i>et al.</i> 2023)
Fungi	<i>Neurospora crassa</i>	Low	Fungus capable of AXT production through genetic manipulation.	(Gmoser <i>et al.</i> 2017)
Fungi	<i>Paracoccus carotinifaciens</i>	Moderate	Bacterium capable of AXT production, used in research.	(Hayashi <i>et al.</i> 2021)



**Table 1.** Biological sources of AXT (Continued).

Source	Scientific/Common Name	AXT Content	Notes	Reference
Fungi	<i>Blakeslea trispora</i>	Moderate	Mucoralean fungus that can synthesize carotenoids, including AXT.	(Choudhari <i>et al.</i> 2008)
Insects	<i>Bombyx mori</i>	Low	AXT synthesis achieved through genetic modification.	(Chieco <i>et al.</i> 2019)
Microalgae	<i>Chlamydomonas</i> sp.	Low to Moderate	Green microalgae capable of AXT synthesis under certain conditions.	(Perozeni <i>et al.</i> 2020)
Microalgae	<i>Scenedesmus</i> sp.	Low to Moderate	Microalgae that can produce AXT as part of their carotenoid profile.	(Aburai <i>et al.</i> 2015)
Microalgae	<i>Spirulina</i> sp.	Low	Blue-green algae containing AXT in small quantities.	(An <i>et al.</i> 2017)
Microalgae	<i>Botryococcus braunii</i>	Low to Moderate	Green microalgae with potential for AXT production.	(Indrayani <i>et al.</i> 2022)
Microbes	<i>Escherichia coli</i>	Low	Genetic engineering can enable AXT synthesis in bacteria.	(Park <i>et al.</i> 2018)
Yeast	<i>Phaffia rhodozyma</i>	High	Widely used commercial source for AXT production.	(Sedmak <i>et al.</i> 1990)
Yeast	<i>Saccharomyces cerevisiae</i>	Low	AXT production possible through genetic engineering.	(Ukibe <i>et al.</i> 2009)

**Fig. 2.** Biological sources containing AXT. Values were given based on dry weight.

Structurally, AXT comprises paired terminal rings connected by a polyene chain. The  $\beta$ -ionone ring holds significance, hosting asymmetrical carbon atoms at positions 3 and 3', bonded to hydroxyl groups (-OH). This configuration is significant, leading to mono- and di-ester formations upon reaction with fatty acids. AXT's polymorphism is seen in stereoisomers and geometric forms, including liberated and esterified versions, found in natural sources (Yang *et al.* 2011).

In nature, prominent stereoisomers include 3S, 3'S and 3R, 3'R, synthesized by *Haematococcus pluvialis* and

*Xanthophyllomyces dendrorhous*, respectively. Synthetic AXT comprises various isomers, including (3S, 3'S), (3R, 3'S), and (3R, 3'R). 3R, 3'R is the dominant stereoisomer found in the Antarctic krill *Euphausia superba* primarily in esterified form. In wild Atlantic salmon, the prevailing form is 3S, 3'S, existing as the free form. The molecular formula AXT is  $C_{40}H_{52}O_4$ , with a molar mass of 596.84 g/mol. These insights reveal AXT's intricate structure and diverse forms, impacting its behavior and interactions across natural and synthetic realms (Sun *et al.* 2023).

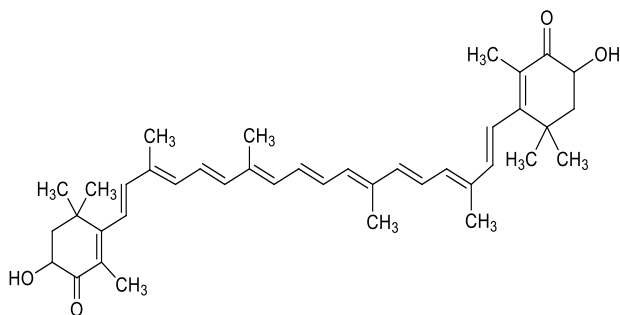


**Fig. 3.** Chemical structure of AXT.

#### Bioavailability, Pharmacokinetics and Safety of AXT

##### Bioavailability

Once released from the food matrix, carotenoids are amassed inside lipid droplets in gastric juices, where they are then incorporated into micelles. These micelles then diffuse into enterocyte plasma membrane. Carotenoids, such as AXT, are carried in circulation via high- and low-density lipoproteins (HDL and LDL, respectively) (Liu *et al.* 2023). AXT and other carotenoids fate relies on their biochemical properties, whereas dietary and non-dietary factors affect their absorption. The content of 3–37 mg/kg of AXT in salmon flesh converts to an intake of approximately 1–7 mg of AXT in a 200-g portion of salmon. The common natural form of AXT in wild salmon is the 3S, 3'S isomer (Odeberg *et al.* 2003). Absorption is affected by dietary habits and smoking; concurrent food consumption tends to enhance absorption, while smoking appears to decrease AXT's half-life. Studies on various animal species, such as mice, rats, dogs, and humans, have investigated AXT absorption from diverse sources (Madhavi *et al.* 2018). In a double-blind trial involving healthy men, daily consumption of 250 g of wild or aquacultured salmon for four weeks yielded differing plasma AXT concentrations. Plasma AXT levels stabilized at 39 nmol/L after consuming wild salmon (3S, 3'S isomer) for six days, and at 52 nmol/L after aquacultured salmon (3R, 3'S) consumption. Interestingly, aquacultured salmon intake led to significantly higher AXT concentrations in plasma on days 3, 6, 10, and 14, though not on day 28. This suggests that AXT intake pattern in plasma mirrors the ingested salmon and that maximal concentrations can be attained within the initial week, regardless of the source (Rüfer *et al.* 2008). Bioavailability and isomer distribution pattern of AXT in human plasma have been investigated while comprehensive studies on AXT's pharmacokinetics and tissue distribution in human skin remain lacking. AXT's lipid-solubility implies improved absorption in the presence of dietary lipids. Oil-based formulations enhance AXT bioavailability; an open parallel study revealed that lipid-based formulations, particularly those with higher hydrophilic synthetic surfactant content, yield the highest bioavailability (Odeberg *et al.* 2003).

It is recommended to consume AXT alongside dietary fats to optimize bioavailability. Future research should replicate these finding using dose aligned with regulatory recommendations. Current literature suggests a lack of

significant focus on enhancing AXT bioavailability, especially for skin tissue. Novel delivery methods like nanoparticles, topical creams, and specific phospholipid complexes show promise and warrant further exploration to enhance AXT bioavailability (Lima *et al.* 2021). Different forms of AXT and other factors affecting its bioavailability are represented in Fig. 4.

##### Pharmacokinetics

Carotenoids undergo absorption akin to lipids, subsequently traversing the lymphatic system to reach the hepatic locale. The efficiency of carotenoid absorption is contingent upon the concurrent dietary constituents. A diet abundant in cholesterol possesses the potential to augment carotenoid absorption, in contrast to a low-fat diet which tends to attenuate it. Following ingestion, AXT interacts with bile acids, leading to the formation of micellar structures within the small intestine.

These AXT-containing micelles experience partial uptake by enteric mucosal cells, thereby effectuating their integration into chylomicra within these cells. Following their release into the lymphatic circulation, chylomicra containing AXT undergo enzymatic hydrolysis by lipoprotein lipase. The subsequent swift clearance of chylomicron remnants by the hepatic organ and other tissues ensues. AXT becomes encompassed within lipoproteins, facilitating its systemic transport to various tissues. Among the diverse repertoire of endogenous carotenoids, AXT is distinguished for its exceptional capacity to shield cells, lipids, and membranous lipoproteins against oxidative impairment (Ambati *et al.* 2014).

##### Safety

Microalgae-derived AXT (i.e. AXT of *H. pluvialis*) has been authorized as color additives in feed for salmon and as a dietary supplement for human consumption in Western countries, Europe, Japan, and the USA. As part of its regulatory framework, the European Food Safety Authority (EFSA), and specifically its Panel on Additives and Products or Substances used in Animal Feed (FEEDAP), recommends an acceptable daily intake (ADI) for AXT at 0.034 mg/kg body weight (bw), or 2.38 mg/70-kg individual per day. Later on, the EFSA's Panel on Dietetic Products, Nutrition and Allergies (NDA) reaffirmed this scientific position maintaining that a conclusion of establishing the safety for 4 mg/day (0.06 mg/kg bw) of AXT was still to be determined (Agostoni *et al.* 2014, Aquilina *et al.* 2014). Notably, studies involving individuals who were administered more than 4 mg of AXT per day reported no adverse effects (Spiller & Dewell 2003, Res *et al.* 2013). First and foremost, even an acute administration of 40 mg of AXT over 48 hours in 32 healthy people was reported to be largely harmless, with only three mild cases (Odeberg *et al.* 2003). Chronic intake of AXT at 16 and 40 mg per day is safe for patients with functional dyspepsia (Kupcinkas *et al.* 2008). FDA has granted approval for direct human consumption of AXT from *H. pluvialis*, permitting dosages up to 12 mg

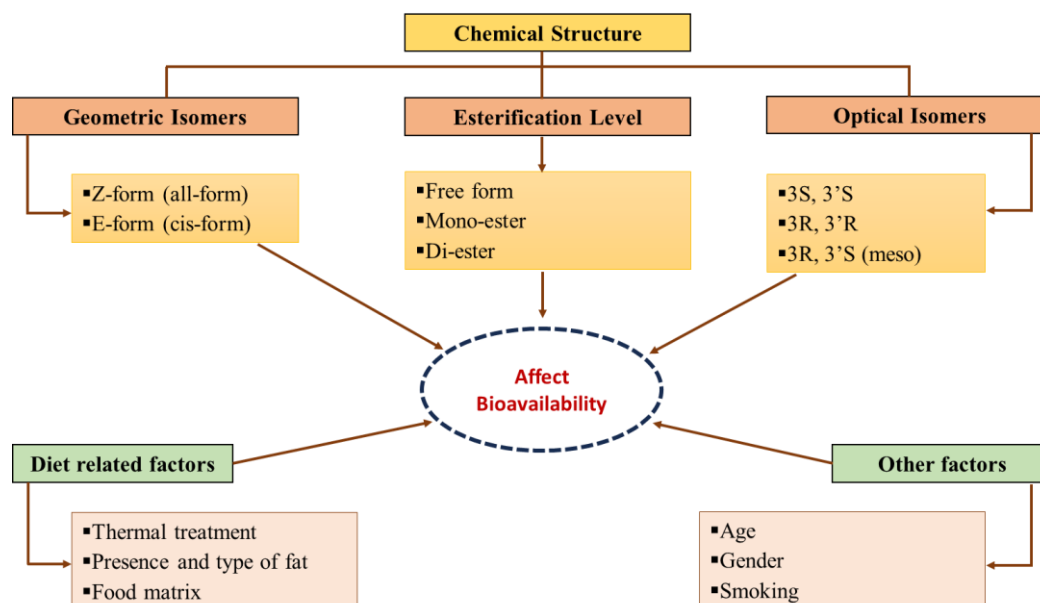


**Fig. 4.** Representation of different forms of AXT and other factors affecting its bioavailability.

per day and up to 24 mg per day for a duration not exceeding 30 days (Visioli & Artaria 2017). Furthermore, supercritical CO<sub>2</sub> extracts sourced from *H. pluvialis* have obtained "novel food" designation from FDA and are acknowledged as having "GRAS" (generally recognized as safe) status (Shah *et al.* 2016).

#### Common mechanism of action and biological activities of AXT

Disease progression is a complex phenomenon influenced by a myriad of factors, each exerting a significant impact on the intricate interplay of health and well-being. A suboptimal diet, characterized by nutritional deficiencies or an excess of detrimental components, compromises the body's immune system and overall functionality, fostering an environment conducive to the development of diseases (Childs *et al.* 2019). Infections, initiated by pathogenic microorganisms, have the potential to overpower the body's defense mechanisms, initiating detrimental cascades that contribute to the progression of diseases (Heinzelmann *et al.* 2002). Smoking, a well-established risk factor, introduces harmful chemicals that promote inflammation and OS. Dysfunctional mitochondrial respiration, along with chronic or acute inflammation, disrupts normal cellular activities, acting as influential forces in disease pathogenesis (Winiarska-Mieczan *et al.* 2023). Environmental factors, encompassing pollution, toxin exposure, radiation, drug metabolism, and ischemia-reperfusion injury, collectively contribute to the intricate network influencing disease progression (Heinzelmann *et al.* 2002). AXT, as a potent antioxidant, assumes a pivotal role in this context by modulating the activities of essential antioxidant enzymes at the cellular level, including superoxide dismutase (SOD), catalase, and glutathione peroxidase. Through the neutralization of free radicals and the reduction of OS, AXT augments the cellular antioxidant

defense system, presenting potential in the prevention of diseases associated with OS (Kim *et al.* 2009). Scientific investigations revealed that AXT supplementation has shown beneficial effects at doses of 6–18 mg/day for 12 weeks, improving HDL (6 & 12 mg), reducing triglycerides and increasing adiponectin (12 & 18 mg). An 8 mg/day dose for 8 weeks lowered visceral fat, triglycerides, and systolic blood pressure. 12 mg/day for 12 weeks improved insulin resistance and reduced LDL, HbA1c, and OS markers. Studies also reported enhanced antioxidant capacity and lipid profile regulation, with no significant impact on BMI or total cholesterol in some cases (Dansou *et al.* 2021). The common mechanism of action of AXT is summarized in Fig. 5.

#### Antioxidant activity of AXT

An antioxidant is a molecule that combats oxidation by neutralizing free radicals and reactive oxygen species (ROS). These highly reactive molecules stem from normal aerobic metabolism, causing oxidative damage to proteins, lipids, and DNA, linked to various disorders (Gutteridge & Halliwell 2010). Endogenous and exogenous antioxidants like carotenoids counter this OS. Carotenoids, with their conjugated double bonds, exhibit antioxidant properties by quenching singlet oxygen and halting chain reactions. These benefits likely result from carotenoid interactions with cell membranes (Mohd Aijaz *et al.* 2023). Compared to other carotenoids including lutein, lycopene,  $\alpha$ -carotene, and  $\beta$ -carotene, AXT holds superior antioxidant activity. AXT found in *H. pluvialis* offers robust protection against radicals in rats. Its distinctive molecular structure, featuring hydroxyl and keto groups, contributes to its potent antioxidant abilities. AXT's antioxidant potency surpasses zeaxanthin, lutein, canthaxanthin,  $\beta$ -carotene, and  $\alpha$ -tocopherol. The polyene chain in AXT traps radicals in cell membranes, while its terminal ring scavenges both inner and outer membrane

radicals (Rao *et al.* 2015). AXT's antioxidant role extends to boosting enzyme activities, as seen in rabbits' diets and ethanol-induced gastric ulcer rats. OS disrupts pro-oxidant/anti-oxidant balance, yielding ROS and free radicals (Augusti *et al.* 2012). Xanthophylls, including carotenoids, counteract this by interrupting radical chain reactions or reacting harmlessly. AXT safeguards against oxidative damage by neutralizing singlet oxygen, scavenging radicals, inhibiting lipid peroxidation, enhancing immune function, and regulating gene expression. Its high antioxidant capacity and polarity make it a promising nutraceutical (Seabra & Pedrosa 2010). *In vivo*, carotenoids like AXT need appropriate tissue transfer and concentration proportional to the oxidizing agent. AXT's antioxidant prowess surpasses

vitamin E, neutralizing singlet oxygen and outperforming other photochemical agents (Kogure 2019).

Age affects AXT activity, being more effective in youth due to enhanced antioxidant enzymes. AXT also enhances membrane fluidity, impeding diffusion and bolstering antioxidant efficacy. Scientific investigations revealed that AXT is highly effective to protect against inflammation, cancer, aging, and age-related macular degeneration, along with promoting overall health. It shields the retina from impairment induced by NMDA and antagonizes OS, activating pathways that trigger antioxidant responses (Kandy *et al.* 2022). AXT activates the PI3K/AKT and ERK pathways, facilitating Nrf2 activation and enhancing enzyme expression for protection against OS (Kavitha *et al.* 2013). SOD, catalase,

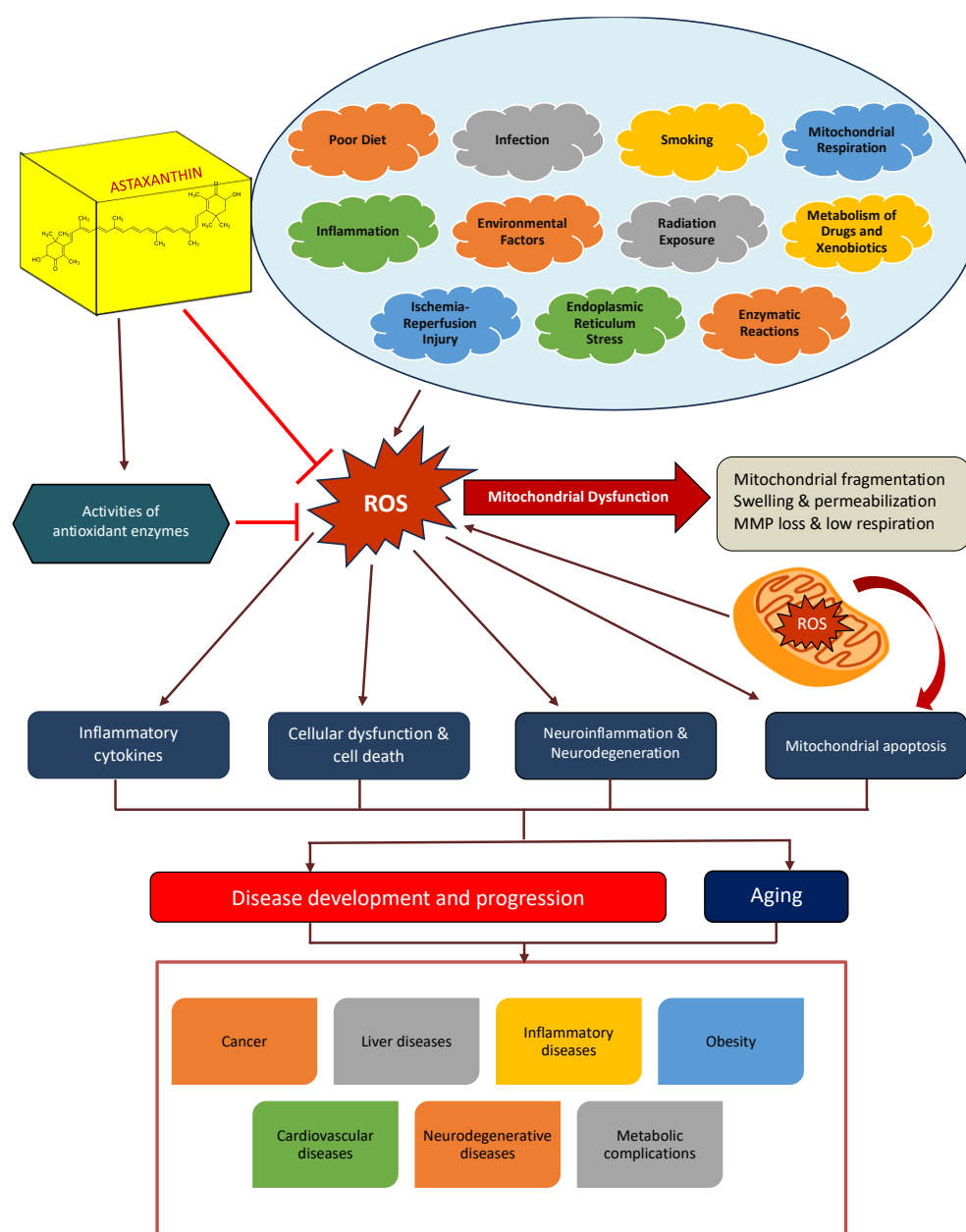


**Fig. 5.** Diagrammatic illustration of disease development and progression through various factors and common mechanism of action of AXT for their prevention.

TBARS, and peroxidase are elevated in rat liver and plasma after AXT supplementation (Polotow *et al.* 2014). In essence, antioxidants like AXT combat oxidative damage by neutralizing radicals and ROS, offering multifaceted protection against various disorders and promoting overall health (Rodriguez-Ruiz *et al.* 2018). In a study by Dansou *et al.* (2021), laying hens were supplemented with AXT at doses of 0, 21.3, 42.6, and 213.4 mg/kg of feed. The results indicated that while AXT improved antioxidant activities, such as enhancing SOD and glutathione peroxidase (GSH-Px) activities and reducing malondialdehyde (MDA) content in both liver and serum, the highest dose (213.4 mg/kg) did not provide additional antioxidant benefits compared to the moderate doses (21.3 and 42.6 mg/kg). Therefore, for optimal antioxidant activity in laying hens, a supplementation range of 21.3 to 42.6 mg/kg of feed is recommended (Dansou *et al.* 2021).

### Antiapoptotic activity of AXT

Neurodegenerative disorders, ischemic stroke, heart ailments, sepsis, and syndromes involving dysfunction in multiple organs are associated with cell death through apoptosis (Sanz *et al.* 2008). Several treatment approaches are available to manage apoptosis. Depending on the specific disease context, AXT may either inhibit or promote apoptosis (Hormozi *et al.* 2019). Intrinsic (mitochondrial) and extrinsic (death receptor) pathways are two primary pathways involved in apoptosis which are influenced by crucial apoptotic proteins (Sanz *et al.* 2008). By influencing these proteins, AXT could modify the course of apoptosis and mitigate associated diseases. AXT has been observed to have a dual impact on apoptosis regulation. It can enhance the phosphorylation of Bcl-2-associated death promoter, while the activation of cytochrome c and caspase 3 and 9 reduces. These effects are mediated through the control of mitogen-activated protein kinase/p38 (p38 MAPK), thereby influencing apoptosis (Li *et al.* 2015). Additionally, AXT activates the survival pathway PI3K/AKT, leading to the improvement of mitochondrial-linked apoptosis (Kim & Kim 2019). Interestingly, AXT has been documented to induce intrinsic apoptotic signaling in a model of oral cancer in hamsters. This is achieved by deactivating ERK/MAPK and PI3K/AKT cascades, ultimately inhibiting NF- $\kappa$ B and Wnt/ $\beta$ -catenin pathways (Kavitha *et al.* 2013). Furthermore, AXT's protective effects extend to retinal ganglion cells, reducing apoptotic cell death and ameliorating conditions like diabetic retinopathy by counteracting OS (Harada *et al.* 2017, Fang *et al.* 2023).

### Anti-inflammatory activity of AXT

Inflammation is a complex series of immune responses that activate as a protective mechanism in response to injuries, to initiate the tissue repair process (White & Mantovani 2013). However, when inflammation becomes excessive or uncontrolled, it can be harmful to the host, causing damage to cells and tissues. In both acute and chronic neurodegenerative conditions, inflammation plays a pivotal role (Liu *et al.* 2012). AXT effectively intervenes

in biological systems to curb the initiation of inflammation (Moh Aijaz *et al.* 2024). The anti-inflammatory properties of AXT hold significance in halting the advancement of central nervous system disorders (Masoudi *et al.* 2021). AXT acts by blocking the NF- $\kappa$ B-dependent signaling pathway, thereby decreasing expression of downstream inflammatory mediators such as interleukin-1 $\beta$  (IL-1 $\beta$ ), interleukin-6 (IL-6), and tumor necrosis factor- $\alpha$  (TNF- $\alpha$ ). NF- $\kappa$ B remains inactive in the cytosol under the influence of inhibitory kappa B (I $\kappa$ B) which is a major inhibitor in normal circumstances. Activation of NF- $\kappa$ B triggers a cascade involving I $\kappa$ B phosphorylation by I $\kappa$ B kinase  $\beta$  (IKK $\beta$ ), I $\kappa$ B degradation through the ubiquitin proteasome pathway, and dissociation of I $\kappa$ B from NF- $\kappa$ B. This exposes NF- $\kappa$ B's nuclear localization signal, thereby regulating the transcription of inflammatory genes (Chang & Xiong 2020). Additionally, AXT displays its anti-inflammatory effects by inhibiting cyclooxygenase-1 enzyme (COX-1) and nitric oxide (NO) in lipopolysaccharide-stimulated BV2 microglial cells. *In vivo* studies have demonstrated AXT's capacity to effectively diminish inflammation in tissues and organs (Pereira *et al.* 2021). AXT's anti-inflammatory prowess extends to diverse conditions, including arteriosclerosis, inflammatory bowel disease, sepsis, rheumatoid arthritis, gastric inflammation, brain inflammatory diseases, and the reduction of bacterial load in mice infected with *Helicobacter pylori* (Bennedsen *et al.* 2000). AXT functions as a potent antioxidant to counteract inflammation's initiation within biological systems (Chang & Xiong 2020). For instance, extracts from algal cells, i.e. of members of the genera *Haematococcus* and *Chlorococcum*, have shown promising results in reducing bacterial load and gastric inflammation in *H. pylori*-infected mice (Wang *et al.* 2000). Studies indicate that AXT can reduce oxidative damage to DNA, thereby enhancing immune responses in healthy human subjects (Park *et al.* 2010). Other research has found that AXT, when combined with *Ginkgo biloba* extract and Vitamin C, leads to reduced inflammation in lung tissues and improved levels of cAMP and cGMP (Haines *et al.* 2011). Furthermore, AXT has demonstrated gastro-protective effects on acute gastric lesions induced by ethanol, possibly due to its influence on various factors such as ATPase inhibition and antioxidant activities (Lee *et al.* 2022). AXT has also been proven effective in mitigating OS, inflammation, and apoptosis caused by high glucose in proximal tubular epithelial cells (Kim *et al.* 2009). Japanese researchers have highlighted AXT's potential for treating ocular inflammation, while its capacity to prevent skin thickening and to reduce collagen loss makes it a promising agent against UV-induced skin damage (Harada *et al.* 2017). In endotoxin-induced uveitis (EIU), a dose-dependent anti-inflammatory effect was observed, with 100 mg/kg AXT showing comparable efficacy to 10 mg/kg prednisolone. AXT improves immune function and reduces inflammation, particularly in individuals with excessive OS, making it a promising candidate for managing inflammatory conditions (Abdelazim *et al.* 2023).



### Anti-obesity activity

Obesity stands as a prominent and widespread public health concern impacting diverse age cohorts globally. Its deleterious outcomes encompass a range of severe ailments such as type 2 diabetes, hypertension, hyperlipidemia, and cardiovascular disorders, mediated by assorted mechanisms (Suhel Alam 2024). The pursuit of alternative, safe agents for combating obesity has spurred considerable attention towards AXT due to its promising anti-obesity attributes (Radice *et al.* 2021). Incorporating AXT into the diet as a supplementary component demonstrates the capacity to thwart weight gain, curtail plasma cholesterol levels, diminish plasma and hepatic triacylglycerol (TAG) content, amplify the expression of endogenous antioxidant genes within the liver, mitigate myeloperoxidase and NOS levels, and render splenocytes less responsive to lipopolysaccharide (LPS) stimulation. Furthermore, it holds potential to preempt obesity-linked disruptions in metabolic processes and inflammatory responses (Xia *et al.* 2020). A study by Aoi *et al.* (2008) unveiled that AXT fosters heightened lipid utilization during physical exercise, culminating in a reconfigured muscular metabolism, heightened physical performance, reduced body adiposity, and enhanced efficacy in muscular activities during exercise (Aoi *et al.* 2008). In a randomized double-blind study involving 23 overweight and obese adults (BMI > 25 kg/m<sup>2</sup>), participants were administered either 5 mg or 20 mg of AXT daily for 3 weeks. The study found significant improvements in OS biomarkers, suggesting potential benefits in managing obesity-related OS (Choi *et al.* 2011). Another study examined the combined effects of high-intensity functional training and AXT supplementation (20 mg/day) over 12 weeks in obese men. Results indicated reductions in body weight, body fat percentage, and improvements in lipid profiles, highlighting the potential of AXT in weight management when combined with exercise (Saeidi *et al.* 2023). AXT emerges as an innovative selective modulator of peroxisome proliferator-activated receptor gamma (PPAR- $\gamma$ ), operating as an antagonist or agonist to exert its beneficial impacts on obesity and insulin resistance (Taghiyar *et al.* 2023).

### Anti-diabetic Activity

OS levels are notably elevated in diabetes mellitus patients, primarily attributed to hyperglycemia-induced dysfunction of pancreatic  $\beta$ -cells and concurrent tissue damage (Yang *et al.* 2011). AXT holds promise in mitigating hyperglycemia-induced OS within pancreatic  $\beta$ -cells, while concurrently enhancing glucose and serum insulin levels. AXT's protective influence extends to shielding pancreatic  $\beta$ -cells against glucose toxicity, and it demonstrates immunomodulatory potential in the context of lymphocyte dysfunction associated with diabetic rats (Kanwugu *et al.* 2022).

In tandem, AXT combined with  $\alpha$ -tocopherol exhibited the ability to counter OS and ameliorate its

effects in streptozotocin-induced diabetes in rats (Yeh *et al.* 2016). This versatile compound also impedes glycation and cytotoxicity induced by glycated proteins in human umbilical vein endothelial cells through the inhibition of lipid and protein oxidation (Mashhadi *et al.* 2018). In metabolic terms, AXT effectively enhances insulin sensitivity in models of high-fat/high-fructose diet-induced obesity, both in spontaneously hypertensive corpulent rats and mice. This effect is attributed to its stimulation of the insulin receptor substrate (IRS)–PI3K–AKT signaling pathway, achieved through a reduction in serine phosphorylation of IRS proteins. Consequently, this leads to improved glucose metabolism through the regulation of metabolic enzymes, particularly in insulin-resistant mice (Naito *et al.* 2004, Zhuge *et al.* 2021). Notably, AXT demonstrates a multifaceted approach to combatting diabetes-associated complications. It effectively decreases urinary albumin levels and exhibits potential in preventing diabetic nephropathy by diminishing OS and curtailing renal cell damage. This encompasses the restoration of enzyme activities in salivary glands and the attenuation of glycation-induced cytotoxicity in human umbilical vein endothelial cells (Zhang *et al.* 2021). Animal studies investigated the effects of AXT on metabolic syndrome features in SHR/NDmcr-cp rats. The rats were administered AXT at a dose of 50 mg/kg body weight per day for 22 weeks, leading to improved insulin sensitivity and lipid metabolism parameters (Hussein *et al.* 2007). A clinical study involving healthy volunteers with prediabetes, participants were administered 12 mg of AXT daily for 12 weeks. The results indicated improvements in glucose metabolism and reductions in modified low-density lipoprotein levels (Urakaze *et al.* 2021). Another randomized clinical, placebo-controlled trial assessed the effects of 12 mg/day AXT over 24 weeks in individuals with prediabetes and dyslipidemia. The study found that AXT improved lipid profiles and reduced markers of cardiovascular disease risk, with trends toward improved insulin sensitivity (Ciaraldi *et al.* 2023). Overall, AXT emerges as a versatile therapeutic candidate, addressing hyperglycemia-induced OS, enhancing insulin sensitivity, and potentially mitigating diabetic complications.

### Immuno-modulatory activity

Immune cells are highly vulnerable to damage from free radicals, particularly due to the presence of polyunsaturated fatty acids (PUFAs) in their cell membranes (Das 2011). The protective role of antioxidants, particularly AXT, in safeguarding immune defenses from free radical harm is significant. While animal studies under laboratory conditions have explored AXT's impact on immunity, clinical research in humans remains limited (Fakhri *et al.* 2018). In comparison to  $\beta$ -carotene, AXT has demonstrated more potent immuno-modulating effects in mouse models. Notably, older animals displayed improved antibody production and reduced humoral immune responses following dietary AXT supplementation. Laboratory investigations

revealed that AXT prompted immunoglobulin production in human cells (Jyonouchi *et al.* 1994). Notably, an eight-week AXT supplementation regimen in humans resulted in heightened blood AXT levels, improved activity of natural killer cells targeting virus-infected cells, increased counts of T and B cells, reduced DNA damage, and significantly lower C-reactive protein (CRP) levels in the AXT-supplemented group (Sekikawa *et al.* 2023).

Both *in vivo* and *in vitro* studies on rats have unveiled AXT's influence on immunity, while human clinical research remains scarce. AXT's heightened immunomodulating effects compared to  $\beta$ -carotene have been evidenced in mouse models. Additionally, aged animals witnessed enhanced antibody production and diminished humoral immune responses through dietary AXT supplementation (Ohgami *et al.* 2003, Donoso *et al.* 2021). Further investigations demonstrated AXT's ability to activate humoral immune and cell-mediated reactions in canines and felines, regulate lymphocytic immune responses *in vitro*, and partly exert *ex vivo* immunomodulatory effects by elevating interferon-gamma (INF- $\gamma$ ) and interleukin-2 (IL-2) production without cytotoxicity (Lin *et al.* 2016). In various *in vitro* settings, AXT showcased the potential to elevate antibody secretory cell production, T-helper cell antibodies, and various immunoglobulins (IgM, IgG, IgA) in response to T-dependent stimuli (Fan *et al.* 2021). An *in vivo* study by Jyonouchi *et al.* (2000) indicated that dietary supplementation with AXT could potentially restore immune responses. In the face of stress, AXT effectively counteracts the decline in immunological functions by boosting immune responses mediated by natural killer (NK) cells and T lymphocytes, while also reducing DNA damage and CRP levels (Jyonouchi *et al.* 2000).

#### Neuroprotective activity

Neurological disorders encompass a range of conditions leading to disability, including both acute injuries and chronic neurodegenerative diseases. The underlying pathogenesis of many of these disorders involves inflammation, OS, and apoptosis (Suescun *et al.* 2019). A compound of particular interest in this context is AXT, which possesses the unique ability to traverse the Blood Brain Barrier (BBB) due to its fat-soluble nature. Given its diverse activities, AXT holds considerable promise as a potential therapeutic option for both acute and chronic neurological diseases (Si & Zhu 2022).

Recent investigations conducted in the laboratory have delved into the biological properties of AXT using an *in vivo* model. The findings from these studies underscore the favorable neuroprotective attributes of AXT in animal models of spinal cord injury (SCI). The heightened metabolic activity within the brain renders it susceptible to OS (Bahbah *et al.* 2021). However, AXT demonstrated the capability to enhance the activities of antioxidant enzymes and mitigate OS markers in distinct central nervous system (CNS) regions. Additionally, AXT exhibited a dampening effect on pro-inflammatory

cytokines such as interleukin-1 $\beta$  (IL-1 $\beta$ ), IL-6, tumor necrosis factor-alpha (TNF- $\alpha$ ), and NOS (Yook *et al.* 2016). In a study on pilocarpine-induced status epilepticus in rats, AXT was administered at a dose of 30 mg/kg body weight every other day for two weeks. The treatment improved cognitive function and reduced neuronal apoptosis, OS, and inflammation in the hippocampus (Deng *et al.* 2019). Furthermore, as alluded earlier, AXT has demonstrated its neuroprotective potential across experimental models of diverse neurological disorders. This efficacy is attributed to its multifaceted mechanisms, including anti-oxidative, anti-inflammatory, and anti-apoptotic actions (Fakhri *et al.* 2019). Notably, AXT's efficacy spans conditions such as Alzheimer's disease, Huntington's disease, Parkinson's disease, amyotrophic lateral sclerosis, traumatic injuries, inflammatory-induced injuries, and age-related dementia. The broad spectrum of functionalities exhibited by AXT in the context of neurological disease treatment underscores its role as a versatile and multi-target pharmacological agent (Fakhri *et al.* 2018).

#### Cardioprotective activity

Elevated generation of reactive oxygen and nitrogen species stimulates transcriptional agents, propelling the development of atherosclerosis, disruption of endothelial function, and harm subsequent to ischemic reperfusion and arrhythmia (Xiang *et al.* 2021). The likelihood of cardiovascular ailments is positively linked to cholesterol concentrations, specifically focusing on low-density lipoprotein (LDL), inflammation and OS form the basis of numerous cardiovascular symptoms (Yang *et al.* 2018). AXT exhibits cardioprotective effects by enhancing inflammation, lipid and glucose metabolism, and antioxidant activity. AXT inhibits free radicals and 7-ketocholesterol formation, curbing atheroma. It prevents arteriosclerosis by inhibiting LDL oxidation, lowering macrophage infiltration, apoptosis, and plaque rupture, enhancing plaque stability via adiponectin (Zaafan & Abdelhamid 2021). AXT reduces pro-inflammatory cytokines, Matrix Metalloproteinase (MMP) activation, and scavenger receptor upregulation in macrophages, regulating atherogenesis related functions. It counters inflammation and OS, curbs lipid peroxidation, thrombosis, and protects against cardiovascular damage in animal models and human cells (Derias *et al.* 2021). AXT ameliorates diabetes-related coagulation by its anti-oxidative and anti-inflammatory effects, increasing red blood cell concentrations. It safeguards against isoproterenol cardiotoxicity through free radical scavenging and antioxidant activity, a potential adjuvant therapy. AXT's impact on coronary disease prevention is underexplored (Krestinina *et al.* 2020). It reduces blood pressure by attenuating the renin-angiotensin system, angiotensin-II, and ROS-induced vasoconstriction, enhancing NO bioavailability and endothelial function, primarily in resistant arteries. AXT improves vascular elastin, arterial wall thickness, and blood fluidity in hypertension. It augments heart mitochondrial function,

reduces pro-inflammatory markers, suggesting a role in cardiac protection (Gao *et al.* 2021). OS and inflammation characterize atherosclerotic cardiovascular disease, making AXT a potential therapeutic due to its antioxidant and anti-inflammatory potential (Kara & Kilitçi 2023). Disodium disuccinate astaxanthin (DDA) shows promise in protecting myocardium, reducing infarct size and enhancing salvage. AXT is detected in myocardial tissues post DDA treatment (Adam Lauver *et al.* 2005). In hypertensive and normotensive rat models, AXT influences blood pressure, increases basal arterial blood flow, elevates nitric oxide, and reduces peroxynitrite levels (Kara & Kilitçi 2023). In mice, AXT elevates heart mitochondrial potential and contractility index. AXT prevents hypercholesterolemia-induced protein oxidation in rabbits through paraoxonase and thioredoxin reductase activity maintenance at dosages of 100 mg and 500 mg/100 g (Augusti *et al.* 2012).

#### Anti-cancer activity

Aerobic metabolism generates reactive species like superoxide, hydroxyl radical, and hydrogen peroxide, while photochemical reactions and lipid peroxidation produce singlet oxygen and peroxy radicals (Martemucci *et al.* 2022). These processes contribute to aging, carcinogenesis, mutagenesis, and degenerative diseases by oxidizing proteins, DNA, and lipids. Antioxidants mitigate oxidative damage, decreasing carcinogenesis and mutagenesis (Sun *et al.* 2020). Carotenoids, notably AXT, attract attention for their anticancer potential due to their inverse correlation with cancer prevalence (Ramamoorthy 2020). AXT surpasses other carotenoids like  $\beta$ -carotene and canthaxanthin in antitumor efficacy. Gap junctional communication is impaired in human tumors due to absent cell-to-cell connections, but AXT's promotion of connexin-43 protein via gene upregulation restores this communication, curbing tumor proliferation (Demirel & Tuna 2021).

AXT exhibits antitumor effects in various cancers, restraining growth and inducing cell death. Moreover, AXT curbs metastasis, inhibits 5- $\alpha$ -reductase to suppress prostate cancer, and triggers anti-invasive pathways (e.g., NF- $\kappa$ B, STAT3, PPAR $\gamma$ ). Downregulating MKK1/2-ERK1/2-mediated thymidylate synthase expression enhances non-small cell lung carcinoma sensitivity to pemetrexed-induced cytotoxicity (Faraone *et al.* 2020). AXT demonstrates preventive effects in carcinogenesis models, including large bowel and tongue cancers. It suppresses bladder and oral cancers, regulates immunity, and delays tumor initiation, implying optimal blood AXT levels safeguard against tumorigenesis. However, AXT supplementation post-tumor initiation may be counterproductive ROS from aerobic metabolism. Singlet oxygen and peroxy radicals arise from photochemical events and lipid peroxidation, contributing to aging and degenerative diseases via DNA, protein, and lipid oxidation (Yasui *et al.* 2011, Immacolata Faraone *et al.* 2020). Antioxidants counteract ROS-induced mutagenesis and carcinogenesis. Natural carotenoids and

retinoids enhance gap junctional communication between the cells. For instance, AXT derivatives improve intercellular communication in primary human skin fibroblasts. AXT exhibits potent antitumor activity compared to canthaxanthin and  $\beta$ -carotene, restraining fibrosarcoma, breast, and prostate cancer growth (Rivera-Madrid *et al.* 2019).

AXT's impact extends to inhibiting cell death, proliferation, and mammary tumors in chemically induced rodents. *Haematococcus pluvialis* extract, rich in AXT, hinders human colon cancer cell progression via cell cycle arrest, apoptosis, and cytokine suppression (Lim & Wang 2020). Nitroastaxanthin and 15-nitroastaxanthin, products of AXT and peroxynitrite, demonstrate anticancer effects. AXT treatment inhibits Epstein-Barr virus and mouse skin papilloma carcinogenesis (Ambati *et al.* 2014).

#### Hepatoprotective activity

AXT, as a potent antioxidant, has demonstrated remarkable preventive and therapeutic effects on various liver conditions. It addresses liver fibrosis, tumors, ischemia-reperfusion injury, and non-alcoholic fatty liver disease by modulating crucial signaling pathways (Li *et al.* 2015). It curtails JNK and ERK-1 activity to enhance liver insulin sensitivity, suppresses PPAR- $\gamma$  expression to reduce hepatic fat synthesis, and inhibits TGF- $\beta$ 1/Smad3 to counteract HSC activation and fibrosis. It also targets JAK/STAT3 and Wnt/ $\beta$ -catenin pathways to impede liver tumor progression, and safeguards against ischemia-reperfusion injury by mitigating apoptosis and autophagy (Jannel *et al.* 2020). AXT's benefits extend to lipid accumulation, insulin resistance, ROS, and lipid oxidation products in the liver. It mitigates these issues by reducing lipid buildup and insulin resistance. It curbs lipid peroxidation (LPO), augments cellular antioxidants like TBARS, glutathione, and SOD, and emerges as a hepatoprotective agent (Li *et al.* 2020). Following liver ischemia-reperfusion injury, AXT treatment maintains hepatic xanthine dehydrogenase and curbs protein carbonyl levels (Bernabeu *et al.* 2023). AXT also intervenes in hepatic stellate cell (HSC) activation and extracellular matrix formation. It accomplishes this by downregulating NF- $\kappa$ B and TGF-1 expression, preserving MMP2/TIMP1 balance, and influencing energy production in HSCs through autophagy modulation and apoptosis stimulation (Zheng *et al.* 2023). AXT effectively counteracts apoptosis and autophagy induced by hepatic IR injury by neutralizing ROS and inflammatory cytokines, attributed to MAPK family inactivation (Wei & Guo 2022). In mouse models, AXT (80 mg/kg) significantly alleviates liver fibrosis through the suppression of profibrogenic factors, possibly via downregulation of NF- $\kappa$ B p65 and Wnt/ $\beta$ -catenin pathways, achieved by inhibiting ERK and PI3K/AKT activation (Zhuang *et al.* 2021). Overall, AXT emerges as a versatile agent for liver protection and treatment, acting on various pathways to address a spectrum of liver-related conditions (Azadian *et al.* 2024).

## Conclusion and future perspectives

AXT represents an exciting and promising nutraceutical and pharmaceutical with innumerable biological activities and health benefits. As a powerful antioxidant, it performs a key function to lower OS, improve inflammation, and prevent cell damage. Its therapy use is widespread in neuroprotection, cardiovascular diseases, metabolic disorders, and cancer prevention. AXT is effective, however, it depends heavily on the dosage, because not all these health problems require the same dosage of AXT to work properly. For general signals of health and antioxidant support, some studies suggest 4–12 mg doses per day while for neuroprotective and cognitive enhancement, clinical results show greater efficacy with higher doses between 6–16 mg per day. In metabolic diseases like diabetes and obesity, AXT has improved insulin sensitivity, glucose metabolism, and lipid regulation when supplemented at 8–12 mg/day. Doses of 5–20 mg daily were shown to inhibit body fat accumulation and improve lipid metabolism for weight management. Cardioprotective effects like decreasing LDL oxidation and improving circulation are noticed in doses of 8–12 mg daily. For instance, AXT has successfully inhibited tumor growth, mediated apoptosis, and prevented metastasis in preclinical studies using higher doses of 10–50 mg/kg body weight in cancer model systems. Indeed, additional clinical trials will be needed to establish accurate cancer-dosage levels for humans. One of the main obstacles in AXT research is guided by its bioavailability, despite its many health benefits. It is usually poorly absorbed in human body, as it is a lipid-soluble compound. In the future, advanced delivery systems, such as nano-emulsions, lipid-based carriers, and phospholipid complexes, should be developed in order to facilitate the absorption and effectiveness of AXT. Moreover, large-scale human clinical trials are warranted to develop dosage guidelines and confirm long-term toxicity. Exploration of synergistic effects of AXT with other bioactive compounds represents another encouraging area of research. Incorporating AXT with other polyphenols, flavonoids, or conventional medicines may yield higher

therapeutic effects, especially for chronic diseases like cancer, cardiovascular diseases, and neurodegenerative diseases. Biotechnological approaches regarding the future AXT production may offer a sustainable and cost-effective alternative for the commercial availability of AXT in the near future. As the global demand for this potent carotenoid is ever-increasing, optimizing microalgae-based biosynthesis together with improving the extraction methods can help to scale up the production of AXT. Moreover, the role of AXT in healthy aging and longevity represents a fascinating research avenue within and beyond the realm of DI diseases. This is important because its ability to resist oxidative damage, optimize mitochondrial function, and modulate inflammatory pathways, indicate that it may help prevent many age-related diseases which include Alzheimer's, Parkinson's, and cardiovascular diseases as well.

Summarizing, AXT appears to be a very promising natural compound with pleiotropic health applications. However, more research is required to fine-tune dosing and enhance bioavailability, along with larger scale clinical trials, in order to capitalize on its potential to do so. With continuous advancements in biotechnology, formulation science, and clinical research, AXT could become a key player in modern medicine, offering innovative strategies for disease prevention, treatment, and overall health improvement.

**Ethics Committee Approval:** Since the article does not contain any studies with human or animal subject, its approval to the ethics committee was not required.

**Data Sharing Statement:** All data are available within the study.

**Author Contributions:** All authors contributed equally to this manuscript in its all stages.

**Conflict of Interest:** The authors have no conflicts of interest to declare.

**Funding:** The authors declared that this study has received no financial support.

## References

1. Abdelazim, K., Ghit, A., Assal, D., Dorra, N., Noby, N., Khattab, S.N., El Feky, S.E. & Hussein, A. 2023. Production and therapeutic use of astaxanthin in the nanotechnology era. *Pharmacological Reports*, 75(4): 771-790.
2. Aburai, N., Sumida, D. & Abe, K. 2015. Effect of light level and salinity on the composition and accumulation of free and ester-type carotenoids in the aerial microalga *Scenedesmus* sp. (Chlorophyceae). *Algal Research*, 8: 30-36. <https://doi.org/10.1016/j.algal.2015.01.005>
3. Adam Lauver, D., Lockwood, S.F. & Lucchesi, B.R. 2005. Disodium disuccinate astaxanthin (Cardax) attenuates complement activation and reduces myocardial injury following ischemia/reperfusion. *Journal of Pharmacology and Experimental Therapeutics*, 314(2): 686-692. <https://doi.org/10.1124/jpet.105.087114>
4. Agostoni, C., Berni Canani, R., Fairweather-Tait, S., Heinonen, M., Korhonen, H., La Vieille, S., Marchelli, R., Martin, A., Naska, A., Neuhäuser-Berthold, M., Nowicka, G., Sanz, Y., Siani, A., Sjödin, A., Stern, M., Strain, S., Tetens, I., Tomé, D., Turck, D., Brantom, P., Engel, K.-H., Pöting, A., Poulsen, M., Salminen, S., Schlatter, J., Van Loveren, H. & Verhagen, H. 2014. Scientific Opinion on the safety of astaxanthin-rich ingredients (AstaREAL A1010 and AstaREAL L10) as novel food ingredients. *EFSA Journal*, 12(7): 3757-3757. <https://doi.org/10.2903/j.efsa.2014.3757>
5. Aijaz, M., Keserwani, N., Yusuf, M., Ansari, N.H., Ushal, R. & Kalia, P. 2023. Chemical, Biological, and

- Pharmacological Prospects of Caffeic Acid. *Biointerface Research in Applied Chemistry*, 13(4): 324. <https://doi.org/10.33263/BRIAC134.324>
6. Aijaz, M., Kumar, A., Ahmad, M. & Ansari, M.A. 2024. Plant-Based Therapies in Parkinson's Disease Management: Mechanisms, Clinical Evidence, and Future Perspectives. *Letters in Applied NanoBioScience*, 13(3): 1-23. <https://doi.org/10.33263/LIANBS133.148>
7. Ambati, R.R., Moi, P.S., Ravi, S. & Aswathanarayana, R.G. 2014. Astaxanthin: Sources, extraction, stability, biological activities and its commercial applications - A review. *Marine Drugs*, 12(1): 128-152. <https://doi.org/10.3390/md12010128>
8. An, J., Gao, F., Ma, Q., Xiang, Y., Ren, D. & Lu, J. 2017. Screening for enhanced astaxanthin accumulation among *Spirulina platensis* mutants generated by atmospheric and room temperature plasmas. *Algal Research*, 25: 464-472. <https://doi.org/10.1016/j.algal.2017.06.006>
9. Aoi, W., Naito, Y., Takanami, Y., Ishii, T., Kawai, Y., Akagiri, S., Kato, Y., Osawa, T. & Yoshikawa, T. 2008. Astaxanthin improves muscle lipid metabolism in exercise via inhibitory effect of oxidative CPT I modification. *Biochemical and Biophysical Research Communications*, 366(4): 892-897. <https://doi.org/10.1016/j.bbrc.2007.12.019>
10. Aquilina, G., Bampidis, V., De, M., Bastos, L., Guido Costa, L., Flachowsky, G., Gralak, A., Hogstrand, C., Leng, L., López-Puente, S., Martelli, G., Mayo, B., Ramos, F., Renshaw, D., Rychen, G., Saarela, M., Sejrsen, K., Van Beelen, P., Wallace, R.J. & Westendorf, J. 2014. Scientific Opinion on the safety and efficacy of synthetic astaxanthin as feed additive for salmon and trout, other fish, ornamental fish, crustaceans and ornamental birds. *EFSA Journal*, 12(6): 35-35. <https://doi.org/10.2903/j.efsa.2014.3724>
11. Augusti, P.R., Quattrin, A., Somacal, S., Conterato, G.M.M., Sobieski, R., Ruviano, A.R., Maurer, L.H., Duarte, M.M.F., Roehrs, M. & Emanuelli, T. 2012. Astaxanthin prevents changes in the activities of thioredoxin reductase and paraoxonase in hypercholesterolemic rabbits. *Journal of Clinical Biochemistry and Nutrition*, 51(1): 42-49. <https://doi.org/10.3164/jcbrn.11-74>
12. Azadian, R., Mohammadalipour, A., Memarzadeh, M.R., Hashemnia, M. & Aarabi, M.H. 2024. Examining hepatoprotective effects of astaxanthin against methotrexate-induced hepatotoxicity in rats through modulation of Nrf2/HO-1 pathway genes. *Naunyn-Schmiedeberg's Archives of Pharmacology*, 397(1): 371-380. <https://doi.org/10.1007/s00210-023-02581-8>
13. Bahbah, E.I., Ghozy, S., Attia, M.S., Negida, A., Emran, T.B., Mitra, S., Albadrani, G.M., Abdel-Daim, M.M., Uddin, M.S. & Simal-Gandara, J. 2021. Molecular Mechanisms of Astaxanthin as a Potential Neurotherapeutic Agent. *Marine Drugs*, 19(4): 201-201. <https://doi.org/10.3390/md19040201>
14. Bennedsen, M., Wang, X., Willén, R., Wadström, T. & Andersen, L.P. 2000. Treatment of *H. pylori* infected mice with antioxidant astaxanthin reduces gastric inflammation, bacterial load and modulates cytokine release by splenocytes. *Immunology Letters*, 70(3): 185-189. [https://doi.org/10.1016/S0165-2478\(99\)00145-5](https://doi.org/10.1016/S0165-2478(99)00145-5)
15. Bernabeu, M., Gharibzadeh, S.M.T., Ganaie, A.A., Macha, M.A., Dar, B.N., Castagnini, J.M., Garcia-Bonillo, C., Meléndez-Martínez, A.J., Altintas, Z. & Barba, F.J. 2023. The potential modulation of gut microbiota and oxidative stress by dietary carotenoid pigments. *Critical Reviews in Food Science and Nutrition*. 64(33): 12555-12573. <https://doi.org/10.1080/10408398.2023.2254383>
16. Binti Ibnu Rasid, E.N., Mohamad, S.E., Jamaluddin, H. & Salleh, M.M. 2014. Screening factors influencing the production of astaxanthin from freshwater and marine microalgae. *Applied Biochemistry and Biotechnology*, 172(4): 2160-2174. <https://doi.org/10.1007/s12010-013-0644-x>
17. Bjerkeng, B., Hatlen, B. & Wathne, E. 1999. Deposition of astaxanthin in fillets of Atlantic salmon (*Salmo salar*) fed diets with herring, capelin, sandeel, or Peruvian high PUFA oils. *Aquaculture*, 180(3-4): 307-319. [https://doi.org/10.1016/S0044-8486\(99\)00206-9](https://doi.org/10.1016/S0044-8486(99)00206-9)
18. Boussiba, S. & Vonshak, A. 1991. Astaxanthin accumulation in the green alga *Haematococcus pluvialis*. *Plant and Cell Physiology*, 32(7): 1077-1082. <https://doi.org/10.1093/oxfordjournals.pcp.a078171>
19. Brotosudarmo, T.H.P., Limantara, L., Setiyono, E. & Heriyanto. 2020. Structures of Astaxanthin and Their Consequences for Therapeutic Application. *International Journal of Food Science*, 2020: 2156582. <https://doi.org/10.1155/2020/2156582>
20. Capelli, B., Talbott, S. & Ding, L. 2019. Astaxanthin sources: Suitability for human health and nutrition. *Functional Foods in Health and Disease*, 9(6): 430-445. <https://doi.org/10.31989/ffhd.v9i6.584>
21. Chang, M.X. & Xiong, F. 2020. Astaxanthin and its Effects in Inflammatory Responses and Inflammation-Associated Diseases: Recent Advances and Future Directions. *Molecules*, 25(22): 5342. <https://doi.org/10.3390/molecules25225342>
22. Chen, J., Hendriks, M., Chatzis, A., Ramasamy, S.K. & Kusumbe, A.P. 2020. Bone Vasculature and Bone Marrow Vascular Niches in Health and Disease. *Journal of Bone and Mineral Research*, 35(11): 2103-2120. <https://doi.org/10.1002/jbmr.4171>
23. Chieco, C., Morrone, L., Bertazza, G., Cappelozza, S., Saviane, A., Gai, F., Di Virgilio, N. & Rossi, F. 2019. The Effect of Strain and Rearing Medium on the Chemical Composition, Fatty Acid Profile and Carotenoid Content in Silkworm (*Bombyx mori*) Pupae. *Animals (Basel)*, 9(3): 103. <https://doi.org/10.3390/ani9030103>
24. Childs, C.E., Calder, P.C. & Miles, E.A. 2019. Diet and Immune Function. *Nutrients*, 11(8): 1933. <https://doi.org/10.3390/nu11081933>
25. Choi, H.D., Kim, J.H., Chang, M.J., Kyu-Youn, Y. & Shin, W.G. 2011. Effects of astaxanthin on oxidative stress in overweight and obese adults. *Phytotherapy Research*, 25(12): 1813-1818. <https://doi.org/10.1002/ptr.3494>
26. Choudhari, S.M., Ananthanarayan, L. & Singhal, R.S. 2008. Use of metabolic stimulators and inhibitors for enhanced production of  $\beta$ -carotene and lycopene by *Blakeslea trispora* NRRL 2895 and 2896. *Bioresource Technology*, 99(8): 3166-3173. <https://doi.org/10.1016/j.biortech.2007.05.051>



27. Ciaraldi, T.P., Boeder, S.C., Mudaliar, S.R., Giovannetti, E.R., Henry, R.R. & Pettus, J.H. 2023. Astaxanthin, a natural antioxidant, lowers cholesterol and markers of cardiovascular risk in individuals with prediabetes and dyslipidaemia. *Diabetes, Obesity and Metabolism*, 25(7): 1985-1994.
28. Crupi, P., Toci, A.T., Mangini, S., Wrubl, F., Rodolfi, L., Tredici, M.R., Coletta, A. & Antonacci, D. 2013. Determination of fucoxanthin isomers in microalgae (*Isochrysis* sp.) by high-performance liquid chromatography coupled with diode-array detector multistage mass spectrometry coupled with positive electrospray ionization. *Rapid Communications in Mass Spectrometry*, 27(9): 1027-1035. <https://doi.org/10.1002/rcm.6531>
29. Dansou, D.M., Wang, H., Nugroho, R.D., He, W., Zhao, Q., Tang, C., Zhang, H. & Zhang, J. 2021. Effects of duration and supplementation dose with astaxanthin on egg fortification. *Poultry Science*, 100(9): 101304.
30. Das, U.N. 2011. Essential fatty acids enhance free radical generation and lipid peroxidation to induce apoptosis of tumor cells. *Clinical Lipidology*, 6(4): 463.
31. Demirel, P.B. & Tuna, B.G. 2021. Anticancer properties of astaxanthin: A molecule of great promise. pp. 427-445. In: Ravishankar, G.A. & Rao, A.R (eds). *Global Perspectives on Astaxanthin*. Academic Press, 824 pp. <https://doi.org/10.1016/B978-0-12-823304-7.00003-9>
32. Deng, X., Wang, M., Hu, S., Feng, Y., Shao, Y., Xie, Y., Wu, M., Chen, Y. & Shi, X. 2019. The neuroprotective effect of astaxanthin on pilocarpine-induced status epilepticus in rats. *Frontiers in Cellular Neuroscience*, 13: 123.
33. Derias, M.S.M., Sabaa, A.E.R.F.A., Osman, A.E.M.M.A., Mohamed, A.E.-H.A. & Abou-bakr Darwish, D.A. 2021. The Potential protective role of astaxanthin on doxorubicin-induced cardiac toxicity in rats. *QJM: An International Journal of Medicine*, 114(Supplement\_1): hcab117.003. <https://doi.org/10.1093/qjmed/hcab117.003>
34. Donoso, A., González-Durán, J., Muñoz, A.A., González, P.A. & Agurto-Muñoz, C. 2021. Therapeutic uses of natural astaxanthin: An evidence-based review focused on human clinical trials. *Pharmacological Research*, 166: 105479. <https://doi.org/10.1016/j.phrs.2021.105479>
35. Fakhri, S., Abbaszadeh, F., Dargahi, L. & Jorjani, M. 2018. Astaxanthin: A mechanistic review on its biological activities and health benefits. *Pharmacological Research*, 136: 1-20. <https://doi.org/10.1016/j.phrs.2018.08.012>
36. Fakhri, S., Aneva, I.Y., Farzaei, M.H. & Sobarzo-Sánchez, E. 2019. The neuroprotective effects of astaxanthin: Therapeutic targets and clinical perspective. *Molecules*, 24(14): 2640. <https://doi.org/10.3390/molecules24142640>
37. Fan, Q., Chen, Z., Wu, Y., Zhu, J. & Yu, Z. 2021. Study on the Enhancement of Immune Function of Astaxanthin from *Haematococcus pluvialis*. *Foods*, 10(8): 1847. <https://doi.org/10.3390/foods10081847>
38. Fang, J., Bai, W. & Yang, L. 2023. Astaxanthin inhibits oxidative stress and apoptosis in diabetic retinopathy. *Acta Histochemica*, 125(6): 152069-152069. <https://doi.org/10.1016/j.acthis.2023.152069>
39. Faraone, I., Sinisgalli, C., Ostuni, A., Armentano, M.F., Carmosino, M., Milella, L., Russo, D., Labanca, F. & Khan, H. 2020. Astaxanthin anticancer effects are mediated through multiple molecular mechanisms: A systematic review. *Pharmacological Research*, 155: 104689. <https://doi.org/10.1016/j.phrs.2020.104689>
40. Faraone, I., Sinisgalli, C., Ostuni, A., Armentano, M.F., Carmosino, M., Milella, L., Russo, D., Labanca, F. & Khan, H. 2020. Astaxanthin anticancer effects are mediated through multiple molecular mechanisms: A systematic review. *Pharmacological Research*, 155: 104689-104689. <https://doi.org/10.1016/j.phrs.2020.104689>
41. Fithriani, D., Ambarwaty, D. & Nurhayati. 2019. Identification of bioactive compounds from *Nannochloropsis* sp. *IOP Conference Series: Earth and Environmental Science*, 404(1): 012064-012064. <https://doi.org/10.1088/1755-1315/404/1/012064>
42. Foss, P., Storebakken, T., Austreng, E. & Liaaenjen, S. 1987. Carotenoids in diets for salmonids. V. Pigmentation of rainbow trout and sea trout with astaxanthin and astaxanthin dipalmitate in comparison with canthaxanthin. *Aquaculture*, 65(3-4): 293-305. [https://doi.org/10.1016/0044-8486\(87\)90242-0](https://doi.org/10.1016/0044-8486(87)90242-0)
43. Gmoser, R., Ferreira, J.A., Lennartsson, P.R. & Taherzadeh, M.J. 2017a. Filamentous ascomycetes fungi as a source of natural pigments. *Fungal Biology and Biotechnology*, 4: 1-25. <https://doi.org/10.1186/s40694-017-0033-2>
44. Gao, H.L., Yu, X.J., Liu, K.L., Zuo, Y.Y., Fu, L.Y., Chen, Y.M., Zhang, D.D., Shi, X.L., Qi, J., Li, Y., Yi, Q.Y., Tian, H., Wang, X.M., Yu, J.Y., Zhu, G.Q., Liu, J.J., Kang, K.B. & Kang, Y.M. 2021. Chronic Infusion of Astaxanthin into Hypothalamic Paraventricular Nucleus Modulates Cytokines and Attenuates the Renin-Angiotensin System in Spontaneously Hypertensive Rats. *Journal of Cardiovascular Pharmacology*, 77(2): 170-181. <https://doi.org/10.1097/FJC.0000000000000953>
45. Gutteridge, J.M.C. & Halliwell, B. 2010. Antioxidants: Molecules, medicines, and myths. *Biochemical and Biophysical Research Communications*, 393(4): 561-564. <https://doi.org/10.1016/j.bbrc.2010.02.071>
46. Haines, D.D., Varga, B., Bak, I., Juhasz, B., Mahmoud, F.F., Kalantari, H., Gesztelyi, R., Lekli, I., Czompa, A. & Tosaki, A. 2011. Summative interaction between astaxanthin, *Ginkgo biloba* extract (EGb761) and vitamin C in Suppression of respiratory inflammation: A comparison with ibuprofen. *Phytotherapy Research*, 25(1): 128-136. <https://doi.org/10.1002/ptr.3160>
47. Harada, F., Morikawa, T., Lennikov, A., Mukwaya, A., Schaupper, M., Uehara, O., Takai, R., Yoshida, K., Sato, J., Horie, Y., Sakaguchi, H., Wu, C.Z., Abiko, Y., Lagali, N. & Kitaichi, N. 2017. Protective Effects of Oral Astaxanthin Nanopowder against Ultraviolet-Induced Photokeratitis in Mice. *Oxidative Medicine and Cellular Longevity*, 2017: 1956104. <https://doi.org/10.1155/2017/1956104>
48. Hayashi, M., Ishibashi, T., Kuwahara, D. & Hirasawa, K. 2021. Commercial Production of Astaxanthin with *Paracoccus carotinifaciens*. *Advances in Experimental Medicine and Biology*, 1261: 11-20. [https://doi.org/10.1007/978-981-15-7360-6\\_2](https://doi.org/10.1007/978-981-15-7360-6_2)

49. Heinzlmann, M., Scott, M. & Lam, T. 2002. Factors predisposing to bacterial invasion and infection. *American Journal of Surgery*, 183(2): 179-190. [https://doi.org/10.1016/S0002-9610\(01\)00866-2](https://doi.org/10.1016/S0002-9610(01)00866-2)
50. Hormozi, M., Ghoreishi, S. & Baharvand, P. 2019. Astaxanthin induces apoptosis and increases activity of antioxidant enzymes in LS-180 cells. *Artificial Cells, Nanomedicine and Biotechnology*, 47(1): 891-895. <https://doi.org/10.1080/21691401.2019.1580286>
51. Hussein, G., Nakagawa, T., Goto, H., Shimada, Y., Matsumoto, K., Sankawa, U. & Watanabe, H. 2007. Astaxanthin ameliorates features of metabolic syndrome in SHR/NDmcr-cp. *Life Sciences*, 80(6): 522-529.
52. Ibrahim, A., Shimizu, C. & Kono, M. 1984. Pigmentation of cultured red sea bream, *Chrysophrys major*, using astaxanthin from Antarctic krill, *Euphausia superba*, and a mysid, *Neomysis* sp. *Aquaculture*, 38(1): 45-57. [https://doi.org/10.1016/0044-8486\(84\)90136-4](https://doi.org/10.1016/0044-8486(84)90136-4)
53. Indrayani, I., Egeland, E.S., Moheimani, N.R. & Borowitzka, M.A. 2022. Carotenoid production of *Botryococcus braunii* CCAP 807/2 under different growth conditions. *Journal of Applied Phycology*, 34(3): 1177-1188. <https://doi.org/10.1007/s10811-022-02682-6>
54. Ip, P.F. & Chen, F. 2005. Production of astaxanthin by the green microalga *Chlorella zofingiensis* in the dark. *Process Biochemistry*, 40(2): 733-738. <https://doi.org/10.1016/j.procbio.2004.01.039>
55. Jannel, S., Caro, Y., Bermudes, M. & Petit, T. 2020. Novel insights into the biotechnological production of haematococcus pluvialis-derived astaxanthin: Advances and key challenges to allow its industrial use as novel food ingredient. *Journal of Marine Science and Engineering*, 8(10): 1-48. <https://doi.org/10.3390/jmse8100789>
56. Jyonouchi, H., Sun, S., Iijima, K. & Gross, M.D. 2000. Antitumor activity of astaxanthin and its mode of action. *Nutrition and Cancer*, 36(1): 59-65. [https://doi.org/10.1207/S15327914NC3601\\_9](https://doi.org/10.1207/S15327914NC3601_9)
57. Jyonouchi, H., Zhang, L., Gross, M. & Tomita, Y. 1994. Immunomodulating Actions of Carotenoids: Enhancement of *In Vivo* and *In Vitro* Antibody Production to T-Dependent Antigens. *Nutrition and Cancer*, 21(1): 47-58. <https://doi.org/10.1080/01635589409514303>
58. Kandy, S.K., Nimonkar, M.M., Dash, S.S., Mehta, B. & Markandeya, Y.S. 2022. Astaxanthin Protection against Neuronal Excitotoxicity via Glutamate Receptor Inhibition and Improvement of Mitochondrial Function. *Mar Drugs*, 20(10): 645. <https://doi.org/10.3390/md20100645>
59. Kanwugu, O.N., Glukhareva, T.V., Danilova, I.G. & Kovaleva, E.G. 2022. Natural antioxidants in diabetes treatment and management: prospects of astaxanthin. *Critical Reviews in Food Science and Nutrition*, 62(18): 5005-5028. <https://doi.org/10.1080/10408398.2021.1881434>
60. Kara, Ö. & Kilitçi, A. 2023. The effect of astaxanthin on amiodarone induced cardiac tissue damage in rat. *Cukurova Medical Journal*, 48(1): 194-199. <https://doi.org/10.17826/cumj.1224847>
61. Kavitha, K., Kowshik, J., Kishore, T.K.K., Baba, A.B. & Nagini, S. 2013. Astaxanthin inhibits NF-κB and Wnt/β-catenin signaling pathways via inactivation of Erk/MAPK and PI3K/Akt to induce intrinsic apoptosis in a hamster model of oral cancer. *Biochimica et Biophysica Acta - General Subjects*, 1830(10): 4433-4444. <https://doi.org/10.1016/j.bbagen.2013.05.032>
62. Kim, S.H. & Kim, H. 2019. Astaxanthin Modulation of Signaling Pathways That Regulate Autophagy. *Mar Drugs*, 17(10): 546. <https://doi.org/10.3390/md17100546>
63. Kim, Y.J., Kim, Y.A.E. & Yokozawa, T. 2009. Protection against oxidative stress, inflammation, and apoptosis of high-glucose-exposed proximal tubular epithelial cells by astaxanthin. *Journal of Agricultural and Food Chemistry*, 57(19): 8793-8797. <https://doi.org/10.1021/jf9019745>
64. Kitahara, T. 1983. Behavior of carotenoids in the chum salmon (*Oncorhynchus keta*) during anadromous migration. *Comparative Biochemistry and Physiology Part B: Comparative Biochemistry*, 76(1): 97-101. [https://doi.org/10.1016/0305-0491\(83\)90177-3](https://doi.org/10.1016/0305-0491(83)90177-3)
65. Kogure, K. 2019. Novel antioxidative activity of astaxanthin and its synergistic effect with vitamin E. *Journal of Nutritional Science and Vitaminology*, 65(Supplement): S109-S112. <https://doi.org/10.3177/jnsv.65.S109>
66. Krestinina, O., Baburina, Y., Krestinin, R., Odinkova, I., Fadeeva, I. & Sotnikova, L. 2020. Astaxanthin prevents mitochondrial impairment induced by isoproterenol in isolated rat heart mitochondria. *Antioxidants*, 9(3): 262. <https://doi.org/10.3390/antiox9030262>
67. Kupcinskas, L., Lafolie, P., Lignell, Å., Kiudelis, G., Jonaitis, L., Adamonis, K., Andersen, L.P. & Wadström, T. 2008. Efficacy of the natural antioxidant astaxanthin in the treatment of functional dyspepsia in patients with or without *Helicobacter pylori* infection: A prospective, randomized, double blind, and placebo-controlled study. *Phytomedicine*, 15(6-7): 391-399. <https://doi.org/10.1016/j.phymed.2008.04.004>
68. Lee, J., Kim, M.H. & Kim, H. 2022. Anti-Oxidant and Anti-Inflammatory Effects of Astaxanthin on Gastrointestinal Diseases. *International Journal of Molecular Sciences*, 23(24): 15471-15471. <https://doi.org/10.3390/ijms232415471>
69. Li, J., Guo, C. & Wu, J. 2020. Astaxanthin in liver health and disease: A potential therapeutic agent. *Drug Design, Development and Therapy*, 14: 2275-2285. <https://doi.org/10.2147/DDDT.S230749>
70. Li, S., Tan, H.Y., Wang, N., Zhang, Z.J., Lao, L., Wong, C.W. & Feng, Y. 2015. The role of oxidative stress and antioxidants in liver diseases. *International Journal of Molecular Sciences*, 16(11): 26087-26124. <https://doi.org/10.3390/ijms161125942>
71. Lim, J.Y. & Wang, X.D. 2020. Mechanistic understanding of β-cryptoxanthin and lycopene in cancer prevention in animal models. *Biochimica et Biophysica Acta - Molecular and Cell Biology of Lipids*, 1865(11): 158652-158652. <https://doi.org/10.1016/j.bbalip.2020.158652>
72. Lima, S.G.M., Freire, M.C.L.C., Oliveira, V.d.S., Solisio, C., Converti, A. & de Lima, Á.A.N. 2021. Astaxanthin delivery systems for skin application: A review. *Marine Drugs*, 19(9): 511-511. <https://doi.org/10.3390/MD19090511>

73. Lin, K.H., Lin, K.C., Lu, W.J., Thomas, P.A., Jayakumar, T. & Sheu, J.R. 2016. Astaxanthin, a carotenoid, stimulates immune responses by enhancing IFN- $\gamma$  and IL-2 secretion in primary cultured lymphocytes *in Vitro* and *ex Vivo*. *International Journal of Molecular Sciences*, 17(1): 44. <https://doi.org/10.3390/ijms17010044>
74. Liu, B.H. & Lee, Y.K. 1999. Composition and biosynthetic pathways of carotenoids in the astaxanthin- producing green alga *Chlorococcum* sp. *Biotechnology Letters*, 21(11): 1007-1010. <https://doi.org/10.1023/A:1005660313289>
75. Liu, F.T., Yang, R.Y. & Hsu, D.K. 2012. Galectins in acute and chronic inflammation. *Annals of the New York Academy of Sciences*, 1253(1): 80-91. <https://doi.org/10.1111/j.1749-6632.2011.06386.x>
76. Liu, X., Xie, J., Zhou, L., Zhang, J., Chen, Z., Xiao, J., Cao, Y. & Xiao, H. 2023. Recent advances in health benefits and bioavailability of dietary astaxanthin and its isomers. *Food Chemistry*, 404: 134605-134605. <https://doi.org/10.1016/j.foodchem.2022.134605>
77. Madhavi, D., Kagan, D. & Seshadri, S. 2018. A study on the bioavailability of a proprietary, sustained-release formulation of astaxanthin. *Integrative Medicine (Boulder)*, 17(3): 38-42.
78. Martemucci, G., Costagliola, C., Mariano, M., D'andrea, L., Napolitano, P. & D'Alessandro, A.G. 2022. Free Radical Properties, Source and Targets, Antioxidant Consumption and Health. *Oxygen*, 2(2): 48-78. <https://doi.org/10.3390/oxygen2020006>
79. Martínez-Cámara, S., Ibañez, A., Rubio, S., Barreiro, C. & Barredo, J.-L. 2021. Main Carotenoids Produced by Microorganisms. *Encyclopedia*, 1(4): 1223-1245. <https://doi.org/10.3390/encyclopedia1040093>
80. Mashhadi, N.S., Zakerkish, M., Mohammadiasl, J., Zarei, M., Mohammadshahi, M. & Haghighizadeh, M.H. 2018. Astaxanthin improves glucose metabolism and reduces blood pressure in patients with type 2 diabetes mellitus. *Asia Pacific Journal of Clinical Nutrition*, 27(2): 341-346. <https://doi.org/10.6133/apjcn.052017.11>
81. Masoudi, A., Jorjani, M., Alizadeh, M., Mirzamohammadi, S. & Mohammadi, M. 2021. Anti-inflammatory and antioxidant effects of astaxanthin following spinal cord injury in a rat animal model. *Brain Research Bulletin*, 177: 324-331. <https://doi.org/10.1016/j.brainresbull.2021.10.014>
82. Mussagy, C.U., Pereira, J.F.B., Dufossé, L., Raghavan, V., Santos-Ebinuma, V.C. & Pessoa, A. 2023. Advances and trends in biotechnological production of natural astaxanthin by *Phaffia rhodozyma* yeast. *Critical Reviews in Food Science and Nutrition*, 63(13): 1862-1876. <https://doi.org/10.1080/10408398.2021.1968788>
83. Naito, Y., Uchiyama, K., Aoi, W., Hasegawa, G., Nakamura, N., Yoshida, N., Maoka, T., Takahashi, J. & Yoshikawa, T. 2004. Prevention of diabetic nephropathy by treatment with astaxanthin in diabetic db/db mice. *BioFactors*, 20(1): 49-59. <https://doi.org/10.1002/biof.5520200105>
84. Odeberg, J.M., Lignell, Å., Pettersson, A. & Höglund, P. 2003. Oral bioavailability of the antioxidant astaxanthin in humans is enhanced by incorporation of lipid based formulations. *European Journal of Pharmaceutical Sciences*, 19(4): 299-304. [https://doi.org/10.1016/S0928-0987\(03\)00135-0](https://doi.org/10.1016/S0928-0987(03)00135-0)
85. Ohgami, K., Shiratori, K., Kotake, S., Nishida, T., Mizuki, N., Yazawa, K. & Ohno, S. 2003. Effects of astaxanthin on lipopolysaccharide-induced inflammation *in vitro* and *in vivo*. *Investigative Ophthalmology and Visual Science*, 44(6): 2694-2701. <https://doi.org/10.1167/iops.02-0822>
86. Park, J.S., Chyun, J.H., Kim, Y.K., Line, L.L. & Chew, B.P. 2010. Astaxanthin decreased oxidative stress and inflammation and enhanced immune response in humans. *Nutrition & Metabolism (Lond)*, 7: 18. <https://doi.org/10.1186/1743-7075-7-18>
87. Park, S.Y., Binkley, R.M., Kim, W.J., Lee, M.H. & Lee, S.Y. 2018. Metabolic engineering of *Escherichia coli* for high-level astaxanthin production with high productivity. *Metabolic Engineering*, 49: 105-115. <https://doi.org/10.1016/j.ymben.2018.08.002>
88. Pereira, C.P.M., Souza, A.C.R., Vasconcelos, A.R., Prado, P.S. & Name, J.J. 2021. Antioxidant and anti-inflammatory mechanisms of action of astaxanthin in cardiovascular diseases (Review). *International Journal of Molecular Medicine*, 47(1): 37-48. <https://doi.org/10.3892/ijmm.2020.4783>
89. Pérez-Rodríguez, L., Jesús, M.-P. & Mougeot, F. 2020. Carotenoid-Based Ornaments as Signals of Health Status in Birds: Evidences from Two Galliform Species, The Red-legged Partridge (*Alectoris rufa*) and the Red Grouse (*Lagopus lagopus scoticus*). pp. 227-251. In: Lawton, J.A. & John, W.V. (eds). *Encyclopedia of Avian Science*, Volume 1-4, 1568 pp.
90. Perozeni, F., Cazzaniga, S., Baier, T., Zaroni, F., Zoccatelli, G., Lauersen, K.J., Wobbe, L. & Ballottari, M. 2020. Turning a green alga red: engineering astaxanthin biosynthesis by intragenic pseudogene revival in *Chlamydomonas reinhardtii*. *Plant Biotechnology Journal*, 18(10): 2053-2067. <https://doi.org/10.1111/pbi.13364>
91. Polotow, T.G., Vardaris, C.V., Mihaliuc, A.R., Goncalves, M.S., Pereira, B., Ganini, D. & Barros, M.P. 2014. Astaxanthin supplementation delays physical exhaustion and prevents redox imbalances in plasma and soleus muscles of Wistar rats. *Nutrients*, 6(12): 5819-5838. <https://doi.org/10.3390/nu6125819>
92. Pulcini, D., Capoccioni, F., Franceschini, S., Martinoli, M., Faccenda, F., Secci, G., Perugini, A., Tibaldi, E. & Parisi, G. 2021. Muscle pigmentation in rainbow trout (*Oncorhynchus mykiss*) fed diets rich in natural carotenoids from microalgae and crustaceans. *Aquaculture*, 543: 736989-736989. <https://doi.org/10.1016/j.aquaculture.2021.736989>
93. Radice, R.P., Limongi, A.R., Viviano, E., Padula, M.C., Martelli, G. & Bermano, G. 2021. Effects of astaxanthin in animal models of obesity-associated diseases: A systematic review and meta-analysis. *Free Radical Biology and Medicine*, 171: 156-168. <https://doi.org/10.1016/j.freeradbiomed.2021.05.008>
94. Ramamoorthy, K. 2020. Anticancer effects and lysosomal acidification in A549 cells by astaxanthin from *Haematococcus lacustris*. *Bioinformation*, 16(11): 965-973. <https://doi.org/10.6026/97320630016965>



95. Rao, A.R., Sarada, R., Shylaja, M.D. & Ravishankar, G.A. 2015. Evaluation of hepatoprotective and antioxidant activity of astaxanthin and astaxanthin esters from microalga-Haematococcus pluvialis. *Journal of Food Science and Technology*, 52(10): 6703-6710. <https://doi.org/10.1007/s13197-015-1775-6>
96. Res, P.T., Cermak, N.M., Stinkens, R., Tollakson, T.J., Haenen, G.R., Bast, A. & Van Loon, L.J.C. 2013. Astaxanthin supplementation does not augment fat use or improve endurance performance. *Medicine and Science in Sports and Exercise*, 45(6): 1158-1165. <https://doi.org/10.1249/MSS.0b013e31827fddc4>
97. Ribeiro, E.A., Genofre, G.C. & McNamara, J.C. 2001. Identification and quantification of carotenoid pigments during the embryonic development of the freshwater shrimp *Macrobrachium olfersii* (crustacea, decapoda). *Marine and Freshwater Behaviour and Physiology*, 34(2): 105-116. <https://doi.org/10.1080/10236240109379063>
98. Rivera-Madrid, R., Carballo-Uicab, V.M., Cárdenas-Conejo, Y., Aguilar-Espinosa, M. & Siva, R. 2019. Overview of carotenoids and beneficial effects on human health. pp 1-40. In: Galanakis G.M. (ed.). *Carotenoids: Properties, Processing and Applications*. Academic Press, 385pp. <https://doi.org/10.1016/B978-0-12-817067-0.00001-4>
99. Rodríguez-Ruiz, V., Salatti-Dorado, J.Á., Barzegari, A., Nicolas-Boluda, A., Houaoui, A., Caballo, C., Caballero-Casero, N., Sicilia, D., Venegas, J.B., Pauthe, E., Omid, Y., Letourneur, D., Rubio, S., Gueguen, V. & Pavon-Djavid, G. 2018. Astaxanthin-loaded nanostructured lipid carriers for preservation of antioxidant activity. *Molecules*, 23(10): 2601. <https://doi.org/10.3390/molecules23102601>
100. Rodríguez-Sáiz, M., De La Fuente, J.L. & Barredo, J.L. 2010. Xanthophyllomyces dendrorhous for the industrial production of astaxanthin. *Applied Microbiology and Biotechnology*, 88(3): 645-658. <https://doi.org/10.1007/s00253-010-2814-x>
101. Roy, V.C., Getachew, A.T., Cho, Y.J., Park, J.S. & Chun, B.S. 2020. Recovery and bio-potentialities of astaxanthin-rich oil from shrimp (*Penaeus monodon*) waste and mackerel (*Scomberomus niphonius*) skin using concurrent supercritical CO<sub>2</sub> extraction. *Journal of Supercritical Fluids*, 159: 104773-104773. <https://doi.org/10.1016/j.supflu.2020.104773>
102. Rüfer, C.E., Moeseneder, J., Briviba, K., Rechkemmer, G. & Bub, A. 2008. Bioavailability of astaxanthin stereoisomers from wild (*Oncorhynchus* spp.) and aquacultured (*Salmo salar*) salmon in healthy men: a randomised, double-blind study. *British Journal of Nutrition*, 99(5): 1048-1054. <https://doi.org/10.1017/s0007114507845521>
103. Saeidi, A., Nouri-Habashi, A., Razi, O., Ataieinosrat, A., Rahmani, H., Mollabashi, S.S., Bagherzadeh-Rahmani, B., Aghdam, S.M., Khalajzadeh, L. & Al Kiyumi, M.H. 2023. Astaxanthin supplemented with high-intensity functional training decreases adipokines levels and Cardiovascular Risk factors in men with obesity. *Nutrients*, 15(2): 286.
104. Sajilata, M.G. & Singhal, R.S. 2008. Isolation and stabilisation of natural pigments for food applications. *Stewart Postharvest Review*, 2(5): 1-29. <https://doi.org/10.2212/spr.2006.5.11>
105. Sanz, A.B., Santamaría, B., Ruiz-Ortega, M., Egido, J. & Ortiz, A. 2008. Mechanisms of renal apoptosis in health and disease. *Journal of the American Society of Nephrology*, 19(9): 1634-1642. <https://doi.org/10.1681/ASN.2007121336>
106. Seabra, L.M.A.J. & Pedrosa, L.F.C. 2010. Astaxantina: Aspectos estruturais e funcionais. *Revista de Nutricao*, 23(6): 1041-1050. <https://doi.org/10.1590/S1415-52732010000600010>
107. Sedmak, J.J., Weerasinghe, D.K. & Jolly, S.O. 1990. Extraction and quantitation of astaxanthin from Phaffia rhodozyma. *Biotechnology Techniques*, 4(2): 107-112. <https://doi.org/10.1007/BF00163282>
108. Sekikawa, T., Kizawa, Y., Li, Y. & Miura, N. 2023. Effects of diet containing astaxanthin on visual function in healthy individuals: a randomized, double-blind, placebo-controlled, parallel study. *Journal of Clinical Biochemistry and Nutrition*, 72(1): 74-81. <https://doi.org/10.3164/jcbs.22-65>
109. Shah, M.D., Ransangan, J. & Venmathi Maran, B.A. 2023. *Marine Biotechnology: Applications in Food, Drugs and Energy*, Springer, 367 pp.
110. Shah, M.M.R., Liang, Y., Cheng, J.J. & Daroch, M. 2016. Astaxanthin-producing green microalga Haematococcus pluvialis: from single cell to high value commercial products. *Frontiers in Plant Science*, 7: 531.
111. Si, P. & Zhu, C. 2022. Biological and neurological activities of astaxanthin (Review). *Molecular Medicine Report*, 26(4): 300. <https://doi.org/10.3892/mmr.2022.12816>
112. Song, G., Zhao, Y., Lu, J., Liu, Z., Quan, J. & Zhu, L. 2024. Effects of Astaxanthin on Growth Performance, Gut Structure, and Intestinal Microorganisms of *Penaeus vannamei* under Microcystin-LR Stress. *Animals*, 14(1): 58-58. <https://doi.org/10.3390/ani14010058>
113. Spiller, G.A. & Dewell, A. 2003. Safety of an astaxanthin-rich *Haematococcus pluvialis* algal extract: A randomized clinical trial. *Journal of Medicinal Food*, 6(1): 51-56. <https://doi.org/10.1089/109662003765184741>
114. Storebakken, T., Foss, P., Schiedt, K., Austreng, E., Liaaen-Jensen, S. & Manz, U. 1987. Carotenoids in diets for salmonids. IV. Pigmentation of Atlantic salmon with astaxanthin, astaxanthin dipalmitate and canthaxanthin. *Aquaculture*, 65(3-4): 279-292. [https://doi.org/10.1016/0044-8486\(87\)90241-9](https://doi.org/10.1016/0044-8486(87)90241-9)
115. Suescun, J., Chandra, S. & Schiess, M.C. 2019. The Role of Neuroinflammation in Neurodegenerative Disorders. *Translational Inflammation*, 241-267. <https://doi.org/10.1016/B978-0-12-813832-8.00013-3>
116. Suhel Alam, M.A. 2024. Complications of cardiovascular disease: the impact of diabetes, dyslipidemia, and metabolic disorders. *World Journal of Pharmaceutical Research*, 13(21): 321-356. <https://doi.org/10.20959/WJPR202421-34375>
117. Sun, J., Yan, J., Dong, H., Gao, K., Yu, K., He, C. & Mao, X. 2023. Astaxanthin with different configurations: sources, activity, post modification, and application in foods. *Current Opinion in Food Science*, 49: 100955-100955. <https://doi.org/10.1016/j.cofs.2022.100955>

118. Sun, S.Q., Zhao, Y.X., Li, S.Y., Qiang, J.W. & Ji, Y.Z. 2020. Anti-tumor effects of astaxanthin by inhibition of the expression of STAT3 in prostate cancer. *Marine Drugs*, 18(8): 415. <https://doi.org/10.3390/MD18080415>
119. Supamattaya, K., Kiriratnikom, S., Boonyaratpalin, M. & Borowitzka, L. 2005. Effect of a *Dunaliella* extract on growth performance, health condition, immune response and disease resistance in black tiger shrimp (*Penaeus monodon*). *Aquaculture*, 248(1-4): 207-216. <https://doi.org/10.1016/j.aquaculture.2005.04.014>
120. Taghiyar, S., Aarabi, M.H., Pourrajab, F., Rad, N.R. & Sharifi-Rigi, A. 2023. Supplement astaxanthin affects PPAR- $\gamma$ /miR-27a axis and metabolic profile. *Gene Reports*, 33: 101838-101838. <https://doi.org/10.1016/j.genrep.2023.101838>
121. Torrisen, O.J., Christiansen, R., Struksnes, G. & Estermann, R. 1995. Astaxanthin deposition in the flesh of Atlantic Salmon, *Salmo salar* L., in relation to dietary astaxanthin concentration and feeding period. *Aquaculture Nutrition*, 1(2): 77-84. <https://doi.org/10.1111/j.1365-2095.1995.tb00022.x>
122. Ukibe, K., Hashida, K., Yoshida, N. & Takagi, H. 2009. Metabolic engineering of *Saccharomyces cerevisiae* for astaxanthin production and oxidative stress tolerance. *Applied and Environmental Microbiology*, 75(22): 7205-7211. <https://doi.org/10.1128/AEM.01249-09>
123. Urakaze, M., Kobashi, C., Satou, Y., Shigeta, K., Toshima, M., Takagi, M., Takahashi, J. & Nishida, H. 2021. The beneficial effects of astaxanthin on glucose metabolism and modified low-density lipoprotein in healthy volunteers and subjects with prediabetes. *Nutrients*, 13(12): 4381.
124. Visioli, F. & Artaria, C. 2017. Astaxanthin in cardiovascular health and disease: Mechanisms of action, therapeutic merits, and knowledge gaps. *Food and Function*, 8(1): 39-63. <https://doi.org/10.1039/c6fo01721e>
125. Wade, N., Goulter, K.C., Wilson, K.J., Hall, M.R. & Degnan, B.M. 2005. Esterified astaxanthin levels in lobster epithelia correlate with shell colour intensity: Potential role in crustacean shell colour formation. *Comparative Biochemistry and Physiology - B Biochemistry and Molecular Biology*, 141(3): 307-313. <https://doi.org/10.1016/j.cbpc.2005.04.004>
126. Wang, X., Willen, R. & Wadstrom, T. 2000. Astaxanthin-rich algal meal and vitamin C inhibit *Helicobacter pylori* infection in BALB/cA mice. *Antimicrobial Agents and Chemotherapy*, 44(9): 2452-2457. <https://doi.org/10.1128/AAC.44.9.2452-2457.2000>
127. Wei, Q. & Guo, J.S. 2022. Developing natural marine products for treating liver diseases. *World Journal of Clinical Cases*, 10(8): 2369-2381. <https://doi.org/10.12998/wjcc.v10.i8.2369>
128. White, E.S. & Mantovani, A.R. 2013. Inflammation, wound repair, and fibrosis: Reassessing the spectrum of tissue injury and resolution. *Journal of Pathology*, 229(2): 141-144. <https://doi.org/10.1002/path.4126>
129. Winiarska-Mieczan, A., Kwiecień, M., Jachimowicz-Rogowska, K., Donaldson, J., Tomaszewska, E. & Baranowska-Wójcik, E. 2023. Anti-Inflammatory, Antioxidant, and Neuroprotective Effects of Polyphenols—Polyphenols as an Element of Diet Therapy in Depressive Disorders. *International Journal of Molecular Sciences*, 24(3): 2258-2258. <https://doi.org/10.3390/ijms24032258>
130. Xia, W., Tang, N., Kord-Varkaneh, H., Low, T.Y., Tan, S.C., Wu, X. & Zhu, Y. 2020. The effects of astaxanthin supplementation on obesity, blood pressure, CRP, glycemic biomarkers, and lipid profile: A meta-analysis of randomized controlled trials. *Pharmacological Research*, 161: 105113-105113. <https://doi.org/10.1016/j.phrs.2020.105113>
131. Xiang, M., Lu, Y., Xin, L., Gao, J., Shang, C., Jiang, Z., Lin, H., Fang, X., Qu, Y., Wang, Y., Shen, Z., Zhao, M. & Cui, X. 2021. Role of Oxidative Stress in Reperfusion following Myocardial Ischemia and Its Treatments. *Oxidative Medicine Cellular Longevity*, 2021: 6614009. <https://doi.org/10.1155/2021/6614009>
132. Yang, H., Jin, X., Lam, C.W.K. & Yan, S.K. 2011. Oxidative stress and diabetes mellitus. *Clinical Chemistry and Laboratory Medicine*, 49(11): 1773-1782. <https://doi.org/10.1515/CCLM.2011.250>
133. Yang, J., Yin, H.S., Cao, Y.J., Jiang, Z.A., Li, Y.J., Song, M.C., Wang, Y.F., Wang, Z.H., Yang, R., Jiang, Y.F., Sun, J.P., Liu, B.Y. & Wang, C. 2018. Arctigenin Attenuates Ischemia/Reperfusion Induced Ventricular Arrhythmias by Decreasing Oxidative Stress in Rats. *Cellular Physiology and Biochemistry*, 49(2): 728-742. <https://doi.org/10.1159/000493038>
134. Yaqoob, Z., Arshad, M.S., Imran, M., Munir, H., Qaisrani, T.B., Khalid, W., Asghar, Z. & Suleria, H.A.R. 2022. Mechanistic role of astaxanthin derived from shrimp against certain metabolic disorders. *Food Science and Nutrition*, 10(1): 12-20. <https://doi.org/10.1002/fsn3.2623>
135. Yasui, Y., Hosokawa, M., Mikami, N., Miyashita, K. & Tanaka, T. 2011. Dietary astaxanthin inhibits colitis and colitis-associated colon carcinogenesis in mice via modulation of the inflammatory cytokines. *Chemico-Biological Interactions*, 193(1): 79-87. <https://doi.org/10.1016/j.cbi.2011.05.006>
136. Yeh, P.T., Huang, H.W., Yang, C.M., Yang, W.S. & Yang, C.H. 2016. Astaxanthin Inhibits Expression of Retinal Oxidative Stress and Inflammatory Mediators in Streptozotocin-Induced Diabetic Rats. *PLoS One*, 11(1): e0146438. <https://doi.org/10.1371/journal.pone.0146438>
137. Yokoyama, A. & Miki, W. 1995. Composition and presumed biosynthetic pathway of carotenoids in the astaxanthin-producing bacterium *Agrobacterium aurantiacum*. *FEMS Microbiology Letters*, 128(2): 139-144. <https://doi.org/10.1111/j.1574-6968.1995.tb07513.x>
138. Yook, J.S., Okamoto, M., Rakwal, R., Shibato, J., Lee, M.C., Matsui, T., Chang, H., Cho, J.Y. & Soya, H. 2016. Astaxanthin supplementation enhances adult hippocampal neurogenesis and spatial memory in mice. *Molecular Nutrition and Food Research*, 60(3): 589-599. <https://doi.org/10.1002/mnfr.201500634>
139. Ytrestøyl, T. & Bjerkeng, B. 2007. Dose response in uptake and deposition of intraperitoneally administered astaxanthin in Atlantic salmon (*Salmo salar* L.) and Atlantic cod (*Gadus morhua* L.). *Aquaculture*, 263(1-4): 179-191. <https://doi.org/10.1016/j.aquaculture.2006.10.021>



140. Zaafan, M.A. & Abdelhamid, A.M. 2021. The cardioprotective effect of astaxanthin against isoprenaline-induced myocardial injury in rats: Involvement of TLR4/NF- $\kappa$ B signaling pathway. *European Review for Medical and Pharmacological Sciences*, 25(11): 4099-4105. <https://doi.org/10.26355/eurev.202106.26052>
141. Zhang, C., Jin, Y., Yu, Y., Xiang, J. & Li, F. 2021. Effects of natural astaxanthin from microalgae and chemically synthetic astaxanthin supplementation on two different varieties of the ridgetail white prawn (*Exopalaemon carinicauda*). *Algal Research*, 57: 102347-102347. <https://doi.org/10.1016/j.algal.2021.102347>
142. Zhang, X., Hou, Y., Li, J. & Wang, J. 2021. The role of astaxanthin on chronic diseases. *Crystals*, 11(5): 505. <https://doi.org/10.3390/cryst11050505>
143. Zheng, Y., Xie, L., Yang, D., Luo, K. & Li, X. 2023. Small-molecule natural plants for reversing liver fibrosis based on modulation of hepatic stellate cells activation: An update. *Phytomedicine*, 113: 154721-154721. <https://doi.org/10.1016/j.phymed.2023.154721>
144. Zhuang, P., Greenberg, Z. & He, M. 2021. Biologically Enhanced Starch Bio-Ink for Promoting 3D Cell Growth. *Advanced Materials Technologies*, 6(12): 2100551. <https://doi.org/10.1002/admt.202100551>
145. Zhuge, F., Ni, Y., Wan, C., Liu, F. & Fu, Z. 2021. Anti-diabetic effects of astaxanthin on an stz-induced diabetic model in rats. *Endocrine Journal*, 68(4): 451-459. <https://doi.org/10.1507/endocrj.EJ20-0699>



## Melatonin - leptin interaction and obesity-related genes

Bülent Gündüz<sup>1\*</sup>, Emine İnci Balkan<sup>2</sup>

<sup>1</sup> Department of Biology, Faculty of Science, Canakkale Onsekiz Mart University, 17020 Çanakkale, TÜRKİYE

<sup>2</sup> Department of Medical Laboratory Techniques, Vocational School of Health Services, Demiroglu Bilim University, 34750 Istanbul, TÜRKİYE

### Cite this article as:

Gündüz B. & Balkan E.İ. 2025. Melatonin - leptin interaction and obesity-related genes. *Trakya Univ J Nat Sci*, 26(1): 93-102, DOI: 10.23902/trkjinat.1619680

Received: 14 January 2025, 13 March 2025, Online First: 21 March 2025, Published: 15 April 2025

**Edited by:**  
Belgin Süsleyici

**\*Corresponding Author:**  
Bülent Gündüz  
[bgunduzbio@comu.edu.tr](mailto:bgunduzbio@comu.edu.tr)

**ORCID iDs of the authors:**  
BG. 0000-0003-0497-8287  
EİB. 0000-0002-2708-2427

**Key words:**  
Agouti-Related Protein (AgRP)  
Endocrine  
Gene Expression  
Neuropeptide Y (NPY)  
Suprachiasmatic Nuclei (SCN)

**Abstract:** Most living organisms have circadian clocks which maintain rhythm in internal cycles of behavior, physiology, and metabolism, allowing them to anticipate the earth's 24-hour rotation. In mammals, circadian integration of metabolic systems optimizes energy gathering and usage across the light and dark cycles. Disruption of circadian rhythms may lead to metabolic dysfunctions such as obesity and obesity-related disorders. The molecular and hormonal mechanism behind obesity is mostly related to mRNA expressions in hypothalamus, and leptin, and melatonin hormone levels. In obesity and related disorders, the chronobiotic hormone melatonin regulates physiological functions such as energy metabolism, body fat, and reproduction by cross-interacting with leptin. Leptin signals satiety by inhibiting Neuropeptide Y/Agouti-Related Peptide (NPY/AgRP) genes in hypothalamus and exerts its effects on food intake, body weight, and the reproductive system. In this review, the molecular and hormonal mechanisms behind obesity were discussed.

**Özet:** Çoğu canlı organizmanın, davranış, fizyoloji ve metabolizmanın iç döngülerinde ritmi koruyan sirkadiyen saatleri vardır ve bu da organizmaların dünyanın 24 saatlik dönüşünü tahmin etmelerine olanak tanır. Memelilerde, metabolik sistemlerin sirkadiyen entegrasyonu, ışık ve karanlık döngüleri boyunca enerji toplanmasını ve kullanımını optimize eder. Sirkadiyen ritimlerin bozulması obezite ve obeziteye bağlı bozukluklar gibi metabolik işlev bozukluklarına yol açabilir. Obezitenin arkasındaki moleküler ve hormonal mekanizma çoğunlukla hipotalamustaki mRNA ifadeleri ve leptin ve melatonin hormonlarının seviyeleriyle ilişkilidir. Obezite ve ilgili bozukluklarda kronobiyotik bir hormon olan melatonin, leptin ile çapraz etkileşime girerek enerji metabolizması, vücut yağı ve üreme gibi fizyolojik işlevleri düzenler. Leptin hormonu hipotalamustaki Nöropeptid Y/Agouti İlgili Peptid (NPY/AgRP) genlerini inhibe ederek tokluk sinyali verir ve besin alımı, vücut ağırlığı ve üreme sistemi üzerinde etkilerini gösterir. Bu derlemede obezitenin arkasındaki moleküler ve hormonal mekanizmalar tartışılmıştır.

### Introduction

Obesity is increasingly recognized as a serious, worldwide public health concern. Even though it is preventable, due to comorbid diseases of obesity such as cardiovascular, reproductive, and endocrine system problems, obesity has become one of the tough disorders in the society (World Health Organization [WHO] 2021). It is an uncontrolled increase in body weight which can be defined as a disorder resulting from a disruption in energy metabolism (Jais & Brüning 2017). Excessive fat accumulation in white adipose tissue or some organs due to an imbalance in energy homeostasis may lead to the development of obesity. Energy homeostasis is managed in the hypothalamic region by a sophisticated network of orexigenic and anorexigenic signals (Kalra *et al.* 1999). There is ample evidence on that suprachiasmatic nucleus (SCN), arcuate nucleus (ARC), pineal gland and white

adipose tissues have important roles in organizing the energy balance of the body (Morgan *et al.* 2003). This complex network system could be easily corrupted by environmental factors (i.e. feeding time) if they last a prolonged time. In this context, this review aims to briefly discuss the role of melatonin and leptin in the development of obesity and changes in obesity-related gene expression.

### Leptin and Obesity, Obesity- Related Genes

As in humans, many animals regulate their body weight, reproduction, and energy gain/expenditure according to various environmental factors (Reiter 1974, Stetson *et al.* 1975). Sustaining vitality depends on the effective use of essential nutrients and energy storage. In this sense, the homeostasis between gained and



OPEN ACCESS

expended energy is critical for all organisms (Galgani *et al.* 2010). Excessive calorie intake and a lack of exercise have been used to explain the dramatic rise in obesity, but this only serves to highlight the need for a new look at the mechanisms underlying how obesity develops and shapes metabolism. Studies have found a connection between obesity and a 24-hour lifestyle and the sleep-wake cycle (Bray & Young 2012, Shochat 2012). At the heart of this link between sleep and obesity is the endogenous rhythm, also known as the circadian rhythm, which is regulated by both genetic and environmental factors. This rhythm controls the expression and/or activity of the hormones and enzymes involved in metabolism. But there is increasing evidence showing that eating habits, mealtimes, and specific nutrients also have an impact on metabolism by affecting circadian clocks (Jamshed *et al.* 2019, Charlot *et al.* 2021). Therefore, metabolic disorders can be caused by circadian rhythm disruptions.

Obesity is a central nervous system disease occurring due to several dysfunctions between hormonal and neurological mechanisms (O'Brien *et al.* 2017). There is clear evidence showing that the circadian clock, controlled by the SCN which is located in the hypothalamus, synchronizes physiological functions to optimize metabolic efficiency. Even though SCN serves as the body's pacemaker, peripheral clocks are also a part of the mammalian circadian system. These coordinated peripheral clocks in other organs send signals to the SCN, the body's main clock (Fig. 1). To induce optimal energy homeostasis, both central and peripheral clocks need to be synchronized. Otherwise, disruption in the circadian clock may result in alterations in gene expression and hormone levels.

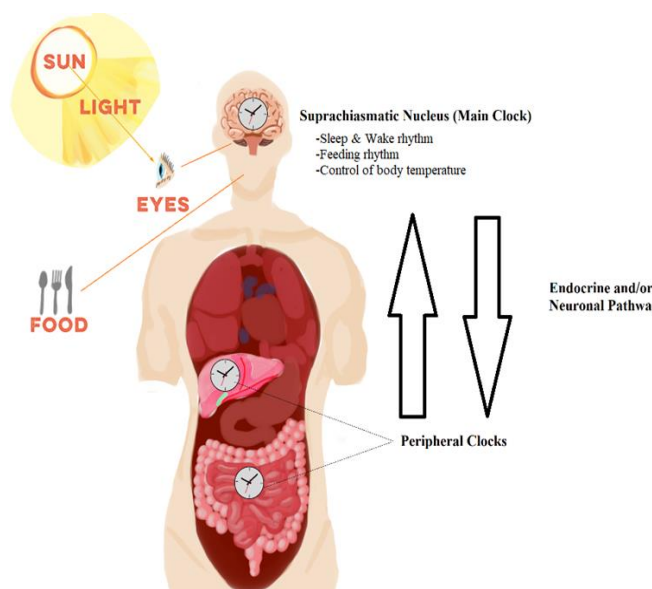


**Fig. 1.** Relationship between main clock and peripheral clocks. There is mutual communication between the SCN and the peripheral clocks. Light is the most important initiating signal of this system.

Through molecular studies, it has been established that all vertebrate cells and tissues display a circadian rhythm. The liver, intestines, and adipose tissue are just a few peripheral tissues of mammals that exhibit independent circadian oscillations (Mohawk *et al.* 2012). The analysis of the gene expression profile in mammals revealed that 3% to 20% of the genes displayed 24-hour expression, and the majority of these genes were involved in metabolic processes. Although organs in the periphery exhibit consistency in their circadian rhythms their functions can be affected if circadian rhythms within or between tissues are disturbed. Differentiation in temporal gene expression has been found to be important in organs involved in glucose and lipid metabolism, such as skeletal muscle, liver, heart, and adipose tissue. The liver and white and brown adipose (fat) tissues have also been found to contain a large number of nuclear receptors with rhythmic activity. Thus, it is possible to figure out the connection between nuclear receptors and clock genes, which regulate energy flow in response to altering physiological needs during the light/dark cycle in metabolism. In this way, the circadian rhythm of metabolic gene expression ensures the best possible exchange between the anabolic and catabolic processes brought on by feeding and fasting periods. For instance, nutrition can maximize the levels of enzymes in adipose tissue. However, it was discovered that the mouse liver experiences a peak in the processes of glycolysis, gluconeogenesis, and fatty acid metabolism overnight. Changes in the circadian rhythms of peripheral *Clock* genes have been linked to an increase in body weight, abnormalities in glucose homeostasis, and blood pressure regulation, all of which contribute to the development of metabolic syndrome. These adjustments may be the result of behavioral or environmental changes, such as a high-fat diet interfering with circadian rhythms.

#### Circadian Rhythm and Metabolism

Many hormones, including insulin, glucagon, adiponectin, corticosterone, leptin, and ghrelin, have been shown to exhibit circadian release. These hormones play important roles in metabolism. It is well known that leptin plays a significant role in the hypothalamus and, when released from adipocytes under physiological conditions, suppresses appetite and accelerates metabolism. The circadian rhythm of leptin was abolished in hamsters as a result of SCN lesion, implying that the circadian clock regulates leptin production (Karakaş & Gündüz 2006). Additionally, unlike healthy animals, rats with SCN-lesions did not increase the level of free fatty acids in plasma after intraperitoneal administration of leptin, indicating that SCN may also play a role in leptin (Li *et al.* 2012). The circadian clock has been implicated in the regulation of metabolism and energy balance in peripheral tissues, in addition to its effects on the endocrine system. The circadian clock conveys this function by mediating the production and/or activity of some metabolic enzymes (glycogen phosphorylase, cytochrome oxidase, lactate dehydrogenase, acetyl-CoA carboxylase, malic enzyme, fatty acid synthase, glucose-6-phosphate dehydrogenase) and transport systems involved in the metabolism of

cholesterol, amino acids, drugs, toxins, glycogen, and glucose and in the citric acid cycle (Marcheva *et al.* 2013).

#### The Effect of Nutrition on Circadian Rhythm

Feeding, one of the strong major environmental signals, is known to impact circadian oscillators. Karakaş *et al.* (2006) demonstrated that locomotor activity of Mongolian gerbils was advanced by the food restriction phase. The neuronal link between the pineal gland and the SCN may be the cause of the mechanism underlying this effect. Food restriction phase advances with the release of rhythmic melatonin hormone by the pineal gland (McArthur *et al.* 1991, Selmaoui *et al.* 2001, Challet *et al.* 2003). Another study revealed that rats fed a high-fat diet had alterations in circadian rhythm. The amplitude of daily pineal melatonin rhythm was shown to decrease in obese rats (Cano *et al.* 2008). In obese Sprague-Dawley rats administration of melatonin reduced body weight and leptin level. However, body weight and food efficiency increased in obese pinealectomized animals. When these animals were treated with melatonin, body weight, and food efficiency were not different from the sham-operated control group (Prunet-Marcassus *et al.* 2003). Likewise, in one of the experiments reported in Gündüz & Karakaş

(2001), daily 4-hour melatonin infusions between 17:00-21:00 inhibited body weight growth in pinealectomized juvenile Siberian hamsters. A recent study also underlined that misalignment of feeding rhythm induces disruption in the circadian clock and obesity. Restricted feeding to active phases of the daily rhythm (night time for rodents) resulted in increased energy expenditure in mice fed high fat diets (Hepler *et al.* 2022). These studies demonstrate the role of melatonin in body weight gain. Given that overeating or dietary content affects circadian rhythmicity and that feeding is a significant environmental signal, it appears that obesity is one of the diseases connected to circadian rhythms.

The relationship between appetite regulation and food intake is crucial to understanding the causes of obesity. Leptin is one of the major elements in this mechanism and is synthesized mainly from adipose tissue into circulation which binds its receptors in hypothalamus (Schwartz *et al.* 1996). This hormone, which is derived from adipocytes, regulates energy metabolism as well as many other processes, including feeding and reproduction (Mercer *et al.* 1996, Meli *et al.* 2004).

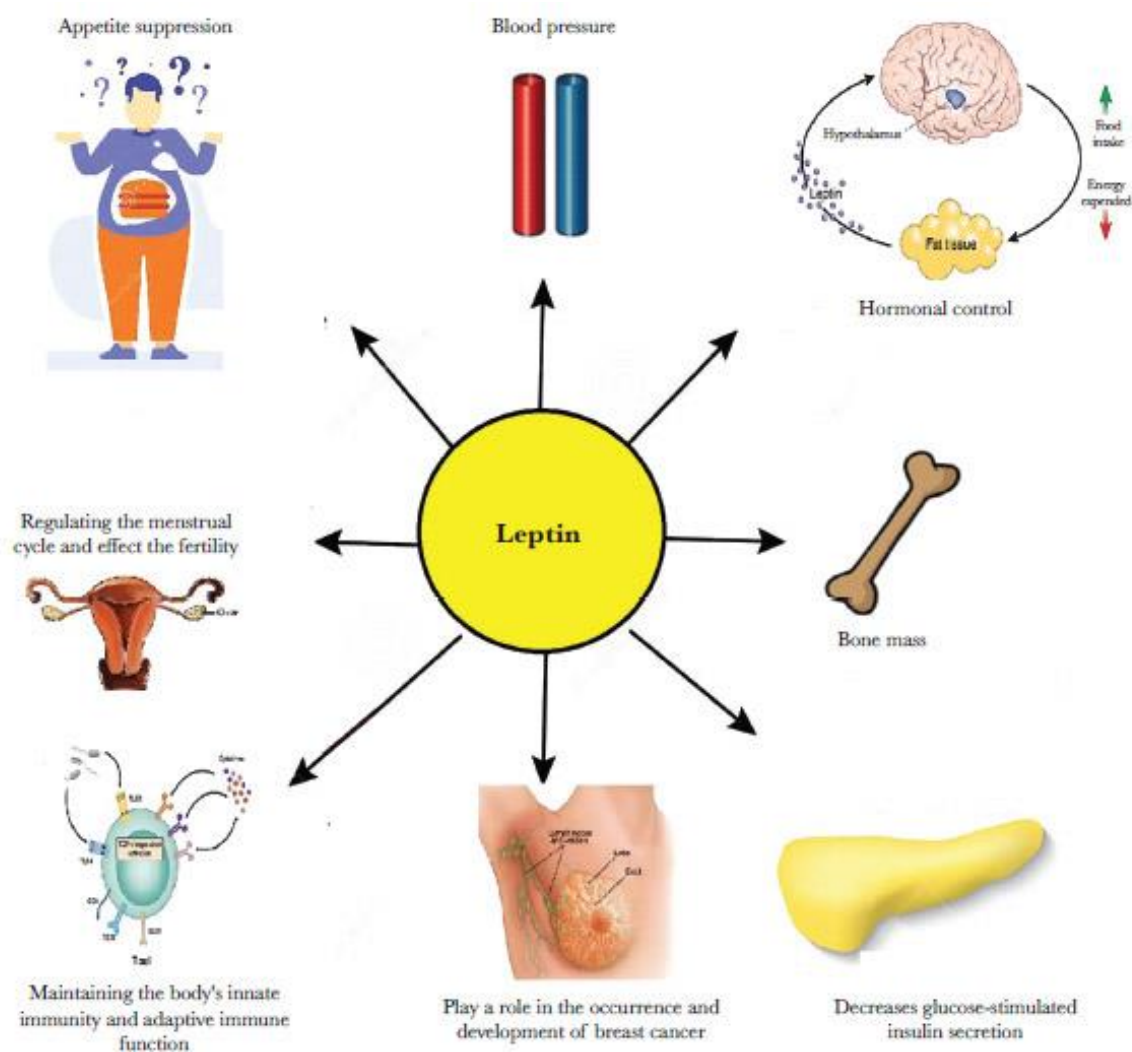


**Fig. 2.** Effects of leptin on different tissues (Al-Hussaniy *et al.* 2021).



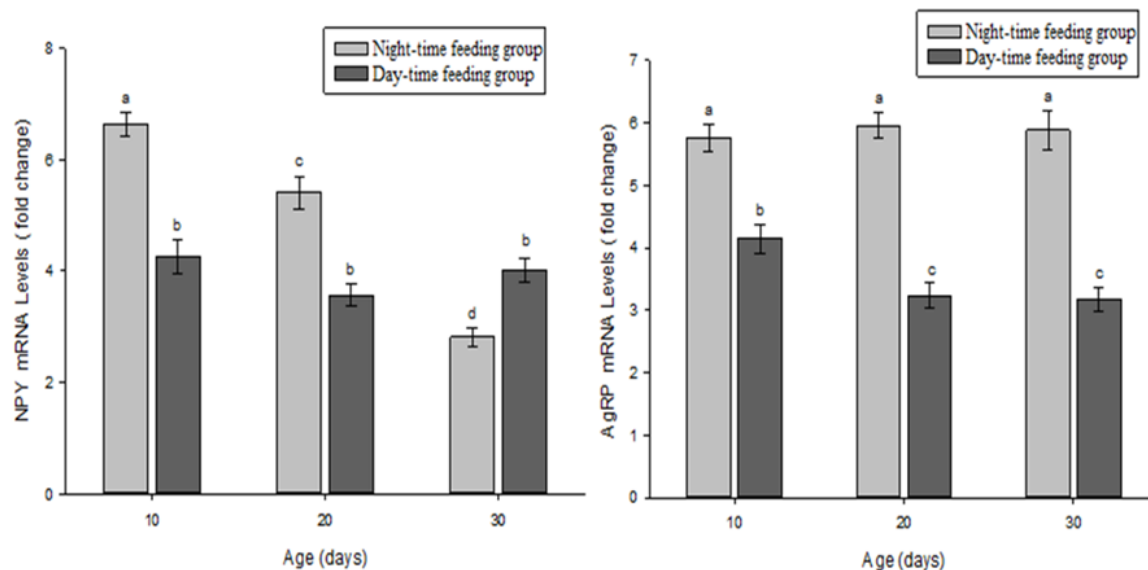


**Fig. 3.** NPY and AgRP mRNA expressions of offspring of Syrian hamsters, *Mesocricetus auratus* (Waterhouse 1838) relative to the *ad libitum* group. Different letters indicate statistical significance.

Leptin inhibits Neuropeptide Y (NPY) and Agouti-Related Peptides (AgRP) via its receptors in the ARC, which are responsible for regulating food intake and energy balance (Schwartz *et al.* 2000). Because NPY and AgRP co-express in hypothalamus, a recent study found that NPY-originated AgRP neurons control feeding initiation via Npy1r signaling, but Npy2r signaling controls locomotion and energy expenditure (Qi *et al.* 2022). Another study showed that the AgRP neurons in mice are inhibited at the start of the dark phase, which prevents them from eating, but that they are stimulated at the start of the light phase, when the mice are full (Krashes *et al.* 2011). The complementary characteristics of NPY and AgRP include the fact that NPY temporarily prolongs hunger after gaining access to food while AgRP controls feeding over a longer period of time. Additionally, feeding was eliminated when NPY was deleted, but not AgRP or GABA, leading researchers to hypothesize that NPY plays a special role in sustaining hunger in the interval between food finding and consumption (Chen *et al.* 2019).

Epidemiological studies on humans and animals have shown that nutrition is essential for the metabolic control of energy balance from very early development (McMillen *et al.* 2008, Varela *et al.* 2021). A food limitation during pregnancy and lactation may alter the offspring's metabolic processes permanently and alter the likelihood of obesity in adulthood (McMillen *et al.* 2005, Martin-Gronert & Ozanne 2006). In our recent study (İnan & Gündüz 2024), we showed how an important maternal factor such as nutrition affects the gene expression of hypothalamic neuropeptides NPY/AgRP in the brains of offspring and how this changes from the early stages of development (up to day 30) (Fig. 3). The findings indicate that dietary modifications during the very early stages of development have a considerable impact on the expression of NPY/AgRP mRNA in offspring. The variation in expression of neuropeptide

genes during and after lactation is notable. Our research shows that feeding the young at different times of the day has the biggest impact during the lactation period, since this was the moment when both NPY/AgRP protein levels and mRNA expression increased. It is well recognized that a mother's poor eating schedule or undernutrition increases the offspring's risk of metabolic problems. Our discoveries could change the course of metabolic disease, provide a new understanding of energy metabolism, and pinpoint new areas for early disease prevention and therapy through nutritional strategies in the early years of life. The neural development of the offspring is influenced by maternal variables during pregnancy, which may also control the programming of dietary neuropeptide gene expression throughout life.

In 1953, Kennedy developed the idea that circulatory impulses produced in proportion to body fat storage regulate appetite and energy expenditure in a coordinated manner to balance body weight (Kennedy 1953). The existence of such circulatory impulses was demonstrated by Coleman in his landmark research on parabiosis in 1973. The obesity gene (*ob*) mutation prevents the formation of a circulating anorexic factor, as demonstrated by Coleman's tests that compared the circulatory systems of two strains of highly obese mice (*ob/ob* and *db/db*) with wild-type animals and with one another. However, he discovered that the diabetes gene (*db*) mutation reduces the responsiveness to this factor. As a result, it was discovered that the *db/db* mutant mouse produced excessive satiety factor but could not respond to it due to a malfunctioning receptor, while the *ob/ob* mutant recognized and responded to same satiety factor but failed to produce it. The *Ob* gene was cloned in late 1994 and revealed to encode a 16 kDa protein known as leptin or the *OB* protein, which is produced by adipose tissue and released into the bloodstream (Zhang *et al.* 1994). When leptin deficit is corrected in *ob/ob* mice, food

intake is significantly decreased, and the obesity condition returns to normal. Therefore, obesity in mice is caused by both leptin resistance (in db/db mice) and leptin insufficiency (in ob/ob animals). Consequently, leptin functions as a crucial negative feedback signal for the regular regulation of food consumption and body weight (Frühbeck *et al.* 1998, Coleman 2010).

The behavior and physiology of experimental animals have been found to be significantly affected by restricting food intake at specific times of the day (limiting the amount and duration of meals without reducing energy intake). It was discovered that two to four hours prior to a meal, experimental animals displayed food expectancy behaviors such as increased locomotor activity, body temperature, corticosterone release, gastrointestinal motility, and activity of digestive enzymes (Nelson & Halberg 1986). All of these data are said to be indicators of the biological clock. Many physiological processes controlled by the SCN are observed to change with the restriction of daytime feeding, and it has been observed that restricted nutrition has an impact on SCN (Tacad *et al.* 2022). In animals with SCN lesions and mutant mice, it has been reported that limited feeding affects circadian

rhythm independently of light (Froy 2007). In addition, studies have shown that limited nutrition affects circadian oscillators in peripheral tissues such as liver, kidney, heart, and pancreas without affecting the rhythm-regulating mechanism in SCN (Oosterman *et al.* 2015). For this reason, it was thought that the regulation of *Clock* oscillators in peripheral tissues with nutrition may play a direct role in the coordination of metabolic oscillations.

Energy restriction or reducing the amount of energy in the diet without resulting in malnutrition has been found to increase rodents' life spans by up to 50% (Barger *et al.* 2003). In addition to increasing life expectancy, energy restriction also delayed the onset of age-related pathophysiological changes such as cancer, diabetes, kidney diseases, and cataracts (Weindruch & Sohal 1997). The mechanism of these effects of reducing energy consumption on aging and lifespan is still not fully understood. The synchronization of peripheral oscillators, however, is believed to be directly mediated by the time of eating or by synchronization of the SCN, which sends humoral or neural signals to peripheral tissues, during the restriction of nutrition and energy intake.

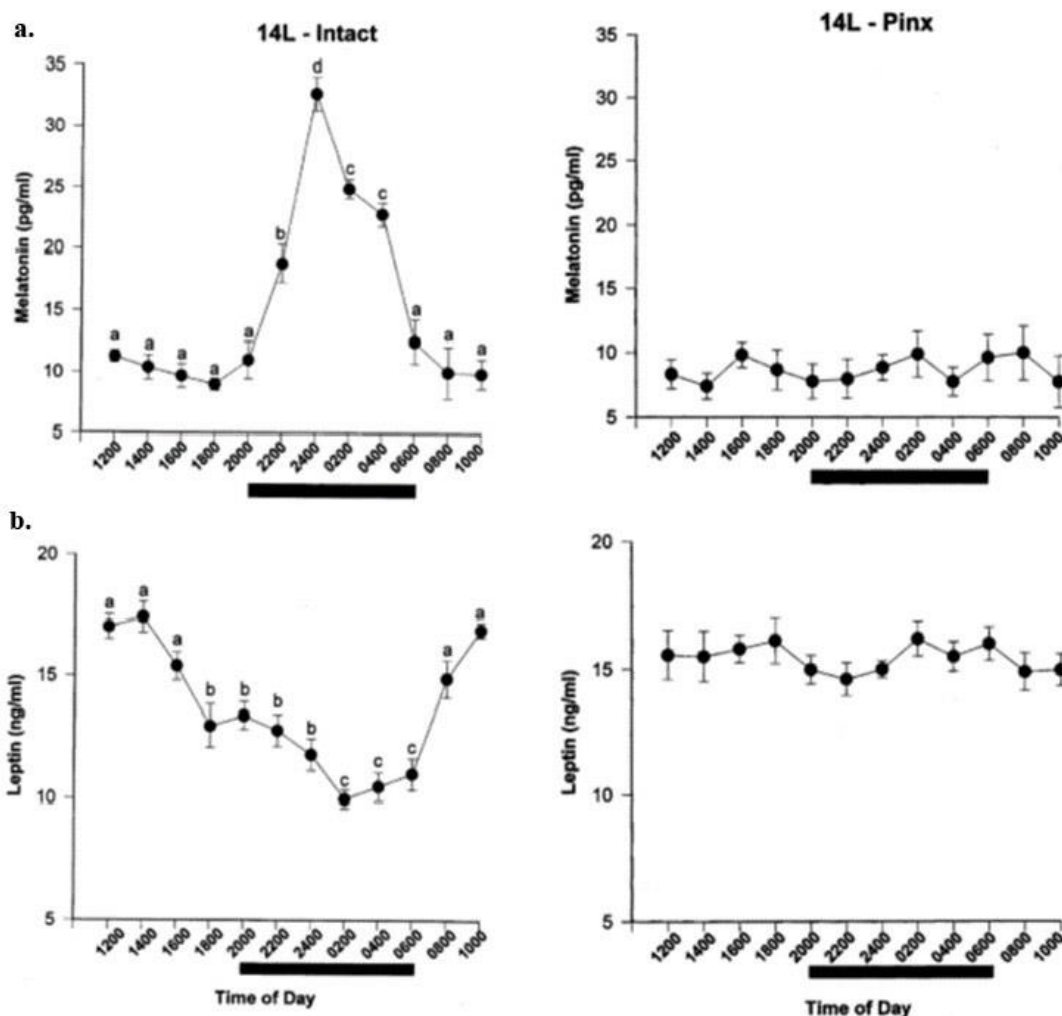


**Fig. 4.** Twenty-four-hour serum melatonin and leptin levels in intact and pinealectomized hamsters in 14L photoperiod. **a.** Melatonin, **b.** leptin (Gündüz 2002).

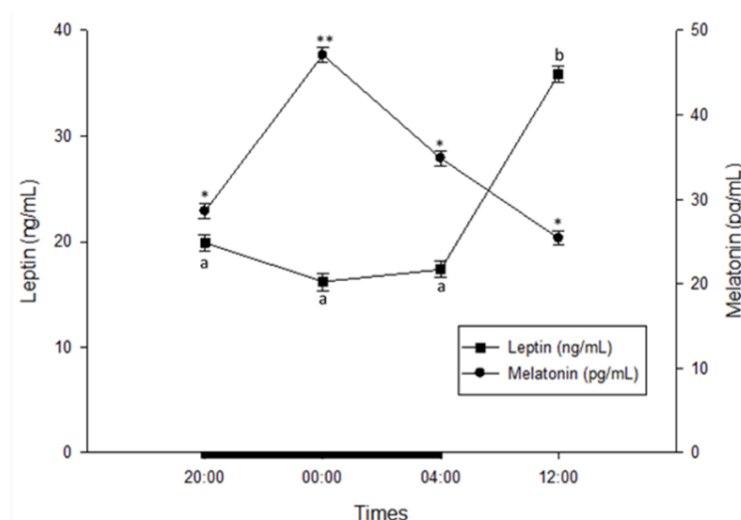


**Fig. 5.** Leptin and melatonin values in male Syrian hamsters (Balkan & Gündüz 2023).

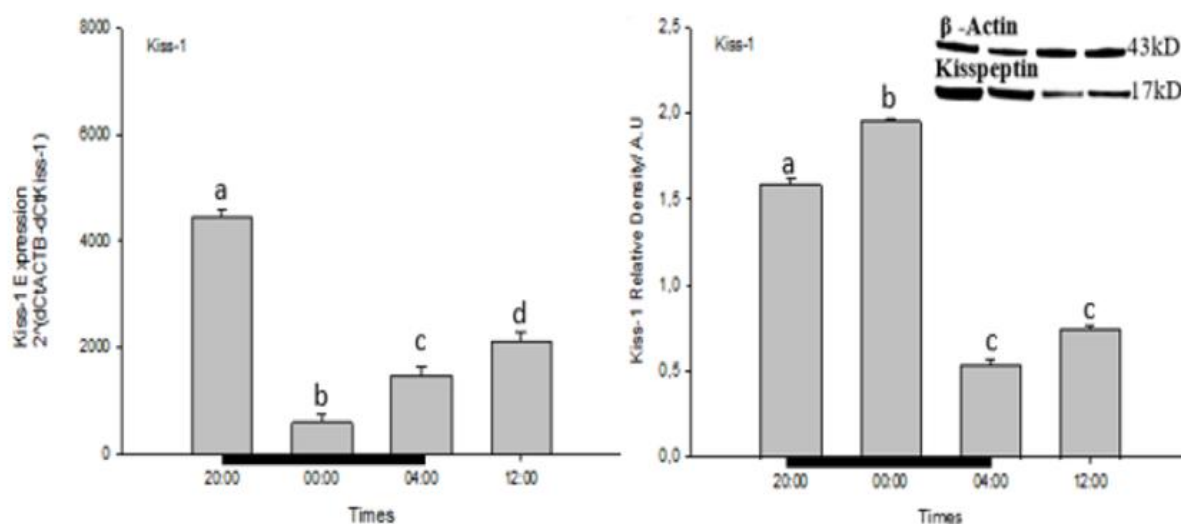


**Fig. 6.** Quantification of mRNA expression and relative protein density changes at different times of day (20:00, 00:00, 04:00, and 12:00). Different letters indicate significant levels (Balkan & Gündüz 2023).

The circadian rhythm of genes involved in controlling energy homeostasis and feeding regulation are intrinsically linked. In our most recent study, nighttime and daytime feeding restrictions reduced the body weight of Syrian hamster pups while increasing NPY/AgRP mRNA expression (Fig. 3) (İnan & Gündüz 2024). To reduce energy requirement in fasting conditions NPY reduces body weight and bone formation (Lim *et al.* 2006, Coupé *et al.* 2009). Although leptin regulate the expression of the NPY/AgRP gene, melatonin also plays a crucial part in the control of food intake. As shown by Gündüz & Hasanoğlu (2016), melatonin increased the expression of NPY/AgRP genes in the hypothalamic region of the brain, but leptin decreased the levels of these neurotransmitters. Moreover, pinealectomy increased leptin hormone levels and decreased AgRP gene expression. Melatonin is therefore a highly effective regulator of feeding-related gene expression (Gündüz & Hasanoğlu 2016).

#### Leptin and Melatonin Interaction (Obesity & Reproduction)

The interaction between leptin and melatonin has been linked to disorders of the reproductive system and other conditions. The reproductive system is very sensitive to nutrients and metabolism. Leptin has a major role in the regulation of food intake and body weight and metabolic gate to the reproductive system (Wade *et al.* 1996). For example, ob/ob mice are genetically infertile. Leptin treatment restores infertility in genetically interfile ob/ob mice (Chehab *et al.* 1996). Low level of circulation leptin due to food restriction is linked to reduced secretion of gonadotropins (Cunningham *et al.* 1999, Karakaş *et al.* 2005).

Melatonin regulates fat metabolism in some mammalian species (Rasmussen *et al.* 1999, Wolden-Hansen *et al.* 2000, Baltacı & Mogulkoc 2007) and Syrian hamsters show an inverse relationship between melatonin

levels and leptin concentration (Figs 4-5) (Gündüz 2002, Balkan & Gündüz 2023).

Melatonin may be the primary regulator of leptin metabolism in raccoon dogs and Syrian hamsters, as evidenced by the fact that leptin levels are reduced and circadian changes of leptin are abolished in animals treated with melatonin (Gündüz 2002, Nieminen *et al.* 2002). The melatonin hormone may have a direct impact on the ob gene's mRNA expression. Zalatan *et al.* (2001) revealed the blocking effect of melatonin on fatty acid transport through melatonin-receptor-mediated mechanism. The hypothalamus of seasonally breeding mammals such as hamsters is programmed differently for long (summer) and short (winter) days. While the hypothalamus is sensitive to the leptin hormone on short days, it becomes resistant to it on long days (Zieba *et al.* 2007). Leptin is modulated by photoperiodical signals in seasonal breeding mammals, according to that study. The role of the pineal gland hormone melatonin in controlling leptin in sheep is demonstrated by the seasonal switch to leptin response (Zieba *et al.* 2007). Melatonin regulates the energy balance by involving three steps, namely food intake, energy storage, and energy expenditure, by sending photoperiodic signals to the central nervous system.

Kisspeptin is a neuropeptide that is primarily produced in the brain of photoperiodic animals that exhibit seasonal reproduction and is thought to have significant effects on the hypothalamic-pituitary-gonadal (HPG) axis. In addition to how kisspeptin affects fertility, current research has focused on how kisspeptin regulates energy balance and body weight (Harter *et al.* 2018). One of our most recent studies found that kisspeptin mRNA expression is low during the dark phase when leptin hormone is low, but peptide release is high (Fig. 6). Although this characteristic exists in Syrian hamster species, some rat and mouse species show a more pronounced linear relationship between kisspeptin and leptin. The discovery that leptin induces kisspeptin gene expression supports the idea that kisspeptin neurons may modify energy balance (Smith *et al.* 2006, Hill *et al.* 2008). Leptin increases the expression of the kisspeptin gene. Kisspeptin neurons do not have melatonin receptors, so it is unclear where melatonin regulates kisspeptin expression (Li *et al.* 2011).

## Conclusion

The circadian clock, an internal timekeeping system, has emerged as a crucial regulator of metabolism and energy balance in peripheral tissues. Beyond its well-known influence on the endocrine system, the circadian clock coordinates metabolic processes in organs such as the liver, adipose tissue, and skeletal muscle. This intricate system ensures that metabolic functions are optimally synchronized with daily fluctuations in environmental cues, such as light-dark cycles and feeding-fasting rhythms. Disruptions to the circadian clock, such as those experienced during shift work or

chronic jet lag, have been associated with metabolic disorders, including obesity, insulin resistance, and dyslipidemia. Although there have been great changes in our lifestyle with industrialization, there has been no change in our genetic structure for about ten thousand years. Today, the incompatibility between genetic structure/lifestyle has paved the way for the development of many chronic diseases. Modern lifestyle has contributed to high energy consumption, unbalanced diet and sedentary lifestyle, causing obesity to become epidemic. However, studies have shown that working at night, exposure to artificial light, and reduction in sleep time, which are one of the most important changes brought about by industrialization, also contribute to the pathogenesis of obesity. Circadian (biological) clock genes and gene products that make up our biological rhythm and are affected by the sleep/wake cycle and have a critical role in important physiological pathways for metabolism. Therefore, determining the relationship between circadian system dysfunctions and changing nutritional balance and obesity development should be considered in the treatment and prevention of obesity.

The interaction between melatonin and leptin extends beyond their direct influence on each other, as they also modulate the expression of key genes involved in energy balance regulation, such as NPY and AgRP. Melatonin has been shown to suppress the expression of NPY and AgRP in hypothalamus, two neuropeptides known for their orexigenic properties, meaning that they stimulate appetite and increase food intake. This inhibition of NPY and AgRP by melatonin suggests a role in appetite regulation and satiety. On the other hand, leptin, a hormone produced by adipose tissue, acts on hypothalamus to decrease appetite and increase energy expenditure. Leptin signaling inhibits the expression of NPY and AgRP, resulting in reduced food intake and increased energy expenditure. The complex interplay between melatonin, leptin, NPY, and AgRP genes highlights the intricate regulatory mechanisms involved in maintaining energy balance and suggests potential therapeutic targets for metabolic disorders. Further research into these interactions may provide insights into the development of interventions for conditions such as obesity and overeating disorders.

**Ethics Committee Approval:** Since the article does not contain any studies with human or animal subject, its approval to the ethics committee was not required.

**Data Sharing Statement:** All data are available within the study.

**Author Contributions:** Concept: B.G., Design: B.G., E.İ.B., Data analysis: B.G., E.İ.B., Writing: B.G., E.İ.B.

**Conflict of Interest:** The authors have no conflicts of interest to declare.

**Funding:** The authors declared that this study has received no financial support.

## References

- Al-Hussaniy, H.A., Alburghaif, A.H. & Naji, M.A. 2021. Leptin hormone and its effectiveness in reproduction, metabolism, immunity, diabetes, hopes and ambitions. *Journal of Medicine and Life*, 14(5): 600-605. <https://doi.org/10.25122/jml-2021-0153>
- Balkan, E.İ. & Gündüz, B. 2023. Adult Male Syrian Hamsters (*Mesocricetus auratus*) Exhibit Daily Oscillations in Their Serum Levels of Melatonin and Leptin As Well As in the Expression of the GnRH, GnIH, and Kisspeptin Genes. *Türk Tarım ve Doğa Bilimleri Dergisi*, 10(1): 68-75. <https://doi.org/10.30910/turkjans.1196793>
- Baltacı, A.K. & Mogulkoc, R. 2007. Pinealectomy and melatonin administration in rats: their effects on plasma leptin levels and relationship with zinc. *Acta Biologica Hungarica*, 58: 335-343. <https://doi.org/10.1556/ABiol.58.2007.4.1>
- Barger, J.L., Walford, R.L. & Weindruch, R. 2003. The retardation of aging by caloric restriction: its significance in the transgenic era. *Experimental Gerontology*, 38(11-12): 1343-1351. <https://doi.org/10.1016/j.exger.2003.10.017>
- Bray, M.S. & Young, M.E. 2012. Chronobiological effects on obesity. *Current Obesity Reports*, 1: 9-15. <https://doi.org/10.1007/s13679-011-0005-4>
- Cano, P., Jiménez-Ortega, V., Larrad, A., Toso, C.F.R., Cardinali, D.P. & Esquifino, A.I. 2008. Effect of a high-fat diet on 24-h pattern of circulating levels of prolactin, luteinizing hormone, testosterone, corticosterone, thyroid-stimulating hormone and glucose, and pineal melatonin content, in rats. *Endocrine*, 33: 118-125. <https://doi.org/10.1007/s12020-008-9066-x>
- Challet, E., Caldelas, I., Graff, C. & Pévet, P. 2003. Synchronization of the molecular clockwork by light-and food-related cues in mammals. *Biological Chemistry*, 384(5):711-9. <http://doi.org/10.1515/BC.2003.079>
- Charlot, A., Hutt, F., Sabatier, E. & Zoll, J. 2021. Beneficial effects of early time-restricted feeding on metabolic diseases: importance of aligning food habits with the circadian clock. *Nutrients*, 13(5): 1405. <https://doi.org/10.3390/nu13051405>
- Chehab, F.F., Lim, M.E. & Lu, R. 1996. Correction of the sterility defect in homozygous obese female mice by treatment with the human recombinant leptin. *Nature Genetics*, 12(3): 318-320. <https://doi.org/10.1038/ng0396-318>
- Chen, Y., Essner, R.A., Kosar, S., Miller, O.H., Lin, Y.C., Mesgarzadeh, S. & Knight, Z. A. 2019. Sustained NPY signaling enables AgRP neurons to drive feeding. *Elife*, 8, e46348. <https://doi.org/10.7554/eLife.46348>
- Coleman, D.L. 1973. Effects of parabiosis of obese with diabetes and normal mice. *Diabetologia*, 9(4): 294-298.
- Coleman, D.L. 2010. A historical perspective on leptin. *Nature Medicine*, 16(10): 1097-1099. <https://doi.org/10.1038/nm1010-1097>
- Coupé, B., Grit, I., Darmaun, D. & Parnet, P. 2009. The timing of "catch-up growth" affects metabolism and appetite regulation in male rats born with intrauterine growth restriction. *American Journal of Physiology-Regulatory, Integrative and Comparative Physiology*, 297(3): R813-R824. <https://doi.org/10.1152/ajpregu.00201.2009>
- Cunningham, M.,J., Clifton, D.K. & Steiner, R.A. 1999. Leptin's role on the reproductive axis: perspectives and mechanisms. *Biology of Reproduction* 60(2): 216-222. <https://doi.org/10.1095/biolreprod60.2.216>
- O'Brien, P., Hinder, L.M., Callaghan, B.C. & Feldman, E.L. 2017. Neurological consequences of obesity. *The Lancet Neurology*, 16(6): 465-477. [https://doi.org/10.1016/S1474-4422\(17\)30084-4](https://doi.org/10.1016/S1474-4422(17)30084-4)
- Froy, O. 2007. The relationship between nutrition and circadian rhythms in mammals. *Frontiers in Neuroendocrinology*, 28(2-3): 61-71. <https://doi.org/10.1016/j.yfme.2007.03.001>
- Frühbeck, G., Jebb, S.A. & Prentice, A.M. 1998. Leptin: physiology and pathophysiology. *Clinical Physiology*, 18(5): 399-419. <https://doi.org/10.1046/j.1365-2281.1998.00129.x>
- Galgani, J.E., Ryan, D.H. & Ravussin, E. 2010. Effect of capsinoids on energy metabolism in human subjects. *British Journal of Nutrition*, 103(1): 38-42. <https://doi.org/10.1017/S0007114509991358>
- Gündüz, B. & Hasanoglu, N. 2016. Molecular evaluation of obesity-related hypothalamic NPY and AgRP gene expressions in melatonin injected and pinealectomized Syrian hamsters (*Mesocricetus auratus*) housed in short and long photoperio. pp. 98. Paper presented at the 41<sup>st</sup> Federation of European Physiological Congress, June 29-July 1, Paris, France.
- Gündüz, B. 2002. Daily rhythm in serum melatonin and leptin levels in the Syrian hamster (*Mesocricetus auratus*). *Comparative Biochemistry and Physiology Part A: Molecular & Integrative Physiology*, 132(2): 393-401. [https://doi.org/10.1016/S1095-6433\(02\)00041-7](https://doi.org/10.1016/S1095-6433(02)00041-7)
- Gündüz, B. & Karakaş, A. 2001. Effects of photoperiod and melatonin infusions on body weight in pinealectomized juvenile siberian hamsters (*Phodopus Sungorus*). *Turkish Journal of Biology*, 25(3): 301-321.
- Harter, C.J., Kavanagh, G.S. & Smith, J.T. 2018. The role of kisspeptin neurons in reproduction and metabolism. *Journal of Endocrinology*, 238(3): R173-R183. <https://doi.org/10.1530/JOE-18-0108>
- Hepler, C., Weidemann, B.J., Waldeck, N.J., Marcheva, B., Cedernaes, J., Thorne, A.K., Kobayashi, Y., Newman, M.V., Gao, P., Shao, M., Ramsey, K.M., Gupta, R.K. & Bass, J. 2022. Time-restricted feeding mitigates obesity through adipocyte thermogenesis. *Science*, 378(6617): 276-284. <https://doi.org/10.1126/science.abl8007>
- Hill, J.W., Elmquist, J.K. & Elias, C.F. 2008. Hypothalamic pathways linking energy balance and reproduction. *American Journal of Physiology-Endocrinology and Metabolism*, 294(5): E827-E832. <https://doi.org/10.1152/ajpendo.00670.2007>
- İnan, P. & Gündüz, B. 2024. Variation of NPY and AGRP mRNA expression in Syrian hamsters according to feeding



- times. *Sigma Journal of Engineering and Natural Sciences*, 42(5): 1336-1343. <https://doi.org/10.14744/sigma.2023.00072>
26. Jais, A. & Brüning, J.C. 2017. Hypothalamic inflammation in obesity and metabolic disease. *The Journal of Clinical Investigation*, 127(1): 24-32. <https://doi.org/10.1172/JCI88878>
27. Jamshed, H., Beyl, R.A., Della Manna, D.L., Yang, E.S., Ravussin, E. & Peterson, C.M. 2019. Early time-restricted feeding improves 24-hour glucose levels and affects markers of the circadian clock, aging, and autophagy in humans. *Nutrients*, 11(6): 1234. <https://doi.org/10.3390/nu11061234>
28. Kalra, S.P., Dube, M.G., Pu, S., Xu, B., Horvath, T.L. & Kalra, P.S. 1999. Interacting appetite-regulating pathways in the hypothalamic regulation of body weight. *Endocrine Reviews*, 20(1): 68-100. <https://doi.org/10.1210/edrv.20.1.0357>
29. Karakaş, A. & Gündüz, B. 2006. Suprachiasmatic nuclei may regulate the rhythm of leptin hormone release in Syrian hamsters (*Mesocricetus auratus*). *Chronobiology International*, 23(1-2): 225-236. <https://doi.org/10.1080/07420520500545821>
30. Karakaş, A., Çamsarı, Ç., Erdiñç, S. & Gündüz, B. 2005. Effects of photoperiod and food availability on growth, leptin, sexual maturation and maintenance in the Mongolian gerbils (*Meriones unguiculatus*). *Zoological Science*, 22(6): 665-670. <https://doi.org/10.2108/zsj.22.665>
31. Karakaş, A., Serin, E. & Gündüz, B. 2006. Food restriction affects locomotor activity in Mongolian gerbils (*Meriones unguiculatus*). *Turkish Journal of Biology*, 30(1): 23-28.
32. Kennedy, G.C. 1953. The role of depot fat in the hypothalamic control of food intake in the rat. *Proceedings of the Royal Society of London. Series B-Biological Sciences*, 140(901): 578-592. <https://doi.org/10.1098/rspb.1953.0009>
33. Krashes, M.J., Koda, S., Ye, C., Rogan, S.C., Adams, A.C., Cusher, D.S., Maratos-Flier, E., Roth, B. L. & Lowell, B. B. 2011. Rapid, reversible activation of AgRP neurons drives feeding behavior in mice. *The Journal of Clinical Investigation*, 121(4): 1424-1428. <https://doi.org/10.1172/JCI146229>
34. Li, A.J., Wiater, M.F., Oostrom, M.T., Smith, B.R., Wang, Q., Dinh, T.T., Roberts, B.L., Jansen, H.T. & Ritter, S. 2012. Leptin-sensitive neurons in the arcuate nuclei contribute to endogenous feeding rhythms. *American Journal of Physiology-Regulatory, Integrative and Comparative Physiology*, 302(11): R1313-R1326. <https://doi.org/10.1152/ajpregu.00086.2012>
35. Li, Q., Rao, A., Pereira, A., Clarke, I.J. & Smith, J.T. 2011. Kisspeptin cells in the ovine arcuate nucleus express prolactin receptor but not melatonin receptor. *Journal of Neuroendocrinology*, 23(10): 871-882. <https://doi.org/10.1111/j.1365-2826.2011.02195.x>
36. Lim, K., Zimanyi, M.A. & Black, M.J. 2006. Effect of maternal protein restriction in rats on cardiac fibrosis and capillarization in adulthood. *Pediatric Research*, 60(1): 83-87. <https://doi.org/10.1203/01.pdr.0000220361.08181.c3>
37. Marcheva, B., Ramsey, K.M., Peek, C.B., Affinati, A., Maury, E. & Bass, J. 2013. Circadian clocks and metabolism. *Circadian Clocks*, 127-155. [https://doi.org/10.1007/978-3-642-25950-0\\_6](https://doi.org/10.1007/978-3-642-25950-0_6)
38. Martin-Gronert, M.S. & Ozanne, S.E. 2006. Maternal nutrition during pregnancy and health of the offspring. *Biochemical Society Transactions*, 34:779-882. <https://doi.org/10.1042/BST0340779>
39. McArthur, A.J., Gillette, M.U. & Prosser, R.A. 1991. Melatonin directly resets the rat suprachiasmatic circadian clock in vitro. *Brain Research*, 565(1): 158-161. [https://doi.org/10.1016/0006-8993\(91\)91748-P](https://doi.org/10.1016/0006-8993(91)91748-P)
40. McMillen, I.C., Adam, C.L. & Mühlhäusler, B.S. 2005. Early origins of obesity: programming the appetite regulatory system. *The Journal of Physiology*, 565(1): 9-17. <https://doi.org/10.1113/jphysiol.2004.081992>
41. McMillen, I.C., MacLaughlin, S.M., Mühlhäusler, B.S., Gentili, S., Duffield, J.L. & Morrison, J.L. 2008. Developmental origins of adult health and disease: the role of periconceptual and foetal nutrition. *Basic & Clinical Pharmacology & Toxicology*, 102(2): 82-89. <https://doi.org/10.1111/j.1742-7843.2007.00188.x>
42. Meli, R., Pacilio, M., Raso, G.M., Esposito, E., Coppola, A., Nasti, A., Di Carlo, C., Nappi C. & Di Carlo, R. 2004. Estrogen and raloxifene modulate leptin and its receptor in hypothalamus and adipose tissue from ovariectomized rats. *Endocrinology*, 145(7): 3115-3121. <https://doi.org/10.1210/en.2004-0129>
43. Mercer, J.G., Hoggard, N., Williams, L.M., Lawrence, C.B., Hannah, L.T. & Trayhurn, P. 1996. Localization of leptin receptor mRNA and the long form splice variant (Ob-Rb) in mouse hypothalamus and adjacent brain regions by in situ hybridization. *FEBS Letters*, 387(2-3): 113-116. [https://doi.org/10.1016/0014-5793\(96\)00473-5](https://doi.org/10.1016/0014-5793(96)00473-5)
44. Mohawk, J.A., Green, C.B. & Takahashi, J.S. 2012. Central and peripheral circadian clocks in mammals. *Annual Review of Neuroscience*, 35(1): 445-462. <https://doi.org/10.1146/annurev-neuro-060909-153128>
45. Morgan, P.J., Ross, A.W., Mercer, J.G. & Barrett, P. 2003. Circadian and Seasonal Rhythms-Photoperiodic programming of body weight through the neuroendocrine hypothalamus. *Journal of Endocrinology*, 177(1): 27-34. <https://doi.org/0022-0795/03/0177-027>
46. Nelson, W. & Halberg, F. 1986. Meal-timing, circadian rhythms and life span of mice. *The Journal of Nutrition*, 116(11): 2244-2253. <https://doi.org/10.1093/jn/116.11.2244>
47. Nieminen, P., Mustonen, A.M., Asikainen, J. & Hyvärinen, H. 2002. Seasonal weight regulation of the raccoon dog (*Nyctereutes procyonoides*): interactions between melatonin, leptin, ghrelin, and growth hormone. *Journal of Biological Rhythms*, 17(2): 155-163. <https://doi.org/10.1177/074873040201700206>
48. Oosterman, J.E., Kalsbeek, A., La Fleur, S.E. & Belsham, D.D. 2015. Impact of nutrients on circadian rhythmicity. *American Journal of Physiology-Regulatory, Integrative and Comparative Physiology*, 308(5): R337-R350. <https://doi.org/10.1152/ajpregu.00322.2014>
49. Prunet-Marcassus, B., Desbazeille, M., Bros, A., Louche, K., Delagrangé, P., Renard, P., Casteilla, L. & Pénicaud, L. 2003. Melatonin reduces body weight gain in Sprague Dawley rats with diet-induced obesity. *Endocrinology*, 144(12): 5347-5352. <https://doi.org/10.1210/en.2003-0693>

50. Qi, Y., Lee, N.J., Ip, C.K., Enriquez, R., Tasan, R., Zhang, L. & Herzog, H. 2022. NPY derived from AGRP neurons controls feeding via Y1 and energy expenditure and food foraging behaviour via Y2 signalling. *Molecular Metabolism*, 59: 101455. <https://doi.org/10.1016/j.molmet.2022.101455>
51. Rasmussen, D.D., Boldt, B.M., Wilkinson, C., Yellon, S.M. & Matsumoto, A.M. 1999. Daily melatonin administration at middle age suppresses male rat visceral fat, plasma leptin, and plasma insulin to youthful levels. *Endocrinology*, 140(2): 1009-1012. <https://doi.org/10.1210/endo.140.2.6674>
52. Reiter, R. 1974. Circannual reproductive rhythms in mammals related to photoperiod and pineal function: a review. *Chronobiologia*, 1(4):365-395
53. Schwartz, M.W., Seeley, R.J., Campfield, L.A., Burn, P. & Baskin, D.G. 1996. Identification of targets of leptin action in rat hypothalamus. *The Journal of Clinical Investigation*, 98(5): 1101-1106. <https://doi.org/10.1172/JCI118891>
54. Schwartz, M.W., Woods, S.C., Porte Jr, D., Seeley, R.J. & Baskin, D.G. 2000. Central nervous system control of food intake. *Nature*, 404(6778), 661-671. hat Ovid: Schwartz: *Nature*, Volume 404(6778): 661-671. <https://doi.org/10.1038/35007534>
55. Selmaoui, B., Oguine, A. & Thibault, L. 2001. Food access schedule and diet composition alter rhythmicity of serum melatonin and pineal NAT activity. *Physiology & Behavior*, 74(4-5): 449-455. [https://doi.org/10.1016/S0031-9384\(01\)00592-3](https://doi.org/10.1016/S0031-9384(01)00592-3)
56. Shochat, T. 2012. Impact of lifestyle and technology developments on sleep. *Nature and Science of Sleep*, 19-31. <https://doi.org/10.2147/NSS.S18891>
57. Smith, J.T., Clifton, D.K. & Steiner, R.A. 2006. Regulation of the neuroendocrine reproductive axis by kisspeptin-GPR54 signaling. *Reproduction*, 131(4): 623-630. <https://doi.org/10.1530/rep.1.00368>
58. Stetson, M.H., Elliott, J.A. & Menaker, M. 1975. Photoperiodic regulation of hamster testis: circadian sensitivity to the effects of light. *Biology of Reproduction*, 13(3): 329-339. <https://doi.org/10.1095/biolreprod13.3.329>
59. Tacad, D.K., Tovar, A.P., Richardson, C.E., Horn, W.F., Krishnan, G.P., Keim, N.L. & Krishnan, S. 2022. Satiety associated with calorie restriction and time-restricted feeding: peripheral hormones. *Advances in Nutrition*, 13(3):792-820. <https://doi.org/10.1093/advances/nmac014>
60. Varela, L., Stutz, B., Song, J.E., Kim, J.G., Liu, Z.W., Gao, X.B. & Horvath, T.L. 2021. Hunger-promoting AgRP neurons trigger an astrocyte-mediated feed-forward autoactivation loop in mice. *The Journal of Clinical Investigation*, 131(10):e144239. <https://doi.org/10.1172/JCI144239>
61. Wade, G.N., Schneider, J.E. & Li, H.Y. 1996. Control of fertility by metabolic cues. *American Journal of Physiology-Endocrinology and Metabolism*, 270(1): E1-E19. <https://doi.org/10.1152/ajpendo.1996.270.1.E1>
62. Weindruch, R. & Sohal, R.S. 1997. Caloric intake and aging. *New England Journal of Medicine*, 337(14): 986-994. <https://doi.org/10.1056/NEJM199710023371407>
63. Wolden-Hansen, T., Mitton, D.R., McCants, R.L., Yellon, S.M., Wilkinson, C.W., Matsumoto, A.M. & Rasmussen, D.D. 2000. Daily melatonin administration to middle-aged male rats suppresses body weight, intraabdominal adiposity, and plasma leptin and insulin independent of food intake and total body fat. *Endocrinology*, 141(2): 487-497. <https://doi.org/10.1210/endo.141.2.7311>
64. WHO (World Health Organization). 2021. Obesity and overweight. <https://www.who.int/news-room/fact-sheets/detail/obesity-and-overweight>. (Date accessed: 10.06.2022).
65. Zalatan, F., Krause, J.A. & Blask, D.E. 2001. Inhibition of isoproterenol-induced lipolysis in rat inguinal adipocytes in vitro by physiological melatonin via a receptor-mediated mechanism. *Endocrinology*, 142(9): 3783-3790. <https://doi.org/10.1210/endo.142.9.8378>
66. Zhang, Y., Proenca, R., Maffei, M., Barone, M., Leopold, L. & Friedman, J. M. 1994. Positional cloning of the mouse obese gene and its human homologue. *Nature (London)* 372: 425-432. <https://doi.org/10.1038/372425a0>
67. Zieba, D.A., Kloczek, B., Williams, G.L., Romanowicz, K., Boliglowska, L. & Wozniak, M. 2007. In vitro evidence that leptin suppresses melatonin secretion during long days and stimulates its secretion during short days in seasonal breeding ewes. *Domestic Animal Endocrinology*, 33(3): 358-365. <https://doi.org/10.1016/j.domaniend.2006.06.004>

## Copyright and License

last category should be indicated in the Acknowledgements section. Otherwise, the names of these people should not be included in the manuscript.

Anyone listed as an author of the manuscript in the table below must fulfil at least one criterion from each of the first two categories in addition to being involved in the third category. The contributions of those who do not meet at least one of the criteria in these first two categories and

- Provide the full names of the authors of your submission to Trakya University Journal of Natural Sciences and the contribution details and contribution rates of each author in the below table.
- The contribution rates declared by the corresponding author will be the major reference in any type of ethical inquiry. The corresponding author may be further asked to provide evidence for the contribution rates declared.
- The types of contributions will be determined by the corresponding author considering the type of the submitted paper.
- The contribution types will be published at the end of the manuscript according to your determinations.

[illegible]



## Instructions to Authors

### Trakya University Journal of Natural Sciences

#### (Trakya Univ J Nat Sci)

**Trakya University Journal of Natural Sciences** is published twice a year in April and in October and includes theoretical and experimental articles in the fields of **Biology, Biotechnology** and **Basic Medical Sciences**. Original studies, research notes, reviews, technical notes, letters to the Editor and book reviews can be published in the journal. The publishing language for all articles in the journal is **English**. On the other hand, authors are required to provide a Turkish abstract also. The Turkish version of the abstract will be supplied by the journal for foreign authors. Abstracts should include an introduction, material and methods, results and discussion sections in summary. The authors should pay attention to research and publication ethics [Committee on Publication Ethics \(COPE\)](#) in preparation of their manuscripts before submission by considering national and international valid ethics. An approval of Ethics and Animal Welfare Committee is mandatory for submissions based on experimental animals and this approval should be provided during the submission of the manuscripts. Articles that have not been published elsewhere previously and whose copyright has not been given anywhere else should be submitted. All responsibilities related to published articles in the Trakya University Journal of Natural Sciences belong to the authors.

#### Submitting articles

Articles should be submitted on the web through <https://dergipark.org.tr/trkinat> and all submissions should be performed online.

Authors, who are already a member of the DergiPark system, can enter in the login section using their "user name" and "password" to submit their articles.

Authors entering the DergiPark system for the first time to submit an article will enter in the "**REGISTER**" section to submit their articles.

#### Article preparation rules

Articles should be submitted to the Journal using **MS Word** preparing **12 points Times New Roman** font and 1.5 row spacing. Author names and contact info must be on the first page, the article must continue on the second page without author names and contact info. The whole article should have been numbered with a **line number** restarting each page. The author's name must not be specified any academic titles. If studies are supported by a foundation, this support should have been written in the acknowledgement section.

Articles should be arranged as below:

**Authors:** The name(s) of the author(s) should not be abbreviated and must be written under the title one by one, with surnames in capital letters. Address(es) should be written in full. Corresponding authors in multiple-authored submissions should be indicated, and the address and e-mail of the corresponding author should be written just under the author(s) list. **No other information about the manuscript should be included in this page. The main manuscript text should start with the following new page and should not include any author-contact information.**

**Title:** Should be short and explanatory and written in capital letters and centered.

**Abstract and keywords:** Turkish and English abstracts should not exceed 250 words. "Keywords" should be written under the abstract in small letters and all keywords should be written using a comma after all. Keywords should not be replica of the title words if it is not obligatory.

The abstract must consist of 1. background, 2. purpose, 3. method, 4. results and 5. main conclusions.

**Introduction:** The aim of the submitted and history of the previous studies should be indicated in this section. SI (Système International) system and abbreviation should be used in the article. Other abbreviations- should be explained once in their first appearance in the text. No "." sign should be used



after abbreviations except those used at the end of a sentence (...the determined distance is 45 m. Therefore, ...).

**Material and Method:** If the submitted study is experimental, the methods of the experiments should be given in detail. The method(s) used in the article should be descriptive for others to repeat. If a widely known experimental method is used, the method does not need to be explained in detail. In this situation, indicating only the name of the experimental method or citing the study who used the method for the first time will be enough.

**Results:** Obtained results should be given in this section without any comment. Results can be explained with tables, figures or graphics, if necessary.

**Discussion:** Results must be discussed, but unnecessary duplications should be avoided. In this section, rather than giving literature data, authors should focus on their results considering similarities and differences with and between previously conducted researches and should discuss possible reasons of similarities and differences. The contribution to science and the importance of the obtained results should also be mentioned as much as possible in this section.

**Acknowledgements:** Should be as short as possible. Thanks are usually made to institutions or individuals who support the study or to experts who reviewed the article before submitting to the journal. The acknowledgement section should be given before the references section in a separate header.

**References:** Unpublished information should not be given as a reference (examples of unpublished references: articles in preparation or submitted somewhere, unpublished data or observations, data obtained based on interviews with individuals, reports, lecture notes, seminars, etc.). However, thesis completed and signed by a jury and articles with DOI numbers given can be used as reference. References should be given at the end of the text, sorted alphabetically by author's surname and should be given with numbering.

#### Reference style:

You can download the Endnote style of TUJNS from <http://www.researchsoftware.com>.

Or you can follow the instruction below.

**Articles:** Surname of the author, the first letter of author's first name. publication year. article title, *the name of the journal*, volume, issue, page numbers. Journal name is written in italics.

*Example:*

#### *Articles with single author*

Surname, N. Year. Article title (First letter of all words small). *Whole name of journal*, Volume (Issue): page range.

Aybeke, M. 2016. The detection of appropriate organic fertilizer and mycorrhizal method enhancing salt stress tolerance in rice (*Oryza sativa* L.) under field conditions. *Trakya University Journal of Natural Sciences*, 17(1): 17-27.

#### *Articles with two or more authors*

Surname1, N1. & Surname2, N2. Year. Article title (First letter of all words small). *Whole name of journal*, Volume (Issue): page range.

Dursun, A. & Fent, M. 2016. Contributions to The Cicadomorpha and Fulgoromorpha (Hemiptera) fauna of Turkish Thrace region. *Trakya University Journal of Natural Sciences*, 17(2): 123-128.

Surname1, N1., Surname2, N2. & Surname3, N. Year. Article title (First letter of words small). *Whole name of journal*, Volume (Issue): page range.

Becen, N., Uluçam, G. & Altun, Ö. 2017. Synthesis and antimicrobial activity of iron cyclohexanedicarboxylic acid and examination of pH effect on extraction in water and organic phases. *Trakya University Journal of Natural Sciences*, 18(1): 1-7.

**Preprints:** Surname of the author, the first letter of author's first name. publication year. article title, *the name of the repository* [**Preprint**], (cited: 12.08.2017). DOI number

Example:

Augustine, D., Rao, R.S., Gns, H.S., Anbu, J. & Saraswathy, G.R. 2022. Anticancer Potential of Eudrilus Eugeniae Coelomic Fluid Protein on SCC-9 Cells-In Vitro Gene Expression entwined with Cutting-Edge In-Silico Strategy, *Research Square*. [**Preprint**] (cited: 02.01.2024).  
<https://doi.org/10.21203/rs.3.rs-439242/v1>

**Book:** Surname of author, first letter of author's first name, Year. *Book title* (name of translator or book editor if present), volume, edition number, press, city, page number.

Example:

Surname, N. Year. *Book Title* (First letter of words small and italic), volume, edition number, press, city, page number.

Czechowski, W., Radchenko, A., Czechowska, W. & Vepsäläinen, K. 2012. *The ants of Poland with reference to the myrmecofauna of Europe*. Museum and Institute of Zoology PAS, Warsaw, 496 pp.

**Book Section:** Surname of author, first letter of the author's first name, Year. Section name, page range. In: (Editor(s) of Book, *Book title*, press, city, page number).

Example:

Surname, N. Year. Section name, page range. In: Editor of Book, *Book title* (First letter of words small and italic), press, city, page number.

Jansson, A. 1995. Family Corixidae Leach, 1815—The water boatmen. pp. 26-56. In: Aukema, B. & Rieger, C.H. (eds). *Catalogue of the Heteroptera of the Palaearctic Region*. Vol. 1. Enicocephalomorpha, Dipsocoromorpha, Nepomorpha, Gerromorpha and Leptopodomorpha. The Netherlands Entomological Society, Amsterdam, xxvi + 222 pp.

**Congress, Symposium:** Surname, N. Year. Presentation title (first letters of all words small), page range. Name of Congress/Symposium, Date (day range and month), place.

Example:

Bracko, G., Kiran, K., & Karaman, C. 2015. The ant fauna of Greek Thrace, 33-34. Paper presented at the 6<sup>th</sup> Central European Workshop of Myrmecology, 24-27 July, Debrecen-Hungary.

**Internet:** If any information is taken from an internet source (articles published in journals and taken from internet excluded), internet address should be written in full in references section and access date should be indicated.

Surname, N. Year. Name of study (First letter of words small). <http://www.....> (Date accessed: 12.08.2009).

Hatch, S. 2001. Student perception of online education. Multimedia CBT Systems. <http://www.scu.edu.au/schools/sawd/moconf/papers2001/hatch.pdf> (Date accessed: 12.08.2009).

References within the text should not be numbered and indicated as in the following examples.

Examples:

... atmospheric pollution is causing by x matter (Landen 2002). If an article has two authors, it should be indicated in the text as (Landen & Bruce 2002) or ... according to Landen & Bruce (2002) .... If there are three or more authors, references should be indicated as (Landen *et al.* 2002) or according to Landen *et al.* 2002 ...

**Graphics and tables:** All photos, pictures, drawings and graphics except tables should be indicated as Figures. Pictures, figures and graphics should be clear and ready to print with the offset technique. The places of all tables and figures should be indicated in the text. All tables and figures should be numbered within the text respectively (Table 1, Fig. 1, Figs 3, 4). Figure numbers and legends are written below the figures, table numbers and legends are written above the tables.

All figures (all pictures, drawings and graphics except table) should also be uploaded to the system separately with 300dpi resolution at least as .tif file using the figure numbers in the files name.

Submitted articles are subjected to prior review by the Editorial Board. Editorial Board has the right to reject the articles which are considered of low quality for publish or those which are insufficiently prepared according to the author guidelines. The articles accepted for consideration for evaluation will be sent to two different referees. Editorial Board decides to accept or reject the submissions for publication by taking into account the reports of referees.

## **COPYRIGHT**

The authors retain the copyright and full publishing rights to the article without any restriction.

## **LICENSE**

All articles published in TUJNS is on the "Open Access" terms. All publications are published under the Creative Commons Attribution 4.0 Generic Licence (CC BY 4.0) (<http://creativecommons.org/licenses/by/4.0/legalcode>) which allows to copy and distribute the material in any medium or format and transform and build upon the material, including for any purpose (including commercial) without further permission or fees being required.

## **EXPLOITATION ENQUIRY AND COMPLAINTS**

All kinds of exploitation doubts and complaints about manuscripts, either published or in the publication process, are evaluated by the Editorial Board. The Editorial Board strictly follows the directives of COPE (Committee on Publication Ethics) during the evaluations. An ombudsman who has no connection with the parts in any stage of the complaint is appointed and a decision is made. Complaints can be sent to the editor in chief by sending an e-mail to [tujns@trakya.edu.tr](mailto:tujns@trakya.edu.tr).

## **POST-PUBLICATION CHANGE AND WITHDRAWAL OF A MANUSCRIPT**

Changes in author ordering, removal or addition of a new author in and withdrawal of a published manuscript can be realized by sending an application to [tujns@trakya.edu.tr](mailto:tujns@trakya.edu.tr). The application e-mail should include the reason of the requested change with the evidences. The reasons and the evidence are discussed and finalized by the Editorial Board. Further submissions of authors of a formerly accepted manuscript undergoing a change process are automatically sent back to the authors until the final decision of the manuscript in process.

## **ADVERTISING**

Advertising applications sent to [tujns@trakya.edu.tr](mailto:tujns@trakya.edu.tr) will be evaluated by the journal owner.

**Editor-in-Chief** : Prof. Dr. Kadri KIRAN

Trakya Üniversitesi  
Fen Bilimleri Enstitüsü  
Balkan Yerleşkesi  
22030 - EDİRNE-TURKEY

Phone : +90 284 235 82 30  
Fax : +90 284 235 82 37  
e-mail : [tujns@trakya.edu.tr](mailto:tujns@trakya.edu.tr)



